

**FLOW AND MIXING STUDIES IN A CO-ROTATING  
INTERMESHING TWIN SCREW EXTRUDER**

**DEVENDRA PAL SINGH**

Being a thesis submitted to The Department of Materials Technology, Brunel, The University of West London, for the award of the degree of Doctor of Philosophy in Polymer Technology.

March 1988

**TO THE KHALSA.**

**ITS CREATOR**

**AND TO GOD TO WHOM IT BELONGS**

Brunel University  
Department of Materials Technology  
Uxbridge, Middlesex UB8 3PH

Devendra P. Singh

Flow and Mixing studies in a co-rotating intermeshing twin screw extruder

Ph.D. Degree  
1988

#### ABSTRACT

The basic understanding of mixing in the process of polymer melt extrusion by twin screw extruder is limited by their geometrical complexity and the interactions of the process parameters.

Mixing and flow in a 100mm diameter, trapezoidal channeled, intermeshing co-rotating twin-screw extruder have been characterised by determination of residence time distribution (RTD) and of the paths taken by tracers added to the melt.

The axial mixing and the effects of various parameters on it were established by studying RTD using tracer techniques. As the tail of the distribution is of paramount importance, the reproducibility of the RTD curve was extensively studied.

Radioactive  $MnO_2$  was used as a tracer and detected by gamma ray spectroscopy, giving more reproducible results than added barytes estimated gravimetrically after ashing.

Shock cooling of the extruder and sectioning of the solidified compound in the screw channels was used to study the flow mechanism.

The maximum throughput achieved, polymer melting mechanism, filled volume and axial mixing are interrelated, and are dependent on the configuration and position of segmented mixing discs present in the screw profile.

In the upstream position these act as melting discs and their efficiency is increased in a closed configuration. Initial melting is achieved over a remarkably short distance along the screw profile.

The screw speed affects the axial mixing which is shown to be related to the net relative pressure change at the screw tips.

A flow model is proposed such that the overall material flow taking place in an anticlockwise direction along the screw channel comprises two separate flow regimes. The upper regime rotates anti-clockwise and is made up of main and small tetrahedron flow and calender flow. The lower flow regime rotates clockwise and is made up of main and small side leakage flows and a portion of the main tetrahedron flow, together with a central flow.

The flow studies show conclusively that the melt from a particular site ahead of the intermeshing zone occupies a predestined site after passing through the intermeshing zone.

## **ACKNOWLEDGMENT**

I wish to express my gratitude to my supervisors Mr. G.R.Sothern and Dr. P.R.Hornsby for their encouragement throughout this work, for their invaluable guidance, useful recommendations, helpful discussions and for reading and commenting upon the manuscript.

I also wish to express my gratitude to Prof. M.J.Bevis from whom I have learned so much. This work would have never finished without his financial help at the crucial time.

Particular thanks are due to my employers Center for Industrial Research, Norway, especially Mr. Dag Slotfeldt-Ellingsen and Mr. Reidar Stokke, for providing facilities during the preparation of this manuscript. Advice and assistance was also contributed by the late Prof. E.Gaspar and late Mr. I.Boyne. Mr. J.Felgate and Mr. J.Gupte provided invaluable technical assistance and John Ion helped with language corrections in parts of the manuscript.

Above all, I would like to thank my family for their continuous support and patience during the course of this work.

Oslo, Norway, March 1988

Devendra P. Singh

## **PERMISSION TO REPRINT**

The permission to reprint the figures from the various publications in this thesis is obtained from their copyright holders and authors, and is greatly acknowledged. The name of Journals/Textbooks from which the figures are reprinted together with their respective copyright holder is listed as below. The reference source is quoted in parenthesis of the each figure caption.

- \* Annual Technical Conference of Society of Plastic Engineers:  
Society of Plastic Engineers Inc.
  
- \* Chemical Engineering Progress : American Institute of Chemical Engineering.
  
- \* Industrial and Engineering, Chemistry and Fundamental : American Chemical Society (copyright 1979).
  
- \* Modern Plastic International : McGraw Hill Publications Overseas Corn.
  
- \* Polymer Engineering and Science : Society of Plastics Engineers Inc.
  
- \* Twin Screw Extrusion by Janssen and Churchill : Janssen (1978).

## CONTENTS

<b>CHAPTER 1. INTRODUCTION</b>	<b>1</b>
<b>CHAPTER 2. LITERATURE REVIEW</b>	<b>8</b>
2.1 Flow and mixing in extruders	13
2.2 Residence time distribution	19
2.2.1 Concepts of RTD	19
2.2.2 RTD functions in some systems	25
2.2.3 Advantages of knowledge of RTD of a system.	26
2.2.4 Limitations of RTD data.	27
2.2.5 Method of monitoring RTD.	27
2.2.6 RTD studies in extruders.	33
2.2.6.A RTD studies in single screw extruders.	34
2.2.6.B RTD studies in twin screw extruders.	35
2.2.7 Interpretation of RTD curves.	42
2.2.8 Residence time distribution models	44
<b>CHAPTER 3. EXPERIMENTAL</b>	<b>46</b>
3.1 Polymer characteristics.	46
3.2 The extrusion line	46
3.2.1 Extrusion line's description	46
3.2.2 Modifications to the extrusion line.	52
3.2.3 Operation.	53
3.3 Determination of RTD using tracer technique	53
3.3.1 Ashing technique.	54
3.3.1.A Selection of tracer.	54
3.3.1.B Introducing the tracer and sampling procedure.	57
3.3.1.C Ashing procedure.	57
3.3.2 Radioactive tracer technique.	59
3.3.2.A MnO <sub>2</sub> as tracer.	61

3.3.2.B	Preparation and irradiation of specimens.	61
3.3.2.C	Errors associated with neutron activation analysis	62
3.3.2.D	Techniques for analysis.	68
3.4	Application of RTD to characterise TS250	75
3.4.1	Process variables	76
3.4.2	Machine variables	76
3.4.3	Material variables	80
3.5	Determination of cross channel flow and transverse mixing	81
<b>CHAPTER 4.</b>	<b>RESULTS AND DISCUSSION</b>	<b>89</b>
4.1	Reproducibility of RTD determination.	89
4.1.1	Tracer effect.	90
4.1.2	Sampling effect	99
4.1.3	Extruder performance	101
4.2	Factors influencing RTD.	102
4.2.1	Throughput rate.	102
4.2.2	Melting behavior.	114
4.2.3	Filled volume.	119
4.2.4	Power consumption.	126
4.3	Influence of variables on RTD	129
4.3.1	Throughput rate.	134
4.3.2	Temperature profile.	145
4.3.3	Screw speed.	149
4.3.4	Pulley size (screw speed).	162
4.3.5	Mixing disc - Position and configuration.	162
4.3.6	Melt pressure - by changing die dimensions.	170
4.3.7	Physical form of polymer.	175
4.3.8	Polymer type.	176
4.4	Flow mechanism in extruder.	182
4.4.1	Various flow, their origins and positions.	194

4.4.1.A	Tetrahedron flow	194
4.4.1.B	Side leakage flow	201
4.4.1.C	Central flow	204
4.4.1.D	Calender flow	205
4.4.1.E	Flight gap flow	205
4.4.1.F	Stagnation flow	205
4.4.2	Flow behaviour in passage along the C-shaped chamber.	206
4.5	Transverse mixing along the extruder.	209
4.5.1	Macromixing.	210
4.5.2	Micromixing.	212
4.6	Relationship between RTD and transverse mixing studies	216
4.6.1	Some typical effects of variables	221
<b>CHAPTER 5.</b>	<b>CONCLUSIONS</b>	<b>223</b>
<b>REFERENCES</b>		<b>230</b>



## CHAPTER 1 INTRODUCTION

Extrusion is one of the most important mixing and forming techniques of polymer processing. With a few exceptions, all thermoplastics can be extruded and many may pass a screw extruder not once but twice during their journey from the reactor to the finished product - first through a pelletizing extruder after the reactor, then through a shaping extruder. More thermoplastics are converted into useful products by extrusion than by any other method.

The extrusion process can be accomplished by a screw rotating in a cylindrical barrel. The feed to the extruder may be solid or it may sometimes be liquid. When fed by a solid, it is called a plasticating extruder while if it is fed by liquid, it is termed as a melt extruder. In a plasticating extruder, the solid feed is introduced at one end of the extruder and as it advances along the extruder length, it is melted, homogenised (mixed) and transported to the die at high pressure and temperature for forming into a product.

As discussed above, one of the functions carried out by the extruder is homogenising or rather mixing. This function of the extruder is of prime importance. The thorough mixing is required to ensure complete dispersion (dispersive mixing) of ingredients and also to create a homogeneous mass, such that each particle has been subjected to the same mechanical and thermal treatment. As the flow path followed by each particle and the shear, temperature and residence time for each particle can vary widely, it can lead to variations in the viscosity of the melt and the final characteristics of each particle. So in an extrusion process it is desirable that particles change position with each other, in order to receive the same average treatment. This

continuous reorientation also distributes additives (distributive mixing) - such as colours, stabilizers, fillers, lubricants, as the case may be - throughout the material thereby rendering the mixture uniform. So in a nutshell it can be said that mixing is of two types - dispersive and distributive.

Dispersive mixing concerns the breaking up of the agglomerates. So the component breaks up only upon reaching a certain yield stress.

Distributive mixing can be achieved only by inducing physical motion of the ingredients. The homogeneity or rather randomness of distribution of components of the material passing through extruder, is achieved by distributive mixing. The distributive mixing can be of two types. First being the axial or longitudinal mixing - in this the distribution of ingredients occurring in axial direction (in direction of flow). The second type being the transverse mixing - in this the randomisation or distribution of the ingredients happening in transverse to flow direction.

Twin screw extruders have established their place in two key areas. These being profile extrusion of thermally sensitive materials and speciality polymer processing operations such as alloying, compounding, devolatilization and chemical reactions etc. . In some of these applications, distributive mixing or rather longitudinal mixing is central to their successful application. The longitudinal mixing is being defined as the random movement in the axial direction, thus making the mixture more random. For example in chemical reactions and in extrusion of thermally sensitive polymers, the time spent by each polymer particle within the extruder (Residence time distribution or RTD) should be the same so that all the particles receive the same treatment. But at the same time the particles have to spend a certain

minimum time within the extruder (residence time) so as to get the thermal treatment, e.g. to achieve good gelation in PVC extrusion. However in other cases, such as in polymer compounding, it is desirable that the time spent by polymer particles, in the extruder, should be different from each other. This would even out the feed irregularities. So detailed information on axial mixing could be instrumental in selecting screw design and extruder type for a particular application area. The theoretical work on characterising of axial mixing (by RTD studies) has been extremely limited ( Janssen et al. 1979 ; Werner and Eise 1979). Some researchers have carried out some work in characterising RTD by using model fluids ( Todd and Irwin 1969 ; Todd 1975 ; Janssen and Smith 1975 ; Kim et al. 1978 and Sakai 1981 ; Kao and Allison 1984). Similarly others have carried out work on the polymer melt in extruders ( Janssen 1979 ; Werner and Eise 1979 ; Kim et al 1980 ; Rauwendaal 1981 and Walk 1982; Nichols et al 1983; Sakai et al 1987). However in all these investigations no one has done work on a large size extruder with polymer melt (it is either based on model system or if a polymer system is used then the size of extruder being small) and no one has studied the complete set of processing variables.

The transfer mixing and flow pattern studies inside single screw extruder have been established for a long time. However, as the mixing mechanism ( distributive mixing ) in twin screw extruders is quite complex and difficult to describe. It is rather difficult to calculate it theoretically. A number of workers have carried out work on the mixing and flow patterns. Most of them have ignored the effect of helix angle and/or intermeshing zone ( Kim et al 1973, Wyman 1975, Burkhardt et al 1978, Denson and Hwang 1980 and Eise et al 1981 ). As the overall extruder performance seems to be dominated by the effect

of the intermeshing region, these studies are of limited use. On the other hand, work that attempts to accurately describe the flow in the intermeshing region can easily become very complex ( Maheshri 1977 and Maheshri and Wyman 1979).

In twin screw extruders, there are several flow regimes which tend to contribute towards axial mixing. So to understand flow and mixing behaviour empirically, the flow behaviour and various leakage flows become rather important. The knowledge of flow is of considerable importance in giving information of the following :,

- (1) In monitoring the flow patterns and extent of intermixing of various zones in the tangential direction thus giving information on temperature uniformity achieved.
- (2) The shear history of material during its passage through extruder.
- (3) In monitoring the stagnant zone detrimental to colour changes and stagnation of temperature sensitive polymers.

In the past some experimental work has been done by various researchers using a model fluid ( Jewmenow and Kim 1973 ; Kim, Skatschkow and Stungur 1976 ; Janssen and Smith 1975 ; Janssen 1978). However up to now, the studies in twin screw extruders have been based on flow visualization techniques using model fluids with either model or actual extruders. Naturally studies are of significant importance but of limited practical use. Some work has been done by the following investigators using actual polymer systems (Kim et al (1975) ; Janssen (1978); Howland and Erwin (1983); Bigio and Erwin (1985); Sakai et al (1987) and Hornsby (1987)). In the case of Howland and Erwin (1983) and Bigio and Erwin (1985), the work is based on low viscosity curable silicone rubber and not on polymer melts. In all these cases it is either the local mixing in a confined chamber of twin screw which is

discussed, or just the interaction between the chambers.

So there is a need for some experimental work in order study the flow mechanism inside the extruder, to recognise the various types of flows and study their contribution in mixing and also to demonstrate how the various operating variables could affect the mixing performance of the extruder. Besides, as the maximum throughput rate is achieved, filled volume, power consumption and melting behaviour give indication on the melt state of the polymer and available flow path to the melt. By studying the effect of variables on the above, this tends to give a clear picture of their influence on the melt state and therefore on its conveying and mixing action.

This kind of work would give a better understanding of mixing process and thus it can be used to design better extruders. The one which are not so much dependent on processing variables and with optimum amount of mixing of various flows. Or at least to be familiar with the parameters which seems to affect the mixing performance substantially.

In this work, the mixing studies were carried out on GKN 250X. The extruder used is a low speed co-rotating intermeshing twin screw extruder. It has a closely fitted flight and channel profile and therefore has a higher degree of positive conveying character. However because of its small mechanical clearances, the processing screw speed is lower.

The mechanism of flow path taken by various flows and their intermixing during their subsequent travel down the channel was studied by use of various coloured tracers. This was done by introducing tracers in the feed, stopping the extruder, freezing the

polymer in solid state, withdrawing the barrel, removing the polymer skeleton and sectioning it. Furthermore an attempt was made to relate these various flows the transverse distributive mixing behaviour.

The longitudinal or axial distributive mixing was characterised by residence time distribution (RTD) studies. The tracer was introduced at the feed hopper and tracer concentration was measured at the output to find the time (distribution) spent by particles inside the extruder. The effect of various variables (processing , material and machine design) on RTD were studied.

This investigative study was unique and different from the other work to date in the following ways.

1. A low speed, co-rotating intermeshing twin screw extruder with closely fitted flight and channel profile was used.
2. An industrial extruder( 100 mm diameter) was used and thus results obtained from this would be more meaningful and realistic for industrial application. Thus it contrasts with experiments and results published on small scale laboratory size extruder from which it is rather difficult to extrapolate the results due to scale up problems. A small extruder generally differs from a large machine in some fundamental respects, e.g. relative gap size, surface to volume ratio and the relative contribution of shear and conductive heating. Particularly if a certain combination of critical factors is being examined the probability of direct correlation is small.
3. It has a devolatilization vent-port as a regular feature, which makes it unique and interesting from other twin screw extruders

studied so far. It behaves as if there are two extruders operating in series mode.

4. The effect of whole range of variables on RTD were studied so as to see the relative effect of variables on RTD.

5. In this study it has been tried to find a link between the effect of variables on RTD with overall behaviour of filled volume, melt behaviour, power consumption and throughput rate etc.

6. The flow mechanism including its various flow constituents were studied in detail together with its correlation with RTD.

## CHAPTER 2 LITERATURE REVIEW

The recent arrival of the twin screw extruder in the polymer field has significantly changed the outlook. They not only compete with single screw extruders but also expand their extrusion potential. For example twin screw extruders commercial significance has steadily increased in specialised operations such as PVC powder and reground processing etc. However there is an enormous variety in twin screw extruders, which differ considerably from each other in their principle of operation. The diversity among twin screw extruders is so large that the comprehensive analysis of all the various types would be an enormous undertaking. Theoretical analysis of twin screw extruders lags behind that of the single screw machines, because of the great variety of design and screw configurations in use.

As mentioned above, several types of twin screw extruders exist which have different conveying characteristics. The diversity among twin screw extruders is so large that a comprehensive analysis of all the various types would be an enormous undertaking. A classification of twin screw extruders is shown in Fig 2.1 .

The classification is based on the intermeshing/non-intermeshing (i.e. whether flights of one screw protrude into the channel of the other screw), direction of screws rotating relative to each other, screw speed and shape of the barrel/screw and relative lengths of the screw. A fuller account is given by Rauwendaal (1981). Some typical screw geometries are illustrated in Fig 2.2 . In this work, a GKN 250X twin screw extruder is used. This was 100 mm in diameter and was similar to the commercial GKN 250 variant except for its extended length and reduced diameter. This extruder falls in the category of low speed co-rotating intermeshing twin screw extruder. Its schematic design is



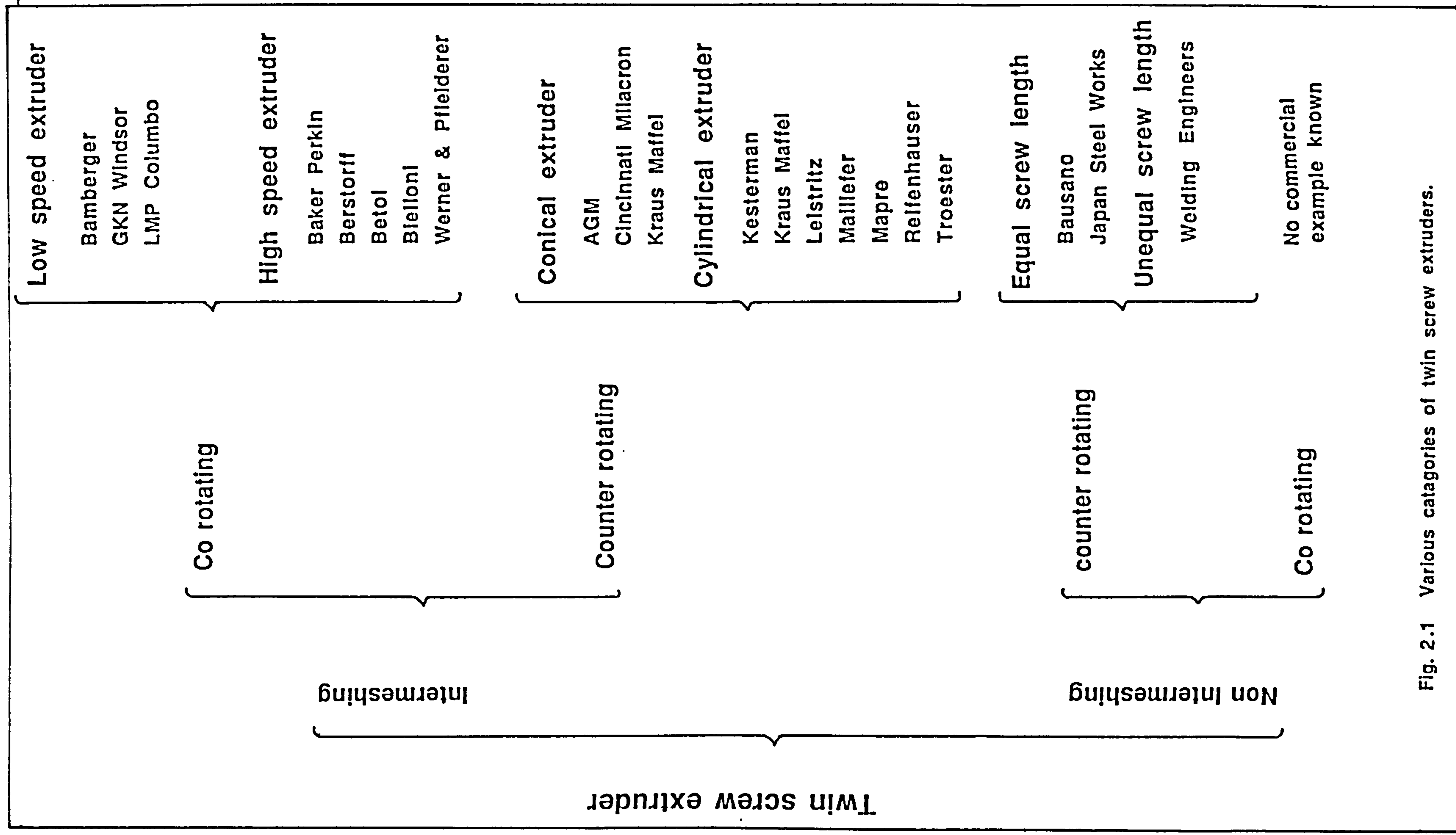


Fig. 2.1 Various catagories of twin screw extruders.

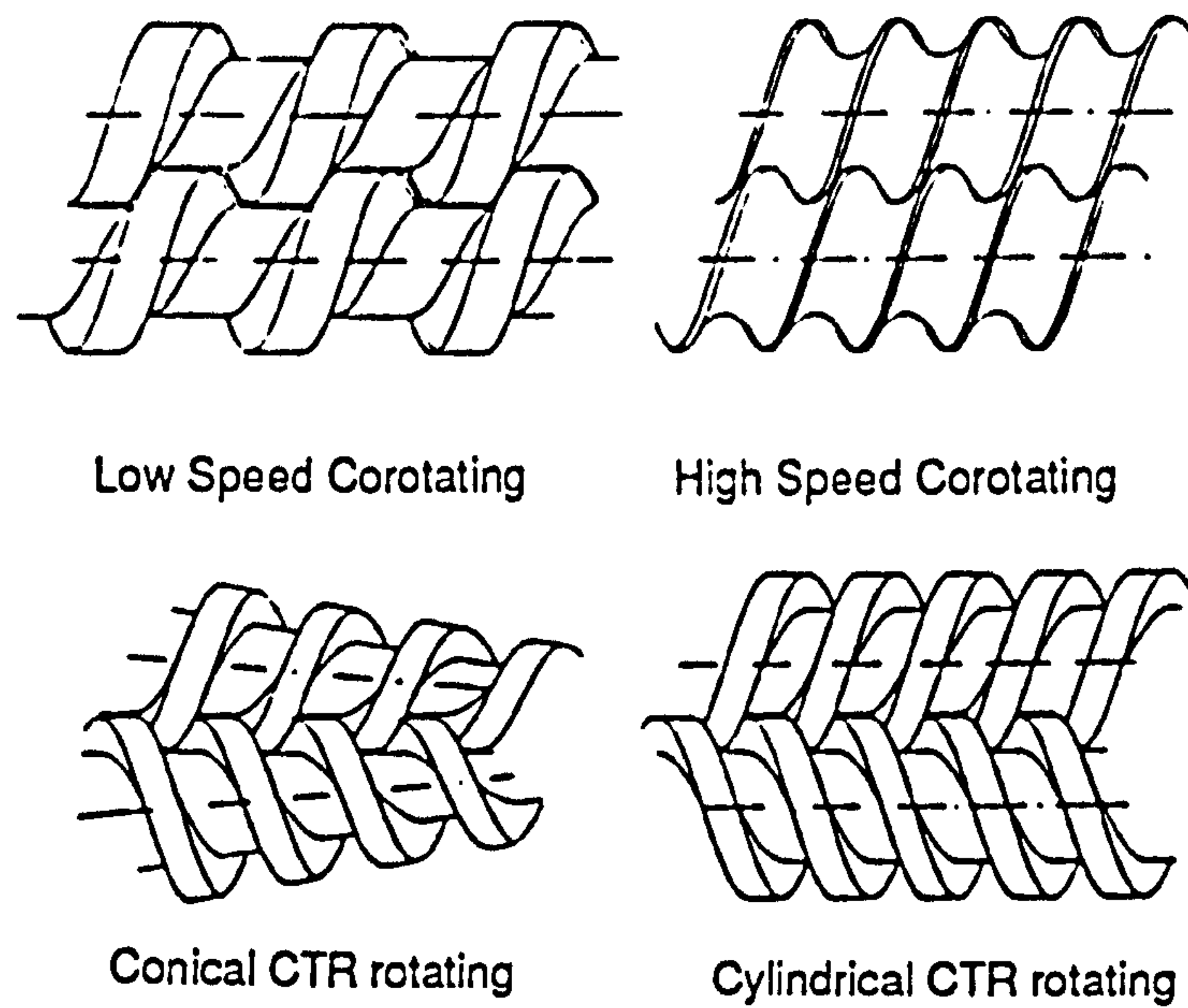
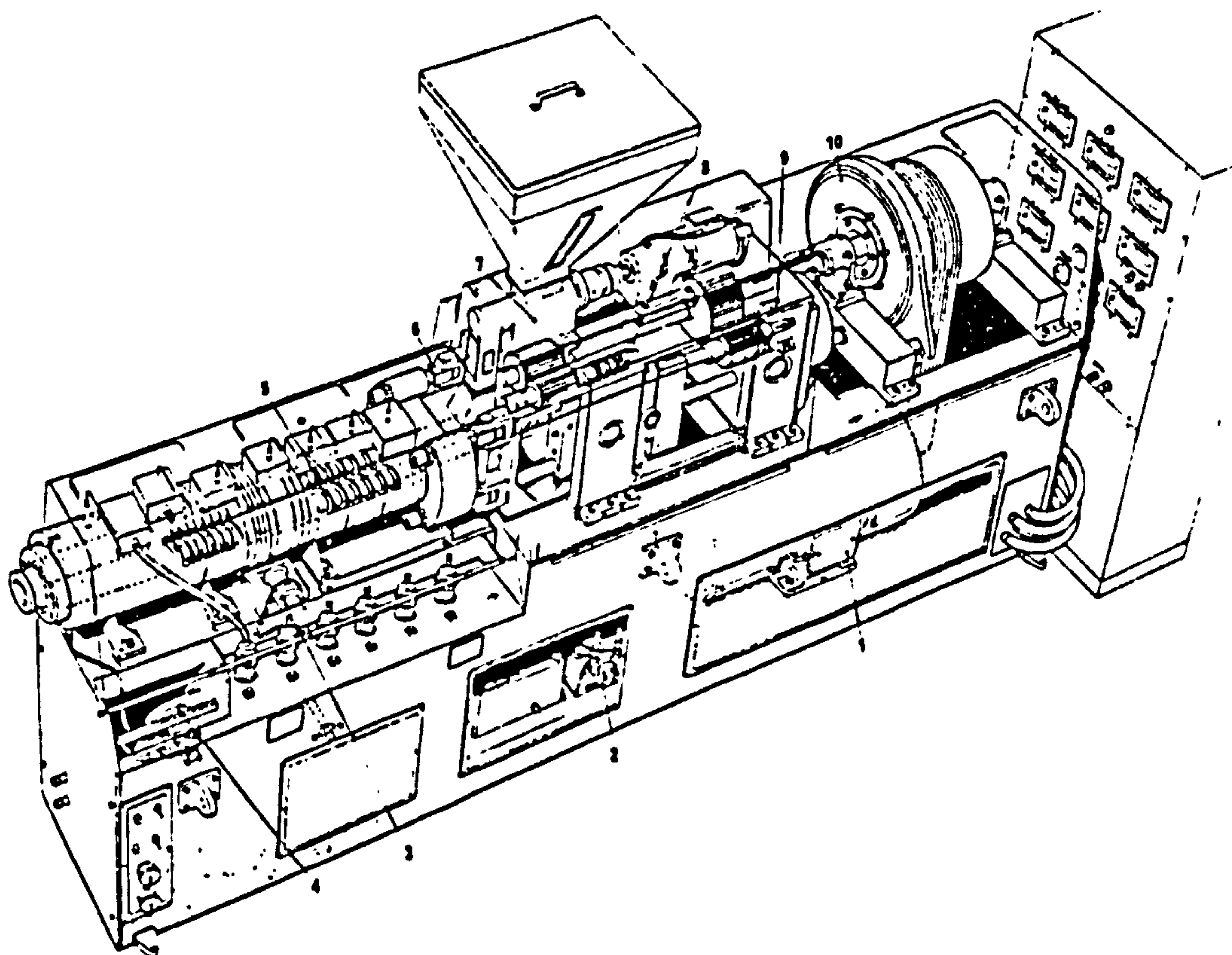


Fig. 2.2 Typical screw geometries of various types (After Rauwendaal 1981)



1, main motor; 2, oil circulation pump; 3, manually operated withdrawal mechanism for trolley mounted barrel; 4, independent oil cooling for front barrel zone; 5, twin screws with interchangeable sections; 6, quick release barrel clamp; 7, controlled material feed; 8, multiple element screw thrust bearing; 9, large diameter standard screw thrust bearing; 10, epicyclic primary gearbox.

Fig 2.3 GKN Windsor TS 250 twin screw extruder (Courtesy GKN Windsor Ltd.)

given in Fig 2.3 . The detailed information on this is given in chapter 3.

Twin screw extruders are successfully used in speciality polymer processing such as in alloying, devolatization, chemical reaction and in profile extrusion. The main requirement and advantage of twin screw extruders in these applications is their ability to give good distributive mixing. The homogeneity or rather randomness of distribution of components of the material passing through extruder is achieved by distributive mixing. Three basic mechanisms of mixing are involved in distributive mixing

- (1) Molecular Diffusion.
- (2) Eddy Diffusion.
- (3) Convection or Bulk Diffusion.

Molecular diffusion is a process that occurs spontaneously driven by a concentration gradient but in polymer processing it is almost insignificant as it occurs extremely slowly. However, it may become of significance in mixing of low molecular weight material e.g. antioxidants, blowing agents etc. The eddy diffusion or turbulent flow being the best to achieve mixing. However the flow becomes turbulent, only when a high Reynolds number has been reached. The Reynolds number depends on the fluid viscosity  $\mu$ , channel diameter  $D$  and average velocity of the flow in the channel  $V$ , the fluid density  $\rho$ , as shown in following equation.

$$Re = \frac{DV\rho}{\mu}$$

However, with the extremely high viscosities associated with polymer melts ( $\approx 10^4$  Pa.sec) turbulent flow is not possible and thus the flow in polymer remains laminar. Thus effective and efficient mixing due to turbulence is never realized. Therefore only convection is the

dominant mixing mechanism in polymer mixing.

The convection mixing can be achieved by two methods:

(a) Bulk rearrangement.

(b) Laminar flow.

(a) Bulk rearrangement: This is achieved by a simple rearrangement of the material that involves a plug type flow and requires no continuous deformation of material. This kind of mixing, through repeated rearrangement of the minor component, can in principle reduce non-uniformities to the molecular level. The repeated rearrangement can be either random or ordered. The former is the process that takes place e.g. in many solid/solid mixers whereas the latter forms part of the mixing mechanism in certain motionless mixers.

(b) Laminar flow: The mixing is also achieved by imposing deformation on a system through laminar flow. It occurs through various types of flow: shear, elongation (stretching) and squeezing (kneading). However, shear flow plays the major role in processing. It is clear that for the interfacial surface to increase both phases must undergo flow. The viscosity ratio plays an important role in laminar mixing. The laminar mixing of polymeric fluid is often a limiting parameter for achieving good mixing in screw extruders.

The decisive variable in laminar mixing is the strain, whereas the rate of application of stress and strain play no role. The interruption in screw or mixing section improves distributive mixing significantly. The simplified theory developed by Mohr et al. (1957) is unable to explain such an improvement. The theory developed by Erwin (1978) can explain such an improved mixing. This is based on

reorientation of interfacial planes as the critical mechanism.

The co-rotating twin screw extruders do have a laminar as well as bulk rearrangement through flow within the extruder. Basically the distributive mixing occurs in two directions viz. in axial direction (in the direction of flow) and in the transverse direction (transverse to direction of transport). As discussed before, the distributive mixing in twin screw extruders occurs as a result of contribution of various leakages. The mechanism for distributive mixing can be studied by the detailed study of the various leakage flows together with the influence of intermeshing zone of twin screw extruder. The knowledge of flow in the intermeshing zone is of considerable importance because it not only improves transverse mixing considerably by providing 90 degrees angle reorientation, an ideal requirement for optimum distributive mixing (Erwin 1978), but it also divides the melt, reblends it, thus giving good axial as well as transverse mixing.

However the longitudinal distributive mixing alone can be studied by the use of the residence time distribution ( RTD ) concept, while the progress in the transverse mixing can be studied by the sectioning the polymer in transverse direction all along the extruder.

## **2.1 FLOW AND MIXING IN EXTRUDERS**

A considerable amount of work regarding flow within single screw extruders, has been carried out and by now it is an established mechanism. The flow studies on single screw extruder were done by Street (1961) using colour sequenced feed stock. Mohr, Clapp and Starr (1961) studied flow patterns in the channel of a model single screw extruder. Shah (1979) and Gailus(1980) investigated the mixing

efficiency by using two streams of pigmented silicone fluid. Boyd (1983) used silicone streams of differing viscosity ratios to examine the behaviour of multiviscosity mixtures in single screw extruder. The above work together with substantial theoretical work on single screw extruders has well established their flow mechanism.

However, twin screw extruder's case is rather different and complicated. This is due to cumulative effect of various factors as mentioned below. The rather late (i.e. recent) arrival on the scene of twin screw extruders in any substantial way. As there exist various types of twin screw extruder differing substantially from each other in mode of operation (Rauwendaal 1981) it is very difficult to generalise them. Furthermore as compared to single screw extruder, the conveying and mixing mechanism in twin screw extruder is rather complex and difficult to describe. A considerable work has been carried out theoretically as well as experimentally which is being reviewed below. The work on mixing and flow pattern was carried out by various researchers such as Kim et al. (1973), Wyman (1975), Burkhardt et al (1978), Denson and Hwang (1980) and Eise et al (1981). However it should be noted that in most of these studies the influence of helix angle or/and intermeshing zone etc. are ignored. As the overall extruder performance (in twin screw extruder) seems to be dominated by the effect of the intermeshing region, these studies are of rather limited use. On the other hand work by Maheshri (1977) and Maheshri and Wyman (1979) shows that the analysis which takes the effect of intermeshing zone in consideration can become quite complex.

A limited amount of theoretical work is being carried out on mixing and flow pattern in twin screw extruders. Wyman (1975) has examined the down channel component of velocity for a leak-proof twin screw

extruder chamber and concluded that the shear rate is the inverted image of a no net flow single screw extruder. Maheshri and Wyman (1979) have concluded that the interaction of the intermeshing second screw lands with the fluid in the chamber, produces a uniform absolute strain for down channel flow in a leak proof chamber and could play an important role in down channel mixing. Kim et al (1973) predicted strain due to the three components of velocity by averaging the shear rate component over the channel depth far from the intermeshing second screw land.

Their analysis only includes the cross channel circulation between the screw flights but ignores the fluid circulation and resultant strain distribution due to the controlled down channel flow. However as the intermeshing second screw land regulates the down channel flow in a twin screw extruder chamber to some degree (depending on leakage), a down channel circulation pattern will exist. So Maheshri and Wyman (1980) examined the combined cross and down channel flow in an idealized leakproof twin screw extruder and concluded that in addition to normal cross channel flow (similar to single screw) fluid circulation between the independent set of channel depths in the down channel direction occurs (in channel direction). This is due to the seal provided by the second screw land. So combined, these two flows give a complex flow path.

Some experimental work is being carried out by various researchers on counter-rotating twin screw extruders to understand the flow and mixing within one chamber and also interaction between the chambers. The flow profile in a model extruder was established by Jewmenow and kim (1973) and Kim ,Skatschkow and Stungur (1976). Jewmenow and Kim established this by injecting aluminum particles in a model fluid of a

polyisobutene solution whilst Kim et al carried it out by using aluminum powder. Good agreement was found with the above work of Jewmenow and Kim. Later on Janssen and Smith (1975) obtained flow profiles by using a model extruder with "Perspex" barrel with aqueous polyvinyl-pyrrolidone solutions. The aluminum particles and coloured dyes were injected and streamlines were observed by video recorder. Later on these streamlines were traced during frame by frame video replay of the tape.

In a single screw extruder the helical flow fluid is fully developed and is essentially the same at all sections along a uniform screw filled with melt. In contrast to this, the essentially closed nature of the chamber in twin screw leads to a flow field of a fully three dimensional character as is clearly established by experiments (Jewmenow and Kim 1973; Janssen and Smith 1975). Because of the great influence of the flight walls a well defined zero velocity layer exists in the chamber dividing fluid moving in opposite directions. Since the flow near the intersecting area cannot readily be analysed numerically, Janssen (1978) investigated it by flow visualisation with colour injection and video recording. To simplify the complex situation he used a disc model and from this he formed a "where to/where from" balance over a cross section of the chamber related to the converging side of the screw ( Fig.2.4). Janssen (1978) also carried some work with real screws by decolouration experiments (i.e. first extruding a coloured compound through extruder followed by extruding a colourless compound) and found that bottom volume mixes very slowly with the bulk of the chamber. Such mixing as does occur is produced mainly by rotation of the processing fluid in the X-Y plane. So he concluded that only if the calender gap was relatively wide, is fluid from this region drawn into this gap where it is sheared and



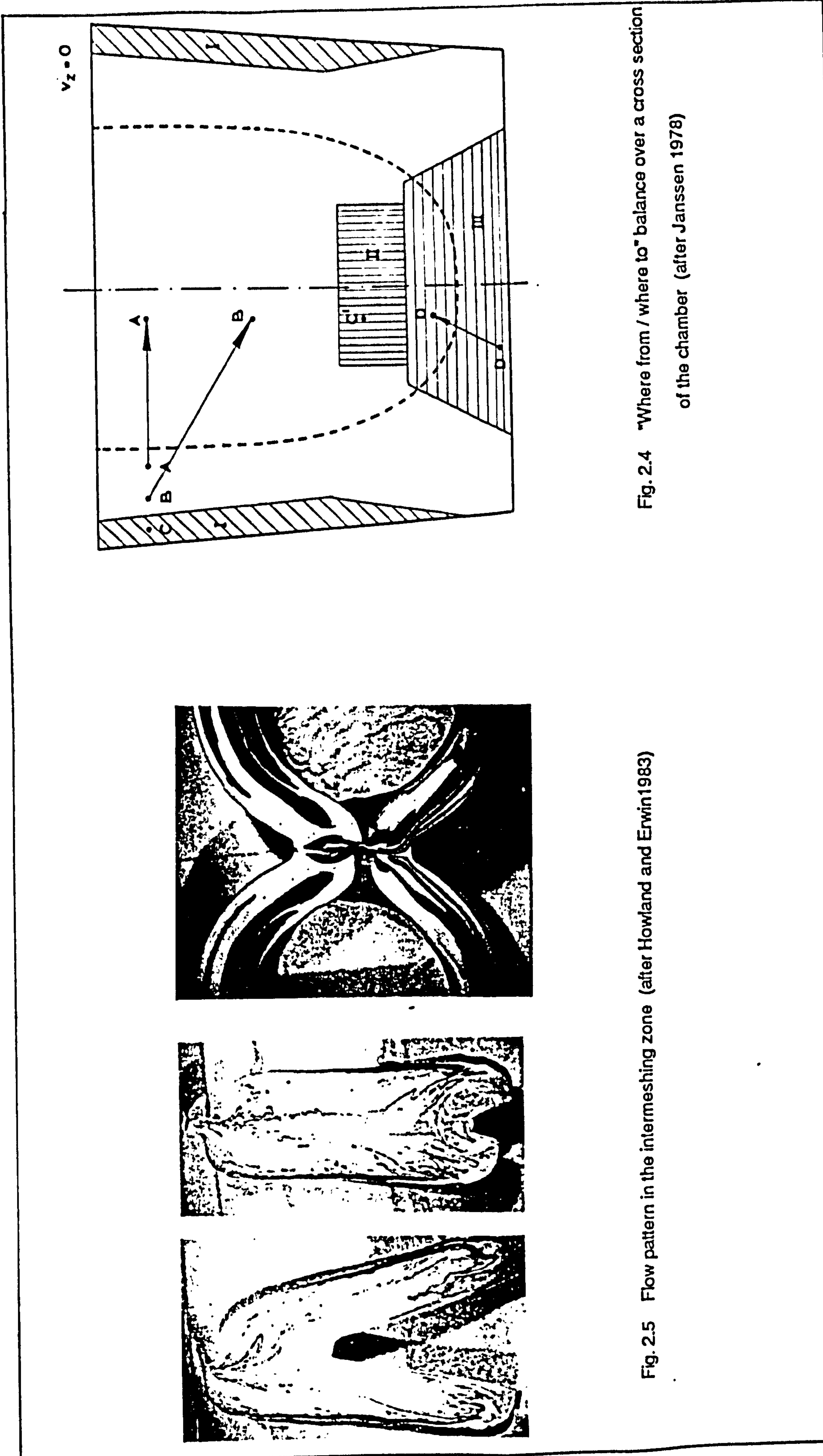


Fig. 2.5 Flow pattern in the intermeshing zone (after Howland and Erwin 1983)

Fig. 2.4 "Where from / where to" balance over a cross section of the chamber (after Janssen 1978)

then mixed with that in the rest of the chamber.

Kim et al (1975) used a twin screw extruder with soft PVC and aluminum powder. The dielectric constant of samples taken out of the C shape was measured and the mixing calculated using a variational coefficient. So they showed that in the middle of the chamber the variational coefficient was much higher than near the intermeshing zone indicating better mixing at the intermeshing zone. Janssen (1978) also carried out work on the interaction between the chambers for four conditions based on the large or no significant calender gap coupled with either a large or small back pressure, during processing.

Howland and Erwin (1983) carried out work on a counter-rotating tangential, non intermeshing twin screw extruder by pumping pigmented curable silicone fluid, curing the fluid and analysing it. In this, the extruder was always operated in a completely filled condition. From these transverse sections, they studied the presence of various flow patterns in sections (Fig 2.5) and also discussed the method to quantify distributive mixing in a transverse plane. As regards the flow mechanism, they showed a backward flow regime in the region created by the flight sweep. This flow then moves in the intermeshing zone, just behind the flight. This flow then penetrates and forms reoriented region across the depth of the channel. This, they showed contributes towards distributive mixing.

Bigio and Erwin (1985) studied the distributive mixing, in a similar study to that described above, in self wiping corotating twin screw extruder. They carried out the experiments by pumping optically pigmented curable silicone fluid, curing the fluid and analysing it. They found that the standard conveying elements provided no

reorientation of laminar stratiform. Therefore, while distributive mixing could be obtained in local regions by use of kneading block arrangements, it was not effectively applied over large sections of the extruder screws.

Sakai et al (1987) studied the flow patterns inside an interchangeable model twin screw extruder (both in co and counter-rotating). They reported that the intermeshed counter-rotating shows a figure of eight shape whilst the flow in co-rotating extruder takes place around the two screws just like as if there is only one oval single screw axes.

Hornsby (1987), while this thesis was in its manuscript form, has reported the flow and mixing in a small co-rotating twin screw extruder. This work is quite interesting one as the extruder on which the work was done, was designed as a result of the current thesis work. The extruder used had a 40mm screw diameter and operated at considerably higher screw speeds than GKN Windsor 250, the extruder used in the present work. He has reported the possible flow paths from where the flow can take place. These possible flow paths are illustrated with the help of section of the polymer screw skeleton. However no proof for such flow paths was given. Further he has shown the presence of two flow regimes in the section of the chamber.

As discussed above, the longitudinal part of the distributive studies can be studied by residence time distribution.

## 2.2 RESIDENCE TIME DISTRIBUTION

2.2.1 Concept of Residence Time Distribution : The longitudinal mixing in an extruder can be conveniently described by studying the

flow of material through it with respect to time. The flow of material through an apparatus can be described by two ideal situations, plug flow and perfect mixing. In a perfect mixer all the elements are perfectly mixed (in longitudinal direction) before leaving the vessel while in plug flow, no longitudinal mixing takes place. However, the extruder never fully satisfies these requirements. Some designs can be considered ideal with negligible errors, whereas other cases deviations from the ideal can be considerable. These deviations can be caused by channelling of fluid through the apparatus, by the recycling of the fluid within the apparatus (backflow) or by the existence of stagnant regions or pockets of fluid in the apparatus.

A knowledge of the flow path taken by the fluid elements in an apparatus (as described above) helps prediction of the exact behaviour of the apparatus. This could be easily deduced if the complete velocity distribution over the range were known. However, in the case of twin screw extruders, it is rather difficult to get precise information regarding velocity distributions. So the other, rather simple, approach is applied concerning the time duration for which individual particles stay in the apparatus. This is described by the term residence time distribution.

This concept of mixing in terms of residence time distribution is valid only in a single component, homogeneous system and is related to the degree of backmixing in a system. This is the mixing that occurs in the primary flow direction i.e. the randomisation occurs in the direction of flow and not transverse to the flow direction ( as discussed before). It differs from the mixing concept in a two component system involving a major and minor component where scale and degree of mixing are studied. In practical application flow through an

apparatus always results in a certain residence time distribution.

Fluid elements entering the apparatus simultaneously will generally leave it at different times. The distribution in residence time can be described quantitatively with two distribution functions which are closely related, viz. the E and the F function. (Bird et. al. 1960).

A. Exit age distribution ( E Function): It is the measure of the distribution of ages of all elements of the fluid stream leaving an apparatus i.e. age distribution of elements at exit or leaving the apparatus. The fraction of the material in the exit stream with residence time between  $t$  and  $(t + dt)$  is given by  $E \cdot dt$ . Since the total area under the E function is by definition equal to unity therefore,

$$\int_0^{\infty} E \cdot dt = 1$$

In practical terms, the exit age distribution curve can be measured from a pulse tracer input signal as stimulus and monitoring its response as output signal i.e. concentration ( $c$ ) as a function of time at a downstream point (Fig 2.6). Since the total area under the E curve function is by definition equal to unity, the concentration readings are normalised for a time invariant system with a constant throughput. This can be done by dividing the concentration in the output by the total amount of tracer injected.

$$E(t) = \frac{c(t)}{\int_0^{\infty} c(t) \cdot dt}$$

where  $c(t)$  is the tracer concentration at the output at time  $t$ .

However  $E(t)$  is dependent on the time. The dimensionless E curve is obtained by plotting  $E(\theta)$  against  $\theta$ .

$$\text{Where } \theta = t/\tau$$

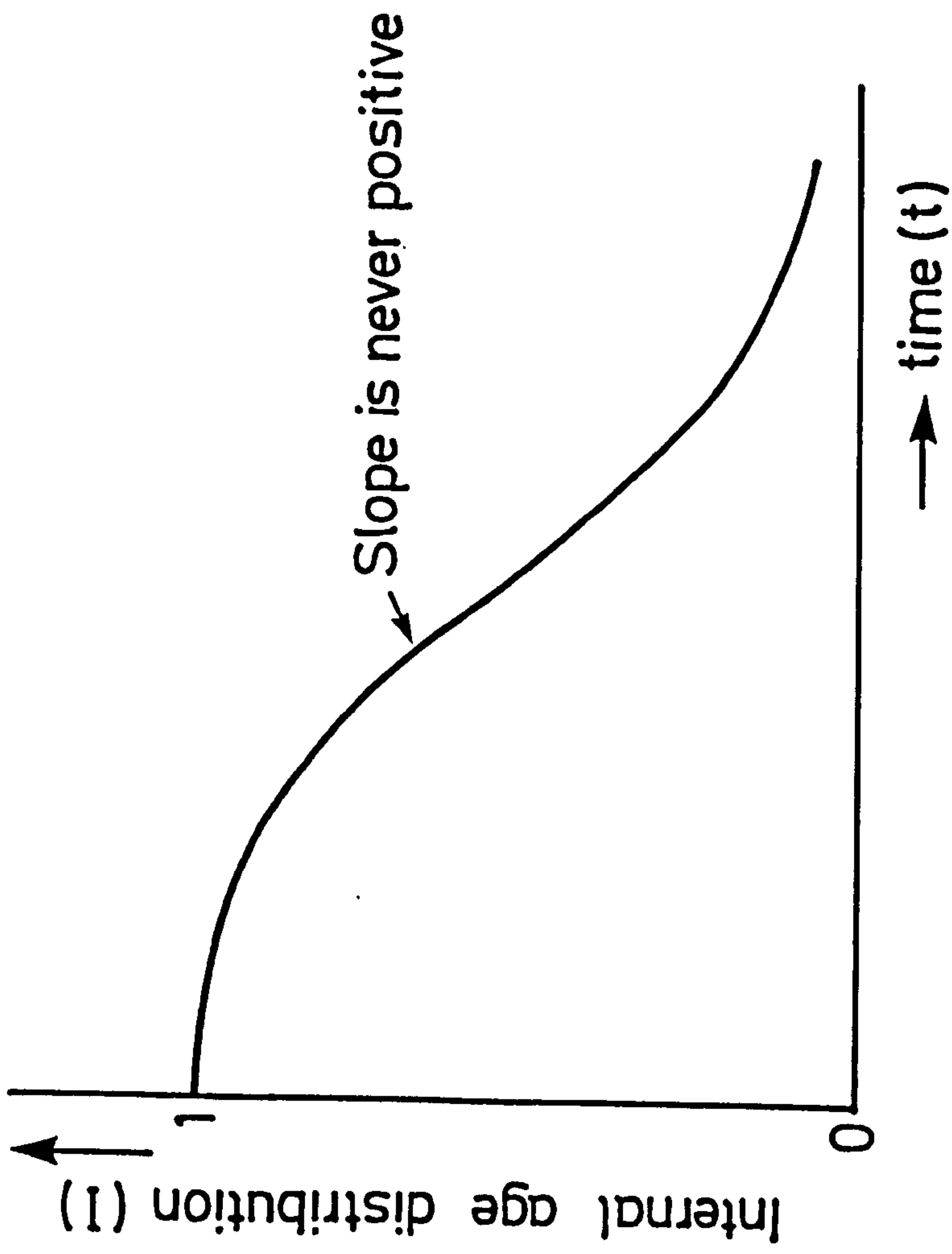


Fig. 2.7 Typical internal age distribution curve

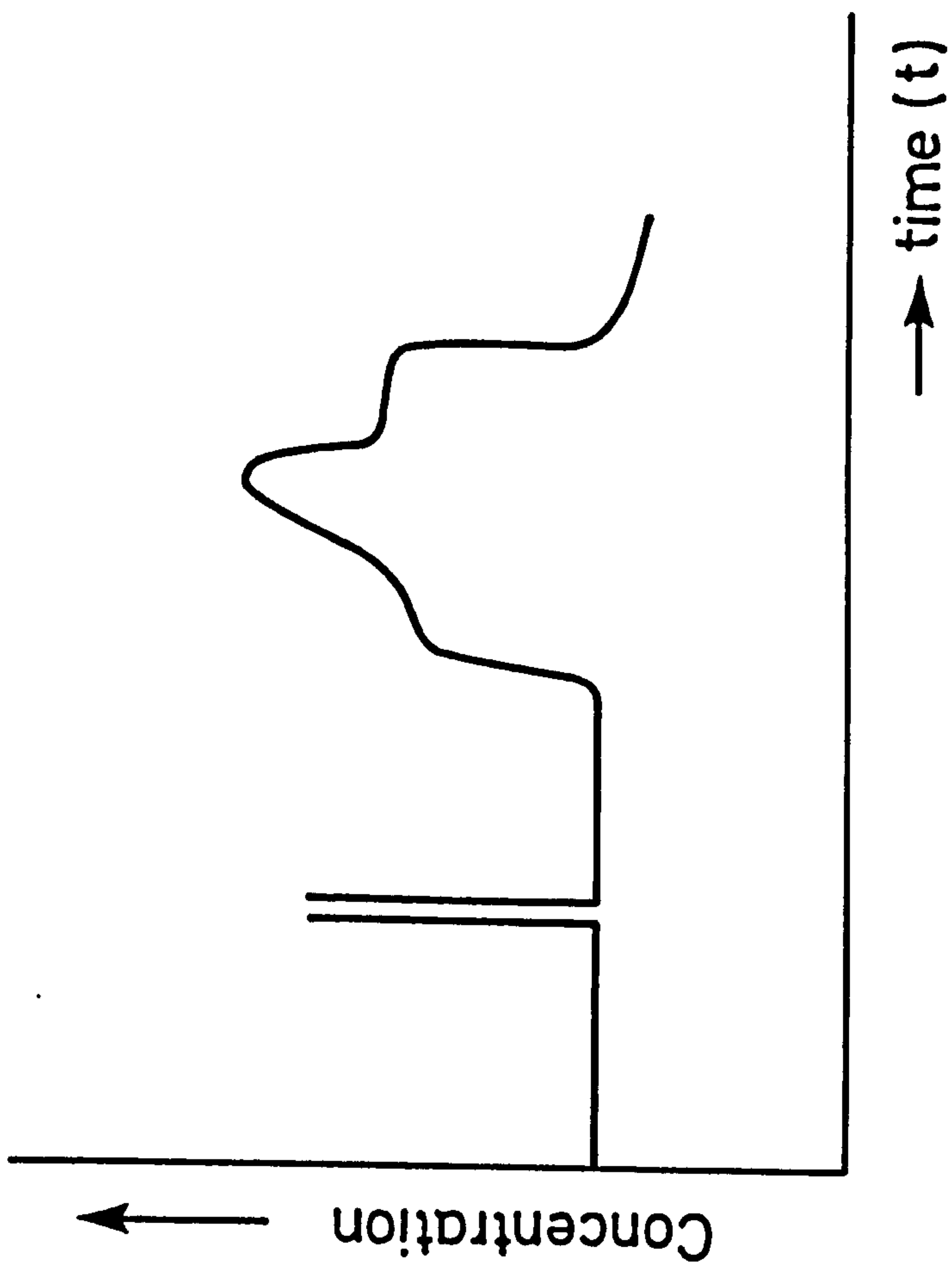


Fig 2.6 Pulse tracer response in a system

Where  $\tau$  is mean residence time. It can be calculated from either

$$\tau = \int_0^{\infty} t.E(t).dt \approx \sum_0^{\infty} t.E(t).\delta t$$

$$= \frac{\sum t.c.\delta t}{\sum c.\delta t}$$

or from

$$\tau = \frac{V_f}{Q_v}$$

where  $V_f$  is the filled volume of the apparatus and  $Q_v$  is the volumetric throughput rate.

B. Internal age distribution: It is the measure of the distribution of ages of the fluid in the apparatus. The symbol  $I$  is a measure of the distribution of ages of the fluid in the apparatus defined in such a way that  $I.dt$  is the fraction of the material with ages between  $t$  and  $(t+dt)$ . Since the sum of all the fractions of the material in the vessel is unity, this sum must also be the total area under the  $I$  versus  $t$  curve. Thus

$$\int_0^{\infty} I.dt = 1$$

A plot of  $I$  against time  $t$  is given in Fig 2.7, as being a typical internal age distribution curve. The advantage of the RTD in integral form is that RTD's of different machines can be readily compared on a one to one basis.

Experimentally this can be obtained by one of the following methods:

(i) By step tracer stimulus: With no tracer initially present in the entering fluid stream, a step signal of concentration  $c_0$  is imposed on the fluid stream entering the apparatus. Then the

concentration-time curve at the apparatus outlet, measuring tracer concentration in terms of inlet tracer concentration and measuring time in reduced units, is called the F curve. I is related to F by following relation:

$$1 - F = I$$

So from the above curve it is easy to get an internal age distribution curve.

(ii) By pulse tracer stimulus: As described earlier in above section 2.2.1.A, the E function can be readily deduced by pulse tracer stimulus. From E function, internal age distribution is calculated by the following relationship

$$F(\theta) = \int_0^{\theta} E(\theta) \cdot \delta t$$

Or better still  $1-F(\theta)$  can be derived from basic principles

$$1-F(\theta) = 1 - \int_0^{\theta} c \cdot \delta \theta$$

While  $c(t) = \frac{c}{c_0}$

$$= \frac{c}{\int_0^{\infty} c \cdot d\theta} = \frac{c}{\frac{1}{\bar{t}} \int_0^{\infty} c \cdot dt} \quad \text{Eqn 1}$$

$$\text{So, } 1 - F(\theta) = 1 - \int_0^{\infty} \frac{c}{\frac{1}{\bar{t}} \int_0^{\infty} c \cdot dt} \times d\theta \quad \text{Eqn 2}$$

However as  $E(\theta) = E(t) \times t$

The equation 2 becomes

$$1 - F = 1 - \int_0^{\infty} E(\theta) \cdot d\theta$$



2.2.2 RTD functions in some model systems: The two extreme flow systems, with respect to the RTD are the plug flow system, which exhibits no RTD and the continuous stirred tank, which exhibits complete back mixing.

A. Plug flow: Elements of fluids which enter the apparatus at the same moment move through it with constant and equal velocity on parallel paths and leave at the same moment. Thus there is no axial dispersion and no RTD.

Therefore, the 1-F curve is described by

$$1 - F = 1 \quad \text{for } t < \tau$$

$$1 - F = 0 \quad \text{for } t > \tau$$

and for the E curve

$$E = 0 \quad \text{for } t \neq \tau$$

B. Perfect mixer flow: A perfect mixer is a vessel in which stirring is so effective that the composition of its contents is identical at all places. The effluent from this vessel has the same composition as its contents.

1 - F curve is described by

$$1 - F = e^{-\theta}$$

and for the E curve

$$E = e^{-\theta}$$

It cuts the ordinate  $\theta = 1$  at  $1/e$  and its initial slope is unity. As shown above, both external and internal RTD functions are identical.

C. Laminar flow in a circular tube: In this case residence time distribution is caused by the differences in velocity and by diffusion. By neglecting the effect of diffusion a relationship can be derived.

For any streamline with velocity  $v$  and residence time  $t$

$$\frac{v}{\langle v \rangle} = 2 \times \left( \frac{1 - r^2}{R^2} \right) = \frac{\tau}{t} = \theta$$

Because the maximum velocity at the centre is twice the mean velocity, both E and F functions are zero for

$$\frac{v}{\langle v \rangle} < 2 \text{ and } \frac{t}{\tau} < 0.5 \text{ respectively}$$

All the above RTD functions, together with some extreme results from the present work, are shown in Fig.4.17.

2.2.3 Advantages of knowledge of RTD: The knowledge of RTD is quite useful as it gives the information on the following:

(a) Cleaning efficiency of the machine: The channelling of fluid or the existence of stagnant pockets are to be guarded against since they always result in decrease in performance. Recycle flow is usually undesirable too, the exception to the rule being certain complex reactions and most autocatalytic and autothermal reactions.

(b) Thermal and deformational history of material through machine: RTD quantifies the above histories experienced by the polymer system during processing and thus it is useful for material requiring closely controlled melt history.

(c) Type of flow in machine: This could play an important part in the design of the machine e.g. most transfer and reaction processes are executed more efficiently under plug flow than under perfectly mixed conditions. A narrow RTD may be essential to limit further widening of molecular weight distribution (MWD) in polycondensation or broad RTD

is required when mixer task is primarily blending of the different constituents and damping of the feed irregularities.

(d) It gives an experimental verification of theoretical model for flow for the extrusion process.

(e) Basis for scale-up: It could be used as a guide to the development of specific equipment and to provide the basis for scale-up where effects of reaction, diffusion and heat transfer are coupled together.

2.2.4 Limitation of RTD data: Residence time is governed by the flow pattern or the path along which the particles move. It does not give any indicative difference in microscopic or macroscopic scale mixing i.e. RTD by itself can not predict whether elements of fluids with same residence time can be considered well mixed.

The particles following the different flow paths can appear at the same time at exit thus giving similar residence time functions. So RTD analysis should be regarded as only supporting evidence on the validity of the proposed reactor flow model.

2.2.5 Method of monitoring RTD: It could be monitored experimentally using stimulus-response technique in which stimulus is applied to system and its response to stimulus is monitored. The stimulus can well be a tracer input signal to the apparatus. It could be a random, cyclic, step or a pulse signal. But for the ease of analysis and because of the close similarity in shape between the output signal and age distribution function, only the pulse signal is commonly used. It involves introduction of tracer as a pulse or delta function and its response is monitored, as shown in Fig 2.6

The tracer system must have the following characteristics.

- (a) A rheological response nearly identical to that of the process stream.
- (b) Be stable in the process environment.
- (c) Should have a large and reproducible response with concentration.
- (d) It should have a linear relationship in response and concentration.
- (e) It should be effective at low concentration which would also satisfy the requirement of a short and instantaneous pulse.
- (f) It should respond slowly with temperature and pressure.
- (g) The detection system must be sensitive, precise, stable and be easily calibrated.
- (h) It should be preferably "visible" throughout the extrudate.

#### TRACER SYSTEMS

Tracer systems have been used extensively in chemical engineering over the years and cover a wide range of techniques. However an extensive survey has been made and only those tracer systems, which could be applicable in extrusion process are discussed here. The advantages and limitations are also summarised in tabulated form.

3.1 METHODS USED FOR RTD DETERMINATION: This is summarized in the table form.

No	Property used as tracer	Equipment/Method used	Material used	Advantages	Disadvantages	References
1	Weight	Ashing of polymer Weighing the inorganic filler	TiO <sub>2</sub>	Cheap, easy to use. Does not require specialist equipment.	1. Long, time consuming process. 2. Applicable to compounds with no inorganic fillers. 3. Higher concentrations required - does affect rheological properties.	Adams (1974)
2	Physical appearance	Microscopic - Physically counting	NaCl crystals in poly-ethylene	Exact, cheap and simple to use. Does not require complicated equipment.	Extremely long and time consuming process.	Kemblowski and Sek (1981)
3	Colour	a) Calorimetric b) Spectroscopy in IR, visible and uv light	Methylene Blue, p-naphthol benzene	Visual monitoring possible while test is in progress (with visible light range only).	1. Limited to optically transparent and thin cross section extrudates. 2. More complex equipment required in polymer system. 3. Non linearity of absorption with concentration. 4. Difficult to monitor at very low concentration (e.g. in tail region of RTD curve), although it is accurate up to 1% concentration.	Bigg + Middleman (1974) Todd (1975) Janssen & Smith (1975) All in model fluids Sebastian & Bicsenberger (1984)
		c) Infra red spectroscopy with IR absorbers and multiinternal reflection		Can be used for opaque extrudates of any thickness.	Only small surface region is analysed. Same limitations as 2-4 in Ja.	

No	Property used as tracer	Equipment/Method used	Material used	Advantages	Disadvantages	References
4.	Conductivity	Measuring increase in electrical conductivity	MnO <sub>2</sub> , KNO <sub>3</sub>	In the detection range normally experienced conductivity is linear with concentration.	It is useful in model systems only. In polymer (plastics) it is of limited use as it depends on other variables (e.g. thickness) which are difficult to control precisely.	Todd & Irving (1969) Todd (1975)
5.	Dielectric		Conductive carbon black, Barium Titanate	1. This is a continuous on line method thus once fitted, should give a number of results rapidly 2. Tracer introduced does not affect melt severely.	1. Capacitance and dielectric is not linear with concentration in the range used. 2. Technique is not very sensitive, as even at 2% concentration (by volume) there is about 0.15% concentration variation on total conc. (about 10% of net concentration). 3. Have to be calibrated for different temperature pressure, deformation condition etc. Even calibration may not apply as because of non uniformity of temperature of extrudate.	Golba J.C. (1988)
6.	Magnetic	Measuring voltage change as relative permeability of core changes.	Iron powder	1. This is a continuous on line method thus rapid result production for various runs. 2. Does not have to calibrate for various temp etc. (unlike dielectric).	1. Complicated due to difference in rheological response between iron filled polymer and normal polymer. 2. Potential intensification of degeneration reaction can take place in presence of high surface area metal powder.	Werner & Eise (1979)
7.		X-ray fluorescence	Antimony oxide, Cadmium selenide	1. Being bright red in colour (cd. selenide) it allows visual following of test.	Requires expensive equipment and special knowledge.	Reumondal (1981) Walt (1982)
8.	Acoustic	Acoustic velocity	Fillers with high elastic modulus	1. Being continuous on line method.	1. Uses specialist equipment, techniques etc. 2. Could be affected by air pockets etc.	Lim et. al.

No	Property used as tracer	Equipment/Method used	Material used	Advantages	Disadvantages	References
9.	Radio-activity	γ-ray counter γ-ray spectroscopy	MnO <sub>2</sub> Cu <sub>2</sub> Cl <sub>2</sub>	<ol style="list-style-type: none"> <li>1. Relatively low radioactivity is required. So less tracer quantity is needed thus similar rheological properties to that of polymer.</li> <li>2. Quick and thus once set up, could generate results for various runs.</li> <li>3. Non destructive.</li> <li>4. Extremely sensitive and accurate</li> <li>5. It does not require transparent material.</li> </ol>	<ol style="list-style-type: none"> <li>1. Extraordinary precautions required in handling of radioactive species.</li> <li>2. Relatively expensive.</li> <li>3. The availability of nuclear reactor facilities and specialist equipment needed for its determination.</li> <li>4. The non trivial calibrations and analysis required to generate RTD curve.</li> <li>5. Polymer system should be free from other ingredients otherwise.</li> </ol>	Zwillichem et al. (1973) Wolf and White (1975 & 1976).
A.		ON-LINE MEASUREMENT (By introducing radioactive tracer in the extruder)		<ol style="list-style-type: none"> <li>1. It is safer than above (9A), as no radioactive material is involved at processing stage. Later on after activation, samples can be processed in a restricted lab area.</li> <li>2. Samples from tail region can be kept large in comparison with those used for peak determination.</li> <li>3. Counting time is not restricted by extrusion velocity.</li> <li>4.-5. Same as above 4+5.</li> <li>6. By this method 4 ppm of Mn in polymer can be detected.</li> </ol>	<ol style="list-style-type: none"> <li>1. It is time consuming and long process.</li> <li>2. Relatively higher tracer quantities required.</li> <li>3. It is destructive testing.</li> <li>4.-7. Same as above 2.-5.</li> </ol>	Wolf & White (1976) Janssen (1976) Schott. (1978)
B.		OFF-LINE MEASUREMENT (By introducing tracer in the extruder and later on activating in nuclear reactor and analysing).				

Amongst all of the techniques discussed above, two tracer techniques were used in this work. These being ashing and radioactive tracer techniques. The radioactive tracer technique was selected because of its accuracy, sensitivity and its flexibility in sample size etc.. Furthermore, because of sensitivity, only a small amount of tracer is required. The small tracer concentration in the polymer does not alter the flow behaviour significantly and thus helps to deduction of the "real" flow behaviour.

#### Review of radioactive tracer technique

A brief account of basic activation theory and its application to present work is described below:

Basic Theory: The basic principle underlying the neutron activation method is that when stable isotopes are irradiated with neutrons, they may give rise to radioactive products as a result of nuclear reactions. The unique characteristics such as the half life and spectrum of the radioactive isotope produced, permit identification of the isotope. The amount of induced activity is proportional to the mass of isotope present in the original material.

The disintegration rate  $I_A$  induced at the end of irradiation time " $t_i$ " and measured at subsequent time " $t_t$ " after the end of irradiation is given by the equation. (Kruger 1971).



$$I_A = \frac{N \sigma \phi W}{3.7 \times 10^7 M} \times \left[ 1 - e^{-0.693 \times t_i / t_{0.5}} \right] \times \left[ e^{-0.693 \times t_t / t_{0.5}} \right]$$

Where

$I_A$  = activity induced at the end of irradiation time,  $t_i$   
(disintegration. $\text{sec}^{-1}$ )

$N$  = Avogadro's number  $6.023 \times 10^{23} \text{ mol}^{-1}$ .

$\sigma$  = cross section of isotope to nuclear reaction ( $\text{cm}^{-2}$ )

$\phi$  = Neutron flux (neutrons  $\text{cm}^{-2} \text{ s}^{-1}$ )

$A$  = Natural abundance of active isotope (fraction)

$W$  = Weight of irradiated sample (g)

$M$  = Atomic weight of the element.

$t_i$  = Time of irradiation (sec.)

$t_{0.5}$  = Half life of produced isotope ( $\text{Mn}^{56}$ ) (sec.)

$t_t$  = time elapsed from end of irradiation (sec.)

There are great difficulties in measuring the exact weight of the irradiated sample as  $\sigma$  is often not known with great accuracy,  $\phi$  is difficult to measure exactly and it is not always easy to determine the absolute disintegration rate. It is for these reason that a comparative analysis is usually carried out. The details of the technique are discussed in section 3.2.2.

**2.2.6 RTD studies in extruders:** The measurement of polymer flow through processing apparatus, in terms of its RTD can provide useful information concerning mixing and conveying characteristics, of the machinery. In addition it can give information regarding the shear and thermal history of the material. This approach has been adopted for many years, for example, in general chemical engineering studies for determining mixing efficiencies in steady flow reactors or blenders. But only in relatively recent times has RTD technique been applied to

polymer processing equipment. RTD functions may be derived and analysed from theoretical principles where appropriate flow models are available, as in the case for single screw extruders (Pinto and Tadmor 1970; Bigg and Middleman 1974). But often direct experimental methods have been employed, especially in twin screw extruders. This is because the conveying mechanism in twin screw extruders is quite complex and difficult to describe by theoretical analysis. The known theoretical analysis of twin screw extruders considers only highly idealized cases of simple geometry, polymer flow properties and operating conditions. The practical applicability of most of this work is quite limited. Besides, twin screw extruders have additional geometrical design parameters.

However RTD studies in extruders can be conveniently divided between single and twin screw extruders.

#### A. RTD studies in single screw extruders

(i) Review of theoretical work: Pinto and Tadmor (1970) derived RTD theoretically, assuming an isothermal Newtonian flow model between parallel plates with no leakage flow. However their model does not predict the influence of process parameters on RTD. But they showed that the channel curvature does influence RTD. This model was extended to a non-Newtonian power law model fluid by Hirschberger (1972) and also by Bigg and Middleman (1974). Sek (1979) proved on the basis of the papers by Roemer and Durbin (1967), Kim and Skathkov (1979) and Tadmor and Klein (1970), that the RTD in an extruder may depend on the leakage flow and radial temperature distribution.

(ii) Experimental (in real systems): Experimental measurements of RTD in both melt and plasticating extruders were carried out by Wolf

and White (1975) who developed a sensitive radioactive tracer technique for RTD measurements and reported a good agreement between experimental and theoretical results.

Schott and Saleh (1976) investigated effect of variables on RTD in 38mm single screw extruder. The variables studied included screw speed, die length, pressure, melt index of polymer, addition of blowing agent and the effect of motionless mixer elements. A radioactive tracer technique was also used. The detailed conditions used are not included in the paper therefore it is of limited practical use.

Kembloski and Sek (1981) investigated RTD in industrial single screw extruders (both in melt and plasticating extruders). The RTD curves were quantitatively characterised using three calculated parameters including dimensionless variance (measure of spread of distribution). The investigation was limited to finding the dependence of dimensionless variance of RTD on dimensionless volumetric output and Reynold's number for which a correlation was found. They concluded that RTD of the material in an extruder depends mainly on the flow mechanism in the melt conveying zone. It was found that resistance to flow through die head of the extruder is important from the RTD point of view, as well as other parameters like screw speed and screw channel depth. Sebastian and Biesenberger(1984)investigated RTD and transverse mixing simultaneously on the same sample, using a colour intensity measurements technique.

## B. RTD studies in twin screw extruders

(i) Theoretical work review : As described before,theoretical work

on twin screw extruder has been extremely limited. Janssen et. al. (1979) made a computational model based on a series of ideally mixed chambers. They assumed that leakage flows in a pump zone have most influence on the residence time. In first three zones, plug flow is assumed. The model further assumes that each chamber is perfectly mixed with the incoming leakage flow in each revolution. This model shows a good agreement with the experimental values of residence time. The mean residence times are within reasonable limits independent of operating changes. However the theory and experimental show differences in RTD when plotted on log-linear scale in the tail region. This shows that the material in the C shape chamber is not ideally mixed.

Werner and Eise (1979) studied conveying characteristics in kneading elements and developed a model based on a number of ideal mixers which is related to RTD spectrum by an axial mixing coefficient.

(ii) Experimental work review: The work done on experimental RTD determination can be conveniently divided into two sections.

a. Model systems.

b. Real systems.

a. Model systems: The work included in this category is the one in which model fluid and/or model devices were used. Todd and Irving (1969) measured RTD in a co-rotating extruder with glucose solution. RTD was determined by an electrical conductivity method.  $\text{KNO}_3$  and  $\text{NaNO}_3$  were used as tracers. They compared the twin screw geometry incorporating a mixing device called the Poly-con. Poly-con can be best described as a series of length of co-rotating paddles of elliptical section, effectively operating as a twin screw extruder with a low positive displacement forward transport. They characterised the

mixing process from a Peclet number (Peclet number is ratio of the back and forth movement compared to the average transport). It can be calculated by multiplying average linear velocity and mixer length and dividing the product by eddy diffusivity - Todd & Irving 1969).

They found that the axial mixing was greater for the continuous twin screw arrangement ( $Pe < 6$ ). It was concluded that Peclet number was independent of feed rate at a constant screw speed. Increasing screw speed from 100 to 200 rpm decreases the Peclet number from 6 to 3. The study overall indicated only minor effect of throughput and screw speed and an overwhelming effect of screw configuration on axial mixing.

Todd (1975) measured RTD in a 101 mm diameter co-rotating extruder with polybutene using methylene blue as a tracer. The technique used to determine RTD have particular attention to the determination of the tail of the distribution curve. The effect of various screw configurations, feed rate, screw speed and viscosity were studied on RTD. It was concluded from this study that the effect of viscosity will be particularly important if the axial distance over which material can be pushed is great provided the time for this spreading is sufficient. Very little axial mixing can be achieved with very low helix angle and with straight paddles. But with helix angles intermediate between the above two, the degree of axial mixing is greater than for either extreme. With straight paddles residence time is not inversely proportional to screw speed, as it is with helical screws. In this paper cumulative RTD curve is plotted on log-probability paper. Janssen (1978) comments on these results that if these data are presented in log-linear co-ordinates, they would show a kink, thus showing two different flow regimes.

Janssen and Smith (1975) reported experiments in a counter-rotating extruder with a PMMA barrel. A step change from clear PVP (polyvinyl pyrrolidine solution) to PVP coloured with methylene blue was imposed and RTD obtained optically. The effect of calender gap (gap in between the flight tip of one screw and screw land of other screw) and die pressure on RTD studied. It was found that the usual response of output concentration to a step change in input concentration when plotted with log-linear co-ordinates shows a kink. This reflects at least partial segregation of fluid passing through the extruder and by implication a limited amount of mixing within the chambers. Only when a wide calender gap, is the kink not significant, suggesting that this geometry is most suitable for good homogenisation.

Kim, Skatschkow and Stungur (1978) have reported experiments in a co-rotating extruder with a viscous medium. Sakai (1981) reported experiments in transparent non intermeshing and intermeshing counter rotating twin screw extruders. The silicone oil was used as a polymer melt model and RTD was studied using an emission diode - glass fibre conductor - photo transistor. The RTD studies were carried out to analyse the effect of various mixing elements designs including pinned, pin full flight screws, continuous rotors, discontinuous rotors etc. A clear dependence of flow behaviour on the mixing element geometry was found.

Kao and Allison (1984) studied RTD in a fully intermeshing co-rotating twin screw extruder (Werner Pfleiderer ZSK 30 type). They studied various variables including throughput, screw speed, barrel temperature. The two screw designs were also studied: one containing four kneading block mixing sections, and the other consisting only of

regular screw bushings. They concluded that although screw configuration was an important variable, for both the configuration the throughput had the largest effect on RTD followed by screw speed whilst barrel temperature change had no effect.

b. Real systems : This category includes the work carried on the polymer melt and extruder devices. Janssen et al. (1979) carried out work on a Pasquetti extruder of 47.7 mm screw diameter and 360 mm effective screw length. This extruder fits in the cylindrical, counter rotating, intermeshing twin screw category. The polymer used was polypropylene and RTD was determined by means of a radioactive tracer technique using manganese dioxide ( $MnO_2$ ) as tracer. The reproducibility of the tracer technique was investigated in detail and special attention was given to the tail of the distribution curve. The effect of die pressure, screw speed and temperature on RTD characteristics were studied. The tail of the RTD becomes shorter at high die pressure while no significant correlation was found for effect of variation in screw speed. They concluded that extruder type studied has remarkably stable RTD characteristics. The results were compared with that of a single screw extruder, an empty pipe and with a theoretical model in which chambers in the extruder are assumed to be well mixed. It was found that a plasticating twin screw extruder does not differ very much from the distribution calculated for a single screw extruder.

Werner and Eise (1979) studied conveying characteristics of a 28 mm diameter Werner & Pfleiderer extruder. This extruder fits in the high speed, co-rotating, self-wiping, intermeshing twin screw category. The polymer used was low density polyethylene and RTD was determined by a relative permittivity method using iron powder as tracer. The effect

of screw speed, throughput rate and different screw designs having different pitches and different width of kneading discs were studied. From these, the degree of fill was calculated and correlation was determined with material transport in the screw and kneading elements. The conveying characteristics of screw and kneading elements were compared by calculating a conveying factor ( $\mu$ ). They showed that kneading disc combinations have lower conveying factor values than screw elements. The conveying factor and, therefore the actual conveying velocity at constant screw speed, increases with an increasing degree of fill.

Kim et al. (1980) studied RTD in a co-rotating extruder with polymer media. Rauwendaal (1981) carried out the evaluation of co- and counter rotating extruders. He studied 28 mm diameter Werner & Pfleiderer extruder, which fits in the high speed, co-rotating, intermeshing twin screw category and 34 mm diameter Leistritz LSM 30.34 of the cylindrical counter-rotating intermeshing twin screw type. The polymer used was high density polyethylene (HDPE) of melt index of 0.2. The RTD was determined by using antimony trioxide as tracer and the concentration of the tracer was measured by X-Ray fluorescence. The effect of throughput and screw speed on RTD characteristics was studied. It was found that both forms of machines show better positive displacement characteristics at high throughput rate and low screw speeds, however, overall the counter-rotating facility showed better positive displacement. A dramatic increase in residence time and widening of RTD occurs when the throughput is reduced to low values, which results in a correspondingly large increase in specific power consumption. The minimum residence time, throughput and specific power consumption are shown to be closely related. In these studies a proportionality is found between throughput and mean



residence time suggesting that the fully filled length of the extruder varies only slightly with changes in screw speed or in throughput.

Walk (1982) carried out experimental work on a non intermeshing counter-rotating twin screw extruder (5.08 mm - of Welding Engineers) using PMMA (of melt flow index of 1.2) as feed material. The tracer used was cadmium selenide, with concentration monitored by an X-Ray fluorescence technique. The effects of screw speed, feed rate, barrel temperature and finally screw configuration on RTD characteristics were studied. The variance of RTD curve and filled volume was calculated. The experimentally determined cumulative distribution curve was compared to various flow models. The studies concluded that a mathematical model combining the equations for plug flow and perfect mixing is a good description of RTD of the extruder studied. The model provides a value, the fraction of plug flow, which can be used to evaluate different screw configurations. The value is independent of operating conditions such as screw speed, feed rate or barrel temperature.

Nichols et al (1983) carried out RTD studies on non intermeshing twin screw extruder. They showed that the mean residence time varied approximately linearly with the inverse flow rate, with deeper channels yielding longer residence times. It was also shown that the mean residence time increased markedly as the screw speed was decreased, with the greatest increase occurring approximately 100 rpm.

Sakai et al (1987) carried out work on model and real twin screw extruders. They analysed the melting behaviour in real extruders and concluded that in non intermeshing twin screws, melting behaviour is very similar to that of single screw extruder. But in case of

intermeshing twin screw extruders, a distinct solid bed and melt pool regions in the channel do not exist, but are intermingled. Further in the model extruder it was shown that the stagnant layer on screw surface, generally present in single screw extruder, is absent in twin screw extruders and co-rotating extruders show a broader RTD as compared to counter-rotating twin screw extruders.

2.2.7 Interpretation of RTD curves: Once RTD has been obtained, it can then be quantitatively described with two distribution functions which are closely related, the E and the F function. However, different researchers, over the years, have tried to get more information from it, basically from the point of applicability in polymer extrusion. Some of them are described below with their relative merits.

(1) Hold back area: It is a measure of degree of positive conveying. It is the difference in area from  $t/\bar{t} = 0$  to  $t/\bar{t} = 1$  between pure plug flow and the actual age distribution curve.

$$A_h = 1 - \int_0^1 F(t/\bar{t}) \cdot d(t/\bar{t}) \quad (\bar{t} = \text{average residence time})$$

However it gives indication of majority of polymer flow and does not describe the tail of distribution curve (Rauwendaal 1981).

(2) Self cleaning number: This number describes the self-cleaning ability of the extruder. It can be calculated from RTD curve as follows.

$$\frac{s}{t} = b - w/t$$

where  $s$  = self cleaning time

$t$  = average residence time

$b$  = width of spectrum

$w$  = distance from turning point describing the longitudinal mixing.

The distance between points of inflection indicates axial mixing whilst the width is influenced by the extent of stagnation (Herrmann and Eise 1981). The self cleaning number for the various residence time spectrums are generally between 2.5 and 5 for polymer melts. This varies depending on product and operating conditions.

(3) Blending efficiency ( $\beta$ ): It is a measure of dispersion in the primary flow direction and is similar to the Peclet number. It can be calculated as follows

$$\beta = 1 - \frac{\Delta A_1}{\Delta A_2}$$

where  $\Delta A_1$  = area between a perfect mixer and mixer in question

$\Delta A_2$  = area between a perfect mixer and a plug flow device.

(4) Dimensionless variance: It is a measure of the spread of the distribution about the mean. It can be calculated as

$$\sigma^2 = \frac{\sum t^2 C}{\sum C} - \left[ \frac{\sum t C}{\sum C} \right]^2$$

As  $\theta = t / \bar{t}$

and therefore,

$$\sigma_{\theta}^2 = \frac{\sigma^2}{\bar{t}^2}$$

For the idealized cases of plug flow and perfect mixing flow, the dimensionless variance takes the value 0 and 1 respectively. For a real systems  $\sigma_{\theta}^2$  varies in range  $0 < \sigma_{\theta}^2 < 1$ . The value of dimension-

less variance enables the evaluation of the deviation of the flow investigated from the limiting cases of plug flow and perfect mixing flow and an approximate comparison of different distributions. For this reason it is used in the present work.

5. Peclet number : This is a number relating the axial mixing in a system. A large Peclet number implies a low axial diffusion. The width or spread of the curve, relating tracer concentration and time, can be used as a measure of axial mixing.

Todd (1975) has suggested a method to calculate the Peclet number of a system. He solved an equation, interpreting the mixer as a semi-infinite column with dimensionless time. He solved one of the derived equations for various Pe numbers, and integrated with respect to  $\tau$  to provide cumulative distribution curves for these. By plotting the logarithm of the ratios of the emergence times for 84% and 16% of the tracer leaving the system against Peclet number, a plot was obtained. From this plot, the determination of the Peclet number becomes a problem of curve matching. A value of Pe greater than 10 represents a case of predominantly plug flow. Further details of this procedure can be found elsewhere (Todd 1975).

2.2.8 Residence time distribution models : As discussed before, there are two ideal flow behaviour, viz. plug flow and perfect mixing. However the conditions in an extruder are neither that of perfect mixing nor of plug flow. So several investigators have suggested various models. Some of those models are described as under.

1. Plug flow number : The flow in extruder does not follows the idealized flow. So the flow can be described by the combination of

these idealized flows, e.g. by seeking the fraction of the flow which follows the ideal flow - say plug flow (Wolf and White 1976).

It can be described as

$$F(\theta) = 1 - e^{-\left[\frac{1}{1-p}\right] [\theta - p]} \quad ; \theta > p$$

$$F(\theta) = 0 \quad ; 0 < \theta < p$$

2. Tank in series : The tanks in series model considers that the screw flights divide the screw into a number of separate chambers equal to the number of turns in the screw (Levenspiel 1972).

$$E(\theta) = \frac{N (N\theta)^{N-1}}{(N-1)!} e^{-N\theta}$$

If N (number of tanks) equals to 1, the model for perfect mixing is obtained and when N equals infinity the plug flow is simulated. The cumulative distribution F(θ) is obtained by graphically integrating E(θ).

## CHAPTER 3. EXPERIMENTAL

This chapter covers in depth the details of the polymers, extrusion line and its operation. It also deals with the operating details of the tracer techniques used and finally with the description of variables studied. Finally it also covers the experimental details for determination of cross channel flow and transverse mixing.

### 3.1 CHARACTERISTICS OF MATERIALS:

The polymer used for the bulk of this work was a commercial injection moulding grade of polypropylene homopolymer in granular form - Propathene\* GW22M and its equivalent in powder form - Propathene GW522M. The injection moulding grade was chosen due to interest in the extruder's compounding application. However, some work was carried out using extrusion grade of polystyrene in granular form - Lustrex\*\* HF66 EX The physical properties of these polymers are tabulated in Table 4.6

The melt flow characteristics of these polymers were obtained using Davenport extrusion rheometer at 200<sup>0</sup>C (192<sup>0</sup>C for polystyrene) over a shear rate range of 100 to 3500 S<sup>-1</sup>. The polymer granules loaded into the barrel were preheated for 15 minutes under compression. A die of 1.04 mm diameter and L:D ratio of 38.3 was used. The pressure was measured using a Dynisco (5000 psi, approximately 35 MN/m<sup>2</sup>) pressure transducer. The flow curves so obtained are given in Fig 4.1 .

### 3.2 THE EXTRUSION LINE

3.2.1 Extrusion line's description : This work was done on GKN Windsor TS 250X co-rotating twin screw extruder. This extruder

---

\* Trade mark of I.C.I.

\*\* Trade mark of B.P. Chemicals

differs from the GKN Windsor TS 250 in being slightly smaller in screw diameter (100 mm instead of 105 mm) and is also slightly longer (  $l:d$  ratio of 17:1) . It was designed to allow for modifications and access to the screws. The screws are of a building block type. The first block is integrated with the shaft onto which various screw elements are mounted. The screw elements consist of further four blocks and five mixing discs segments. The screw elements are secured against turning by means of fitted keys and held on the shaft by means of a threaded screw tip. The twin screws are of the closely intermeshing type. An important feature of these screws are the segmented "mixing" discs (covered by British Patent BP 1264415 of 1972). The name "mixing discs" is a misnomer as these discs act both as melting and mixing discs. Sometimes they are named by their prime function. So when they are placed upstream it is referred as melting disc and when placed downstream, they are referred to as mixing discs. However for ease of convenience, these are hereafter referred to mostly as the mixing discs.

The screw consists of two sets of intermeshing mixing discs each rotatable with one of the screws and each having five axially spaced mixing discs. The perspective and details of mixing disc segment are given in Fig 3.1 . Each of these mixing discs has twelve circumferentially spaced gaps forming flow paths for the polymer melt. The mixing discs are adjustable relative to each other to vary the position of the gaps in the flanges of one mixing disc relative to the position of gaps in flanges of the other mixing disc. The details of various screw segments and settings and positions of mixing discs are shown in Fig 3.2 and 3.3 together with the details in Table 3.1 . The overall picture of the extruder is given in Fig 2.3.

**TABLE 3.1. SPECIFICATIONS OF GKN WINDSOR 250X.**

Direction of rotation	:	Co
Screw Diameter	:	100 mm
Centre Distance between two screws	:	85 mm
Flight Depth	:	15 mm
Length to Diameter Ratio	:	17:1
Screw Speed	:	up to 30 rpm (variable)-small pulley up to 60 rpm (variable)-large pulley.

**DETAILS OF SCREW SECTION**

	Length (cm)	Pitch (cm)	Flight (cm)	Land	Land * (cm)	Helix Angle
Feed Section	33.50					
Compression Section	17.78	3.175	0.635		1.27	21 <sup>0</sup> 7'
Devolatilization Section	34.93	3.81	0.965		2.54	15 <sup>0</sup>
Compression Section	36.83	3.175	0.635		1.27	21 <sup>0</sup> 7'
Metering Section	33.50	3.175	0.637		1.27	21 <sup>0</sup> 7'

**DETAILS OF MIXING DISCS**

Overall 5 pairs of mixing discs 12 slots -  
6.35 mm wide Equispaced slots with 3.175 mm  
radius.

Thickness of mixing disc = 13.3 mm.

Length of Mixing Discs.

For 3 short base M.D 28.57 mm

For 1 medium base M.D 44.45 mm

For one large base M.D 57.45 mm

Thus overall M.D length (set of 5) = 130.47 mm.

\* This is the length of screw section which is without thread.  
It is the total of length of both sides.



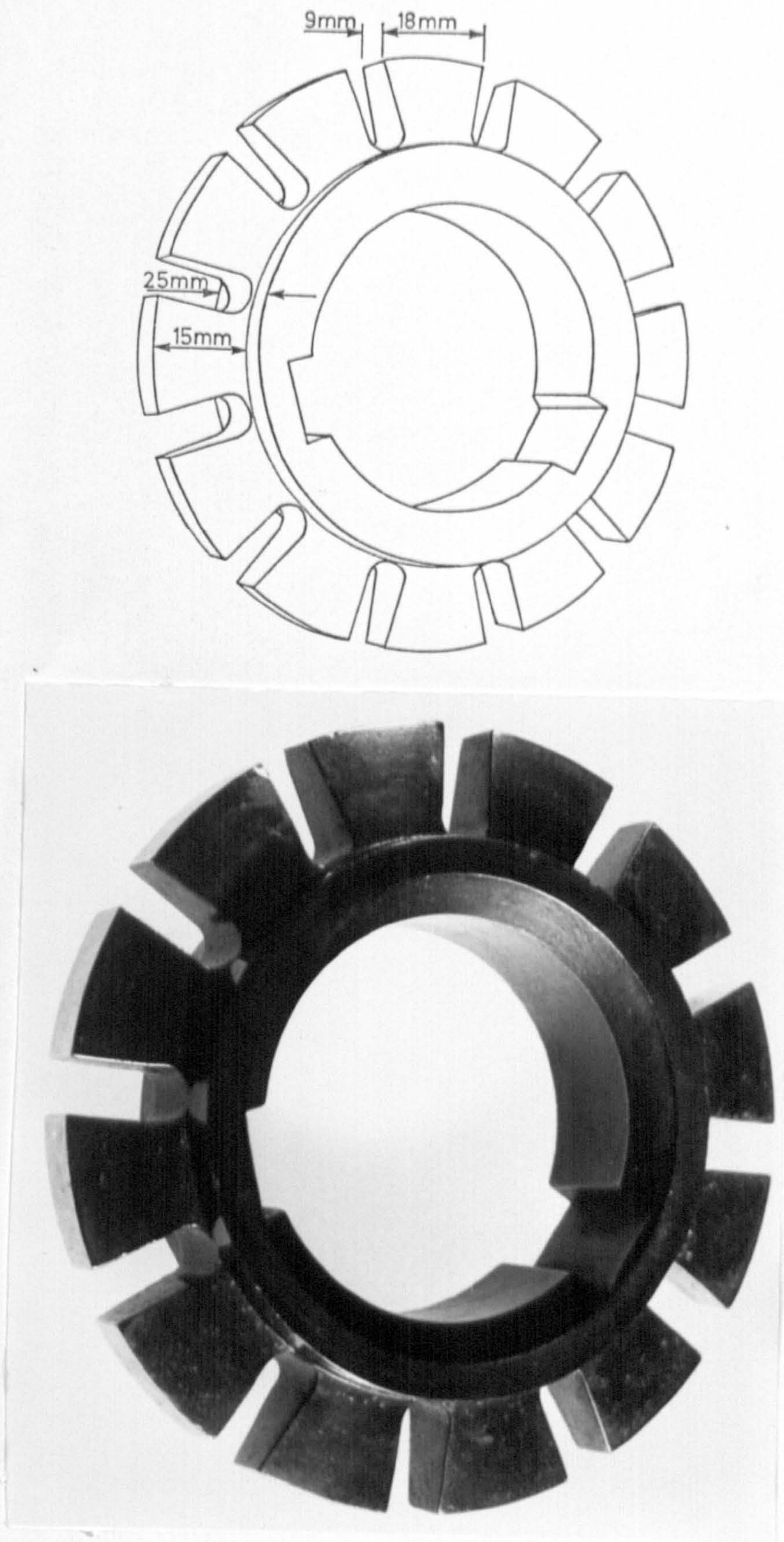
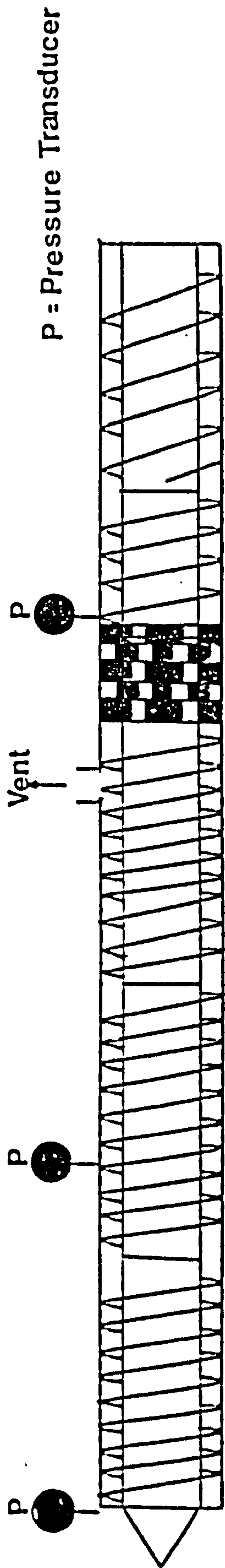
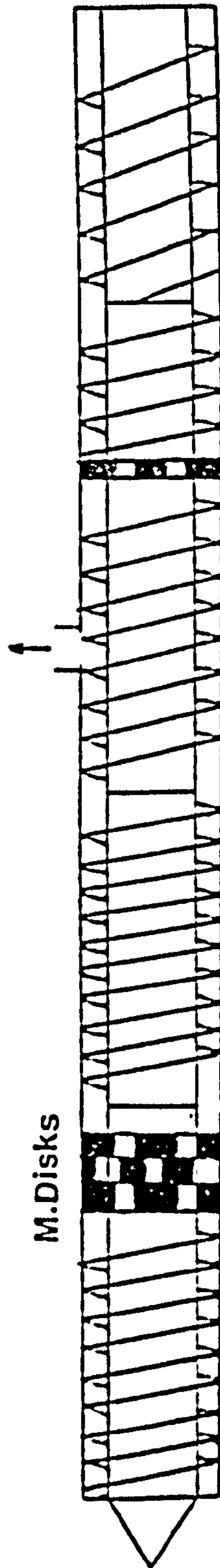


Fig. 3.1 A perspective of mixing disc segment



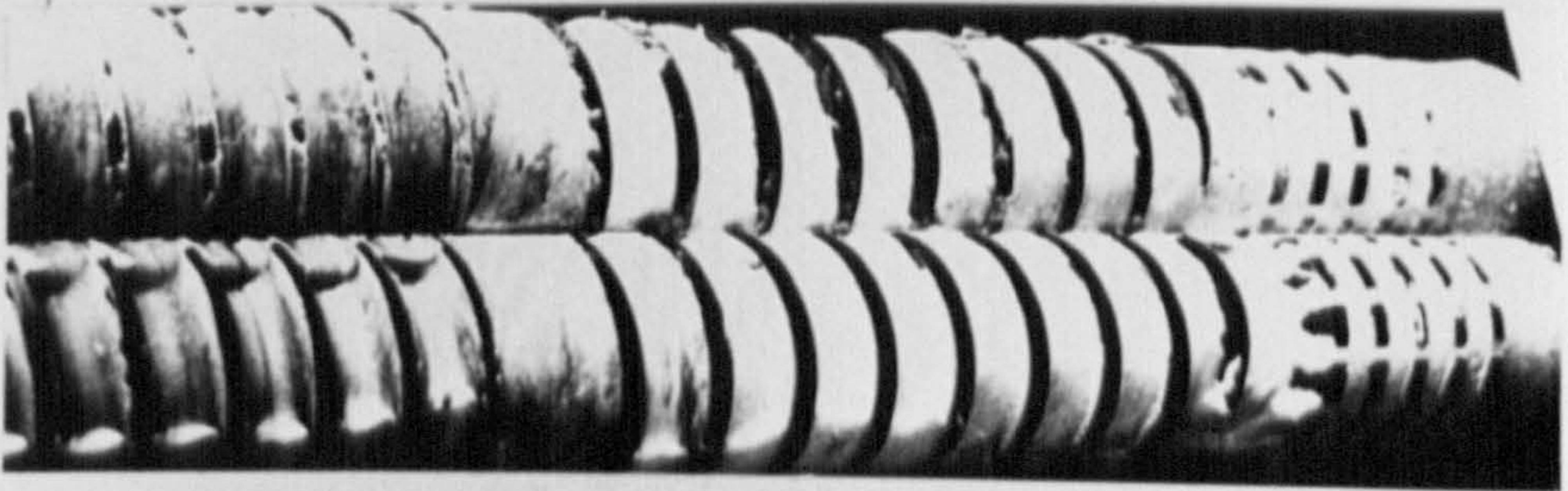
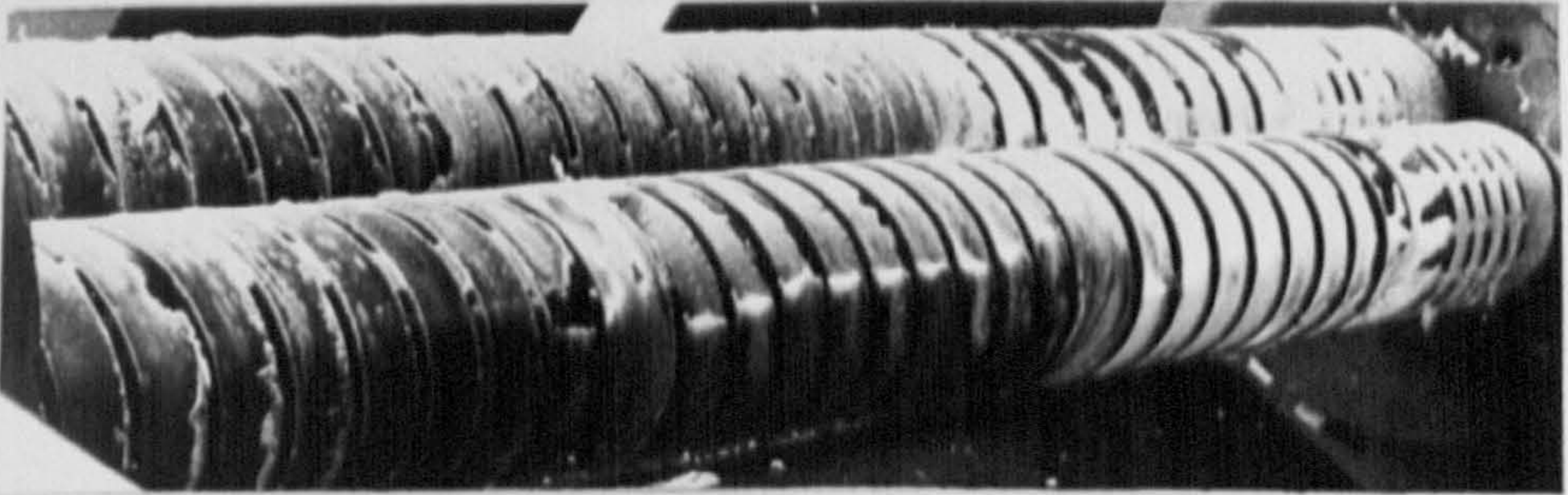
Upstream Mixing Disc Configuration



Downstream Mixing Disc

Fig. 3.2 Schematic diagramme of various screw segments and settings.

M.D. in 'Upstream Position'



M.D. in 'Downstream Position'

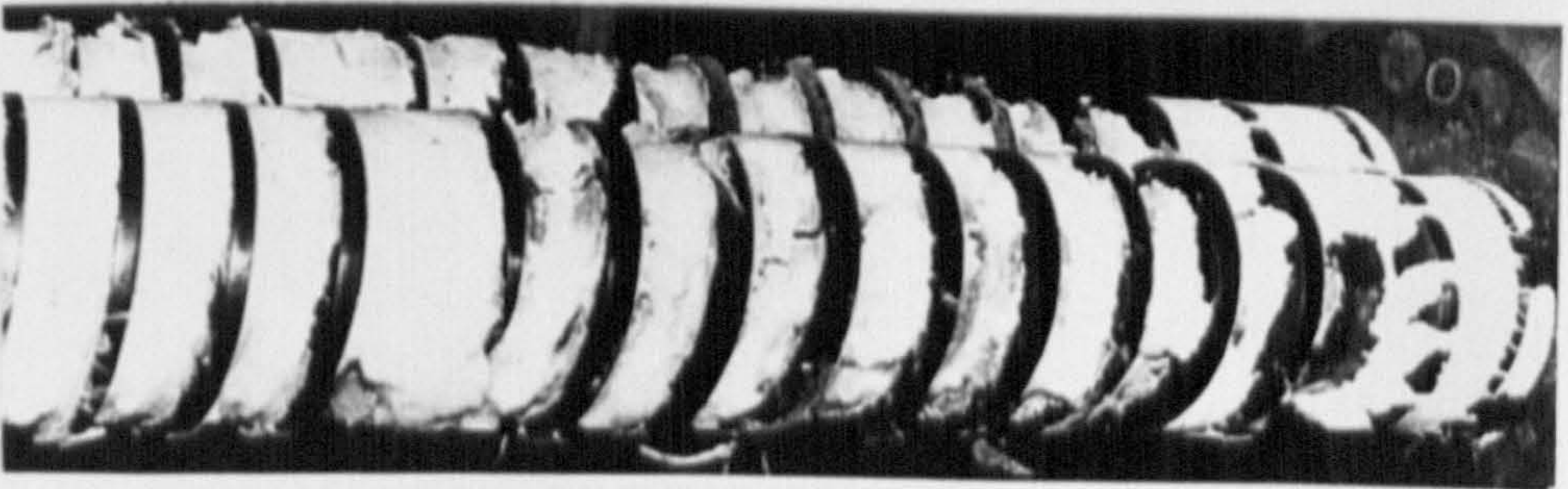
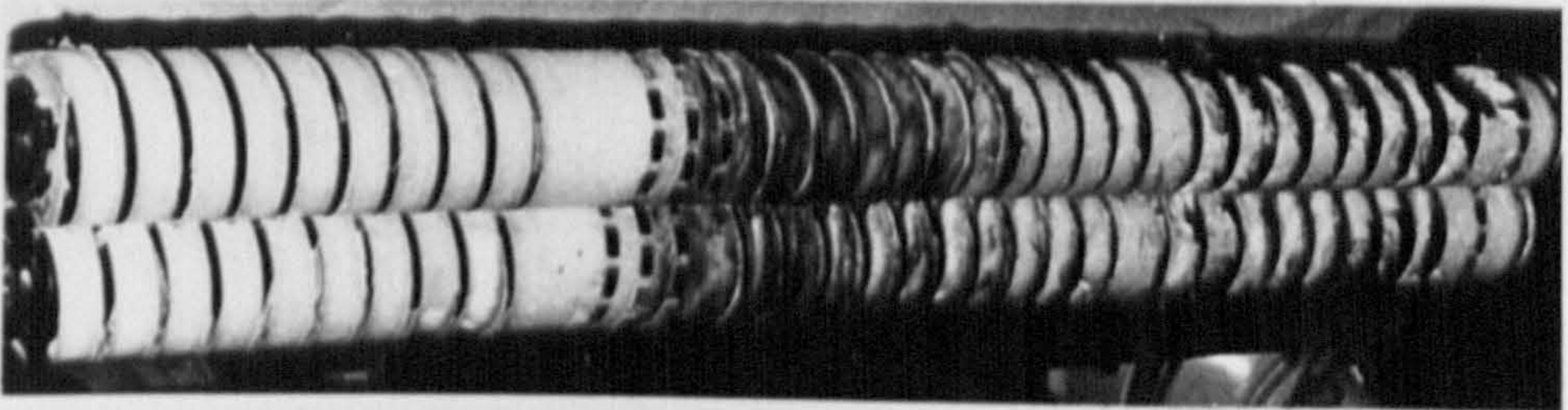


Fig. 3.3 Mixing disc positions in GKN Windsor 250X

The twin screw extruder line consisted of the following units. Twin screw extruder, a strip die, strip cooling bath, sizing plates, Floataire 165 mm capacity caterpillar haul off unit, and a Floataire 100 mm capacity travelling saw unit. The material was fed into the extruder by a volumetric feeder regulated independently from screw speed. Thus the amount of material fed did not change with screw speed. Flood feeding would result in overloading of the extruder drive, due to torque limitations. Three 0.5 tonne polymer storage bins and an automatic pneumatic conveying system were installed to cope with the supply of feed stock. The extruder had three holes located axially along the barrel and five holes in the adapter plate situated at the screw tip. The locations are shown in Fig 3.2 . Five Dynisco pressure transducers were installed in these holes to give pressure readings at various locations. The strain gauge attached to fly wheel at  $22^{\circ}$  angle gave a measure of screw torque and together with ammeter readings gave an indication of current input to mechanical drive of extruder. The temperature of the melt extrudate was measured using a thermo-probe (Digitrons model 2751-K).

3.2.2 Modifications to the extrusion line: The progress of the work was considerably slowed down due to the initial installation problems, associated delays and the extensive machine modifications and repairs done during the programme. The modifications included

- (a) The screw cleaning and stripping proved to be a very time consuming operation. The screw tips were modified to enable prestressing when fitting screw segments, which assisted in preventing the ingress of molten polymer between the segments.
- (b) A special support assembly was designed and constructed for barrel removal while extruder is filled with polymer - for shock cooling and barrel withdrawal experiments.

(c) A new larger pulley was manufactured to permit running at higher screw speeds. This necessitated raising the main motor platform by 50 mm to accommodate the existing Poly V belt drive.

(d) The clamp system of the "Floataire" 100 mm capacity travelling saw unit was adjusted and modified to cut 7.5 cm wide strips into short lengths which could then either be stored for analysis or granulated for recycling using a Cumberland granulator.

(e) Problems were encountered with overshooting of the barrel temperature during the start up. However, it was reduced by heating the extruder to initial preset low temperature followed by setting to the required temperature.

3.2.3 Operation: In all, about two tonnes of polymer was extruded on this machine during the course of this project. Due to the size of the machine, a long running time of the extruder was necessary to achieve steady state, e.g. it took approximately 2.5 hours at 9 rpm. The criterion used to establish the steady state was the stability in the temperature profile along the whole extruder. To save material, reground material feed was used initially e.g. say first two hours at 9 rpm. The extruder was kept scrupulously clean as the analytical technique used was very sensitive to contaminants. The hopper feed control was calibrated for the polymer feedstock used.

### 3.3 DETERMINATION OF RTD (TRACER TECHNIQUE DEVELOPMENT)

Two tracer techniques were used to determine the Residence Time Distribution characteristics of the extruder. Both the techniques were started at the same time, but the ashing technique being simpler, required shorter development time. The ashing technique gave initial trends in effect of various variables. i.e. qualitative effect of variables on RTD. However, as discussed later, the radio-active

technique was more accurate and sensitive, therefore it was extensively used to characterise the various conditions.

3.3.1 Ashing technique: This involved burning of the extrudate containing an inert inorganic filler collected at known time intervals and weighing the ash. This technique was chosen mainly for being cheap, easy to carry out, rather simple in principle, not requiring any special apparatus and expertise. The factors which dictated the choice of filler were the stability of the filler at higher temperature (used in the procedure to get rid of carbonaceous products), density of the filler and its effect on rheological properties of the polymer melt system. The density is important parameter as the higher density would give more weight for the same volume used, thus giving more accuracy to the detection.

#### A. Selection of tracer

In the present study silica and Barytes were chosen from a range of available fillers

(1) Silica: Silica (Gasil 35 - a product from Crosfield Ltd.) was initially chosen as tracer because of associated interest in project of silica dispersion in polypropylene by a co-worker. At the time it was thought that both investigations could result in establishing a relationship between degree of dispersion and RTD.

(a) Preparation of tracer compound: This was prepared by using an oil heated Joseph Robinson two roll mill (0.3 x 0.15 m) with even speed rolls. The front and rear roll temperatures were 170<sup>0</sup>C and 115<sup>0</sup>C respectively. First polypropylene granules were fed to the mill and on formation of a continuous band, silica (40 % by weight) in the

powder form was added to the melt. Cross blending was done to ensure concentration uniformity throughout the mix. The material was taken off the roll mill in approximately 1 mm thick sheet form. It was then granulated in a Cumberland granulator. The tracer compound so obtained was in the form of irregular shaped particles with dimensions determined by retention on a 4 mm screen. Very fine particles of this tracer compound were discarded.

(b) Heat stability of silica: A crucible was heated in a "Carbolite furnace at  $600^{\circ}\text{C}$  for 24 hours and then cooled to room temperature in a vacuum desiccator for 16 hours. The crucible was then weighed accurately and a known amount of silica was placed in the crucible. The crucible was then again heated for 8 hours at  $600^{\circ}\text{C}$  in the furnace. The crucible was cooled in a vacuum desiccator for another 16 hours and then weighed accurately to five decimal places. The silica tracer showed an overall loss of 7.3 % in weight. This could be due to some volatile present. However, on exposure to air for one hour it regained 0.34 % of weight.

However, due to considerable loss in weight at elevated temperature, and its comparatively low density ( $2100 \text{ kg/m}^{-3}$ ) form, it was considered necessary to use an alternative inert filler as the tracer.

(2) Barytes: Barytes (Fordabar ground barytes 200 mesh - a product from Wilfred Smith Ltd, High Street, Edgware) was also chosen as a tracer. This was done because of its inherent higher density ( $4200 \text{ kg/m}^3$ ), its inert nature and heat stability at  $600^{\circ}\text{C}$ . The barytes grade used contains approximately 92.7% barium sulphate, 2.05% silica and 0.49% iron ( $\text{Fe}_2\text{O}_3$ ).

(a) Preparation of tracer compound: It was prepared in the same manner as in the case of the silica tracer except front and rear roll temperatures were set at  $190^{\circ}\text{C}$  and  $170^{\circ}\text{C}$  respectively.

(b) Heat stability of barytes: The same procedure as described above for silica was used for ashing and the loss in weight after 8 hours of heating at  $600^{\circ}\text{C}$  was found to be 1.1 %. However, this weight loss remained the same even at an extended heating time of 24 hours.

(c) Flow curve of the tracer compound: The apparent viscosity - shear rate behaviour of barytes in polypropylene at 40 % by weight concentration was obtained using Davenport extrusion rheometer. Measurements were made at  $200^{\circ}\text{C}$  using the same procedure, as described in Section 3.1 and the flow curve is given in Fig 4.1 .

(d) Filler distribution in the tracer compound: The ashing of barytes compound (which is to be used as tracer) was carried out using the procedure described later (by the slow degradation method). The residue was weighed and found to be 40 % of the initial masterbatch weight thus giving an indication of uniform dispersion of barytes in the compound.

As a result of these observations, barytes was finally chosen as the preferred tracer, due to its inherent higher density ( $4200\text{ kg/m}^3$ ), its inert nature and heat stability at  $600^{\circ}\text{C}$  (only a loss of 1 % which also remains constant as compared to 7.3 % loss in the case of silica where this loss tends to change with humidity. Thus on exposure to normal atmosphere, the silica powder shows a gradual increase in weight as compared to when in vacuum desiccator).



B. Tracer inclusion and sampling procedure: Steady state extrusion was achieved and then 80 g of barytes compound (40 % by weight) was added. The initial samples were taken after the extruder had been running for a period coinciding with the minimum residence time (e.g. 8 minutes at 9 rpm screw speed), and samples were taken at appropriate intervals, ranging from 20 seconds to 2 minutes. Sampling was discontinued before the ashing technique's limit of detection. This was established experimentally, as discussed later. However, as the sampling duration is shown to have an effect on the result (Fig 4.8 ) the overall sampling duration in different runs was chosen to lie in 0.75 to a maximum of 5.0 units of dimensionless time. The samples were taken from the whole width of the strip. The effect of sampling position was studied by comparing samples from the centre and edges of the strip extrudate. The samples from the strip were cut in small pieces (about 2 mm) so as to be packed neatly into the crucible. The results quoted in this section were obtained following the slow degradation method (see later).

C. Ashing procedure: The concentration of tracer was determined in the samples from the output. This involved heating the samples to a temperature at which no carbonaceous residue remained, thus leaving inorganic inert filler. Two procedures were used to measure the tracer concentration.

(1) Direct burning off: This involved initially heating a set of crucibles in furnace at  $600^{\circ}\text{C}$  for 24 hours and cooling these at room temperature in a vacuum desiccator for 16 hours. The crucibles were weighed accurately and a known amount of sample in the form of small pieces was placed in crucibles. The crucibles were then placed in a furnace at  $600^{\circ}\text{C}$  for eight hours. During this time all the polymer

was burnt off and only barytes powder was left. The crucibles were then again cooled to room temperature in a vacuum desiccator for another 16 hours. The crucible and ash were then weighed accurately.

However, when the reproducibility of this technique was checked, it was found unsatisfactory. The cause of the above behaviour is thought to be the rapid burning off of the samples, thus some of the barytes and the burning polymer comes out of crucible together with the evolving flames.

(2) Slow degradation method: The procedure described above was used except the approach for burning off the samples. In this procedure the crucibles with samples were initially heated at  $380^{\circ}\text{C}$  for eight hours (slow degradation of the polymer) followed by heating at  $600^{\circ}\text{C}$  for another two hours (to burn off all the carbonaceous products). The initial degradation temperature of  $380^{\circ}\text{C}$  was determined experimentally as being the maximum temperature at which samples did not catch fire (below onset of ignition) or boiled over crucible while still degrading at relatively high rate. For this method a special ashing furnace "carbolite" was used which also had special venting facility.

This procedure is different and modified from the method described in ASTM D817-72. In this standard platinum crucibles are used, and it is suggested to burn off the samples directly over the flame.

This technique gives much more reproducible results compared to one in which the polymer containing tracer compound is heated directly to  $600^{\circ}\text{C}$ . The reason for this being that in the modified technique most of the polymer is slowly degraded and when the temperature is raised to  $600^{\circ}\text{C}$ , there is very little combustible material left and thus no

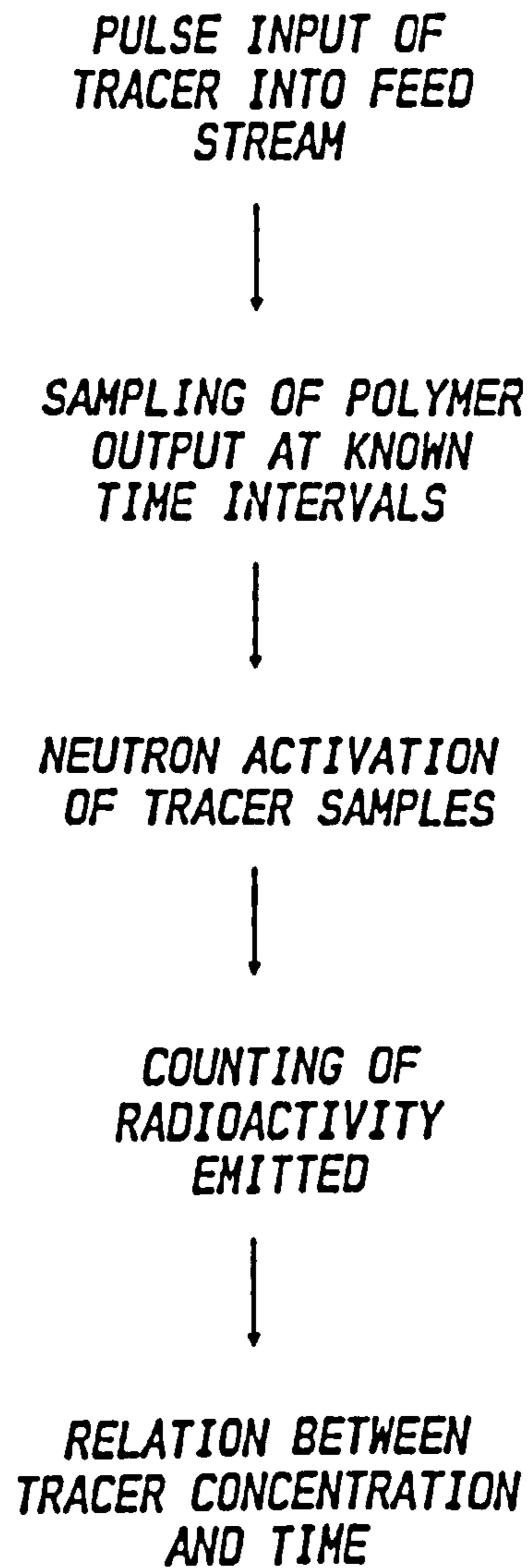
"swirling action" takes place.

The reproducibility of the technique using the above method was determined by taking samples adjacent to each other from the same extrudate. Furthermore the effect of magnitude of the final temperature reached in the ashing procedure, was also determined. The results are shown in Fig 4.4 . It clearly shows that relatively reproducible results are obtained using above method. The final ashing temperature (in between 500 and 600<sup>0</sup>C) does not affect the results substantially.

3.3.2 Radio-active tracer technique: This involved adding MnO<sub>2</sub> compound tracer to the polymer in the extruder, then irradiating the samples with thermal neutrons and determining the concentration of MnO<sub>2</sub> , by measuring the induced radioactivity. This technique is very accurate and sensitive and has been used by various researchers, Wolf and White (1976), Janssen (1978), in the past in the extrusion process. A schematic representation of steps involved is given in Fig.3.4.

The activity induced is proportional to the quantity of Mn present in the sample. Therefore, from equation of section 2.2.5, when other terms and constants are known, concentration of Mn tracer can be determined. But this has serious drawbacks as (i) the magnitude of activation cross section of the target element, i.e. Mn is not sufficiently accurately known. (ii) The flux may vary during the irradiation process. (iii) A self shielding correction must be worked out or be experimentally determined or else some procedure must be adopted to render self shielding effect negligible. (iv) The efficiency of the detector must be known. However, in RTD studies, only relative concentrations are required to calculate RTD curve, so

FIG. 3.4 DETERMINATION OF RTD BY NEUTRON ACTIVATION ANALYSIS



this procedure becomes quite simple as only count rates are taken. These count rates give a comparative concentration for various samples.



In the present study a considerable amount of work was carried out on the choice of procedure within the scope of this technique and in the choice of nuclear reactor etc (Hornsby et al 1985). Finally the reproducibility of the technique was also established extensively.

A.  $\text{MnO}_2$  as tracer: The tracer was prepared by adding 5 % by weight of  $\text{MnO}_2$  powder to polypropylene.  $\text{MnO}_2$  powder (Mallinckrodt Inc.) used was analytical grade and was minimum 99 % pure. The maximum limit of impurities are alkaline earth 0.2 %, chloride 0.01 %, insoluble in acid 0.05 %, nitrate 0.05 %, sulphate 0.05 %.  $\text{MnO}_2$  was chosen as a tracer because it ( $\text{Mn}^{56}$ ) has a short life of 2.5785 hours. The irradiation site was at a distance (approximately 80 kilometers). This half-life gave a sufficient cover for delay in transport and in counting while it also gave a reasonable residual activity as not to pose problems for disposal.

The procedure and conditions for preparation of masterbatch were the same as in 3.3.1.A . The apparent viscosity - shear rate behaviour of this compound was obtained using Davenport rheometer using same method as in 3.1 and results are shown in Fig 4.1 .

(B). Preparation and irradiation of specimens.

(1) Preparation of Specimens: 10 g of tracer containing 5 %  $\text{MnO}_2$  was introduced instantaneously at the feed port of the extruder. The samples of precise weight were taken from the centre of the extruded

strip at appropriate intervals ranging from 20 seconds to 2 minutes (described in detail in 3.3.1.B). The samples were then compression moulded in the form of discs of 21 mm diameter and 3 mm thickness. The mould consisted of three plates of dimensions 0.3 x 0.3 m. The two outer plates were thin stainless steel plates while central plate was a steel plate of 3 mm thickness having 25 equally spaced 21 mm diameter holes. The polyethylene terephthalate release film was used when moulding the specimens. The material was heated in the mould at  $170^{\circ}\text{C}$  for 5 minutes in electrically heated upstroke press (Moore of Birmingham) at contact pressure and then cooled under pressure in a water cooled downstroke press (Bradley & Turton) for 3 minutes. The samples were then neatly trimmed and accurately weighed.

(2) Irradiation of the specimens: The prepared specimens were systematically packed in a plastic tube (2.2 cm diameter and 65 cm long) with one reference disc (with known amount of  $\text{MnO}_2$ ) placed at the top and bottom ends. The prepared samples were irradiated with thermal neutrons in a Reactor at Atomic Weapon Research Establishment (AWRE) in Aldermaston. Two neutron fluxes ( $1.6 \times 10^{12}$  and  $3.2 \times 10^{11}$  neutron  $\text{cm}^{-2}$ ) were investigated for the effect of non uniform activation in beta and gamma ray counting. The details are given below under the heading of non uniform activation. However, because of the unavailability of the high neutron flux reactor, due to its higher usage, all the subsequent irradiations were done at lower neutron flux. Once the specimens had been irradiated, they were returned to Brunel University with minimum delay for counting of the induced radioactivity of  $\text{Mn}^{56}$  decaying to  $\text{Fe}^{56}$ .

(C). Errors associated in neutron activation analyses: There are various errors associated with neutron activation analysis. These

have been discussed by Kruger (1971). These errors can be broadly classified into three categories as shown below.

- (1). Errors associated with activation of sample.
  - (a) Flux inhomogeneities
  - (b) Neutron self shielding (pile effect)
  
- (2). Errors associated with measurement of activity
  - (a) Self absorption
  - (b) Specimen geometry
  - (c) Delay time
  
- (3). Errors associated with data counting
  - (a) Background correction
  - (b) Dead time correction
  - (c) Counting statistics

As the above errors can arise in neutron activation analysis, steps were taken either to make the factor ineffective by adjustment of parameters or to minimize its magnitude and make corrections for their effect. In the following paragraphs, the cause for these errors are discussed together with steps taken to minimize the errors.

- (1). Errors associated with activation of sample : From the neutron activation process, a non uniform activation occurs in the samples packed in the tube. This is considered to be due to the flux inhomogeneities in the reactor and the neutron self shielding of the sample along the tube. Both of these effects lead to a non uniform activation along the tube and are considered in detail as follows

(a) Flux inhomogeneities: The unperturbed flux in a reactor may be expected to be fairly constant under irradiation conditions although a spatial flux gradient may exist in the vicinity of an irradiation position. The flux gradient can be particularly large, so the irradiation position in nuclear reactor is chosen with an insignificant flux gradient. However, as discussed above, the spatial flux gradient present in reactor would lead to a produced activity gradient, i.e. a successive increase or decrease in activity amongst the samples with same concentration along the tube.

(b) Neutron self shielding: The material can absorb neutrons and thus the neutron flux becomes progressively smaller with its travel through material. However, this effect could lead to a non uniform activation if the position of tube in the reactor is such that neutrons travel through one end of the tube to the other end. In such a case, due to self shielding the neutron flux becomes progressively smaller and thus leads to a differential activation along the tube.

The effect of above two parameters on non-uniform activation was determined experimentally for two neutron fluxes ( $1.6 \times 10^{12}$  and  $3.2 \times 10^{11}$  neutron  $\text{cm}^{-2}$ ). The polypropylene samples containing 0.5 % w/w  $\text{MnO}_2$  tracer were packed in a plastic tube and after irradiation, were counted for gamma rays for each of the sample. After making all the corrections, the induced activity Vs sample position in tube was plotted (Fig 3.5). The higher neutron flux shows a straight line and shallow gradient while low neutron flux shows a non linear relationship with much steeper gradient. However due to a heavy work schedule the high neutron flux source was unavailable most of the time so it was necessary to use the low neutron flux. One sample with 0.5 % w/w of  $\text{MnO}_2$  concentration in polypropylene was placed at each



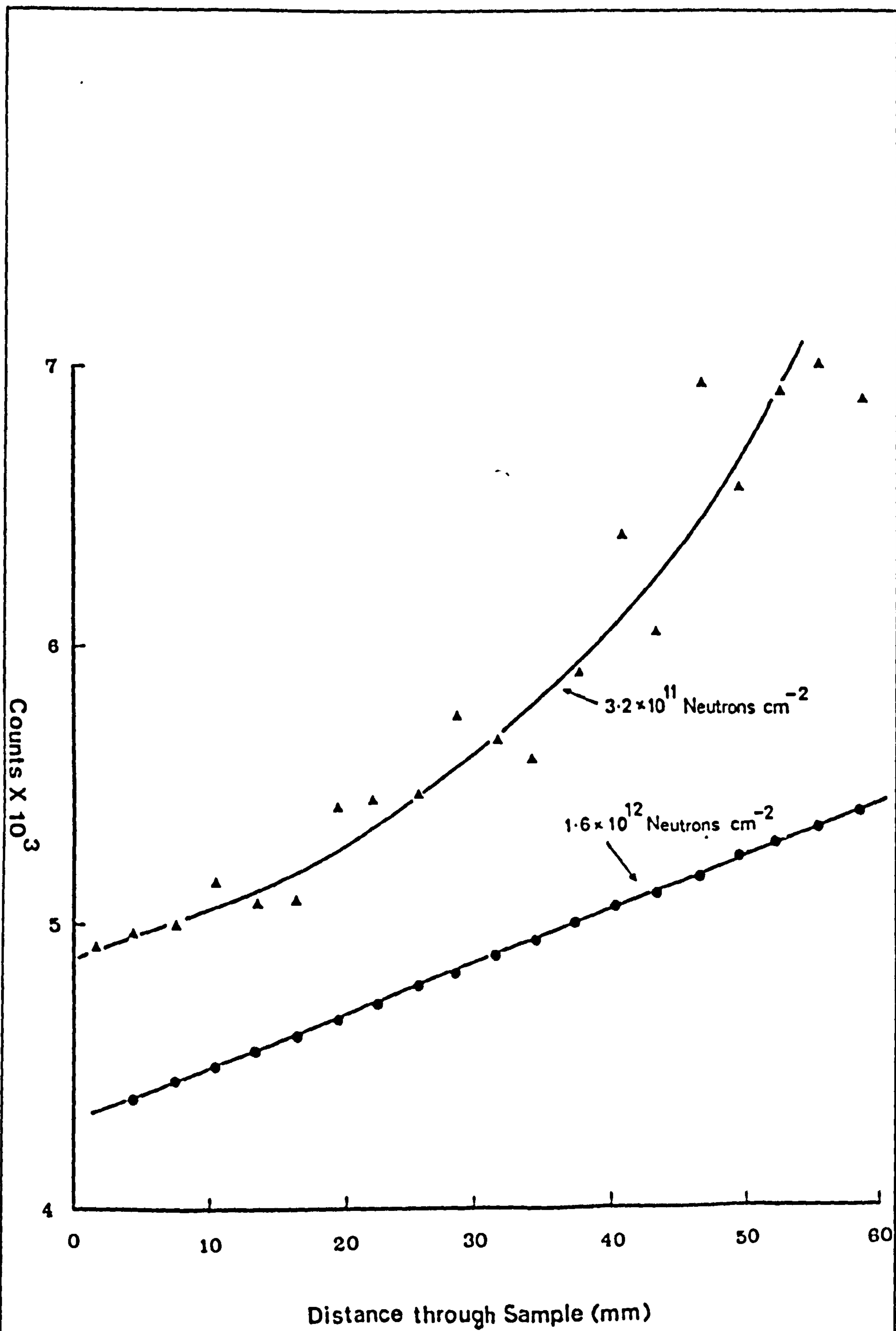


Fig. 3.5 Effect of neutron flux on neutron activation uniformity.

end of the tube so as to check the magnitude of correction which found to remain the same (as shown in Fig 3.5).

2. Errors associated with measurement of activity.

(a) Self absorption: The absorption and scatter of emitting rays in the sample itself can cause error. After certain thickness, the linear relationship in count rate and thickness, is not maintained and the count rate stabilizes for very thick sample. However, this self absorption should not present any serious error because this effect would be of the same degree in all the samples. The sample dimensions were kept virtually identical for all the tests.

(b) Specimen geometry: Radiations generally escape from the samples in all directions and only those particles actually directed towards the counter can be counted. So whilst counting, the sample shape, position, position of the probe and its shape, distance between probe and sample etc. are kept constant. This is done so that the same fraction of particles will always be counted. In other words measurements are made under conditions such that the detection coefficient, i.e. the ratio of measured activity to disintegration rate remains constant.

(c) Delay time: The radionuclide  $Mn^{56}$  decays with its characteristic half life after irradiation. So as to get a comparative induced activity, the induced activity of each sample is calculated at some fixed arbitrary time. At a time  $t$  from the arbitrary time its activity  $A_t$  is given by relationship

$$A_t = A \exp (-0.693 t/t_{0.5})$$

where  $t_{0.5} = 2.5785$  hours.

(3). Errors associated with count data.

(a) Background correction: Due to cosmic radiations, the counting system registers some of these counts. In scintillation counting system used, this is found to be about  $100 \text{ counts min}^{-1}$ . So when counting the radiations from the samples, these background counts are also counted. So to get the net counts, these background counts are subtracted from the indicated counts. The samples with low activity pose problems. Thus these samples give low count rate together with a high noise level of background and thus the net counts are statistically not very accurate.

(b) Dead time correction: All detectors of radioactive radiation have an inherent recovery time following interaction of a radioactive ray and during this period a second incident can not be recorded. This is of the order of microsecond for a scintillation counter. The measurement of the activity was performed using the live time mode of the pulse height analyser, this permits automatic correction of the count rate for dead time losses.

(c) Counting statistics: Due to the random nature of radioactive decay process, the relative statistical standard error ( $\sigma$ ) for the accumulated counts is given by the equation.

$$\text{Relative std.deviation } (\sigma) = \frac{\sqrt{N}}{N} = \frac{1}{\sqrt{N}}$$

where N is the number of counts counted.

The irradiation time of 7 minutes was calculated from equation of section 2.2.5 for the samples so as to get a high count rate range (say 100-20,000 counts  $\text{min}^{-1}$ ) so that higher counting statistics could be obtained.

(D). Techniques for analysis: The  $\text{MnO}_2$  (Manganese dioxide) tracer concentration was analysed by neutron activation analysis. The samples containing  $\text{MnO}_2$  were irradiated with neutrons.  $\text{Mn}^{56}$  decays by giving beta and gamma rays. The energy level constitution of beta rays are 2.838 MeV (47 %), 1.028 (34 %), 0.718 (18 %) and 0.30 MeV (~ 1%), and gamma rays have the energy levels 0.85 (98.87 %), 1.81072 and 2.113054. The concentration of Mn tracer could be determined by counting either of the two rays. Both of these have some merits of their own. Generally the choice of method of counting is based on the method giving the highest count rate with the greatest precision. The following counting techniques being evaluated in the present work especially from the point of view of reproducibility of the results.

(1). Gamma counting: The detection of the  $\gamma$  ray emitted by the active tracer was made with a sodium iodide probe and a scintillation discriminator counter (Canberra). All of the gamma rays emitted by the specimen were counted. The counting schedule adapted was such as to count less radioactive sample at the start and higher concentration specimens later. All the specimens were counted at constant geometry. This was achieved by fixing the detector in a horizontal position and placing the sample in a fixed position on a "perspex" plate holder. After counting all the specimens, the corrections were made to the counts to compensate for background counts, decay of radio nuclide during counting procedure and unequal activation of specimens in the irradiation process. For the fixed setting the background counts were

determined by counting gamma rays without putting any specimen under NaI probe before and after the total specimen counting. The mean of these counts was subtracted from the sample count. As the resolution time, for counter, is much less than  $1 \mu\text{s}$ , the possible range for counting is from 100-100,000 counts  $\text{min}^{-1}$ . The irradiation time of seven minutes in low neutron flux of  $3.2 \times 10^{11}$  Neutron  $\text{cm}^{-2}$  was chosen to give a count rate range of 100-20,000 counts  $\text{min}^{-1}$  (calculated from equation of section 2.2.5).

The gamma ray counting is preferred to beta ray counting because a number of corrections such as self absorption and dead time can be avoided. Furthermore as the concentration of tracer in samples varies from very high in some to very low in some, it renders beta counting unsuitable for high count rates as the dead time correction becomes excessive and thus unreliable.

Disadvantages of gamma ray counting : As discussed above, this technique suffers seriously from the inaccuracy at the low count rates. The concentration of  $\text{MnO}_2$  in the sample would be expected to range from a high value at the stage just after breakthrough which is associated with the mean residence time, to a very low value in the tail region, thus having two extremes of concentration. In the above method where scintillation counter was used, the counts at higher concentrations are quite accurate, as it has microsecond dead time. But counts of the sample with low count rate are not accurately determined as the scintillation counter, as discussed above, has a rather higher background count.

The reproducibility of this technique was determined by analysing two sets of specimens from adjacent positions of a run (Fig 4.5 ).

(2) Beta - gamma ray counting: In this technique both beta and gamma rays were counted. At higher concentration the gamma rays were counted using scintillation counter described above while at lower concentration the beta rays were counted using organic quench Geiger-Muller counter tube with Panax counter. The voltage in Geiger-Muller counter was set in the region of plateau, i.e. where an applied high voltage Vs count rate curve for sample of fixed disintegration rate yields a plateau. The plateau for the tube used was 300 volts long and the increase in count rate with an applied voltage was less than 3% per 100 volts. Similar to gamma ray counting, various errors are associated with beta ray counting. So the corrections were made for background counts, dead time correction, non uniform activation and the decay of radionuclide during counting. The decay correction was made using equation in section 3.3.2 C, and correction for non-uniform activation was made by using the curve in Fig 3.5.

The Geiger-Muller counter has the benefit of having rather low background count, and for the assembly used it was 8 counts  $\text{min}^{-1}$  (as compared to 100 counts  $\text{min}^{-1}$  for gamma scintillation counter). Thus this is quite accurate when the tracer concentration is quite low and therefore offers a low limit of detection.

All detectors of radioactive radiations have an inherent recovery time following interaction of a radioactive ray and during this period a second incident can not be recorded. This can be somewhat greater than 100  $\mu\text{s}$  for Geiger-Muller counter. To offset this effect a known dead time of 200  $\mu\text{s}$  was set electronically in the counter and a corresponding correction was made from the standard correction table. Under electronically set dead time ( $\tau$ ) the observed counting rate is

related to the true counting rate by the relation.

$$N \text{ true} = \frac{N_o}{1 - N_o \cdot \tau}$$

where  $\tau$  is electronically imposed deadtime and  $N_o$  is the observed count rate. However, this error is not significant in samples with count rate less than 10,000 counts per minute but above this count rate, the error is quite significant.

It is clear from the above discussion that low count rates are best counted with Geiger-Muller counter (beta ray counting) while high count rates are best counted with Scintillation counter (gamma ray counting). The two count ranges were covered in this way with count rate covered by both the above counters, were counted for beta and gamma counts and appropriate corrections were made to them. A ratio was then calculated in beta and gamma counts obtained from same sample, which served as conversion factor to convert beta counts to equivalent gamma counts. Once all counts have been obtained in gamma count value, RTD data were calculated.

Beta to gamma count ratio was found to vary from 1.63 to 2.16 which was quite reasonable. However, when its reproducibility was checked by re-irradiating, the ratio varied from 1.72 to 2.34. This increased deviation could be attributed to the presence of active contamination. Furthermore Geiger-Muller counter was found to be sensitive to voltage fluctuation which occurred over the span of counting data. However, by replacing the "Panax" counter by 'Canberra' counter the stability improved substantially.

As some manganese decays to iron on irradiation, which on subsequent second irradiation, could contribute towards the total count.

Therefore to check reproducibility two sets of specimens from adjacent position of a run were used instead of using one set and re-irradiating it (Fig 4.6 ).

C. Gamma ray spectroscopy: In this technique the amount of energy dissipated by the gamma ray in its interaction with the NaI crystal is measured using photomultiplier tube and pulse height analyser. The pulses are sorted by height in step function and each channel counts only those pulses in the narrow pulse height step. So using this technique only gamma rays from Mn tracer (selected energy range) were counted thus avoiding interference from other active elements.  $Mn^{56}$  gives radiation of energy 847 KeV. However, the radiations from  $Mn^{56}$  can also give rise to the peak (in spectrum of energy channels) at high energy level (1380 KeV) which is formed due to the summation of the energy deposited in a detector either by random or coincidence gamma rays within the resolving time of the system or by true coincident in the decay of  $Mn^{56}$ . The absence of any interference in measurement of 847 KeV photopeak of  $Mn^{56}$  was checked by measuring the half life which was found to be 2.5 hours in agreement with the published value for  $Mn^{56}$ .

The apparatus consists of cylindrical NaI (Tl) crystal detector coupled with 800 channel (Packard model 942) analyser together with Packard spectrazoom integrator and a Visual display unit. The channel on this set up were calibrated using  $Na^{22}$ ,  $Co^{60}$  and  $Cs^{137}$  which represent energies of (511 and 1280), (1170 and 1330) and 662 KeV respectively. The calibration curve was constructed by plotting the known gamma photopeak energies along the Y-axis against the channel number along the X-axis. The time of irradiation (40 minutes at low neutron flux) was calculated (equation in Section 2.2.5) as to give a



count rate, for the specimens with very low tracer concentration, which was distinct from background after an initial decay time of two hours( transport time), while at the same time not making the specimens with higher concentration of tracer "too hot", i.e. too active. Furthermore the counting time was also adjusted to the sample activity, e.g. longer for specimens with lower tracer concentration. During transport and handling the radioactivity decayed to 60 % of original value. The limit for the most active specimens was arbitrarily chosen to give 20 % dead time for assembly. The counting schedule adopted was such as to count the less active samples at the start and the higher concentration (highly active) samples later.

The analyser was set on a timing system which permits counting in live time mode. Thus in this mode the timer only operates during the time when an analogue to digital converter is accepting the counts. Thus it gives an automatic compensation for analyser dead time.

Because of the inherent nature of the electronic counting system, the peak in gamma ray spectrum of a radionuclide drifts sometimes. This phenomenon was observed particularly at high count rate. To minimize such potential source of error the integration and read out for a given spectrum were performed over a constant number of channels, the range starting from a point located at fixed number of channel from that with the maximum count rate.

As discussed before the number of accumulated counts does have an effect on accuracy of the method. The radioactive decay process is a random process and relative statistical standard error,  $\sigma$ , for the accumulated counts,  $N$  is given by equation.

$$\sigma = \frac{1}{\sqrt{N}}$$

A large number of counts were accumulated to minimize the statistical standard error. In general approximately  $10^5$  counts were accumulated for each sample to yield a statistical standard error of about 0.1 %.

However, samples with low concentration of tracer do show a very low count rate, but even in these a minimum of  $10^3$  counts were accumulated in some cases by counting over a period of 12 minutes. This yields a standard error of about 3 %. It is not possible to count the weaker samples for any more longer time than as stated above. This is due to the relatively short half life and thus restricted time span available for sets of samples.

In order to evaluate the photopeak areas, initially two methods were utilized - Total peak area method (Baedeker 1971) and Sterlinski's method (Sterlinski 1968). Total peak area method was chosen for detailed study and hence results are based on this method unless otherwise stated. After evaluating the photopeak area, the corrections were made for weight of sample, background counts, non uniform activation, delay time and self absorption etc., similar to that in gamma ray counting.

The reproducibility of this technique was established by irradiating and counting the two sets of specimens taken from adjacent positions from an extrudate (Fig 4.9 ).

So overall it can be said that by using radioactive tracer technique, the tracer concentration can be measured to a high degree of accuracy when account is taken of potential errors arising from activation of

the sample, measurement of the radioactivity, or analysis of count data. Reproducibility of the technique is good, particularly when combined  $\gamma$ - and  $\beta$ -ray or  $\gamma$ -ray spectroscopy counting procedures are employed. One likely source of error, which may result in some irreproducibility at very low tracer concentration, is tracer agglomeration.

Ashing of polymer containing a dense mineral powder, such as barytes, provides an alternative means for assessing tracer concentration.

Although this method has limited accuracy at low amounts of tracer (an order of magnitude less than the radioactive technique), the experimental and analysis procedures are much less complex, requiring inexpensive and readily available facilities. A further point of concern is the effect of the mineral tracer on the melt rheology of the polymer, particularly at high filler loadings.

There are various other factors which can significantly effect the reproducibility. These are discussed later in section 4.1 . These include the effect of position of sampling (analysed by taking samples from the centre and edges of the same strip, at same position along the length - Fig.4.10 )and the effect of two different extruder runs using the same conditions - Fig.4.9 ).

### **3.4 APPLICATION OF RTD TO CHARACTERISE TS250X EXTRUDER**

Once the tracer technique had been established, then RTD studies were carried out on GKN Windsor 250X to study the influence of variables on it. Since the variables available on the extruder are to a certain extent interdependent, it is not generally possible to see the effect of only one variable, keeping others constant. However, every effort

was made to keep other variables constant with the commercial relevance of the results in mind. In all of the following runs granular polypropylene (GWM 22) being used unless otherwise stated. Manganese dioxide tracer was used and samples were collected for radioactive analysis. However, for some runs barytes tracer compound was also used and samples were taken for ashing analysis. When both the tracers were used for similar runs, then the run for  $MnO_2$  tracer was performed first followed by run for barytes because of the sensitivity of the radioactive tracer technique towards contaminants which could result from barytes compound if used initially. After using barytes, the extruder was cleaned by further running it for some time with reground polypropylene (e.g. say at 9 rpm for further 30 minutes).

The runs carried out are tabulated in Table 3.2 and are described in the following headings. The detailed information on these, however, are given in Table 4.1. The justification for the selection of the variables studied is discussed in chapter 4. The variables studied can be broadly categorised as follows:

1. Process variables
2. Machine variables
3. Material variables

3.4.1 Process variables: The variables studied in this category are set up type i.e. which processor can change from control console.

A. Throughput rate: The feed to the extruder is governed by the variable hopper feeder. Two runs using the identical conditions but different throughput rate were carried out. In the first run the

TABLE 3.2 DETAILS OF THE VARIABLES STUDIED

NUMBER	VARIABLES STUDIED	MIXING DISC POSITION	MIXING DISC CONFIGU	SCREW SPEED (RPM)	REMARKS	REF. RUN NO:
A.	PROCESS VARIABLES					
1.	Throughput rate	Upstream	Open	9		A 4 and 5
2.	Temperature profile	Upstream	Open	9		A 4 and 6
3.	Screw speed <sup>a</sup>					
B.	MACHINE VARIABLES					
1.	Pulley size - small	Upstream	Open	9, 18, 27		A 1, 2 & 3
	- large	Upstream	Open	21, 42, 60		A 13, 14 & 15
2.	Mixing disc position & config.					
(i)	Upstream position & open					A 1, 2 & 3
(ii)	Upstream position & closed					A 7, 8 & 9
(iii)	Downstream position & open				P.P. powder	A 27, 28 & 29
(iv)	Downstream position & closed					A 21, 22 & 23
3.	Melt pressure at screw tips	Upstream	Closed	9		A 7, 10 & 12
C.	MATERIAL VARIABLES					
1.	Polymer form - granules & powder	Downstream	Closed	9, 18, 27		A 21, 22 & 23 VS A 24, 25 & 26
		Upstream	Open	21, 42, 60	Large pulley	A 13, 14 & 15 VS A 16, 17
2.	Polymer type - polystyrene & polypropylene					A 13, 14 & 15 VS A 18, 19 & 20

<sup>a</sup> The effect of screw speed was studied for most of the conditions. The details on this can be seen in Table 4.1

feed rate was adjusted until material began to emerge from the vent port and the feed was reduced to give the maximum permissible output without this happening. In the second run the feed was reduced by a further 13 % weight of the previous feed (A4 and A5).

B. Temperature profile: Two runs were carried out using identical conditions except for temperature setting on the heating zones. In first run the standard temperature setting was used (as used in all the other runs) while in second run the temperature setting was reduced by  $10^{\circ}\text{C}$  in Zone 3 and 4 (see Fig 3.2), mixing discs are situated in Zone 4 (run A4 and A6).

C. Screw speed: In this work this variable was most comprehensively studied. Three screw speeds, covering the whole available speed range, were used with maximum output. As these screw speeds were studied by changing other variables, these are described under appropriate variables.

3.4.2 Machine variables: In this category those variables are included which involves the change in the parts of the extruder or in screw profile.

A. Pulley size: The pulley is connected to main motor and it drives epi-cyclic gearbox (10 in Fig 1.2) through Poly V belt. Thus increasing the motor pulley diameter would increase the screw speed. So a large pulley was manufactured at Brunel University as to replace the smaller pulley thus increasing the maximum screw speed of the extruder from 30 to 60 rpm. The two sets of runs, one for each pulley system, were performed at three screw speeds. (Run A 1,2,3 and A 13,14,15). In a big pulley system, the output was restricted by

available current rather than conveying capacity. The runs at maximum speed were also performed using barytes tracer.

B. Mixing discs: The screws are of a building block type. The mixing discs are five pairs of slotted disc type with two sets of slots cut in the internal diameter. Thus being segmented in construction, have two main variants available.

(a) Position along the screw length

(b) Configuration of the discs relative to each other.

The configuration of the discs can be varied by virtue of slots in their internal diameter which fit on to the screw shaft. Thus in the "open" position, all the slots of mixing discs, coincide with each other, while in "closed" position the slot or space in one mixing disc coincides with the solid flange of the other(next) mixing disc and this in turn coincides with the gap of the next mixing disc. Thus making the longest possible travelling passage for polymer melt. As regards to the position of the mixing discs along the screw, two positions were chosen ( Fig 3.2 ).

(a) All the five pairs of mixing discs situated at 5 to 6.5. L:D position i.e. nearer to hopper end or "UPSTREAM POSITION".

(b) One pair situated at 5 l:d ratio position while the other three pairs are situated at 13 l:d position i.e. nearer to die end or "DOWNSTREAM POSITION". By separating mixing discs at two positions , spacer segments (just tubular structure with outside diameter equal to screw land) were included thus total segments decreases from five to four mixing discs.

So in this study, runs at three screw speeds (9, 18 and 27 rpm) were carried out on the following screw settings.

- (i) Upstream
  - (a) Open mixing discs
  - (b) Closed mixing discs
- (ii) Downstream
  - (a) Open mixing discs
  - (b) Closed mixing discs

C. Melt pressure: Melt pressure at the screw tips was varied using a strip die with provision of varying die lip gap in thickness. The upper die lip could be moved and fixed in position with positioning screws. As the die lip gap was varied, it was associated with change in melt pressure at the screw tips. These runs at die lip gaps of 2.15, 4.8 and 6.25 mm were performed at screw speed of 9 rpm (run A7, 10 and 12).

3.4.3 Material variables: This category includes the work carried out using different form or type of polymer feed.

A. Polymer form: In this the polypropylene homopolymer as granules was compared with its equivalent powder form. For both polymer forms, the feed was adjusted to give the maximum output.

B. Polymer type: The two types of polymer, polypropylene and polystyrene granules were compared. Once again suitable temperature profiles for both were chosen. The feed rate was adjusted as to give the maximum output without material coming out of vent port. The mixing discs arrangement in screws being "upstream" and "open" setting.



For each polymer runs at three screw speeds (21, 42 and 60 rpm) were carried out (run A13, 14, 15, and A18, 19, 20). The  $MnO_2$  tracer compound used for polystyrene was made using polystyrene as base polymer and using the same technique as used for preparation for polypropylene/ $MnO_2$  tracer compound.

### 3.5 DETERMINATION OF CROSS CHANNEL FLOW AND TRANSVERSE MIXING

The flow inside the extruder was established by using a coloured tracer, combined with a shock cooling - barrel withdrawal technique.

In this technique the extruder was run to steady state and then coloured tracer granules were introduced through the feed hopper. The polypropylene masterbatch containing carbon black (Plasblack PP 1359 of Cabot Carbon, UK) and 10% red pigment (Masterbatch number 401 of I.C.I.) were used as tracers. After a precalculated time from the tracer input in the extruder, the extruder was stopped. The extruder was then shock cooled by circulating oil (at  $40^{\circ}C$ ) through hollow channelled barrel section (A Churchill oil heat exchanger was connected up with the extruder barrel). The schematic diagram is given in Fig 3.6. The connections on the extruder were made such that one outlet from the heat exchanger cooled zone 5, while the other outlet cooled zone 6 and 4 respectively, in series. Thus cooling rates achieved were fastest in zone 5 followed by zone 6 and then zone 4. Zones 1,2 and 3 were not cooled as the tracer was introduced from the vent port. The oil in turn was cooled with water through the heat exchanger.

The oil temperature reached its maximum of about  $100^{\circ}C$  within the first ten minutes thus indicating a much shorter time to cool the polymer in the extruder. The temperature reading of various zones are

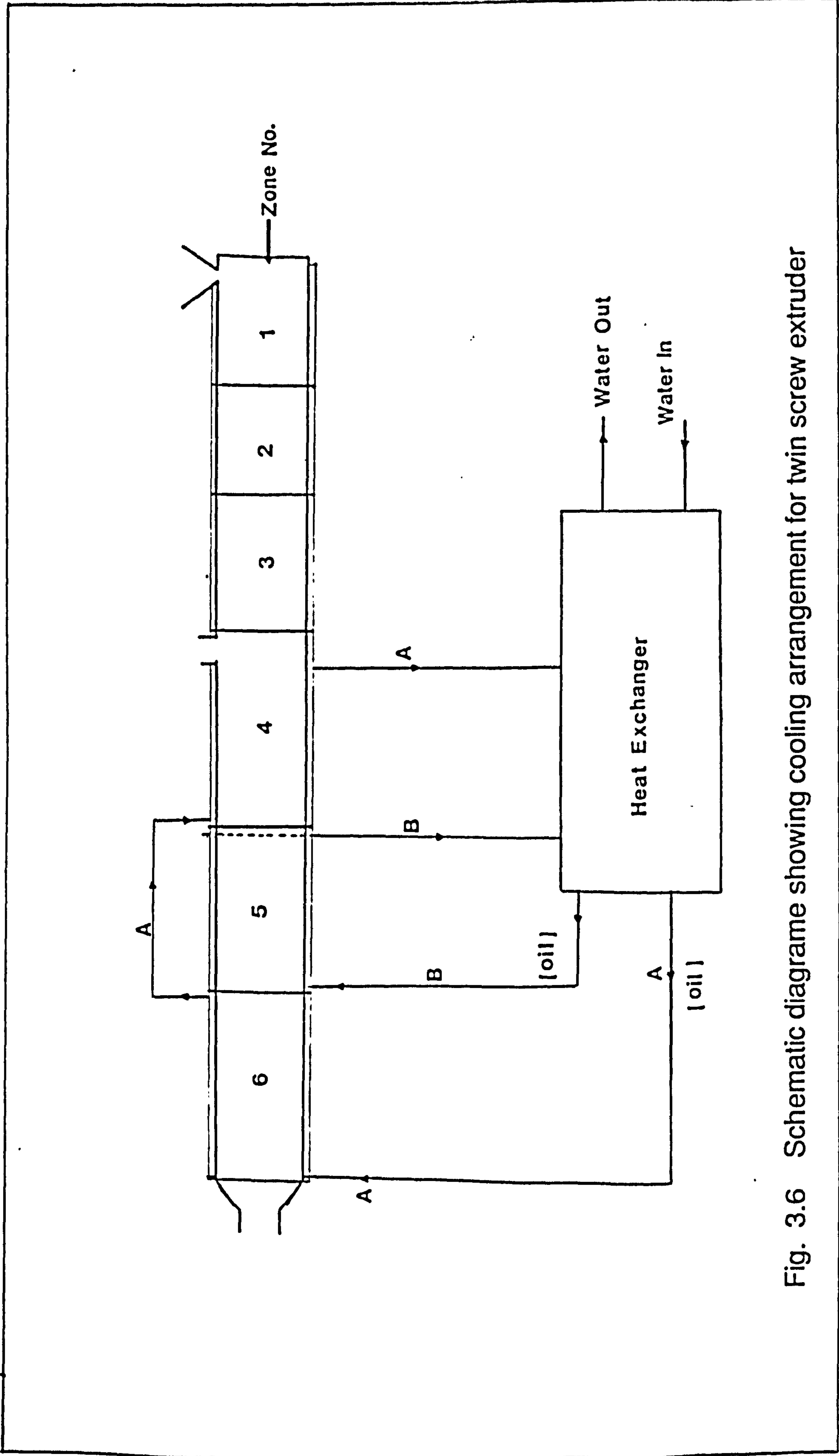


Fig. 3.6 Schematic diagram showing cooling arrangement for twin screw extruder

given in Fig 3.7. Once the extruder was cooled to room temperature, the die head and adapter were removed. A barrel withdrawing adapter, manufactured at Brunel, was fixed onto the barrel. With the help of a hydraulic jack, the barrel was withdrawn. After unscrewing the screw tip caps from the screw spline, the screw segments together with frozen polymer "in situ" were pulled off the screw splines. The screw segments were unscrewed out of the solidified polymer skeleton. Some oil can be introduced in the ingress as to facilitate the removal. The Fig 3.8 shows the screw with solidified polymer, the screw skeleton. This was then sectioned at predetermined places, as shown in Fig 3.8.

There is a problem of voiding in the material which occurs due to differential rate of cooling. This occurs inevitably as a large volume of molten polymer is rapidly cooled. This happens as the polymer in contact with the metal cools rapidly, due to better heat transfer from the metal and therefore leaving the polymer in the centre of the channel relatively molten. So when this is eventually cools, the voids are created. The sections of about 0.4 mm thick were cut using a bandsaw fitted with a locating jig. This arrangement of locating jig cuts a parallel section and supports the polymer skeleton during cutting. A fine cutting blade with appropriate speed gives the required smooth surface. The speed of cutting blade is dependent on the polymer system used. The sections so cut is shown in Fig 3.9 together with one section, as seen magnified using transmitted light.

To study the overall flow within the extruder, it is essential to have a flow pattern generated by extension of single coloured polymer granule. However intermixing can be observed by mixing of two different coloured polymer streaks. These would then also give indication of various zones in the chamber and probably an indication

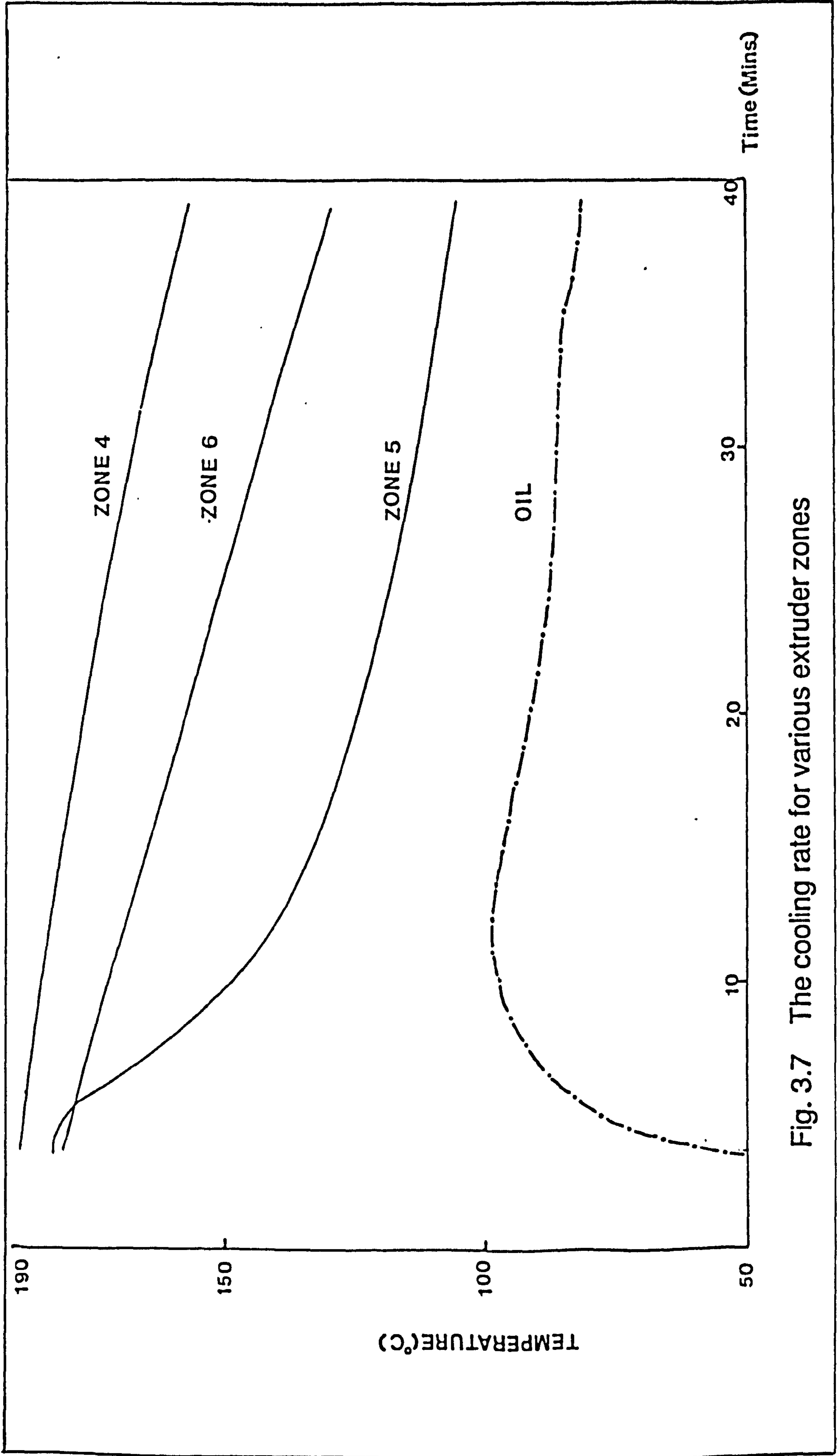


Fig. 3.7 The cooling rate for various extruder zones

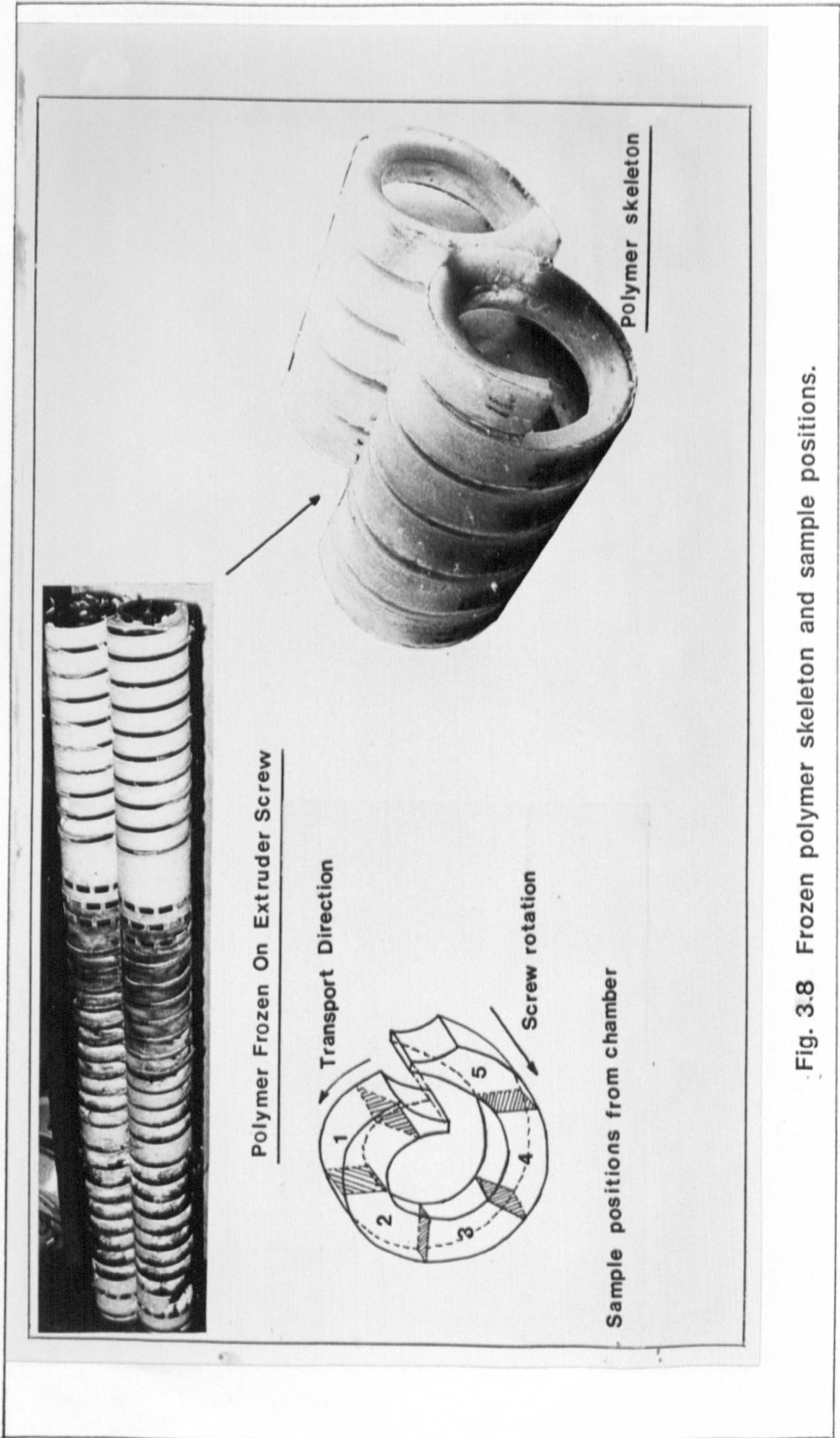


Fig. 3.8 Frozen polymer skeleton and sample positions.



Fig. 3.9 Transverse section of screw channel.

of the flow mechanism. For this purpose colour tracer granules were dropped in every third flight, with alternate black and red colour granules. The relative position inside the channel of tracer is not so important, as it is only added to see the flow path of different regimes. So by introducing at several random places, a complete picture is obtained.

The transverse mixing and its progression along the extruder length was studied by observing macro- and micro-mixing in the screw chambers. The sections were cut for both studies along the whole length, at pre determined places, so the progress in mixing could be established.

In the case of macromixing, carbon black masterbatch was added to the polypropylene granules feed, at timed intervals, as to give 40 ppm by weight of carbon black in polypropylene. This type of concentration gives a grey colour to the coloured/dark portion of polypropylene. This grey colour distribution in white polymer background enables study of mixing possible with naked eye. So for this, the sections were cut at fixed places (at first 1/5th distance from intermeshing zone, as shown in Fig 3.8 shaded area ) along the extruder using a bandsaw, as described above. The photographs of such various sections, cut along the screw length is given in Fig 4.67 . The number mentioned in this figure underneath every section is the channel number and L or R means left or right screw and M.D. means mixing disc location.

Similarly the micromixing was studied by adding carbon black masterbatch as to give 2% by weight overall carbon black concentration in the polymer matrix. The 10  $\mu$ m thick sections were cut at fixed places all along the screw sections both in left and right screws.

These sections were then viewed through a transmitted light microscope and photographed. These sections have voids which are produced as a result of large volumes of melt being cooled rapidly. The unpigmented polymer and voids are distinguished from each other by using crossed polars and thus making voids appear grey, unpigmented polymer white and carbon black pigmented polymer black. However, once major unpigmented polymer areas were absent, then crossed polars were not used, as then merely shape distinguishes between striations and voids. These sections were then analysed for progressive mixing along the length. The photographs of such sections are given in Fig 4.68 and Fig.4.69 .



## CHAPTER 4 RESULTS AND DISCUSSION

### **BACKGROUND TO ANALYSIS OF RTD :**

The twin screw extruder's conveying characteristic is quite complicated which becomes even more confusing due to the effect of intermeshing zone and leakage flows. This makes it rather difficult to determine the velocity profile accurately and from it RTD. However RTD can be determined experimentally which gives an insight on the conveying mechanism. But RTD results should be interpreted carefully as they give an indication of the time spent inside the extruder, measured at outlet and so two different flow patterns may give rise to the same age distribution. Therefore RTD results should be regarded as only supporting evidence to the flow models. Furthermore as RTD is related to the degree of backmixing in a system, which is the mixing that occurs in the primary flow direction and it does not give any indicative difference in microscopic and macroscopic scale mixing. That means RTD by itself cannot predict whether elements of fluids with same residence time can be considered well mixed.

4.1 Reproducibility of RTD determination: In extrusion process the time dependent degradation of the polymer and self cleaning actions are important. So the tail region of the RTD curve, which represents only minute amount left over after passage of majority of the material is quite important. However, the precise detail about this tail and effect of other parameters on it, can truly be obtained if the whole of the method and tracer technique used is quite reproducible. The reproducibility for the whole of the method was studied.

The reproducibility study can conveniently be divided into three main phases.

1. Tracer effects      2. Sampling effect      3. Extruder performance

4.1.1 Tracer effects: Although tracer technique gives a good picture of RTD, however it suffers from various limitations which could have serious implications. Some of these limitations can be overcome by careful planning while others remain unresolved. However, the results obtained are viewed with these limitations in mind, giving a more realistic approach. The limitations caused by use of tracer can be broadly classified into two main effects.

A. Effect of tracer on flow: In the RTD studies by tracer technique it is assumed that tracer has the same flow pattern as polymer. However, as method relies on quantitative estimation of tracer after "let down" in extrudate and as it has a short input time, the tracer concentration in polymer at input has to be high. In the case of ashing tracer technique, method relies on weighing of the tracer. A lower level of detection limit requires a higher concentration used and thus 80 g of 40 % w/w of Barytes concentrate as tracer was used. Viscosity of a filled polymer melt increases with filler concentration. The filler chosen (Barytes) was such as to impart minimum effect on rheological properties of the melt. In the case of radioactive tracer, as the detection limit is of quite low concentration (compared to ashing tracer technique), a small amount of tracer was used. So only 10 g of  $\text{MnO}_2$  masterbatch containing 5 % w/w of  $\text{MnO}_2$  in polypropylene was used. It has been reported that heavily filled polymers show an increase in viscosity. The way in which these heavily filled tracer masterbatches would behave in extrusion process was studied using Davenport capillary rheometer. The results are given in Fig 4.1.

However, this test only provides a limited information essentially because of difficulty in interpretation and also the important features of the extrusion process are not simulated by this test. The shear rate range investigated was 85 to 3500  $\text{sec}^{-1}$ . As discussed by DeBoo and Schneider (1978) the shear rates of significance in the single screw extrusion process are those in the melt film (1000-3000  $\text{sec}^{-1}$ ) and those in melt pool (50-100  $\text{sec}^{-1}$ ).

So this whole range of shear rate was covered in the study. Since only one capillary was used (38.3:1 L/D ratio) the entrance effect was not taken into account and thus reported viscosity is higher than true viscosity. The Rabinowitsch correction was also not made. However, as the work was done on one capillary, it gives a comparative value. When compared with virgin polypropylene, masterbatch containing 5 % w/w of  $\text{MnO}_2$  has lower viscosity at low shear rate range. The molecular reduction due to milling is more than increase due to incorporation of  $\text{MnO}_2$ .

However, at higher shear rate, the viscosity tends to be similar. This is because filled thermoplastic has more pronounced structural viscosity and thus flow curves converge with increasing shearing velocity (DeBoo and Schneider 1978). Thus at higher shear rate, as found in extrusion process, it would behave similar to polypropylene and thus give more accurate result. However, barytes masterbatch (40 % w/w) shows a consistent increase in viscosity over the whole shear rate range. This means that the compound would show a retarded motion as compared to polypropylene and thus give RTD curve with more stagnation than actually present.

As discussed before in section 3.3.2 D, in neutron activation analy-

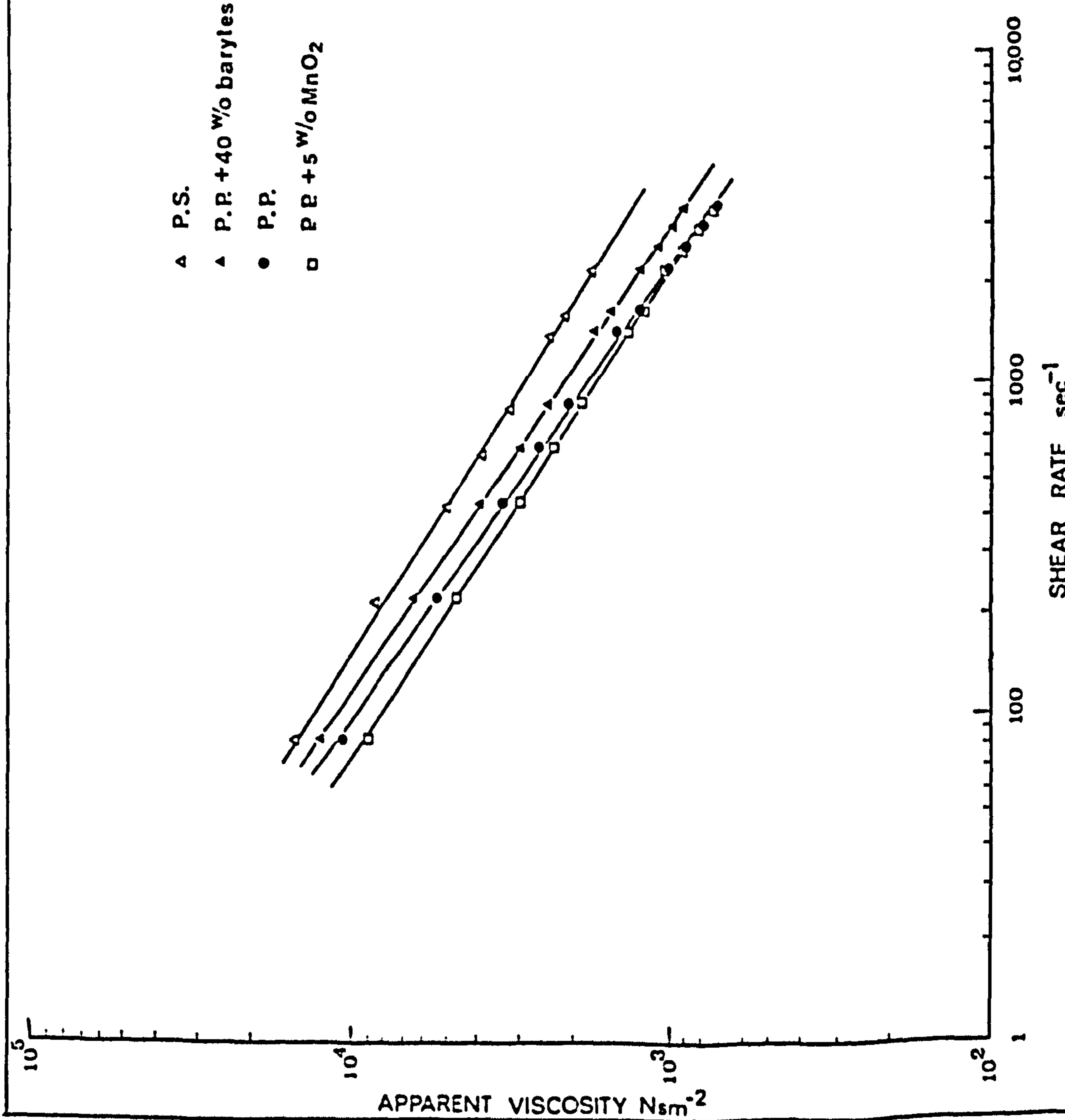


Fig. 4.1 Comparison of the rheological properties of virgin polymers and masterbatches containing tracer powders.

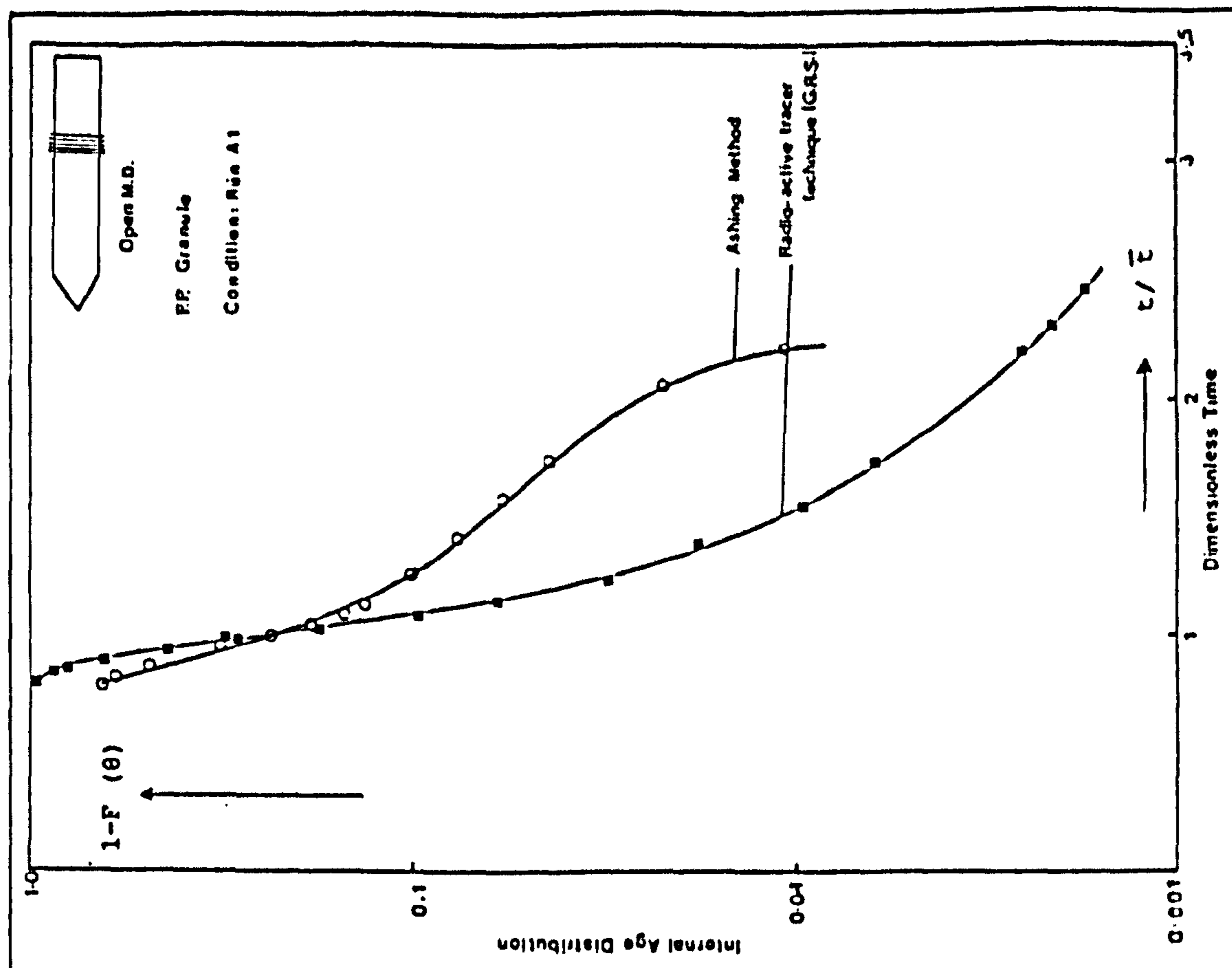


Fig. 4.2 Comparison of two tracer techniques for a similar extruder run.

sis, Gamma ray spectroscopy technique was found to be the best suited for the purpose. Logically this technique was used for all the further investigations, unless otherwise mentioned. Although considerable number of runs were analysed with the ashing tracer technique as well. As discussed before, this ashing technique does not give accurate results. Thus the results obtained by this technique are not given in this thesis except as an example in Figure 4.4, 4.8 and 4.10. The results obtained by ashing technique and by Gamma Ray spectroscopy are compared in Fig 4.2.

B. Amount of tracer material used: The amount of tracer used in experiment can also effect the results. To study this effect, two quantities of  $MnO_2$  tracer (10 and 20 g) were used (Fig 4.3). The RTD curve from 20 g tracer shows a slightly longer tail with not much difference in overall longitudinal mixing to that obtained with 10 g. This clearly shows that the tracer amount itself can affect the RTD results significantly especially below the concentration of 5 % of total amount.

This is probably due to different flow behaviour of masterbatch particles in unmolten form. As the  $MnO_2$  masterbatch granules are relatively smaller in size as compared to base polymer, this relative size could give rise to different flow behaviour in unmolten form. So this adds to the different flow observed.

C. Reproducibility of the tracer technique

1. Ashing technique: The reproducibility of the ashing technique "slow degradation method" was studied. In this case samples were taken from the adjacent positions in extrudate and results calculated.

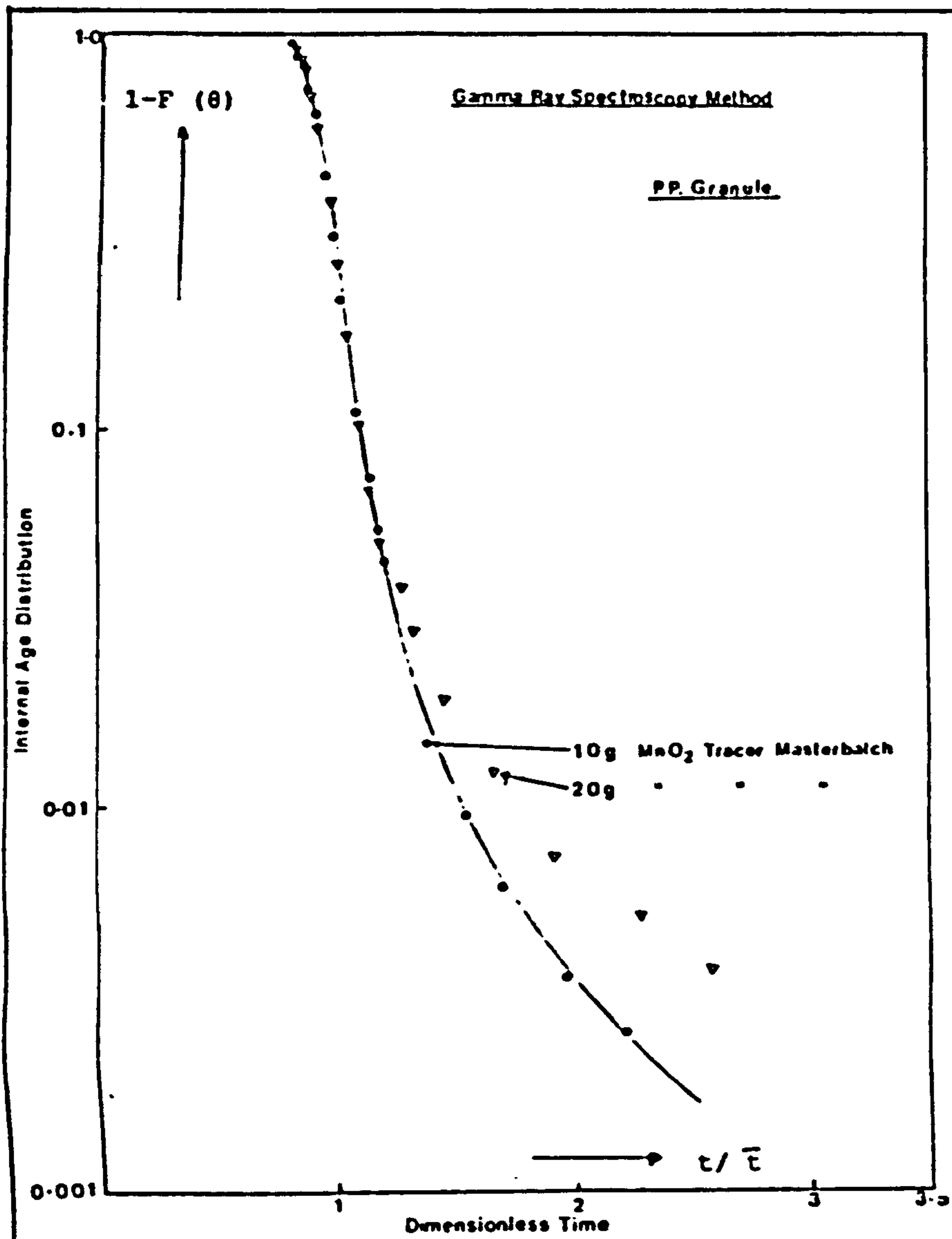


Fig.4.3. Effect of tracer amount.

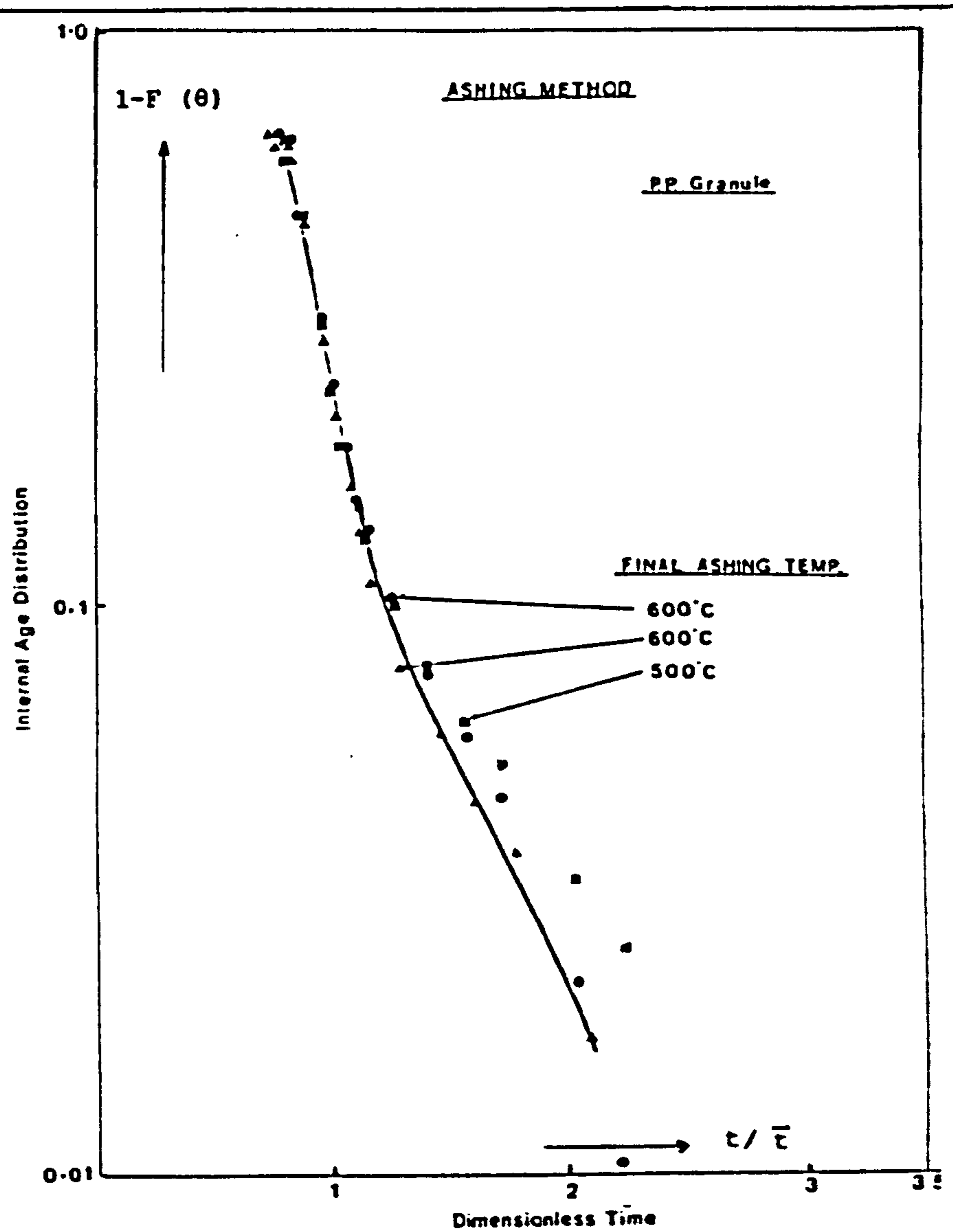


Fig. 4.4 Effect of final ashing temperature (For ashing method only).

Tracer Technique Reproducibility.

The final temperature used for ashing was  $600^{\circ}\text{C}$ . The results are given in Fig 4.4. Although due to the limited sensitivity the lower end of the RTD tail can not be measured and hence limited to 98 %, but up to that range the reproducibility is quite good. The final ashing temperature selection is quite important. At  $500^{\circ}\text{C}$  the curve obtained shows somewhat more stagnation. This may be due to the presence of some carbonaceous products. However by using  $600^{\circ}\text{C}$  the results become quite reproducible, up to 98% of total flow. The stability of the barytes at  $500\text{-}600^{\circ}\text{C}$  was confirmed by heating the barytes powder on its own and precisely determining the weight loss which accounted for only 0.1 % .

2. Radioactive tracer technique : In this technique  $\text{Mn}^{56}$  is used as tracer which has very low limit of detection. As discussed before the rays emitted from active Mn can be counted by three methods. The reproducibility of all these three methods was determined. One set of sample was taken for all the three methods and results were obtained after activation. The samples were allowed to decay completely. Again, after a few days, the sets of samples were reactivated and recounted and thus their reproducibility determined. The results so obtained are given in Fig 4.5, 4.6, 4.7 & 4.9 . Gamma ray method (Fig 4.5) shows an overall reasonable reproducibility, being quite good up to 90 % of the flow beyond which it shows some deviations in results. As compared to ashing technique, this technique has lower detection limit and thus detection of tail for longer time. However the reproducibility of results is somewhat inferior to that of ashing technique. The reason for such a poor reproducibility in the results at lower end is due to the high background (higher counts) in scintillation counting and total of low count rate available from weaker samples in tail region. Furthermore, due to limited time

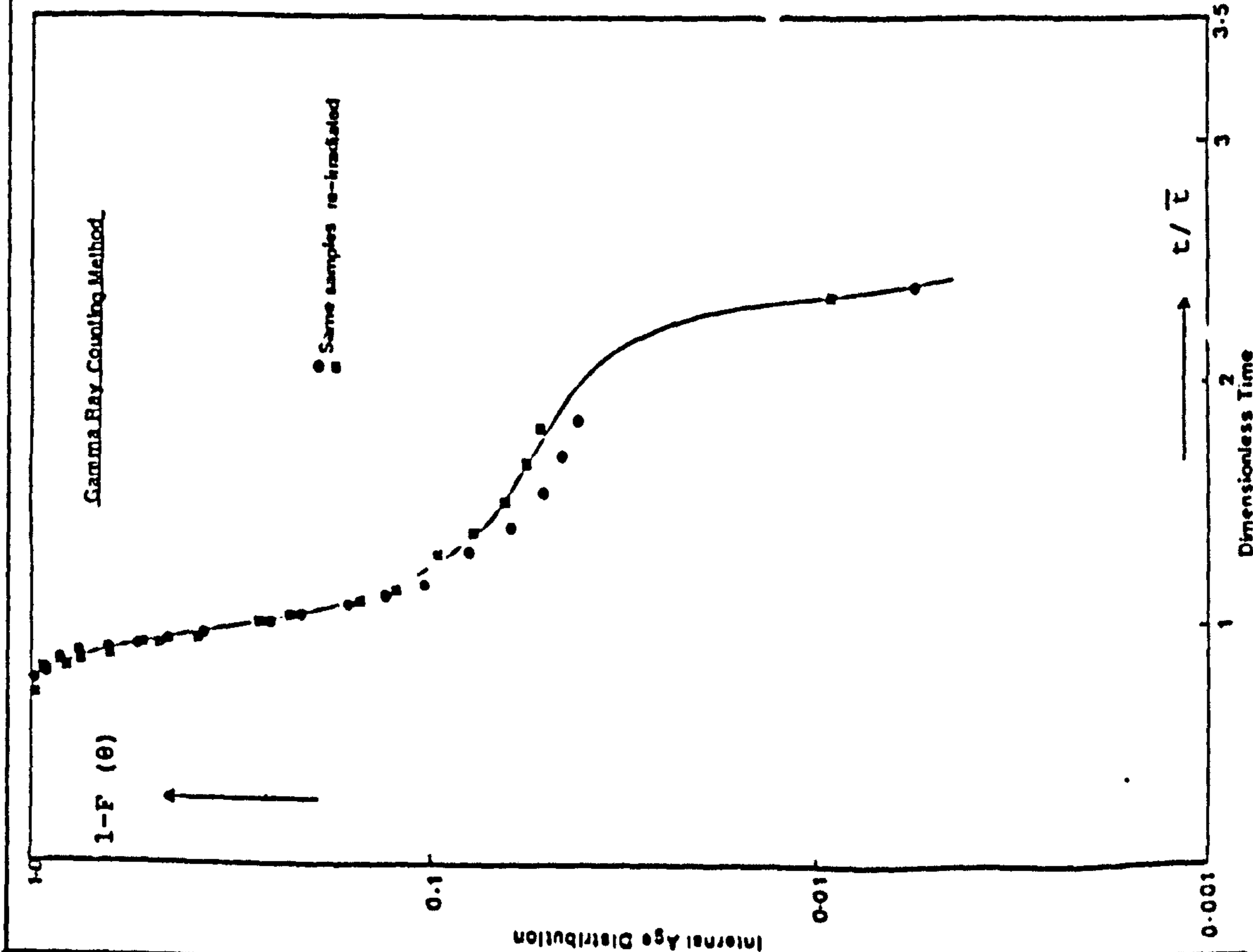


Fig. 4.5 Reproducibility of Gamma ray counting technique.

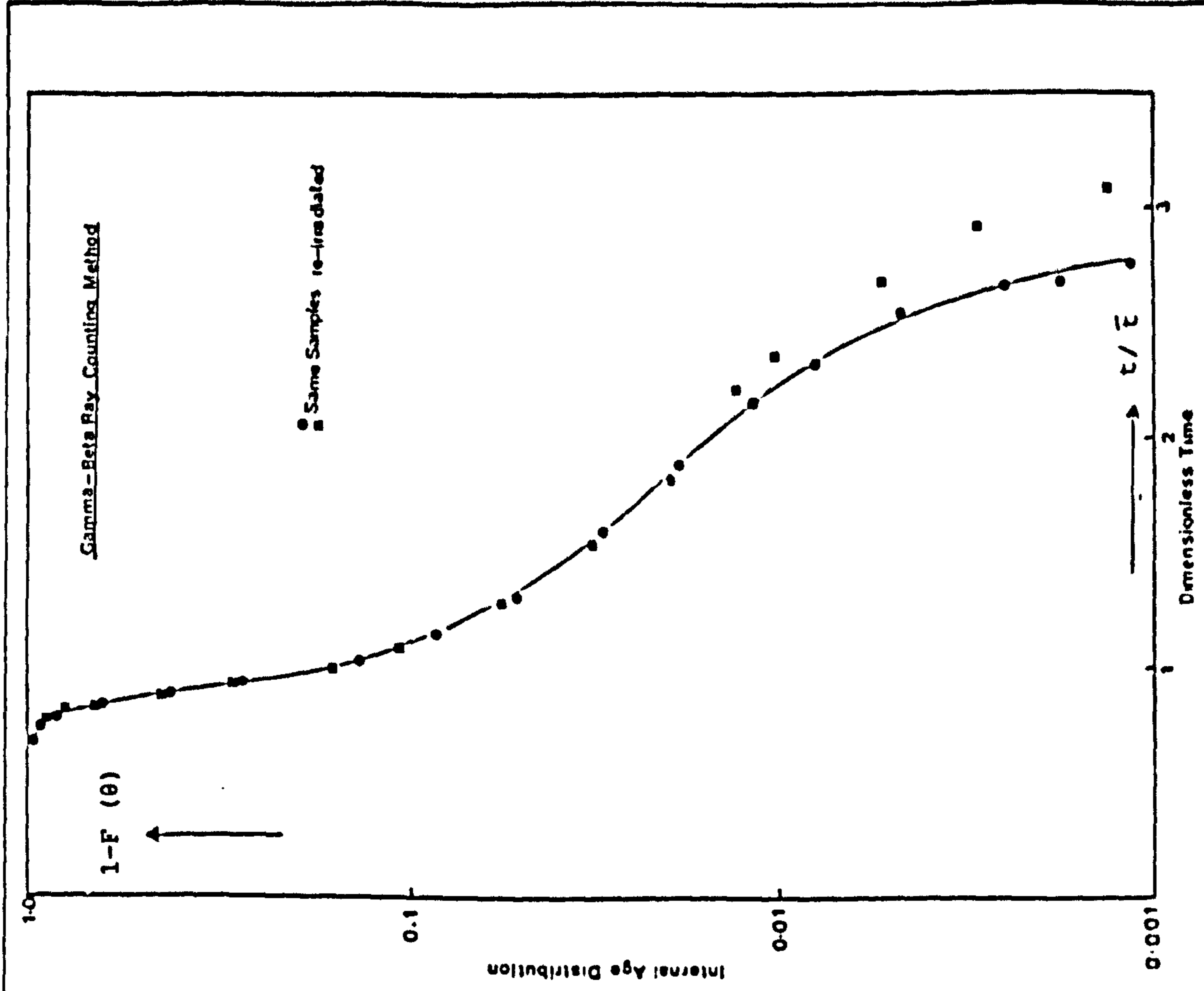


Fig. 4.6 Reproducibility of Beta-Gamma mixed counting technique.

Tracer Technique Reproducibility.



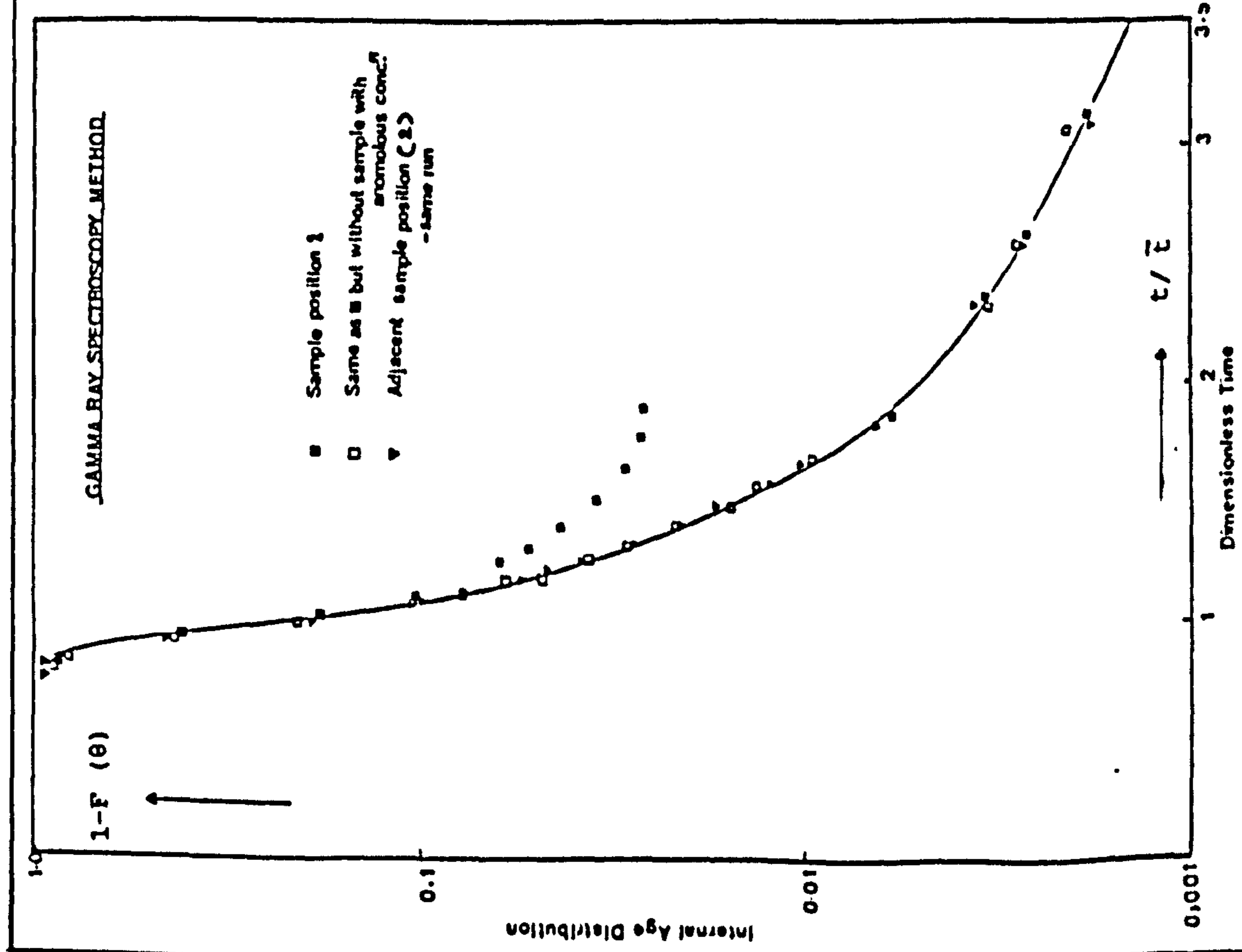


Fig. 4.7 Effect of agglomeration and reproducibility in GRS counting method.

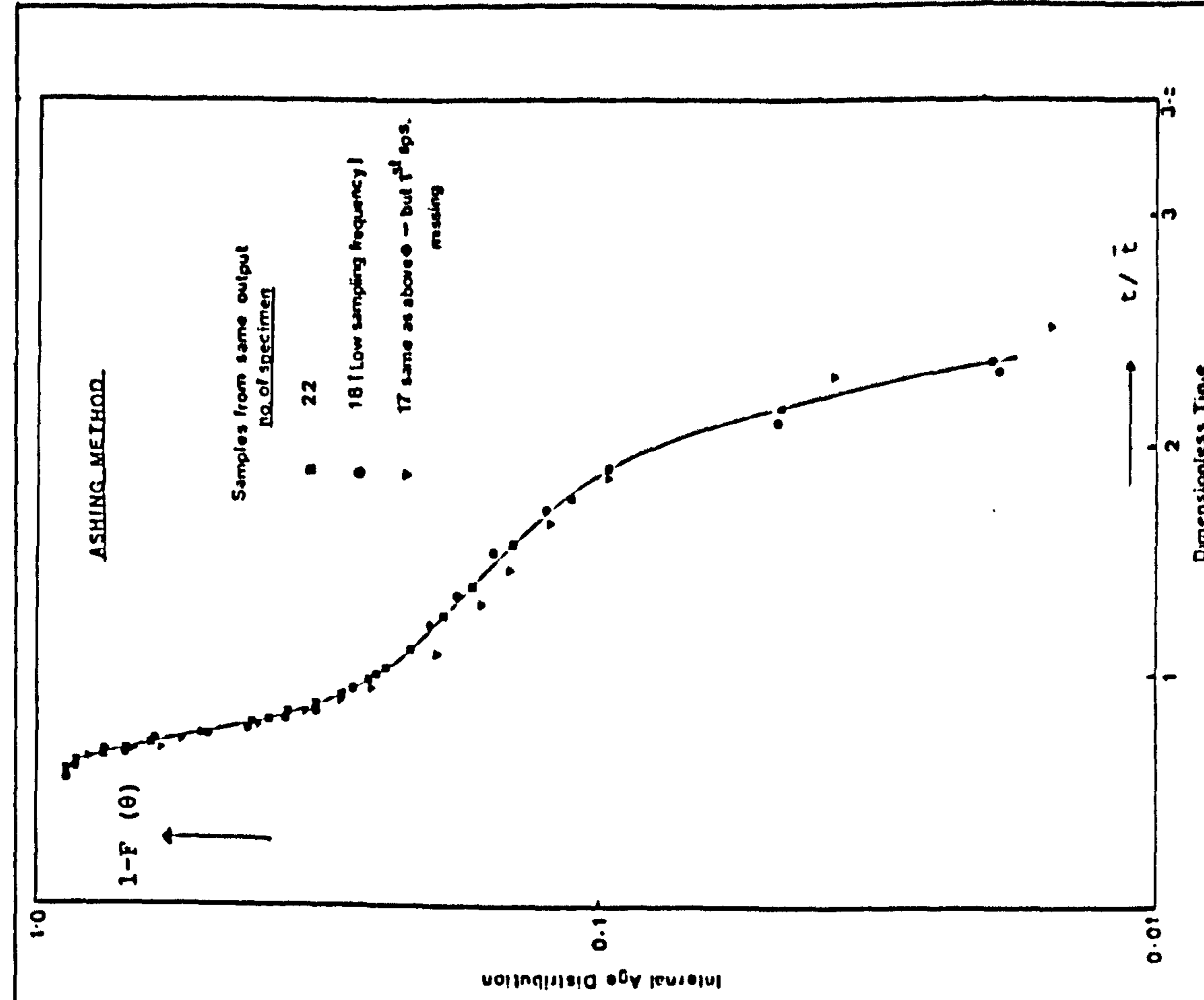


Fig. 4.8 Effect of sampling procedure on reproducibility.

Tracer Technique Reproducibility.

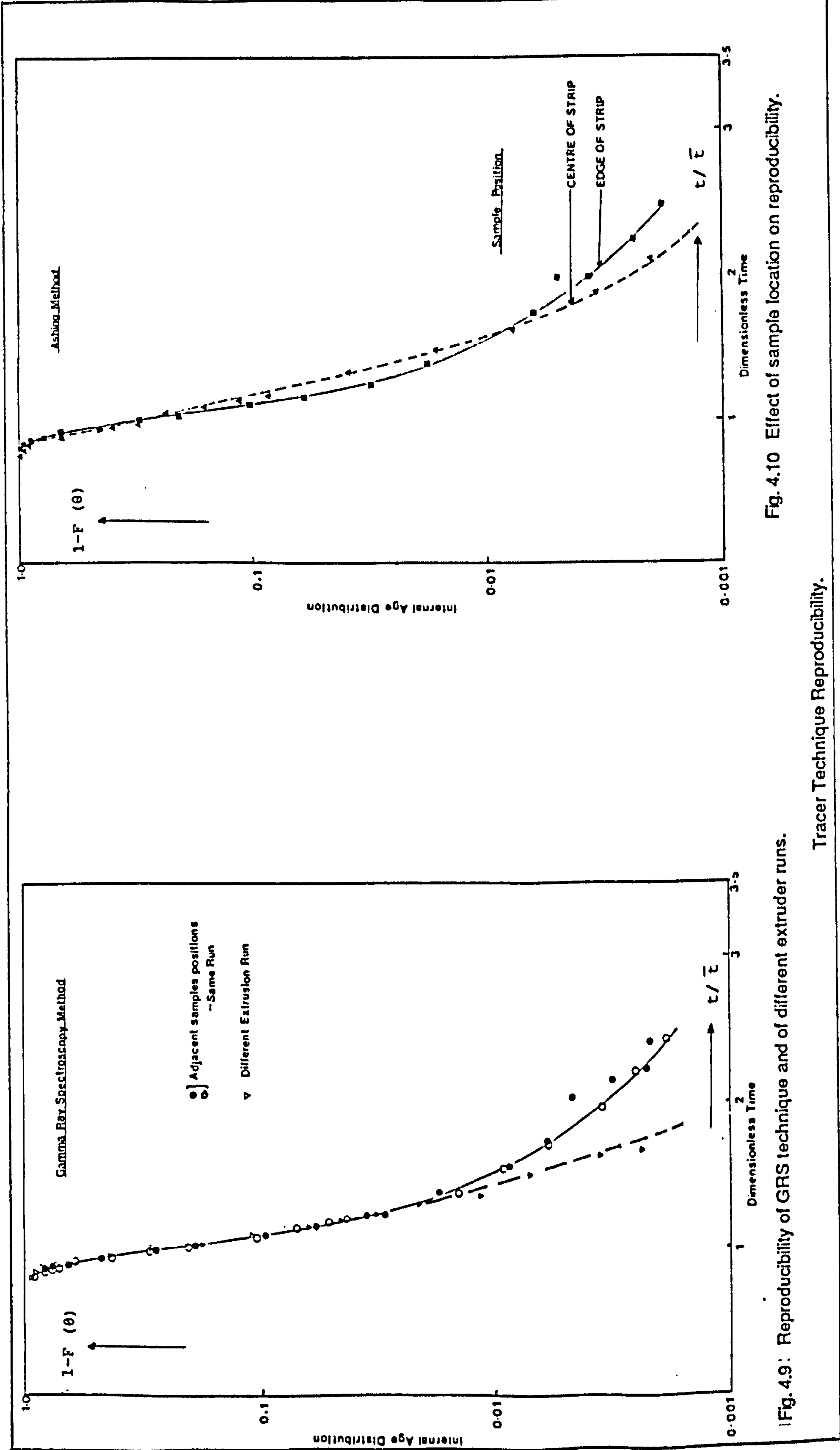


Fig. 4.9: Reproducibility of GRS technique and of different extruder runs.

Fig. 4.10 Effect of sample location on reproducibility.

Tracer Technique Reproducibility.

duration available for counting (net 6 hours experimental time available), a higher total count was not possible from weak samples and thus not very statistically accurate results were achieved.

The reproducibility of the results obtained by beta/gamma ray method (Fig 4.6) shows much improvement over gamma and ashing technique. As discussed earlier in section 3.3.2.D, the improvement was achieved because of accuracy of beta ray counting at low count rate, associated with low background count, and gamma ray counting at high count rate, as scintillation counter has low dead time. The reproducibility is quite good up to about 99 % of the flow beyond which it shows some deviation. In the case of gamma ray spectroscopy (Fig 4.7 and 4.9), a further improvement in reproducibility over the previous methods was obtained and this extends to 99.5 % on the same samples. Thus there is a further substantial improvement on beta/gamma mixed counting, especially in the tail region.

4.1.2 Sampling effect : The various factors associated with the sampling do affect the RTD. These are discussed below.

A. Sample time: As the RTD result is obtained from all of the samples taken in a run and it shows an overall (cumulative) effect of these samples. So the variables such as the duration of the total sampling period, the number of the samples taken, or the time at which the sampling started etc. can have an effect on RTD. To get results, which could then be compared with each other, requires eliminating these variables, which if not carefully controlled can affect RTD. Comparing two calculations from the same set of samples, shows that extending the sampling time broadens the overall RTD curve (Fig 4.8). However, the number of samples within the given sampling time range

does not affect the result. This is clearly shown in Fig 4.8 where two sets of results are calculated, one with 22 samples while other with only 18 samples. The sampling time is of significant importance. Thus initial samples (associated with minimum residence time) are more detrimental, if not taken into account, as compared to the later samples (associated with samples in the tail region). So by leaving out only one sample, associated with the start of the distribution curve, can influence and thus shift the whole curve (Fig 4.8).

B. Sample position : As the samples are taken from the output at a minimum time interval of 20 seconds, it represents a rather long strip of polymer output. So sample from a similar axial position but next to each other along the strip were taken and results obtained. The sample shows quite good reproducibility up to 99.3 % of the total flow, beyond which there is a slight deviation (Fig 4.9). There is obviously more deviation in this case than the case when one set of samples was irradiated, counted and then after complete decay was reirradiated and recounted. This suggests that though tracer is nearly well distributed but still lacks complete homogeneity in the area along the strip. However across the strip, it is a different case. Due to the near laminar flow, velocity profiles are present over the cross section. This leads to the difference in the samples taken from the centre and the edge of the strip. Two such sets of samples were prepared and results calculated by ashing technique (Fig 4.10). The RTD curve for samples taken from centre demonstrates an overall spread and thus more longitudinal mixing. Similarly overall less stagnation occurs in the centre as compared to the edge. This is due to the stagnation occurring due to the die geometry.

C. Agglomeration: As discussed above, manganese tracer is

considered to be in well dispersed form in the masterbatch. However, it was noticed that sometimes rather big agglomerates of tracer occurred in the output. On one occasion, run at high screw speed, a whole  $MnO_2$  masterbatch particle was present in the output. This quite clearly indicated extruder's inability to completely melt and distribute the whole of the polymer passing through it at this condition. Janssen (1978) also observed such a behaviour, of small agglomeration, in his studies. The samples with agglomeration of  $MnO_2$  do give an erroneous result. However, they are quite obvious in the final calculated concentration form and do show up as a discrepancy. If left in calculation, this would give a RTD curve with a different shape. Fig 4.7 shows a typical curve with and without this erroneous concentration.

4.1.3 Extruder performance : Finally the sensitivity of the RTD to the extruder settings was considered. Janssen (1978) also carried out similar work. The fluctuation in extrusion condition may have been caused by the temperature fluctuations or a small fluctuation in feed rate in the extruder. As the machine was quite big and took rather a long time to achieve steady state, even then the temperature always varied, though within a very narrow range. So two runs were performed on extruder with same temperature settings and RTD's were determined. Fig 4.9 shows the results obtained. The overall reproducibility is quite good up to the 99%, after which the two curves show different tail regions. So it can be said that although the accuracy of the measurement holds well up to 99.5%, but the reproducibility due to the extruder's fluctuations make it difficult to be accurate beyond 99%. This should be kept in mind when comparing the effect of variables.

## 4.2 FACTORS INFLUENCING THE RTD:

The variables in extrusion process which affect either the polymer state, or its flow behaviour or the flow path of material, lead to a change in RTD. In this study it is tried to change one variable at a time. As the variables in the extrusion process are interdependent, it was achieved with limited success.

The RTD studies were carried out by changing various parameters viz. Polymer, processing variables and machine variables. An overall trend was observed in the following four important aspects as a function of the effect of other variables. As the following four parameters do affect the melt state and the available flow path of the polymer melt, the effect of various variables on the following gives an in depth insight of their effect on mixing behaviour and so on the RTD results.

### 4.2.1 Throughput rate

### 4.2.2 Melting behaviour

### 4.2.3 Filled volume

### 4.2.4 Power consumption

4.2.1 Throughput rate: In these experiments, a maximum throughput was aimed for. The work has given an insight of how the changing of one parameter such as polymer form or mixing disc location changes the maximum achievable throughput. This in turn, has given information about melting behaviour/polymer packing in the pre-vent- port section or the pressure generation in post-vent-port section. This is because the throughput of GKN Windsor 250X, as shown below, is affected by the limitation in the availability of the space in pre- vent-port section or the pressure generation in the post vent-port section.

The throughput of an extruder of a given diameter is generally restricted by

- (a) Geometry of the inlet
- (b) Melting capacity of the machine
- (c) Pressure generation in the devolatilization region
- (d) Drive power of the machine
- (e) Polymer conveying capacity of the extruder (design)
- (f) Screw speed

In GKN Windsor 250X the conveying capacity of the inlet zone and other zones was quite high. The drive power of the machine was quite high (in small pulley assembly) for various processing conditions (except for run A9 and 23) So the main restriction imposed on the throughput was the pressure generation in the devolatilization zone. However on changing the pulley to bigger size the available torque was reduced and consequently throughput was limited by drive power/torque (Run A 13 to A 20- see current consumption in Table 4.1 where current rating of 50-60 ampere shows torque restriction). However beyond a certain output, the heating capacity of the machine was insufficient and thus polymer was not completely molten. Moving the disc to backward position i.e. in upstream position, the polymer was melted but then due to the limited available torque, the output was reduced.

In this research programme the throughput obtained by the extruder was basically restricted by the extruder's capacity in conveying the melt past the devolatilization zone. The conveying past the vent-port was controlled by

- (a) Melting behaviour/polymer packing in pre vent-port section.
- (b) Pressure generation in post vent-port section.

TABLE 4.1 : DETAILED CONDITIONS OF EXTRUSION RUNS - PART 1

MIXING DISCS		Run No.	Screw speed	Output (kg/hr)	Current (amp.)	Screw Torque (KNM)	Melt pressure MN/m		Remarks
							Before Mixing Disc	At screw Tips	
Position	Config-uration	Small Pulley System							
U P S T R E A M	O P E N	A1	9	33.1	23	1.86- 2.07	-	2.48	
		A2	18	63.8	28	2.62- 2.86	-	3.24	
		A3	27	89.1	38	2.86- 3.26	-	3.72	
		A4	9	34.3	33	2.62- 2.78	-	2.27	
		A5	9	29.8	27	2.15- 2.23	-	1.58	Lower feed rate
		A6	9	34.3	40	3.26- 3.34	-	2.20	Lower temp. profile
	C L O S E D	A7	9	35.3	35	-	-	3.79	
		A8	18	73.2	50	-	-	4.00	
		A9	27	-	55	-	-	4.41	
		A10	9	35.3	35	-	-	4.12	2.15 mmx76 mm Die opening
		A11	9	35.3	37	-	-	4.12	" + Tracer through vent port
		A12	9	35.3	32	-	-	2.65	6.25x76 mm Die opening
C L O S E D	A21	9	30.8	26	1.83- 1.98	0.69	2.9		
	A22	18	74	50	3.5- 3.66	4.34	4.41		
	A23	27	105	53	3.05- 4.21	5.1	4.89		
	A24	9	30	17	1.11- 1.19	0	2.76	Polypropylene Powder	
	A25	18	64.5	27	2.15- 2.31	1.59	3.89	"	
	A26	27	95.4	32	2.56- 2.62	2.34	4.48	"	



TABLE 4.1 : DETAILED CONDITIONS OF EXTRUSION RUNS - PART 2

MIXING DISCS		Run No.	Screw Speed (Rpm)	Output (kg/hr)	Current (amp.)	Screw Torque (KNM)	Melt Pressure MN/m <sup>3</sup>		Remarks
							Before Mixing Disc	At Screw Tips	
Position	Configuration	Small Pulley System							
		DOWNSTREAM	OPEN	A27	9	28.7	18	1.59	-
A28	18			60.1	24	1.98	-	3.72	"
A29	27			97	33	2.78	-	4.48	"
		Large Pulley System							
UPSTREAM	OPEN	A13	21	53	60	2.45	2.27	2.89	
		A14	42	83.1	57	2.44	3.44	3.51	
		A15	60	113.5	60	2.48	2.48	3.93	
		A16	21	58	55	2.42	2.75	3.44	Polypropylene Powder
		A17	60	116	55	2.29	3.08	4.20	"
		A18	21	45.6	63	2.54	-	3.51	Polystyrene Granules
		A19	42	88	60	2.51	-	3.17	"
		A20	60	-	60	2.47	-	-	"

**NOTES FOR TABLE 4.1 PART 1 & 2**

1. The following temperature profiles were set for various runs.

	Zone 1 to 8 temp. °C
(i) For run A6	175, 185, 175, 165, 185, 181, 175, 190
(ii) For run A18, 19 & 20	130, 130, 135, 145, 150, 160, 165, 165
(iii) For all other runs	175, 185, 185, 175, 185, 181, 175, 190

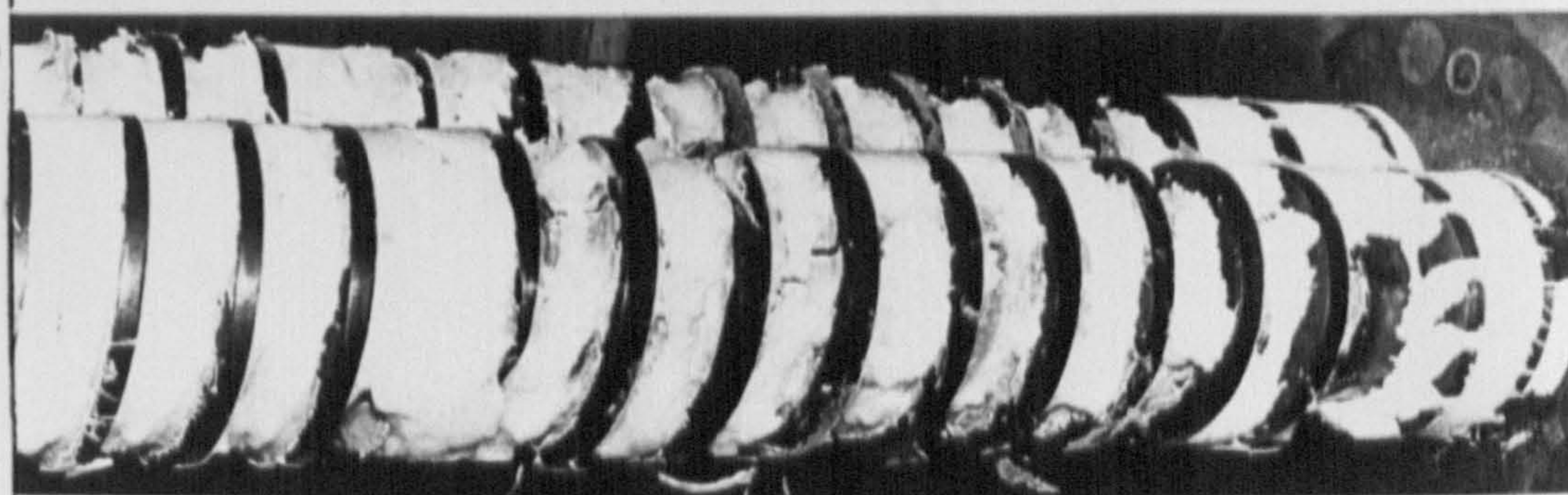
2. The die opening used was 4.8 X 76 mm

3. The screw torque was calculated as  
Screw torque (NM) = Force (Kg) X 9.8 X Cos 22 X 0.35 (m)

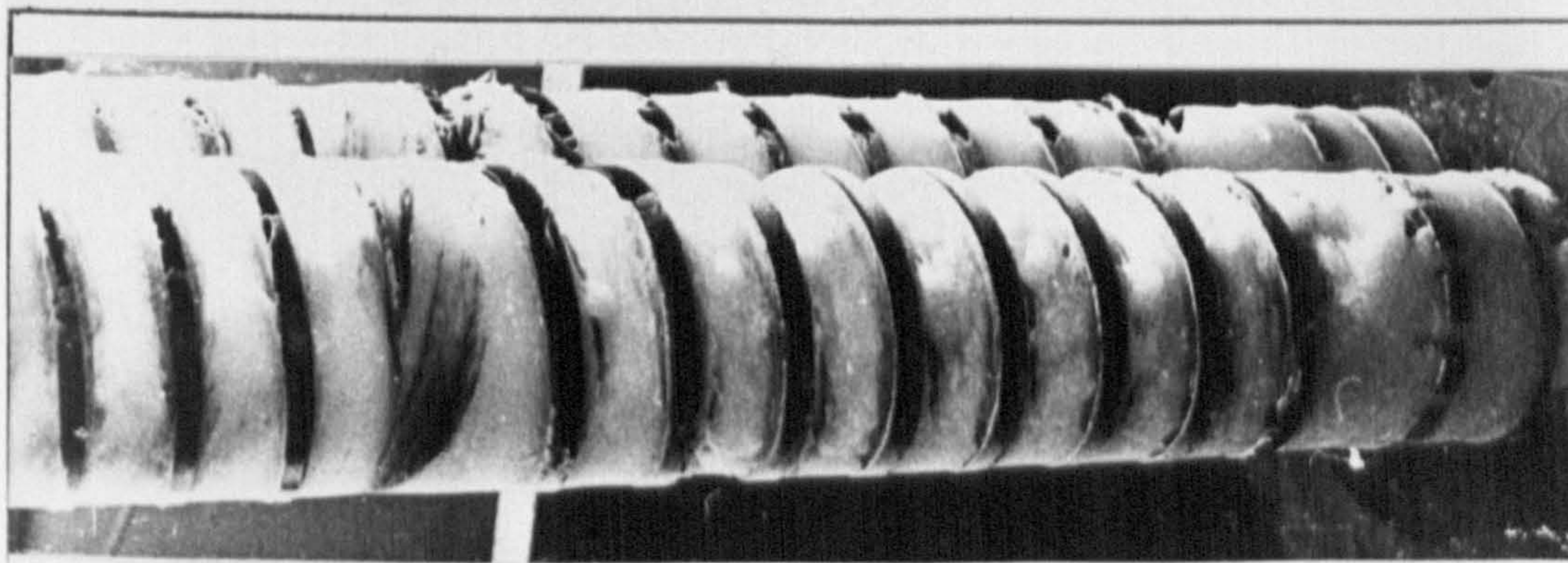
where force was measured on flywheel at angle of 22° at  
distance of 0.35 meters.

Thus the throughput rate obtained under one given condition gives an indication about its influence on the melting behaviour, relative pressure generation of the screw arrangement and the passage of the polymer. The throughput rate directly affects the degree of fill which in turn also directly affects the power consumption.

If the output is controlled by polymer in pre-vent section then obviously it would be affected by factors affecting the volume of material in pre-vent zone. The main part is played by melting mechanism, heat generation and upstream pressure generation. This is clear in the case of polypropylene granules where an increase in throughput results by changing the discs configuration from open to closed in upstream position. (Table 4.3 A reference Run A1, 2 and A7 and A8). This shows an increase of 6.6 and 14% by weight at 9 and 18 rpm screw speed respectively. The closed configuration of mixing disc imparts more resistance to flow and thus associated higher pressure generation at the point results in more melting and compaction. This is confirmed by barrel withdrawal technique. The photograph (Fig 4.11) shows two different throughput rates at the same screw speed. The condition with higher throughput rate shows higher filled volume (Fig 4.11). Mixing discs in upstream position also function as melting discs and moving them to downstream position results in less pressure build up in upstream position which is associated with less melting. Thus in downstream position (i.e. one mixing disc left in upstream position while rest are moved in downstream position) it results in a reduction in output at low screw speed (about 7%-Table 4.3A reference Runs A7, 21). However this associated reduction in output is not observed at high screw speed (Table 4.3A reference Runs A8, 22). It could be that one mixing disc in upstream location at high screw speed



Partially Filled Screw Section



Highly Filled Screw Section

Fig.4.11 Effect of throughput rate on screw filling .

TABLE 4.2 A

BASIC DATA →		Minimum Residence Time (mins)	Mean Residence Time (mins)	Stagnation time (Dimess Time) for 1% material	Vaiance X 100	Hold back area	Filled Volume cm <sup>-3</sup>	Throughput rate (Kg./hr)	REMARKS	Reference runs
<b>SMALL PULLEY SYSTEM</b>										
UPSTREAM	Mixing Disc									
	Con-fig.									
	Screw speed → Polymer ↓ type									
		9   18   27	9   18   27	9   18   27	9   18   27	9   18   27	9   18   27	9   18   27		
		9.5	12	1.55	2.07	0.41	8826			A 1
		--	5.4	1.51	0.85	0.91	---	33.1	63.8	A 2, 3
		9.25	11.5	1.53	1.02		8865	34.3		A 4
	Granule	10	13	2.39	1.99	0.44	8608	29.8		A 5
		9	11.3	1.03	0.59		8613	34.3		A 6
		8.7	11.3	1.57	1.32	0.55	8864	35.3		A 7, 8, 9
	Granule	9	11.4	1.67	1.32	0.43	8942	35.3		A 10
		9	11.3	1.49	1.24	0.62	8864	35.3		A 12
	Powder	10	13.04	2.08	2.99	0.08	8317	28.7		A 27, 28, 29
		9.6	12.20	1.54	1.43	0.49	8350	30.8		A 21, 22, 23
	Powder	10.6	13.64	2.04	3.07	0.13	9093	50		A 24, 25, 26
<b>LARGE PULLEY SYSTEM</b>										
	Screw Speed -----	21	42	60	21	42	60	21	42	60
		5.3	7.2	1.67	0.89	0.64	8480	53		A 13, 14, 15
	Granule	--	6.3	2.82	2.36	--	8120	58		A 16, 17
	Powder	--	7.8	1.5	--	0.79	5988	45.6		A 18, 19, 20
	Polystyrene Granules	3.3	4.6	2.14	0.89	0.82	6815	--		--

TABLE 4.2 B

BASIC DATA		Throughput Rate ( Kg. / hr. )	Current ( Ampere )	Throughput / Current ( Kg. / hr. / Amp. )	Net S.E.C. ( J / Kg ) X 10 <sup>5</sup>	Motorload ( J ) X 10 <sup>5</sup>	REMARKS	Reference runs			
UPSTREAM	Mixing Disc	SMALL PULLEY SYSTEM									
	Position Con-fig.	Screw speed Polymer type									
UPSTREAM	OPEN	9   18   27	9   18   27	9   18   27	9   18   27	9   18   27					
		33.1		1.44   2.28   2.48	1.81	70.17		A 1			
		63.8   89.1	23   28   38		2.72   3.38	193.9   331.4		A 2, 3			
		34.3	33	1.11	2.45	93.98		A 4			
		29.8	27	1.14	2.19	75.7	Low polymer feed	A 5			
	CLOSED	34.3	40	0.90	3.0	113.2	Low temp. profile	A 6			
		35.3   73.2	35   50   55	1.07   1.56				A 7, 8, 9			
		35.3	35				Narrow gap on die lip	A 10			
		35.3	32	1.10			Wide gap on die lip	A 12			
		28.7   60.1   97	18   24   33	1.59   2.73   3.23	1.52   1.90   2.60	53.9   134.6   283.3		A 27, 28, 29			
DOWNSTREAM	CLOSED	30.8   74   105	26   50   53	1.34   1.64   2.19	1.85   3.08   3.79	67.1   248.6   428.4	Current restrn. in A 23	A 21, 22, 23			
		30	17   27   32	1.87   2.38   3.08	1.0   2.11   2.47	40.2   156.7   266.2		A 24, 25, 26			
	OPEN	LARGE PULLEY SYSTEM									
UPSTREAM	Screw Speed -----		21   42   60	21   42   60	21   42   60	21   42   60					
	OPEN	Granule	53   83.1   113.5	60   57   60	1.06   1.57   1.99	3.21   4.07   4.34	193.9   386.4   560.7	A 13, 14, 15			
		Powder	58	55	1.16	2.73	2.89	3.88	191.4	517.4	A 16, 17
		Polystyrene Granules	45.6   88	63   60   60	2.54   2.51   2.47	3.88   3.97	201	397.7	A 18, 19, 20		

Table 4.3 : Correlation of mixing disc configuration, polymer form and throughput

A. POLYPROPYLENE GRANULES

Mixing disc	9 rpm	18 rpm		27 rpm	
configuration	output (Kg/hr)	output (Kg/hr)	* ratio	output (Kg/hr)	ratio
open-upstream	33.1 (A1)**	63.8 (A2)	1.92	89.1 (A3)	2.69
closed-upstream	35.3 (A7)	73.2 (A8)	2.07	-	-
closed-downstream	30.8 (A21)	74 (A22)	2.40	105 (A23)	3.40

B. POLYPROPYLENE GRANULES Vs. POWDER

Mixing disc	polymer	9 rpm	18 rpm		27 rpm	
configuration	form	output (Kg/hr)	output (Kg/hr)	ratio	output (Kg/hr)	ratio
Closed-downstream	powder	30 (A24)	64.5 (A25)	2.15	95.4 (A26)	3.18
	granule	30.8 (A21)	74 (A22)	2.4	105 (A23)	3.40

C. POLYPROPYLENE POWDER

Mixing disc	9 rpm	18 rpm		27 rpm	
configuration	output (Kg/hr)	output (Kg/hr)	ratio	output (Kg/hr)	ratio
closed	30 (A24)	64.5 (A25)	2.15	95.4 (A26)	3.18
open	28.7 (A27)	60.1 (A28)	2.09	97 (A29)	3.37

\* It is the ratio of throughput at given screw speed and that of at 9rpm.

\*\* The numbers in brackets refers to run numbers.

is sufficient to generate enough restriction to flow rate, and associated rise in pressure generated. Thus there is associated rise in temperature due to restricted flow and thus melting. However at low screw speed the polymer flow rate is comparatively low and thus less pressure generation at mixing disc (in upstream position). So to generate the similar pressure, more mixing discs are required at upstream position (Fig 3.2).

The increase in output for setting of upstream mixing disc is achieved because there is more space and pressure generation before the vent port section which is available for melting. Besides, the pressure generation in post-vent port section is low. This is due to the presence of mixing disc in downstream position. Otherwise high pressure generated would force the material out of vent port.

On comparing the form of polymer, for closed/downstream setting on mixing disc, the granules show a better output than powder (Table 4.3B - Run A21, 24 and Table 4.2A -Run A21 to A26). The low throughput for powder can be explained by inability of the one pair of melting discs (in upstream position) to completely fuse the powder and thus less compaction of partially molten polymer. As the pressure at vent port restricts the volumetric throughput, the powder throughput reduces due to partial melting and low bulk density. This is clearly shown by associated data on two sets of runs (Table 4.2A Run A21 to 26). Thus granules show higher throughput which leads to higher melt pressure at pre-melting disc position (i.e. upstream) and at die end position (shown by transducers). The runs with powder show higher filled volume (due to early but partial melting of powder) which leads to higher minimum and mean residence time and higher variance. The calculated filled volume studies (Table 4.2A) and barrel withdrawal studies



(section 4.4) confirm that powder polymer gives higher filled volume. Due to low surface area, the granules remain partially fused and thus show much higher melt viscosity and thus higher current consumption and screw torque.

However changing the position of mixing discs i.e. moving the mixing discs to "upstream" position and operating extruder at twice the screw speed (by changing the pulley size in the drive) changes the whole of the scene.

The increased number of mixing discs in upstream position (five pairs Vs one pair) associated with increased polymer flow rate through them (due to increased speed) leads to increase in pressure generation at pre-mixing disc positions (Table 4.1 part 2 Run A13, 15 Vs A16, 17). This helps the melting of the powder and thus better polymer compaction than occurs in the above case (Downstream mixing discs Run A21 to A26). This better melting and compaction leads to the transport of more polymer and thus increase in throughput than with granules. This leads to higher melt pressure at the end as well. However powder still shows a higher variance and filled volume. This is due to early melting of the powder (as discussed above). The granules show a higher current consumption and a higher screw torque (discussed above).

This conclusively proves the part played by the mixing discs in upstream positions as melting discs. This was supported by observations made by barrel withdrawal technique which showed that the polymer melting was substantially improved by the presence of mixing discs in "upstream" position. Besides, the pre-mixing disc space is found to be packed with partially molten polymer if all the mixing discs were present in upstream position. In the case of one mixing

disc in upstream position and the rest in downstream position this space is only partially filled.

The throughput relationship with mixing discs configuration in downstream position while using polymer in powder form shows interesting results (Table 4.3 C Run A24 to A32). At low screw speed (9rpm) the closed disc configuration shows the highest throughput rate followed by open disc configuration. However at higher screw speed (27 rpm) the trend is quite opposite. It could be due to the fact that at low screw speed, the volume of the incoming polymer melt and back pressure generated from mixing disc plays an active part in determining the output. At low speed probably the closed disc configuration (Run A24) consumes a higher power as compared to open mixing disc configuration (Run A27). This results in higher melting and thus better conveyance due to compaction. However at higher screw speed there is a proportional increase in throughput in closed disc configuration as shown by a factor of 2.15 and 3.18 for two speeds (Table 4.3C). But in the case of open disc, there is a substantial increase in output. It could be that enough pressure is generated in these cases to give improved melting and transport as compared to closed discs where optimum is already achieved at low speed.

4.2.2 Melting behaviour: This is an important aspect of extrusion process and it gives a clear indication about physical state of the polymer which in turn determines the flow behaviour. As the physical state of polymer affects RTD substantially, the physical variables which change the melting behaviour, would obviously change the flow behaviour and thus RTD. The melting behaviour is believed to be influenced by screw speed, mixing disc position and configuration, the form of the polymer used and temperature profile. The melting

process will influence the ratio of molten to unmolten polymer in extruder. One typical example for such a relationship between RTD and processing variable is the restriction imposed by vent port. This physical volume conveyance restriction affects the the degree of fill which in turn affects the pressure build up at die inlet and thus in turn the flow profile in main stream. The pressure at die inlet also affects mixing in "C" shape chamber and also leakage at flight tips. Besides, limited melting could affect the unmolten centre position which then affects the flow behaviour. So this change in melting behaviour affects the flow in numerous ways and thus the resulting RTD.

The melting process in single screw extruder is now fairly well understood. Three alternative mechanisms have been found by various investigators.(shown in Fig 4.12 ) as reviewed by Lindt (1981). Mechanism A is characterised by the existence of a distinct melt pool in contact with the pushing flight of the screw (Maddock 1959, Vermeulen et.al 1971). In mechanism B the dominant melt pool is absent but a centre core of solid material is present, which during the melting diminishes in both depth and width. The melt is accumulated in the molten film surrounding the bed. Mechanism C shows the existence of a distinct melt pool in contact with trailing flight. Lindt (1981) explained the reason for change of position of melt pool being cross channel circulation and leakage flows over the flight, which is related to the pressure component of the leakage flow. Fig 4.12 shows schematically the three different flow patterns of the transverse circulation which can arise during melting. The melting mechanism A is essentially closed transverse circulation around the solid bed. The transition from mechanism A to B to C is characterised by circulation pattern being gradually overridden by the leakage flow.

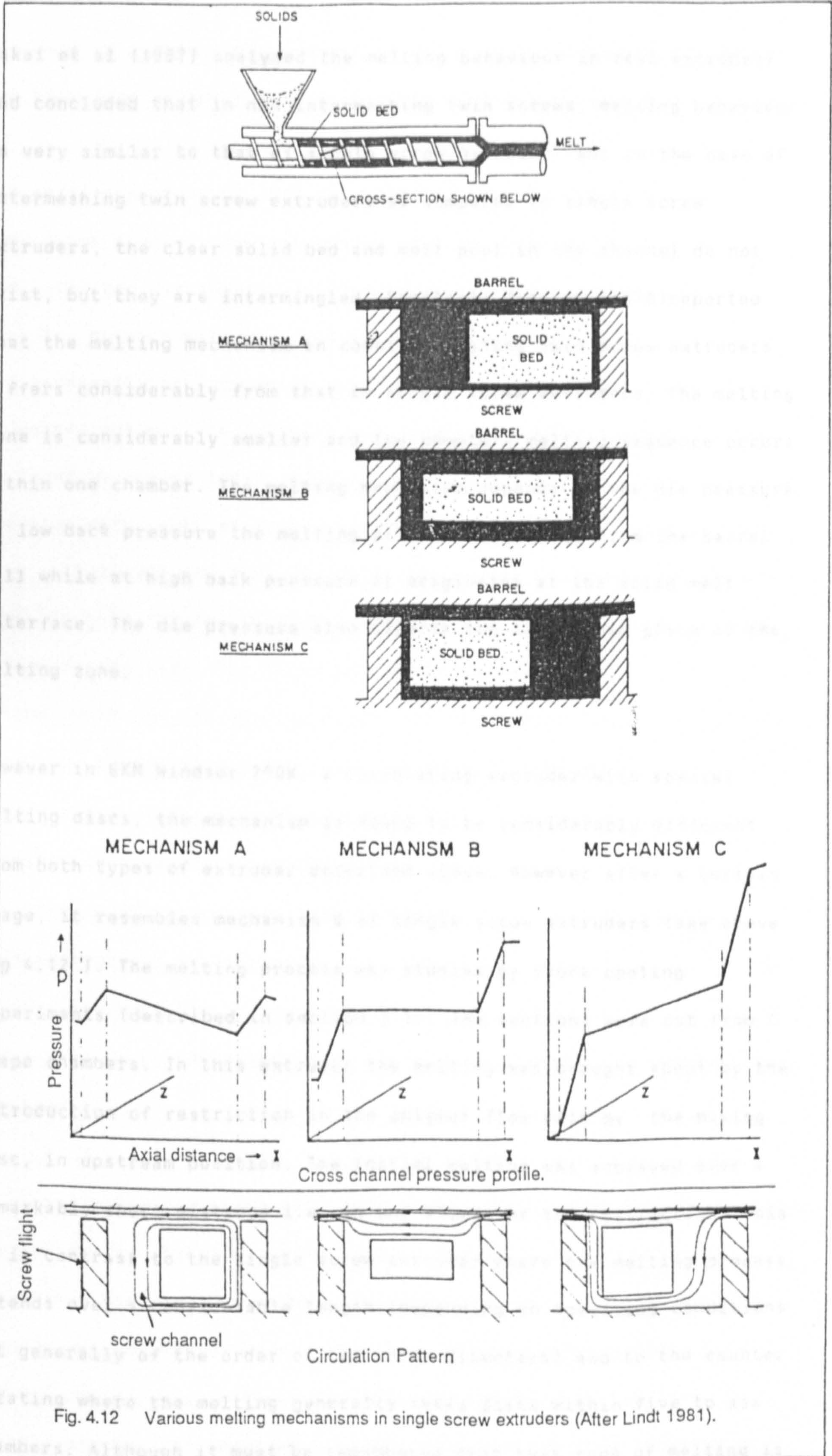


Fig. 4.12 Various melting mechanisms in single screw extruders (After Lindt 1981).

Sakai et al (1987) analysed the melting behaviour in real extruders and concluded that in non intermeshing twin screws, melting behaviour is very similar to that of single screw extruder. But in the case of intermeshing twin screw extruders as compared to single screw extruders, the clear solid bed and melt pool in the channel do not exist, but they are intermingled. Similarly Janssen (1978) reported that the melting mechanism in counter-rotating twin screw extruders differs considerably from that in single screw extruders. The melting zone is considerably smaller and the complete melting sequence occurs within one chamber. The melting mechanism depends on the die pressure. At low back pressure the melting process originates from the barrel wall while at high back pressure it originates at the solid melt interface. The die pressure also affects the length and place of the melting zone.

However in GKN Windsor 250X, a co-rotating extruder with special melting discs, the mechanism is found to be considerably different from both types of extruder described above. However after a certain stage, it resembles mechanism B of single screw extruders (see above Fig 4.12 ). The melting process was studied by shock cooling experiments (described in section 3.5). The sections were cut from C shape chambers. In this extruder the melting was brought about by the introduction of restriction in the polymer flow path by the mixing disc, in upstream position. The initial melting was achieved over a remarkably short distance i.e. in one step-over the restriction. This is in contrast to the single screw extruder where the melting process extends over a considerable length (depending on operating conditions but generally of the order of ten screw diameters) and to the counter rotating where the melting generally takes place within five to six chambers. Although it must be remembered that this type of melting is

achieved as a result of presence of mixing discs in the screw design and therefore is not common to all the co-rotating extruders.

The melting process in this extruder is similar in some aspects to some large single screw extruders. In this, like large single screw, the solid bed was apparently located in the middle of the chamber, once the polymer melt has crossed the main melting discs. The solid bed apparently is located in the middle of the chamber between layers of molten polymer. It steadily and slowly decreases in size (similar to found by Dekker 1976). However the presence of some interruption in the flow path, such as discontinuity in screw thread, can disturb the flow pattern and therefore can force the mixing of molten with unmolten part. In this the low thermal conductivity of polypropylene also plays a significant part. The solid unmolten core represents an isolated polymer unit and its melting depends on the barrel temperature, heat generated by shearing and power consumption during the course of it overcoming pressure barrier at mixing discs. However the solid unmolten core seems to mix fairly well by interruptions in the flow path (Fig 4.67 as given on page number 213) and thus enhances the melting process. The interruptions in the flow path are caused either by the interruptions in the screw flight (due to segmented nature of the screw) or by the presence of the mixing discs etc in downstream position.

In single screw extruders, a similar approach is taken to enhance the melting process by interrupting the solid bed in centre. The ODM (organised distributive mixing, from Rheotec- 1982 ) screw provides homogeneous melt by ensuring a regular, frequent redistribution of plasticated material between the area in contact with the screw flights and that in the centre of the flow path. It does this by a

multiflight screw section with the flight starts staggered circumferentially at an angle between  $120^\circ$  and  $360^\circ$  - Fig.4.63.

4.2.3 Filled volume: The actual filled volume of the extruder is important from the RTD point of view. In a chamber at the hopper end the process material is usually a granular solid and there is a considerable amount of air present. So there can be little pressure difference developed between adjacent chambers (Janssen et.al 1976). For this reason the flow of the material in this part of the machine can be regarded as plug flow. At the first set of mixing discs, melting starts. However the actual extent of melting depends on various variables. Once the polymer is in molten form, flow profiles are formed and RTD results. So it is the molten volume which actually determines the RTD. The filled volume in the twin screw can be dependent on the two parameters.

1. Degree of fill
2. Polymer melt zone length

1. Degree of fill: The degree of fill does not influence the RTD directly. This is because the axial velocity of the polymer melt is independent of the degree of fill of the screw (Booy 1980). However it (degree of fill) affects it indirectly, by creating pressure at the screw tips. The pressure buildup and thus associated pressure gradient affects the polymer flow path (relative flows through various flow paths - as described later on in section 4.4) and the flow profile in polymer melt.

The degree of fill, in GKN Windsor 250X, is influenced by feed rate of the polymer at hopper and by the volumetric conveying capacity of the screw section in the vent port region. However the conveying in the

vent port zone is influenced by melting capability of pre-vent zone of the extruder. The melting capability is the sum of heat input by heater bands and shear heat generated while crossing the mixing discs.

2. The polymer melt zone length affects the RTD in the following manner.

(i) It changes the total filled volume of the extruder, as the different lengths of the melt zone with same degree of fill would give different filled volumes. The conveying characteristics of the filled and compacted volume is different from that of the loosely filled zones.

(ii) The polymer melt zone length, also determines the relative amounts of four possible zones. So in a condition with longer polymer melt zone, the zone where solid/melt co-exist would be longer than the condition with shorter polymer melt zone. Therefore as a result of changing polymer melt zone length, the relative amounts of four possible zone would change. These zones being those of particulate solids conveying, of melting where in solid and melt co exist, of melt conveying by partially filled chambers and of fully filled chambers.

The melt zone length is controlled by melting behaviour which in turn depends on various factors including temperature of polymer, set temperature profiles, polymer form, mixing disc configuration (only in upstream position) and screw speed.

The influence of processing variables on filled volume has been studied by some investigators. For counter-rotating extruder Rauwendaal (1981) has plotted the reciprocal throughput against mean



residence time at different screw speeds and throughputs and found a linear relationship. The proportionality between  $\bar{t}$  and  $Q^{-1}$  indicates that the filled volume of the extruder is about constant. This becomes clear from a well known relationship,

$$\text{Mean residence time} = \frac{\text{Filled volume}}{\text{volumetric throughput}}$$

He concluded that the fully filled length of the extruder varies only slightly with changes in screw speed or in throughput.

Similarly Janssen (1978) carried out work on counter-rotating extruder regarding the melting zone which can be considered to be closely related to the melt zone length studies. This is because the earlier the melting position in extruder the longer would be melting zone. He found that melting starts at a point that is more sensitive to screw speed than to total die pressure. As regards to the melt state, the melting process itself is more dependent on the die pressure than screw speed. So in short, the screw speed does not affect the length but only the location of the melting zone. The die pressure affects both the length and the place of the melting zone. The former effect is a reflection of the time needed to bring the solids up to their temperature.

In the present studies the relationship between the filled volume and mean residence time was studied and it was found that filled volume decreases with increase in screw speed (indicated by the low mean residence time value) for most of the conditions. However for one condition it remains constant (Fig 4.13).

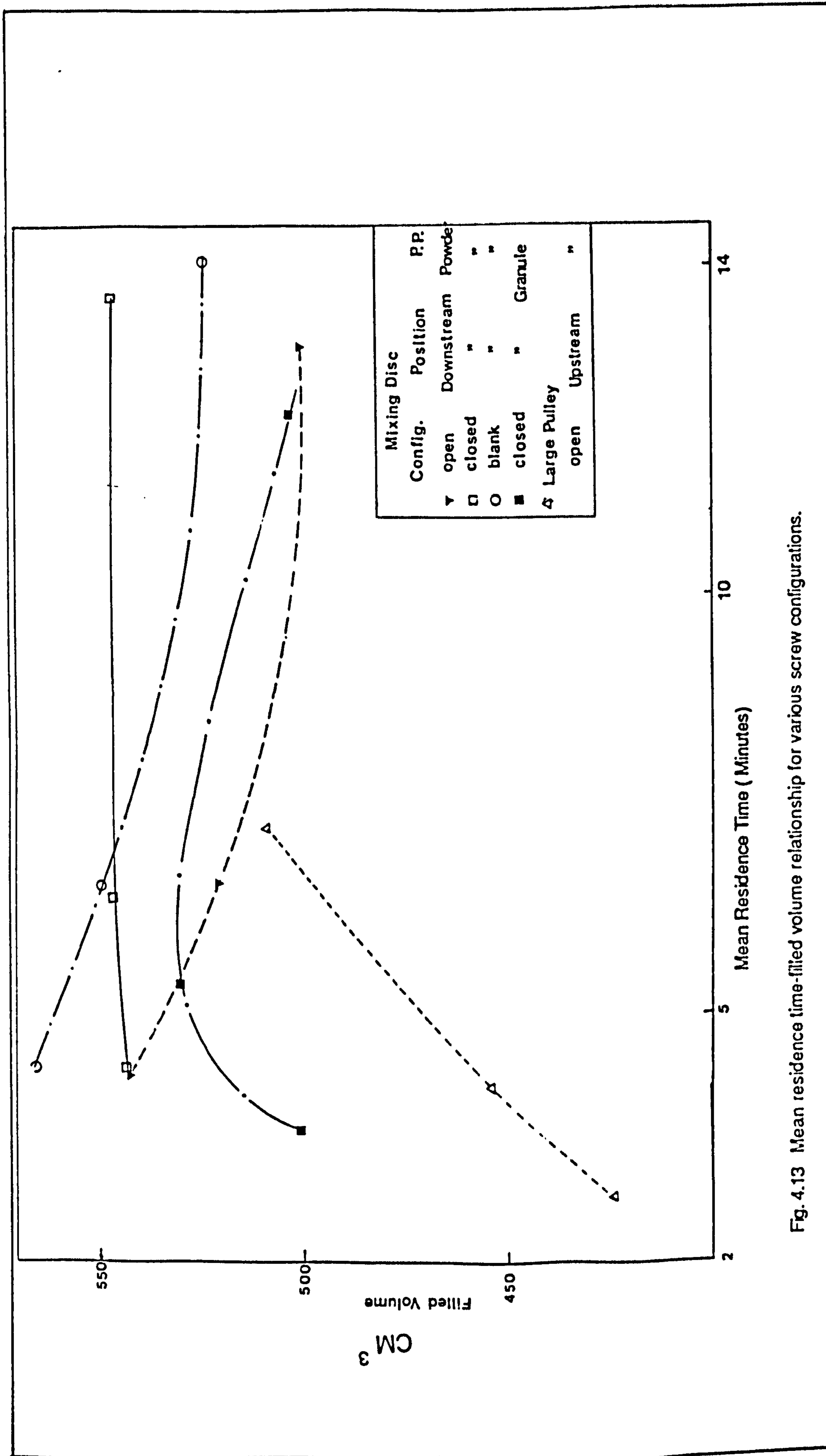


Fig. 4.13 Mean residence time-filled volume relationship for various screw configurations.

Table 4.4 Distribution of the material within the various flights  
in a mixing section after few turns of the screws  
(after Martelli 1983)

No. of turns	1	2	3	4	5	6	7	8	9
0	0	0	0	0	0	0	0	0	0
0	100	0	0	0	0	0	0	0	0
1	30	70	0	0	0	0	0	0	0
2	9	4.2	4.9	0	0	0	0	0	0
3	2.7	18	44	34	0	0	0	0	0
4	0.8	7.5	26	41	24	0	0	0	0
5	0.2	2.8	13	30	36	16	0	0	0
6	0.07	1	6	18	32	30	11	0	0
7	0.02	0.3	2.5	9.7	22	31	24	8	0
8	0.00	0.1	1	5	14	26	29	18	5

The filled volume studies show that it is reasonably constant for various conditions except in low feed rate (A5) or when feed is restricted due to power or torque requirements (Run A13 to 15). The runs with mixing discs in upstream, open position - for both normal and modified pulley system (and thus increase in screw speed) show a decrease in filled volume with increase in screw speed. (Run A1, 2, 3, and A13, 14, 15). The reason for this is that at high screw speed the residence time is low and melting is delayed. The heat needed to warm the solids up is about three times the latent heat required to complete the melting process. ( $2.8 \times 10^5$  J/Kg and  $8.4 \times 10^4$  J/Kg respectively - Janssen 1978). The decrease in filled volume of run with low set temperature profile on extruder (Run A6) can similarly be explained.

However on changing the mixing discs configuration to closed in upstream position or moving these to downstream position, a complete reversal of trend is found. In these cases the filled volume increases with increase in screw speed (indicated by the low mean residence time value). But the reasons for this filled volume in both of these cases are different, as explained below.

For upstream mixing discs in closed position (Run A7, 8) there is a net overall gain in filled volume as compared to upstream open disc configuration (Table 4.2 A). This is probably due to more resistance offered by closed configuration and thus more pressure builds up. This is supported by the shock cooling experiments where an extended polymer melt zone was found before closed mixing discs as compared to open mixing discs (similar to work as shown in Fig 3.3). The increase in pressure build up in front of mixing discs improves melting which in turn helps compaction of polymer and thus overall melt volume

increases in post mixing disc screw section.

For downstream mixing disc position, (Run A21, 22 and 23), however, there is a net overall loss in filled volume as compared to upstream open disc configuration. But in common with above condition, there is an increase in filled volume with increase in screw speed except when available current/torque is a restriction (A23). In this setting (downstream position) only one mixing disc is present in upstream position and it acts as a melting disc. As this one disc is not sufficient to cause restriction to flow, low heat dissipation and thus poor melting and poor packing of polymer results. As transportation across vent-port is restricted by a fixed volume, poor packing of melt leads to reduced polymer transport and thus less filled volume (Run A21 Vs A1). As is clear from the foregoing discussion the vent port makes this machine behave as if there are two extruders in series. Thus it is completely different from any twin screw extruder so far studied by other workers.

However increase in screw speed increases the flow rate of material through melting discs (output/hour/revolution). In these conditions probably the one melting disc, in upstream position, is sufficient to cause a relatively high pressure build up in front of melting disc and thus increase in melting. This leads to compaction of polymer which in turn gives filled volume. A similar trend is observed when using mixing discs in downstream position with polypropylene powder. In the case of closed disc configuration (Run A24, 25, and 26) maximum filled volume is achieved at 9 rpm screw speed. At this screw speed the main melting is done by one melting disc in upstream position while the rest is completed by closed disc configuration. The increase in screw speed does not cause any improvement for this setting. However in

"open disc" configuration (Run A27, 28, 29), at low screw speed the filled volume is low due to poor melting by the first melting disc in upstream position and less contribution by open discs in the downstream position. But increase in screw speed causes the pressure build up at first melting disc and consequently increase in filled volume occurs. This is enhanced by contribution of open mixing discs which, due to increase polymer flow rate, exert a significant back pressure or rather a restriction to flow.

The melting characteristic of powder polypropylene is quite different to that of granules. The large surface area of powder enhances the melting rate and thus for similar heat available powder shows a faster melting. The bulk density of the powder is low as compared to granules. On comparing the powder with granules for similar conditions, (Run A21 to A24) although the melt temperature is similar, the throughput and thus melt pressure are higher for the powder indicating that powder has higher filled volume. This is probably due to early melting in powder which leads to overall longer molten zone rather than filling of the chambers.

4.2.4. Power consumption: This is an important consideration from technical as well as economic point of view. As described in Chapter 4, a minimum amount of energy consumption would be desirable to achieve good distributive and dispersive mixing.

In this work, power consumption was studied by calculating the specific energy consumption (SEC) and polymer processed per unit current (Throughput/current). Net SEC (specific energy consumption) was calculated from screw torque and screw speed as follows.

$$\text{Specific energy consumption} = \frac{2 \pi \times n \times M}{m}$$

where  $n$  = Screw speed (Rev/sec)

$m$  = Mass throughput rate (Kg/sec)

$M$  = Screw torque (NM)

Whilst,

Screw torque (NM) = Force (Kg)  $\times$  9.8  $\times$  distance (M)  $\times$   $\cos 22^{\circ}$  \*

\* Strain gauge attached to fly wheel at  $22^{\circ}$  angle.

The net SEC can be indicative of shearing undergone (work input) by the polymer during its passage through extruder. By carrying out theoretical work Denson and Hwang Jr (1980) concluded the following points.

1. One third to nearly half the power is consumed in the clearance region of the co-rotating twin screw extruder.
2. The power consumed in flow in the cross channel direction (Circulatory flow within the channel) is rather negligible.
3. There is a linear relationship in power consumed with flow rate and pressure gradient in the down channel direction (axial flow down the channel).

The effect of various factors on SEC can be explained as follows. The mechanical energy from the extruder motor is transferred into heat by frictional and viscous resistance. It follows that filled volume or higher pressure at screw tips would also lead to higher torque, provided other variables remain constant. This is because unmolten polymer, due to its particulate structure (in unconsolidated form as compared to molten form where the granular boundaries disappear), does not offer significant resistance to screw rotation as compared to

polymer melt. In short a higher SEC value would lead to excessive generation of heat and hence a temperature rise. The individual cases will be discussed under separate headings. But for general interest the cases dealing with throughput rate and mixing disc configuration are discussed.

4.2.4.1 Throughput Rate: The condition with low throughput rate (Run A4 -see table 4.1 part 1 for details on runs and table 4.2B for SEC values) shows a low SEC value, and marginally higher throughput/current value as compared to the run with similar conditions but higher throughput rate (Run A5). The run with low throughput rate shows a decrease in filled volume. So it is clear that decrease in filled volume leads to low SEC. However it was found that once the extruder is nearly full, any increase in throughput leads to a sharp increase in the power consumption. The barrel withdrawal studies (discussed in section 4.4) have conclusively proved (section 4.2.1) that increase in throughput rate increases the overall fill of the screw and thus filled volume (Fig 4.11). Thus this increase in filled volume probably leads to more leakage flow which leads to sudden increase in power consumption. This result is similar to the result of theoretical work carried out by Denson & Hwang Jr who stated that the One third to nearly half the power is consumed in the clearance region of the co-rotating twin screw extruder.

4.3.4.2. Mixing Disc Configuration: On comparing runs at high speed with mixing disc in downstream position (A26, 29, 32) it becomes quite clear from throughput/current ratio that closed disc configuration consumes more energy than when discs are open. However it is not advisable to compare results at different screw speeds. This is because not only the throughput is changed but associated losses in



the drive occur together with the lateral forces on the screws which are obviously related to power loss. The heat transfer from heater bands is low and to maintain the enthalpy of system, more mechanical dissipation has to occur and thus more loss of power.

### 4.3 INFLUENCE OF VARIABLES ON RTD :

The residence time of a polymer particle leaving the co-rotating twin screw extruder consists of the sum of the residence times it experiences in the solid transport zone ( $t_s$ ), melt zone ( $t_m$ ) - a zone where the polymer is fully molten but the chambers are only partially filled (this also includes the devolatilization zone) and pump zone ( $t_p$ )- where chambers are fully filled and pressure build up occurs.

The influence of the die can not be overlooked. However it is assumed to be constant within the range effect of variables.

$$t_t = t_s + t_m + t_p$$

Firstly the general flow mechanism of polymer melt along the screw is discussed in detail together with all the possible leakage flows. The effect of a selected variable is assessed by studying.

1. the associated changes in other variables (i.e. variables not changed willingly). This is because in extrusion process, the variables are interdependent.
2. the effect of all these changed variables on the overall flow mechanism. These variables affect by changing
  - a. the flow path available to polymer
  - b. melt state of the polymer which includes the filled volume and length of the complete melt zone, i.e. zone filled with molten polymer (both semi and completely filled). This includes the

effect of leakages.

a. Flow path.

The flow path contributes considerably in spreading RTD. The passage formed by the trapezoidal channels is triangular in shape and its area is defined by the angle of the flank of the flights (Fig 4.62). Due to this change of shape at intermeshing zone, a considerable amount of reorientation of the material takes place. Furthermore, because of differences in diameter in which the material lies, different linear velocity results for different layers. So the high linear velocity for the layer near the tip of flight and lower for those near the core of the screw causes mixing. The division of the melt at intermeshing zone enhances the spreading of the melt. This is shown in Table 4.4 and Fig 4.16 where the colour of the material is suddenly changed and the concentration of the old material in the first flight decreases very rapidly (Martelli 1983).

b Melt State of the Polymer.

i) Flow in first two zones:

It has been shown that in a single screw extruder the first two zones contribute very little to the spread of RTD (Lovegrove and Williams 1973). In the first two zones, i.e. in solid transport zone and in the melt zone the leakages are negligible and the flow in these zones can be assumed to be plug flow. Furthermore Kemblowski and Sek (1981) have shown that in a single screw extruder a relationship exists between the RTD concerning melt extrusion as well as plasticating extrusion, which indicates that RTD of the material in the extruder depends on the flow mechanism in the pump zone. The contribution of the melt film to the RTD was investigated by Lidor and Tadmor (1976)

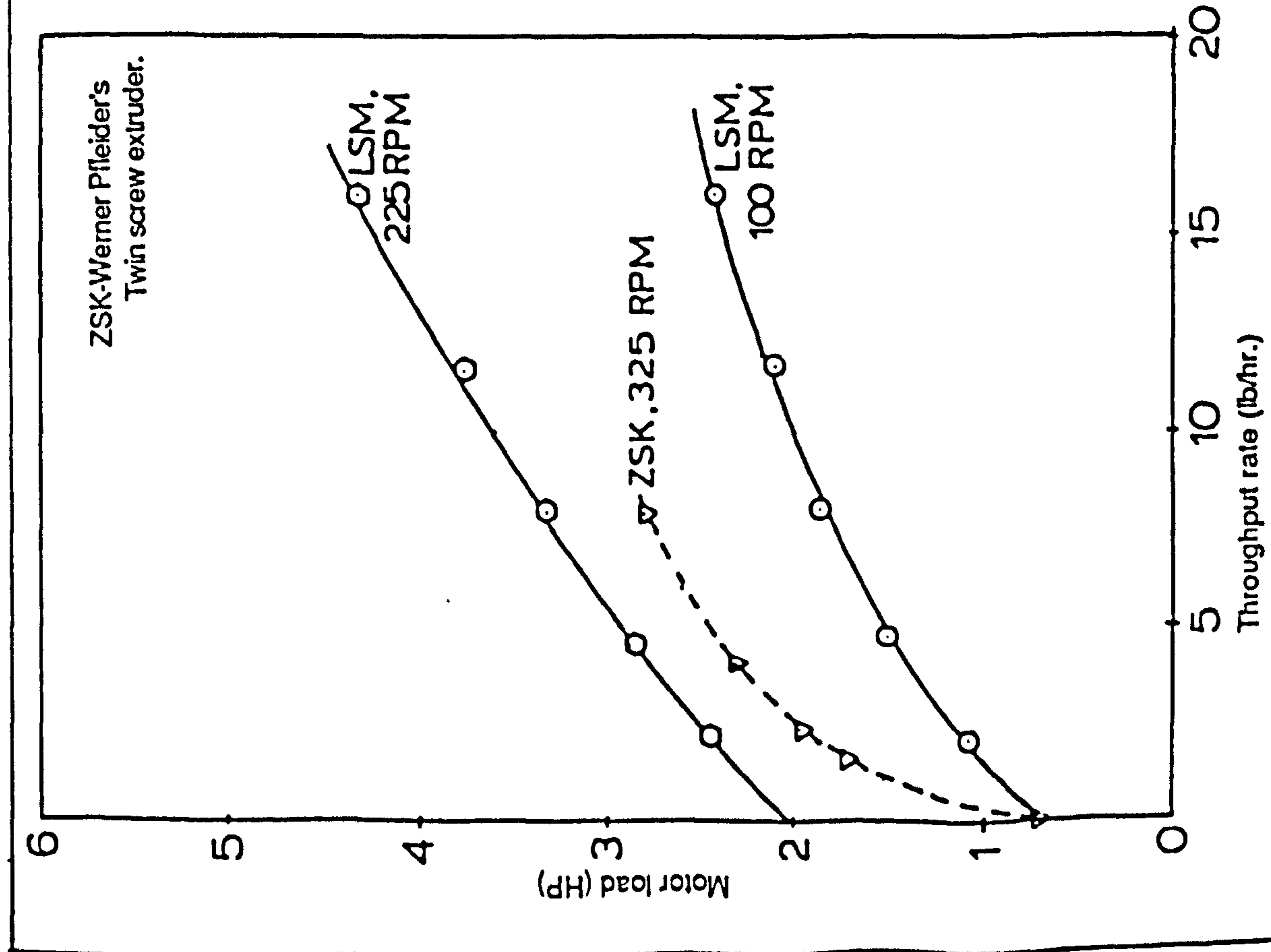


Fig. 4.14 Relationship in throughput and motor load for different extruders (Rauwendaal 1981)

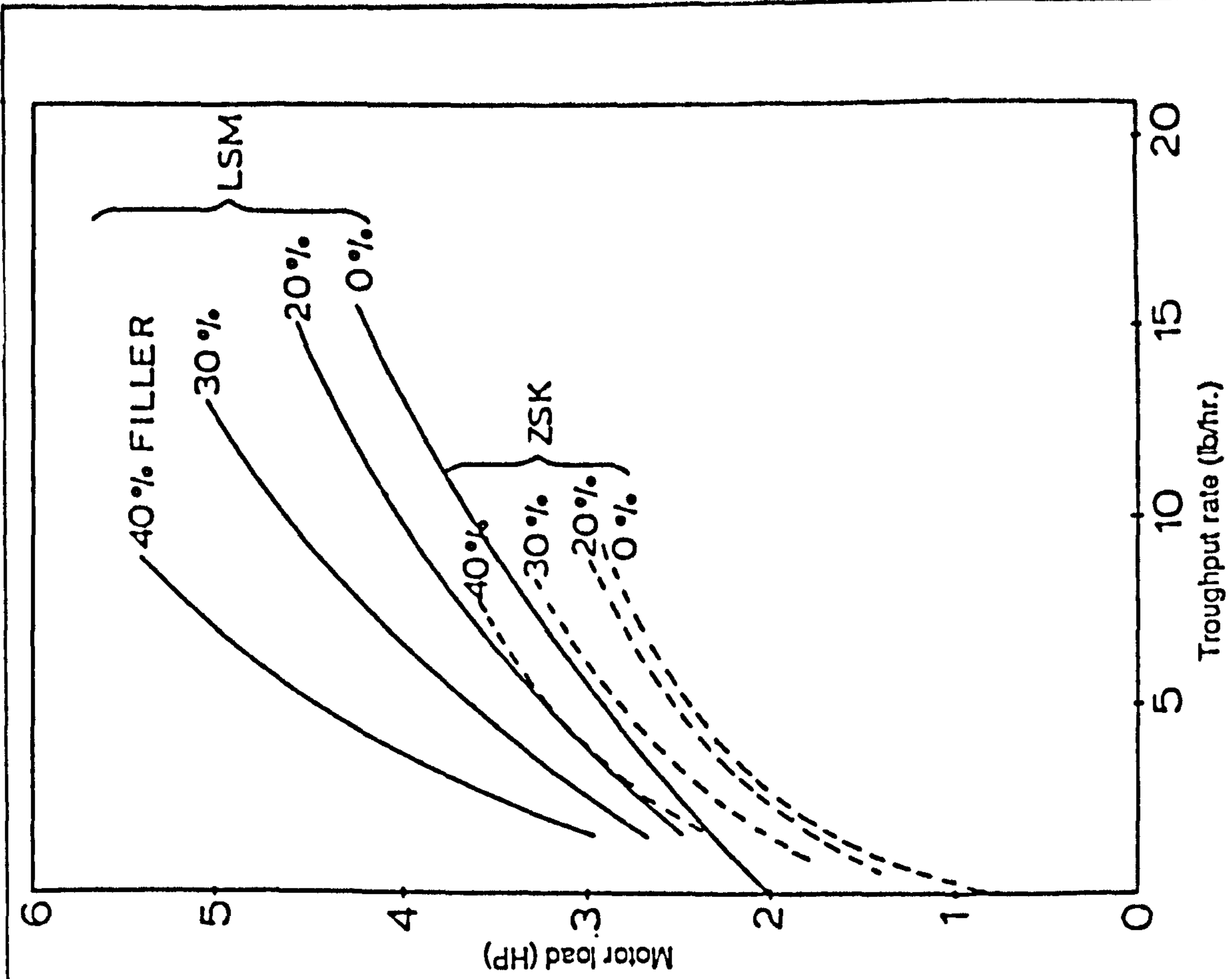


Fig. 4.15 Relationship in throughput and motor load for filled materials for two extruders (After Rauwendaal 1981).

Fig. 4.16 Distribution of material within various flights for two conditions (Martelli 1981).

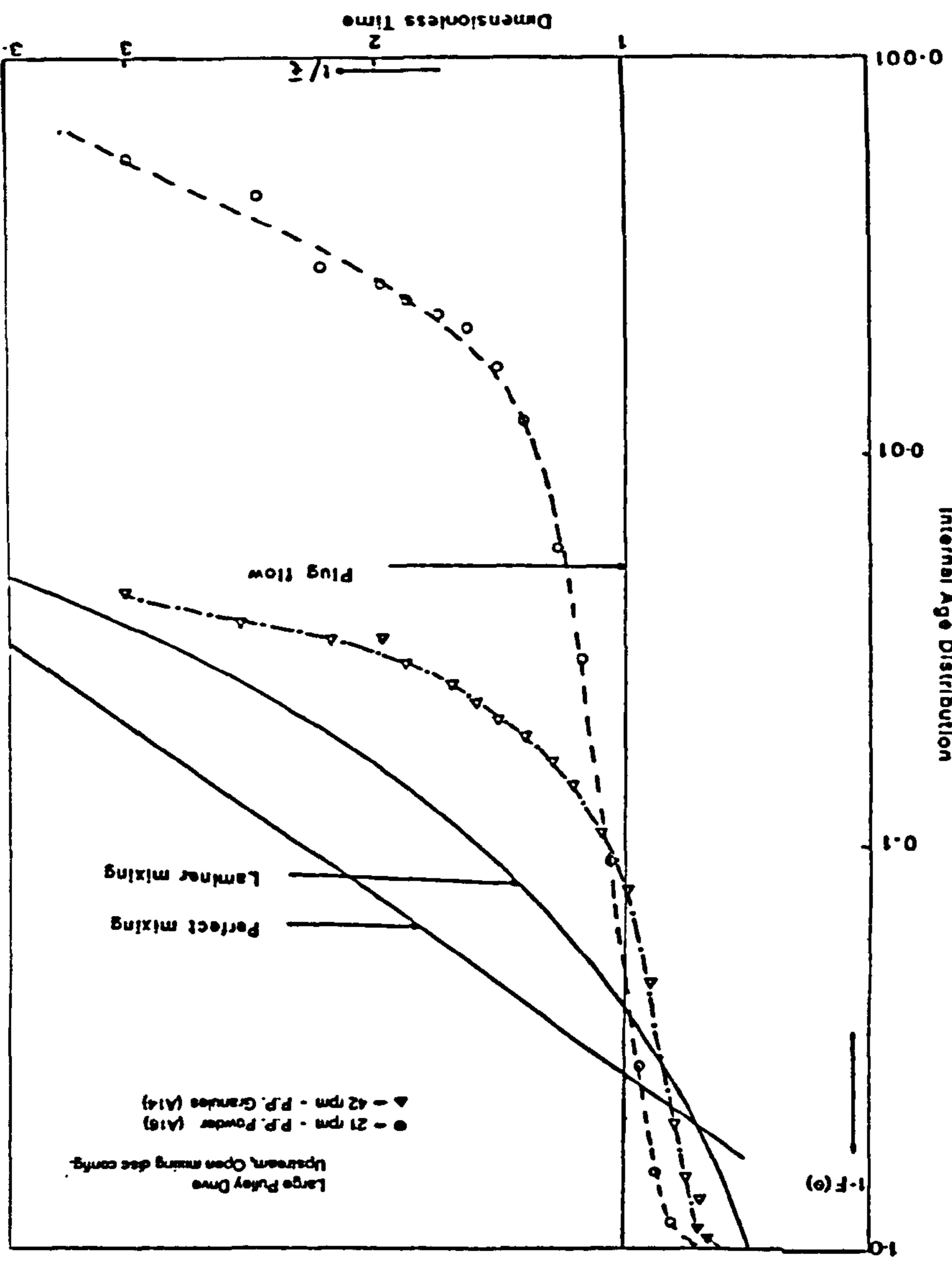
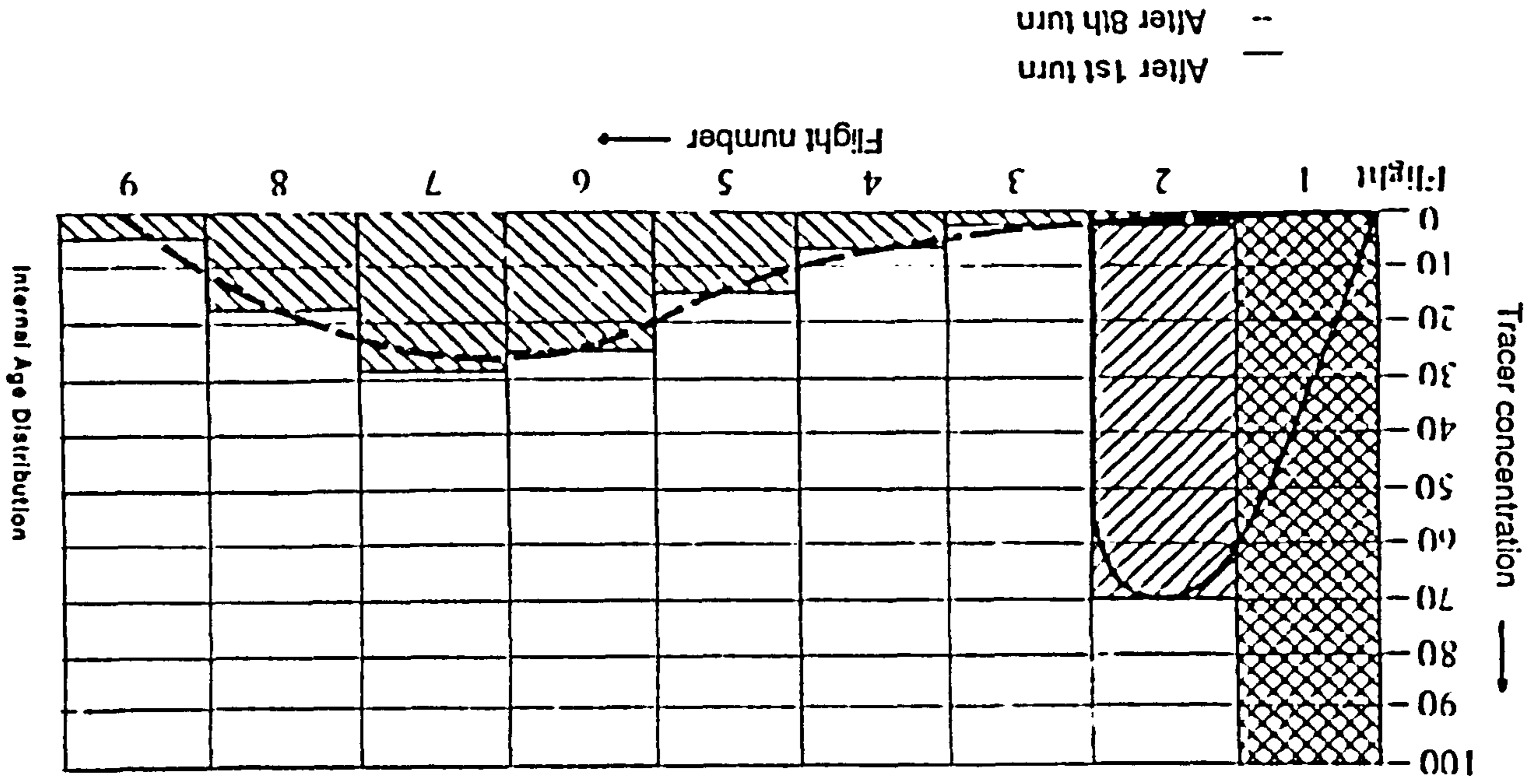


Fig. 4.17 RTD for some ideal flows together with results from

GKN Windsor 250X twin screw

in single screw extruders. Their result indicated that the contribution due to melt film in RTD was negligible.

On transferring the above findings to the first two zones of twin screw extruder the following becomes apparent. The polymer in the first two zones is in a non-molten state, so that distributive mixing due to flow profile in polymer does not take place. Consequently plug flow occurs. But due to different flow paths formed, along the screw, some spread in RTD occurs (Fig 4.54). These different flow paths are formed as a result of intermeshing of two screws (as discussed in point "a" as above). The flow of polymer and its distribution in various other chambers are shown in Fig 4.55.

ii Flow of polymer in pump zone: The flow of polymer in this region results primarily from frictional and viscous forces. But due to intermeshing screws (unlike single screw) the material is constrained and physically prevented from rotating with the screws. A barrier is formed for backflow due to intermeshing regions thus giving a limited positive displacement action. The balance between drag flow and pressure flow largely determines transport due to the openness of the channel. The conveyance never reaches zero even in difficult cases, as in sticky materials. This is because of the wiping action of the screws. Therefore a so-called forced conveyance exists. The material is redistributed at the intermeshing zone. This flow behaviour is discussed in detail in section 4.4 .

For the ease of understanding some typical RTD curves together with some extreme results from present studies are shown in Fig 4.17. This figure shows that the flow in GKN Windsor varies from one extreme (approaching to plug) to another extreme (approaching laminar mixing).

Some further information was extracted out of the RTD curve obtained from these studies, similar to the approach taken by some researcher earlier (discussed in section 2.2.7). The holdback area and dimensionless variance were calculated from the RTD curves. The hold back area gives an indication of the overall flow pattern. This is somewhat similar to the concept of blending efficiency and therefore the blending efficiency is not calculated. The dimensionless variance gives the measure of the spread of the distribution about the mean. This in turn gives an indication of the axial mixing of the extruder. As regards the flow models, the flow model based on the concept of plug flow number fails to represent the present flow. The model flow based on this plug flow number shows a straight line relationship on log linear plot whilst the RTD curves from the present work show a non-linear relationship on similar axes.

Now having covered in general the flow and RTD characteristics, the effect of various variables can be studied.

For convenience, the variables are considered in three categories:

1. Processing variables
2. Machine variables
3. Materials variables

The processing variables are those which can be changed by the machine controls instantaneously, while machine variables are those which necessitate change in hardware of the machine. The material variables are self explanatory. The detailed conditions of each run are shown in Table 4.1. and details on the variables studies are given in table 3.2.

4.3.1 Effect of throughput rate: In closely intermeshing twin

screw extruders, the throughput rate is a realistic variable as the extruder shows a positive conveyance of the polymer, largely independent of the frictional relations.

At a constant screw speed in GKN Windsor, the throughput rate and consumed current show a linear increase initially. But at higher throughput rate there is a substantial increase in the current with a small increase in throughput rate. From this it follows that it is not always economical to obtain maximum output from the extruder but instead to operate it at slightly lower throughput. Conventionally up to now the generally applied limitations on output used to be the acceptable melt temperature and process stability. But in view of above observation the efficiency should also be added to the list.

The effects of throughput rate have been extensively studied by various investigators. In the present work two different throughput rates at a constant screw speed were compared. The first throughput being the maximum achievable and second being 13 % less than the first (33.1 kg/hr vs 29.8 kg/hr - Run A4 and A5). This reduction in throughput rate leads to a 30 % decrease in melt pressure at the screw tip (from 2.27 to 1.58 MN/m<sup>2</sup>). Obviously this decrease in the melt pressure would reduce the associated leakage flows in the completely filled zones especially towards the screw end. The polymer processed per unit current (the ratio of throughput rate and current) shows an increase with decrease in throughput thus indicating less work input to the polymer at low throughput level (Table 4.2). This again adds evidence to the above stated observation that increase in throughput, at the same screw speed, leads to a substantial increase in current consumption. This is associated with decrease in screw torque which once again reflects the smaller work input.

The change in throughput rate affects residence time significantly. The minimum residence time increases slightly in real time value with decrease in throughput rate (from 9.25 to 10 minutes). Similar trends were observed by Rauwendaal (1981) and Walk (1982). The work by Rauwendaal shows that the relationship in throughput and minimum residence time is a hyperbolic one (Fig 4.19). Walk observed that increase in throughput rate is associated with decrease in the minimum residence time which tends to level off at higher rates. However a completely reversed relationship is seen if the residence time values are made dimensionless. The results from the experiments carried out show a decrease in minimum residence time (dimensionless) with reduction in throughput rate (from 0.8 to 0.77 - Table-4.2A) thus tending towards Newtonian fluid flow for which the value is 0.75. Walk's results, if converted to dimensionless form, give similar trends.

Mean residence time, however, increases with decrease in throughput rate (Table-4.2A), similar to that reported by Walk (1982), Hermann and Eise (1981) - Fig 4.20. The barrel withdrawal results (Fig 4.11) show that increased throughput rate leads to highly filled screw sections. The longer mean residence time at low throughput rate, at the same screw speed is caused by the available free space as compared to the higher throughput case where a higher filled volume shows that the screw sections are more packed. The packed screw sections give polymer melt little chance to "rattle around" or rather restricts the free movement of polymer melt in the "C" shape channel. Similarly Tucker and Nichols (1987), by their work on counter-rotating non-intermeshing twin screw extruder, have found that the mean residence time varied approximately linearly with the inverse flow rate. They



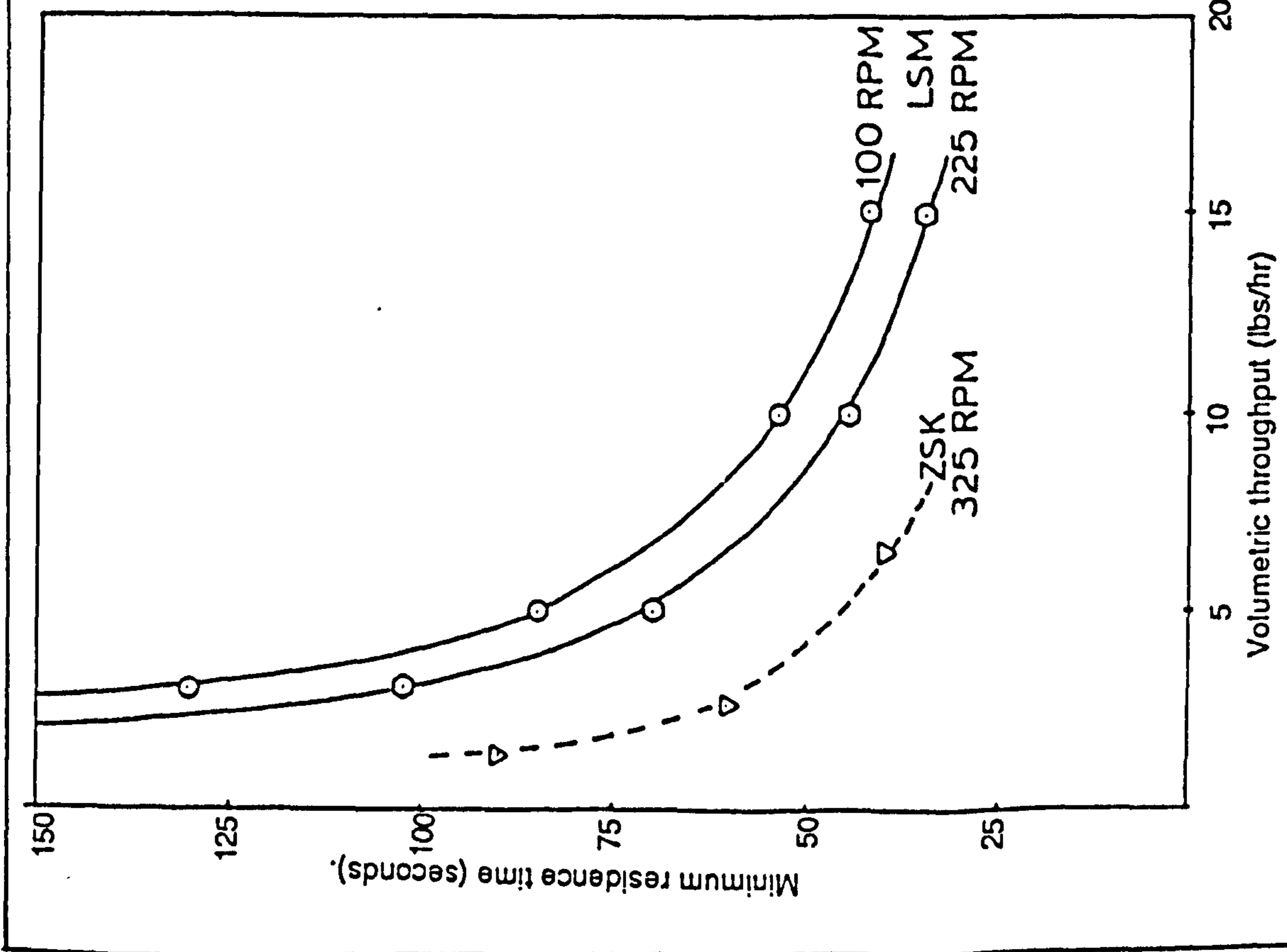


Fig. 4.19 Relationship in throughput and minimum residence time (Rauwendaal 1981).

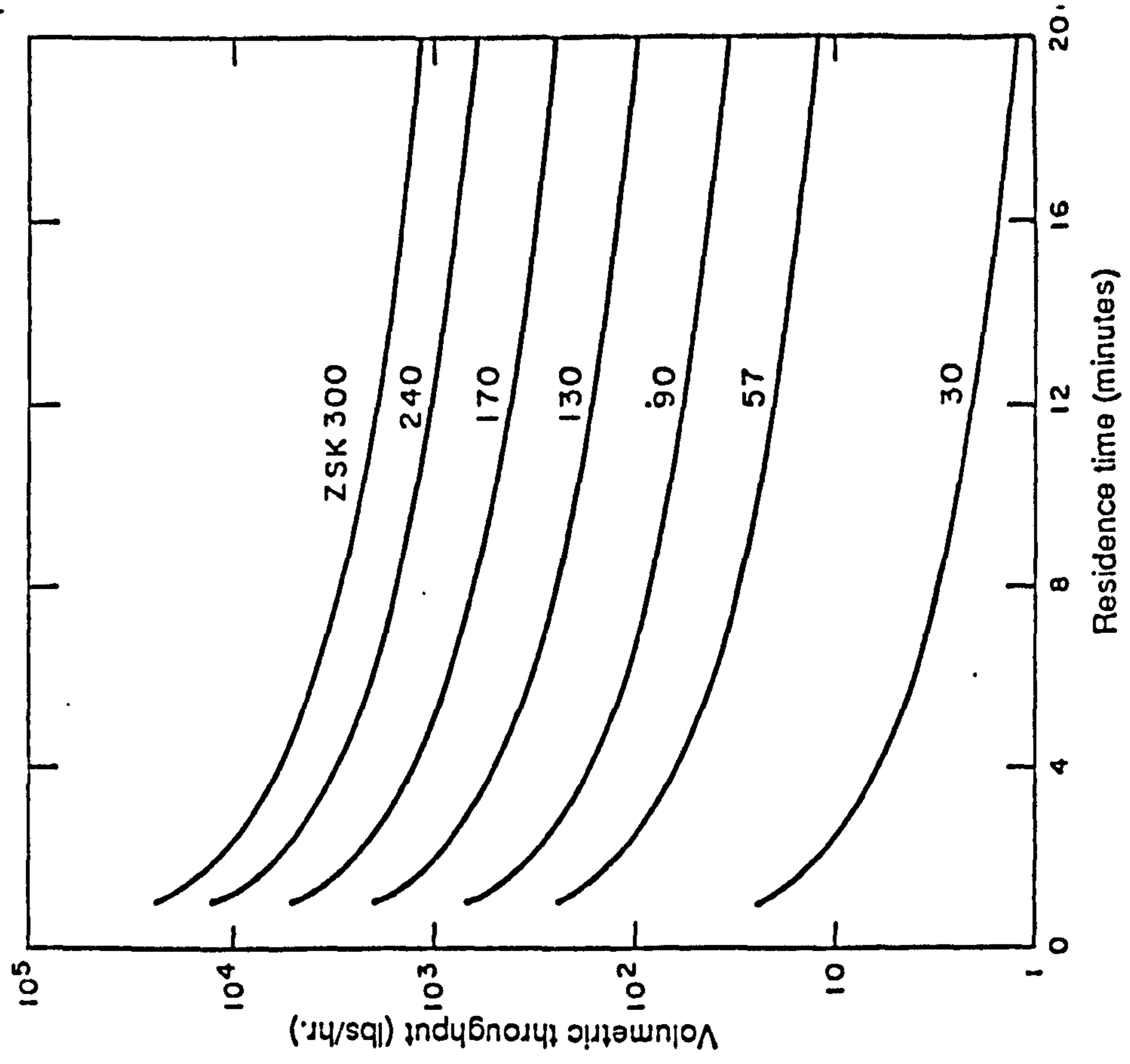


Fig. 4.20 Relationship in throughput and residence time (Herman and Eise 1981).

have, in their paper, presumed it to be an effect of free volume.

The effect of throughput rate on the overall RTD is being extensively studied by various other investigators. Theoretical studies based on a Newtonian isothermal flow model in single screw extruder (Pinto and Tadmor 1970) show that RTD is not affected by processing variables. But the model taking account of curvature indicates that the RTD is dependent on the operating conditions. Pinto and Tadmor (1970) have shown that the deviation from the parallel plate model increases as the flow rate is increased at a constant screw speed (Fig 4.21). At high throughput rate the conveying becomes more positive moving nearer to plug flow. Similar results were reported by Bigg and Middleman (1974) who showed that for a fixed power law index fluid the same behaviour is observed (Fig 4.22). In this figure  $G_z$  is variable throughput. In the present studies, a similar trend was observed. When plotted on the same axes, (as that of Bigg and Middleman 1974), the curve shows the same trend as that of Bigg and Middleman. Low throughput has relatively less portion of flow as vertical line (vertical portion represents plug flow). High throughput shows more plug flow. However as both of these conditions represent rather highly filled volume, the extreme case of low throughput (e.g.  $G_z = 0.5$ ) is not seen. This is also clear from Fig 4.23 which shows that the flow becomes more positive (move towards plug flow) at higher throughput. The lower throughput shows early emergence of melt, and 90 % of the material leaves at less time (dimensionless) than that of higher throughput rate, but last 10 % shows much longer and broader tail suggesting more axial mixing overall. Similarly Rauwendaal (1981) showed both in co and counter-rotating extruders that high degree of fill gives more plug flow behaviour (Fig 4.24). The results from the present work are plotted on the same axes (Fig 4.24). It

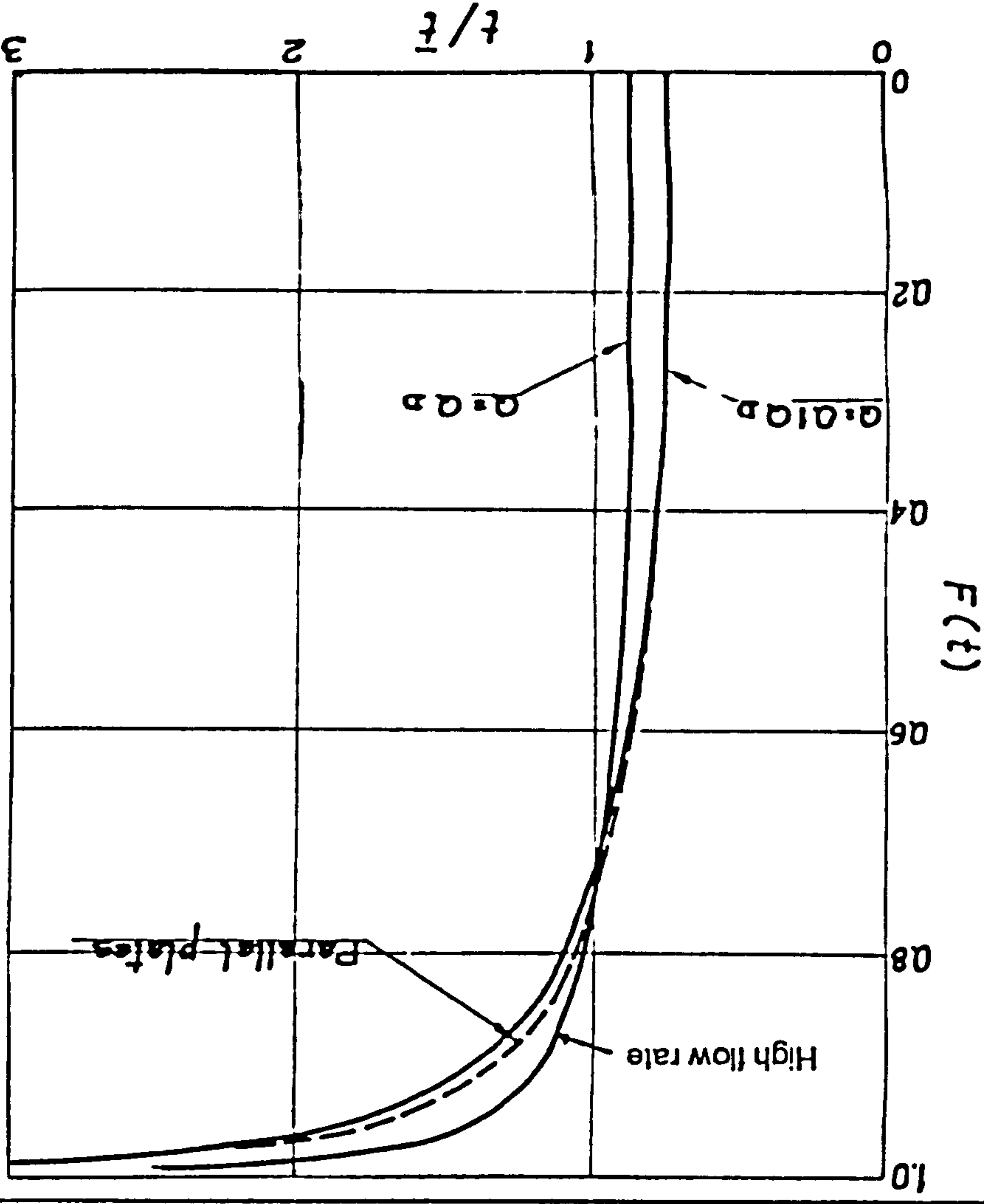


Fig. 4.21 Acomparison of the function  $F(t)$  calculated on the basis of

the "parallel plate" and "curved channel" models (After Pinto & Tadmor 1970)

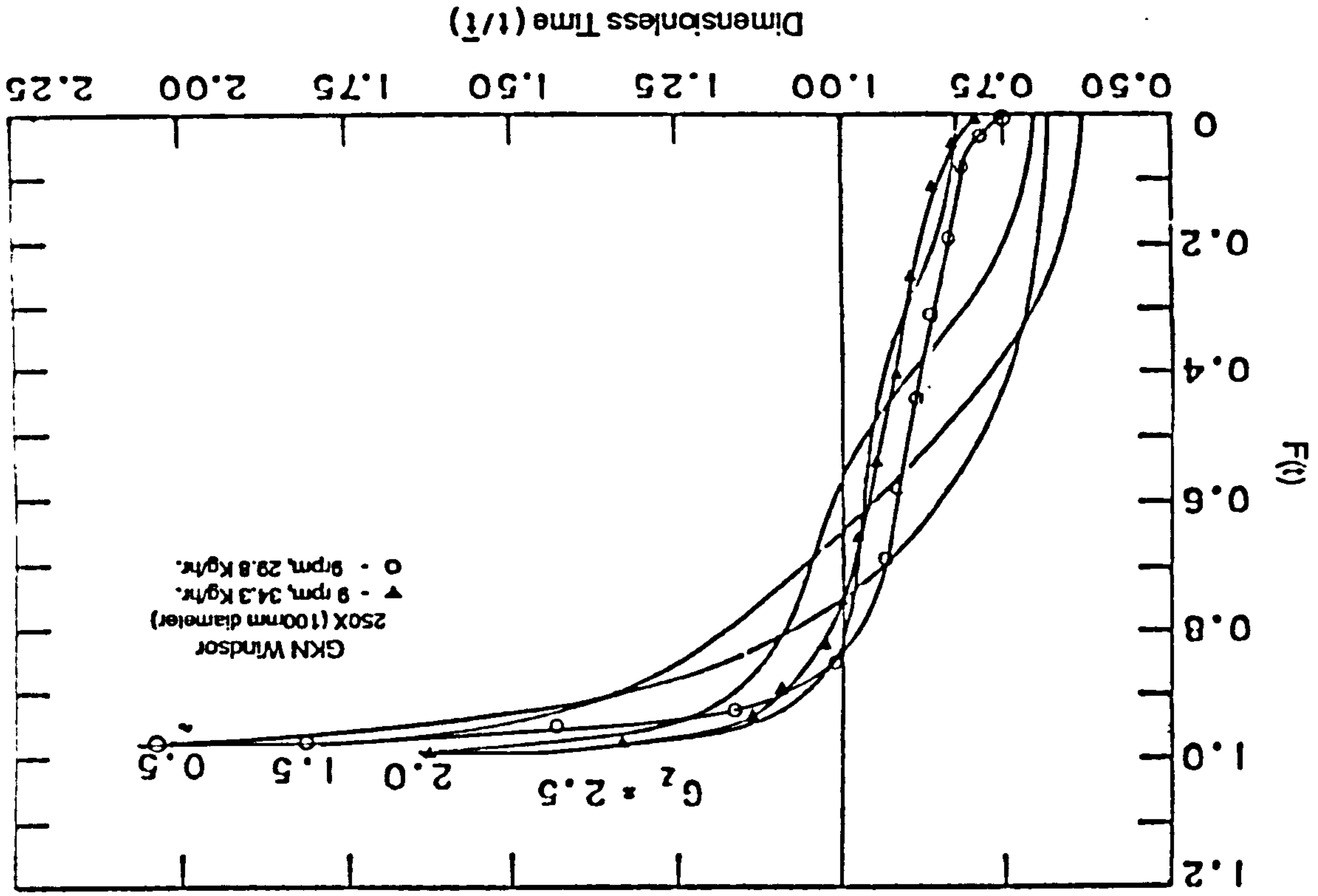


Fig. 4.22 RTD curve for various variable throughputs ( $Gz$ ) for fluid with power law index of 0.2 (after Bigg and Middleman 1974) together with experimental results on GKN Windsor 250X

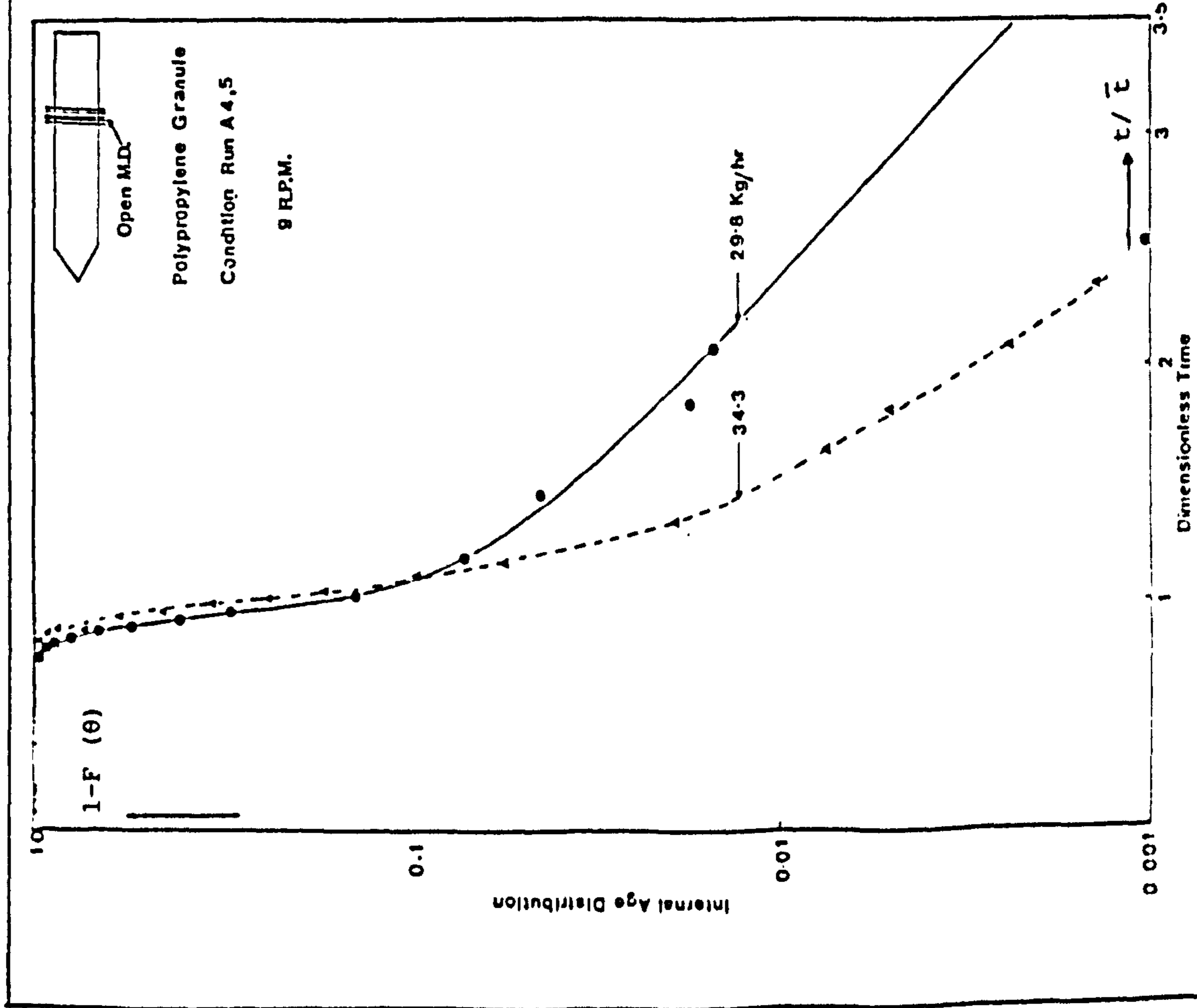


Fig. 4.23 Effect of polymer throughput rate on RTD.

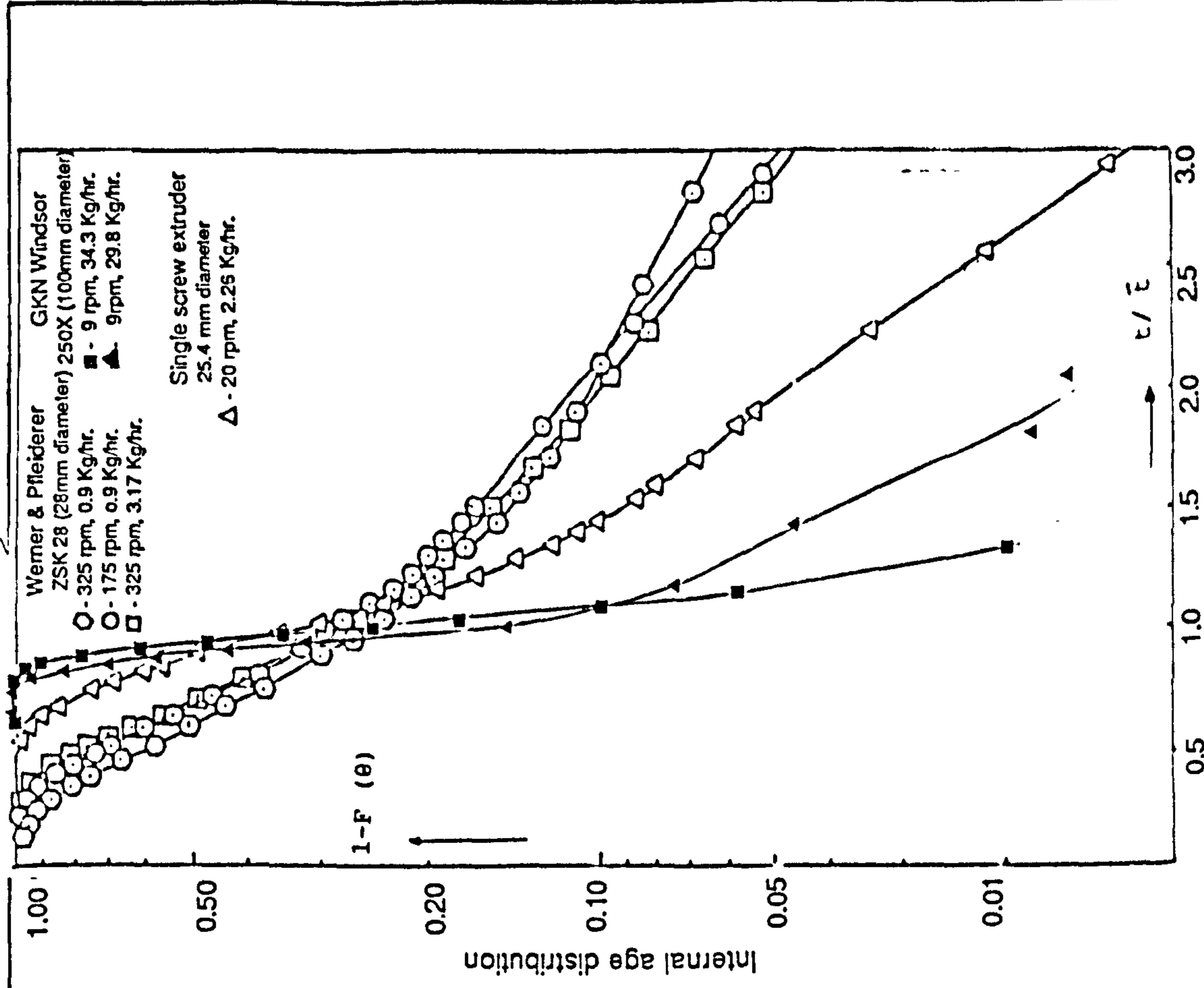


Fig. 4.24 RTD for different extruders for various conditions (results for single screw & Werner Pfleiderer are from Rauwendaal 1981).

shows a similar trend to that found by Rauwendaal (1981). However the flow curve is quite revealing. It shows that the flow in GKN Windsor is substantially more plug type than the extruders tested by Rauwendaal (1981) viz. Werner & Pfeleiderer.

The reason for plug flow behaviour at higher throughput rate could be as follows.

1. At low throughput rate, the filled volume decreases as compared to that at high throughput (shown by barrel withdrawal experiments - section 4.2.3). So at low throughput rate, the polymer has more unoccupied space inside the screw channel (because of low amount of polymer melt inside the extruder) during passage through the extruder. This could lead to more free movement rather than compact movement (as in high throughput) and could lead to more intermixing with other polymer axially and thus to greater axial mixing.

2. The heat for melting is derived from shearing of the polymer and from heat transfer from barrel wall. For the same heat input from the heater bands, there is restricted melting at higher output at same screw speed. This is because less energy per unit polymer mass is available at high throughput rate as compared to low throughput rate at the same screw speed. Furthermore the increase in throughput rate is associated with a decrease in residence time, and this once again reduces heat transfer (due to limited time available inside the extruder) and thus melting. In the present work it was found that at higher screw speed and at higher throughput rate a certain amount of unmolten polymer was coming out in the extrudate. The partially molten polymer does not show a typical viscous flow and up to a certain level of unmolten fraction shows a rather plug flow motion. This is because of restricted motion and difficulty in slipping past other polymer

particles. This above explanation is further supported by the work of Lidor and Tadmor (1976) who have reported similar results for 2.54 cm diameter single screw extruder (Fig 4.25). They show that at a given throughput rate the RTD curve shows a good axial mixing. However, as the throughput rate is increased, the RTD curve starts to show a portion of vertical line (see Fig 4.25). This portion in the curve increases as the throughput rate is increased. They found this to correlate with the amount of solid or unmolten particles in the extrudate.

3. The velocity distribution is dependent on the position of zero shear stress point ( $Y_{oz}$ ). This is a function of pressure gradient, viscosity etc. (Hermann, Burkhardt and Jakopin 1977). The flow rate and  $Y_{oz}/h$  (where  $h$  is height) are dependent on each other, and thus changing the throughput does change velocity distribution which once again changes the RTD.

Todd (1974) showed that in co-rotating extruders, axial mixing was much more strongly affected by equipment features than by feed rate. When plotted on log probability paper, different feed rate does give similar conveying for 90 % of material, but the other 10 % of material flows in a different manner. The material stagnates at higher throughput rate. A similar trend was seen in the present work when plotted on log probability paper (Fig 4.27). However, in this case 80 % of the flow (rather than 90% as discussed above) shows a rather flat and linear relationship between the dimensionless time and internal age distribution, but for the last 20 % of the flow, the flow characteristic changes and it appears as if this portion of flow (20%) is following a different regime. On the same figure (Fig 4.27), the results from work of Todd (1969) are plotted. This comparison shows

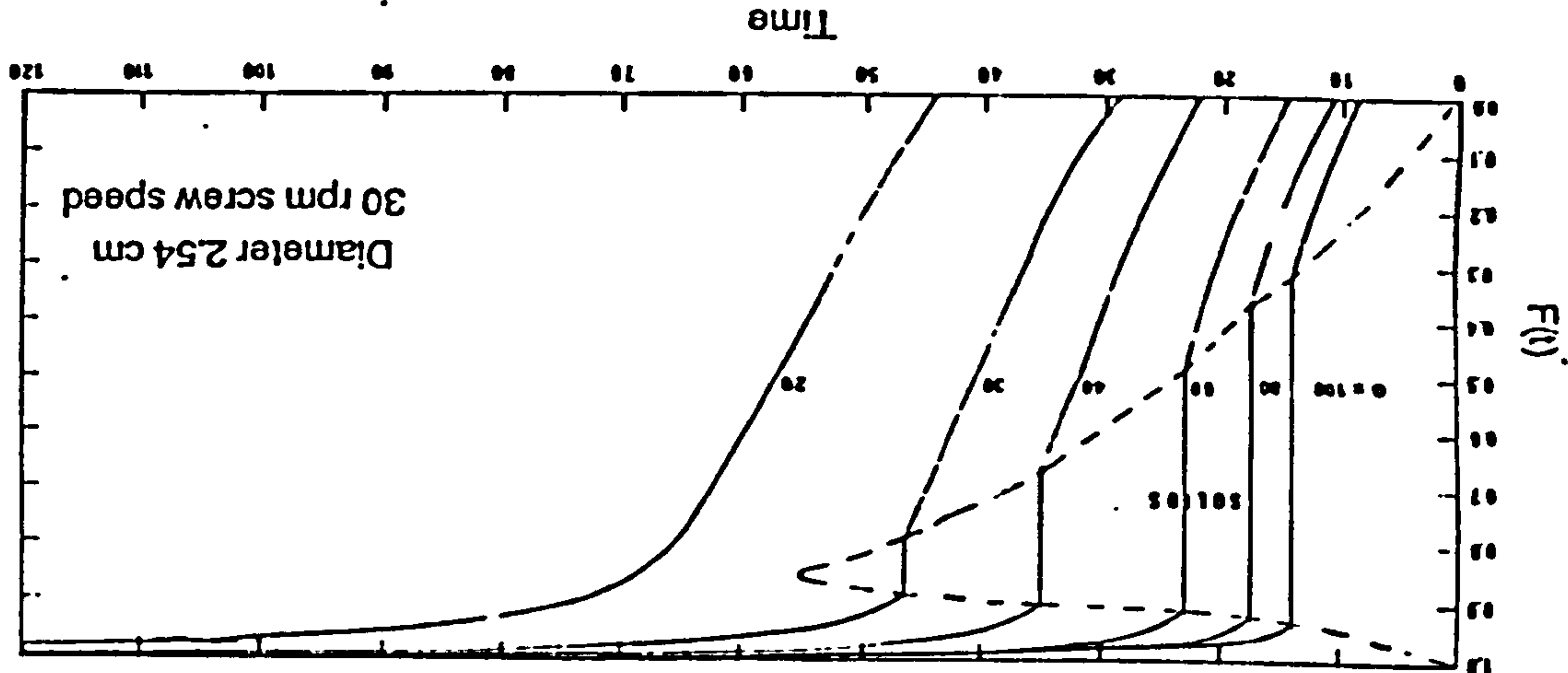
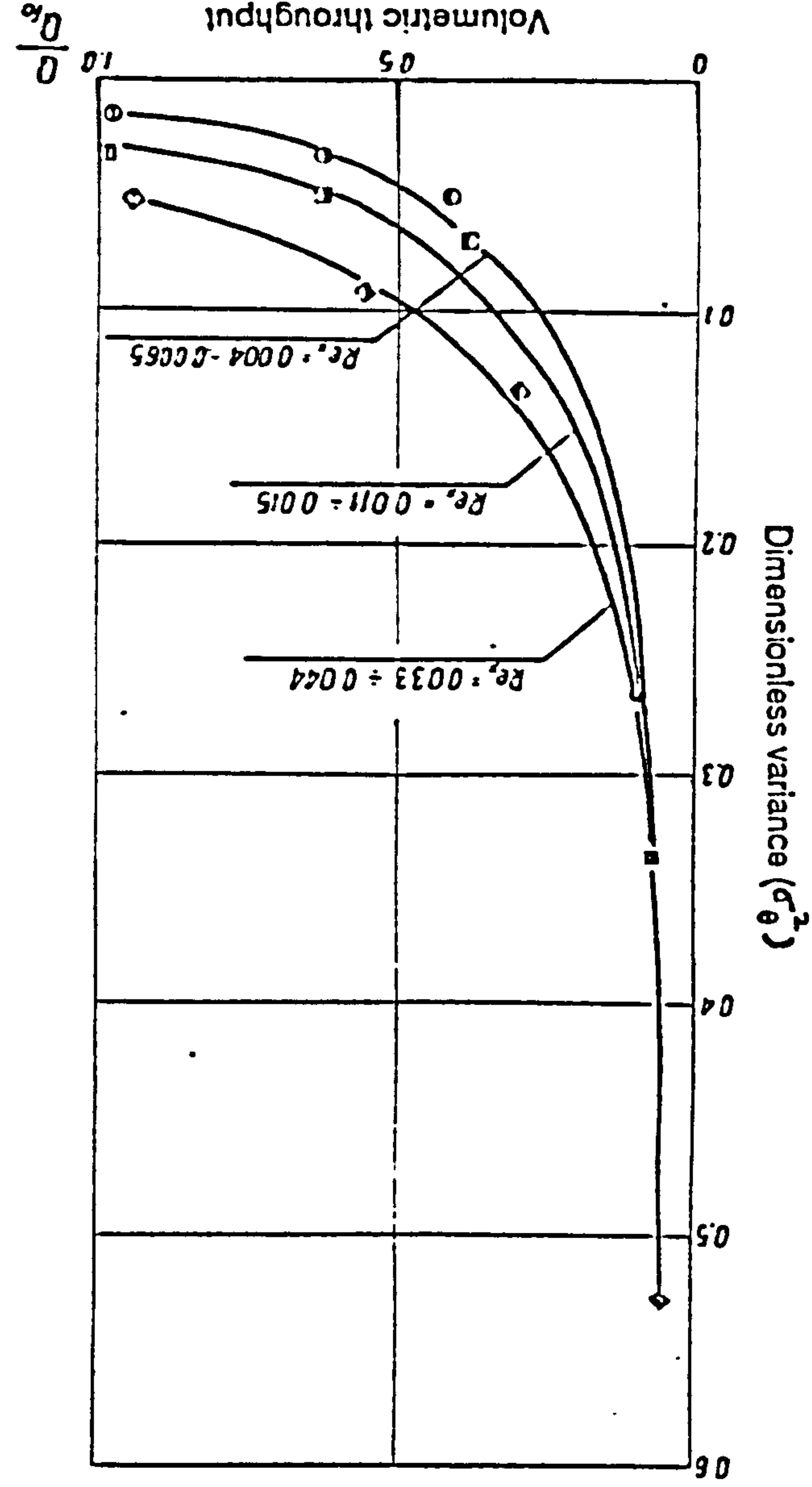


Fig. 4.25 RTD for various throughput rates (G) at constant screw speed (Alter Lidor & Tadmor).

Fig. 4.26 Variance Vs. volumetric throughput for potato syrup extrusion for various conditions (Alter Kembloski 1981 - see original article for details of captions).



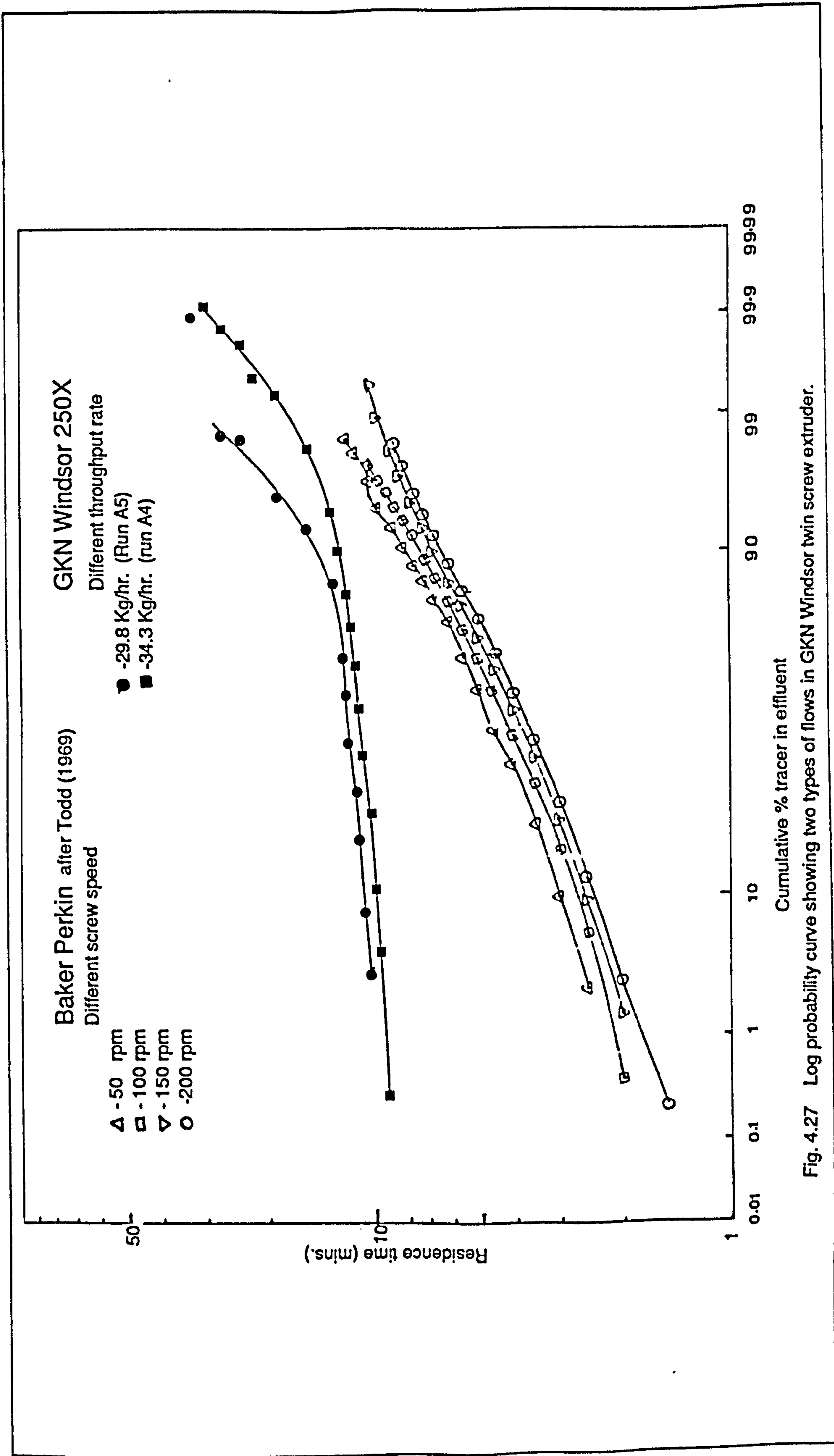


Fig. 4.27 Log probability curve showing two types of flows in GKN Windsor twin screw extruder.



that the GKN Windsor has more plug flow as compared to Baker Perkin's twin screw extruder. The flatness of the plot shows the plug type of flow.

The value of variance of RTD, which is the measure of spread of distribution, does show the difference numerically. The decrease in throughput at constant speed is associated with an increase in variance from 102 to 190, which means a broader RTD. These results are similar to that reported by Walk (1982) for non-intermeshing twin screw extruder (Table 4.5).

Kemblowski and Sek (1981) have shown that in a single screw extruder, at constant screw speed and Reynolds number the dimensionless variance decreases with increase in dimensionless volumetric throughput, reaching minimum value with a free outlet and approaching unity when die is closed (Fig 4.26). This once again confirms that at high throughput, a more plug like flow behaviour is observed due to the effect of velocity distribution.

4.3.2 Effect of temperature profile: Two runs were performed using identical conditions except in the second case the temperature setting was reduced by  $10^{\circ}\text{C}$  in zone 3 and zone 4 (Run A4 and A6 - Fig 4.28). The mixing discs were situated in the zone 4 of the barrel (Fig 3.2).

The change in the temperature profile can have a major effect in the three respects.

- a. Coefficient of friction in between the metal and polymer
- b. Viscosity of the polymer melt
- c. Filled volume

TABLE 4.5 : VARIOUS CONDITIONS FOR RTD STUDIES & ASSOCIATED RESULTS  
(AFTER WALK 1982)

screw config.	variable studied	screw speed (RPM)	barrel temp °C	feed rate (kg/hr)	$t_{min}$ (sec)	$\bar{t}$ (sec)	dim. less <sup>*</sup> $t_{min}$ (sec)	$\sigma^2$	$V_f$
1	screw speed	200	218	82	30	45	0.66	344	47.9
1	"	275	218	82	24	43.9	0.55	300	45.3
1	"	450	218	82	20	32.4	0.62	124	33.6
2	feed rate	300	218	45	43	76.4	0.56	714	49.4
2	"	300	218	68	33	54	0.61	463	53.0
2	"	300	218	91	30	44.9	0.66	401	57.0
2	"	300	218	113	26	33.1	0.78	153	53.6
2	screw geom.	200	218	82	40	58.2	0.69	359	67.5
3	reprodu:	200	218	82	38	57.9	0.66	204	68.8
3	"	200	218	82	38	60.4	0.63	247	69.6
3	temperature	200	232	82	38	63.2	0.60	347	71.7
3		200	260	82	38	62.2	0.61	450	73.1

Where  $V_f$  is filled volume

\* Dimensionless  $t_{min}$  is calculated as

$$\text{Dim. less } t_{min} = \frac{t_{min}}{\bar{t}}$$

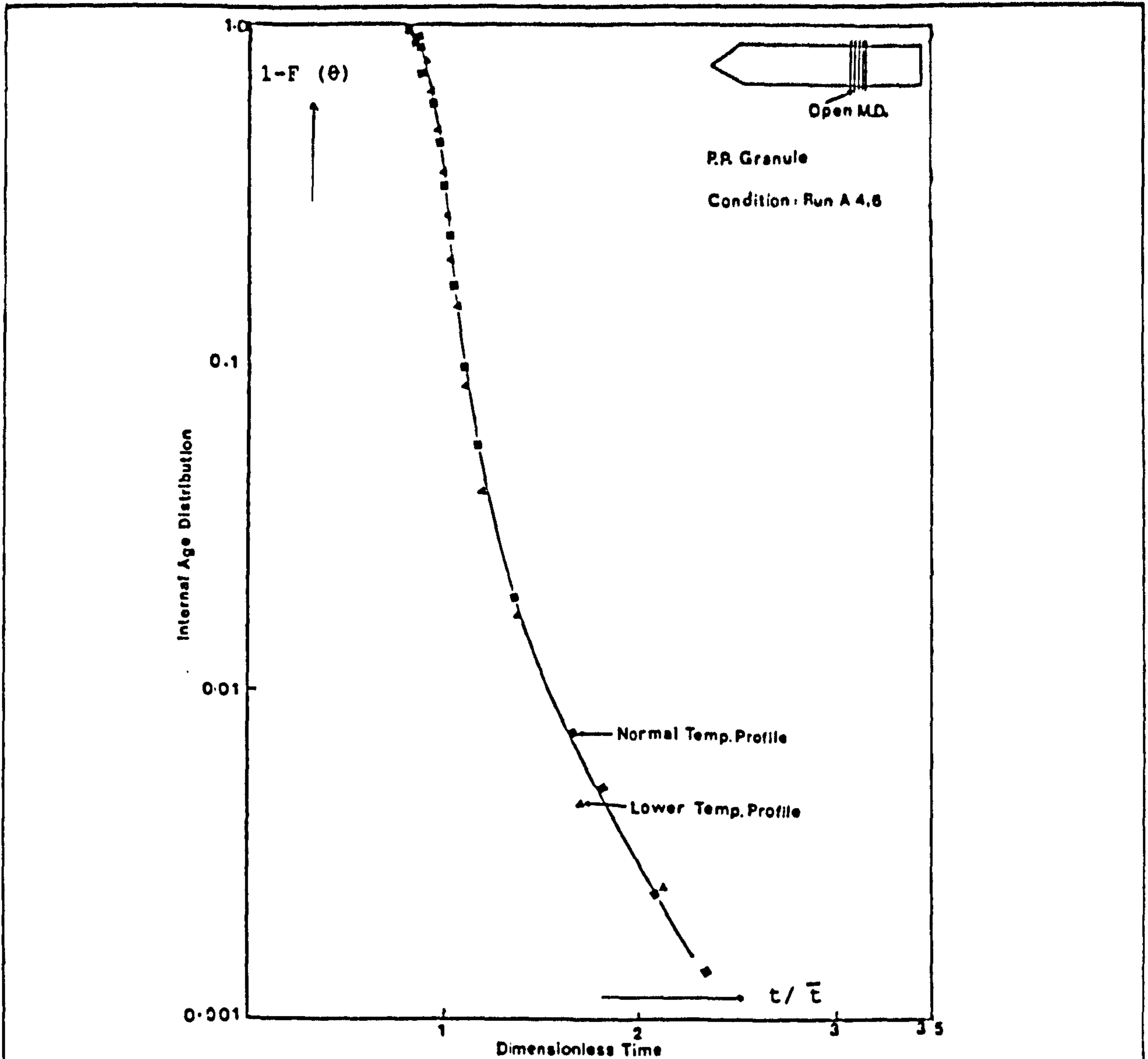


Fig. 4.28 Effect of extruder temperature profile on RTD.

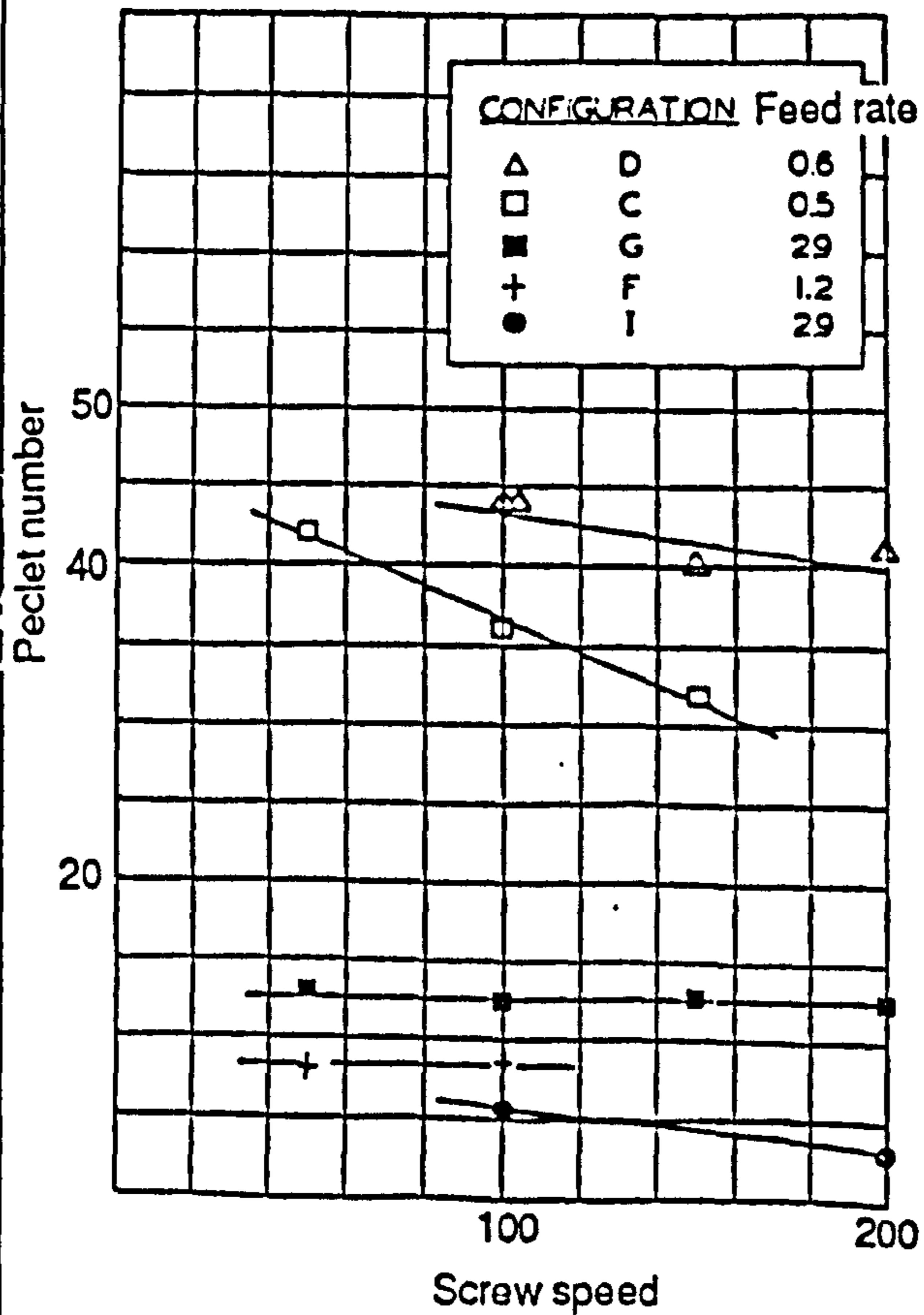


Fig. 4.30 Effect of rotor speed on Peclet number (After Todd & Irving 1969).

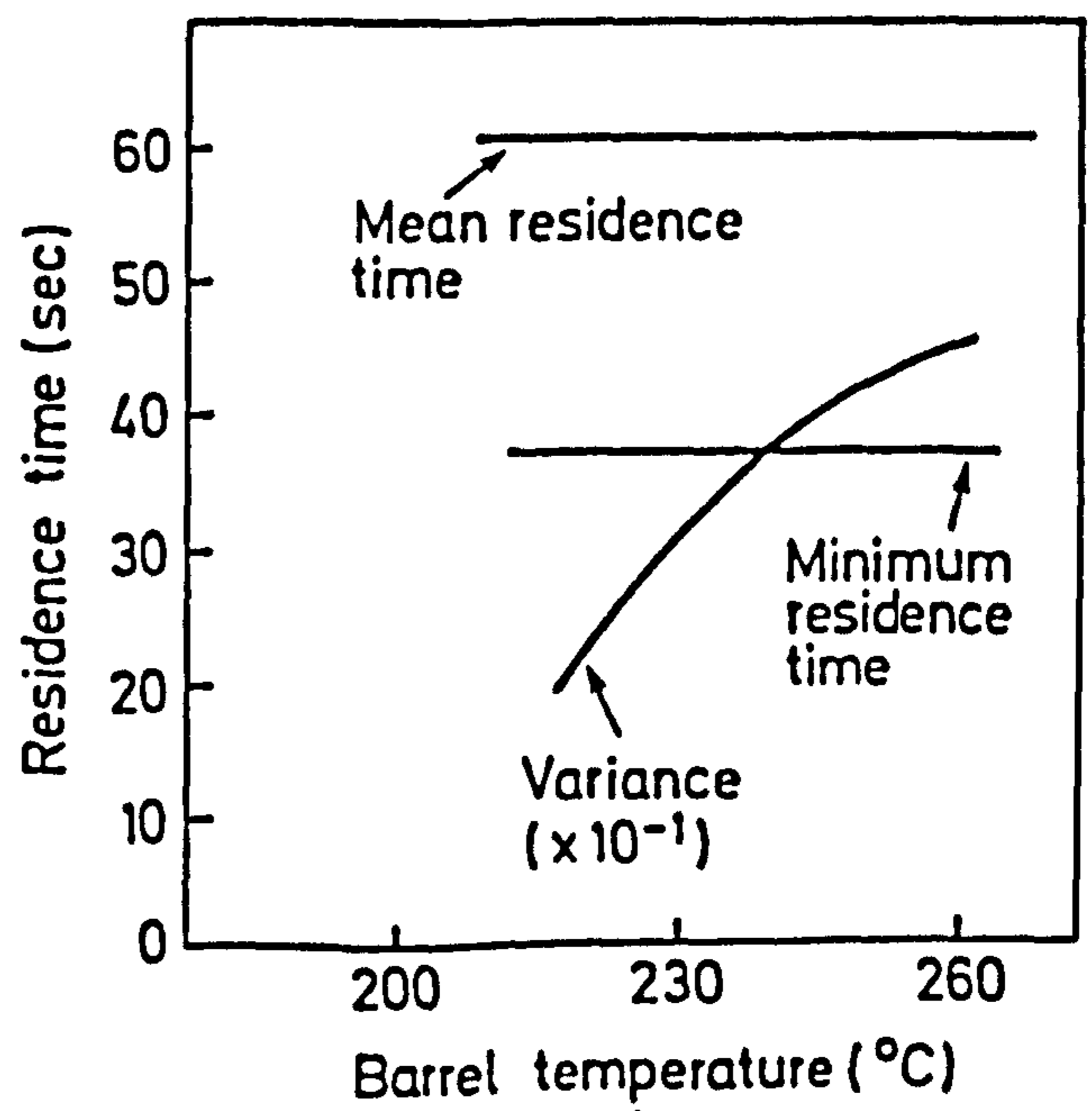


Fig. 4.29 Residence time Vs barrel temperature (After Walk 1982)

a. Coefficient of friction: The conveying in single screw extruders depends on the frictional coefficient of the polymer, its temperature and steel temperature. But in co-rotating twin screw extruders the material is conveyed semi-positively in the C shape chambers (as compared to counter-rotating where there is a positive conveyance due to the closed C shape chambers ). So the friction does play a small part in conveying. Because co-rotating extruders basically have interconnected C shape chambers so there is no direct cut-off in the flow direction (vs. counter-rotating). But at the same time the screws wipe each other and so there can be no prolonged stagnation. So the temperature of barrel relative to the screw is important in that the feed zone must be well below the adhesion temperature of the polymer. As material can stick to a warm screw it reduces the effective chamber volume and thus the throughput.

b. Viscosity: The viscosity can affect the RTD results by affecting the manner in which the polymer flows in a given path and also a reduced viscosity can increase the relative leakage flows. In the present case, two RTD results for different temperature profiles, as shown in Fig 4.28, do not show any significant difference to each other (within the accuracy of the tracer technique) thus showing similar flow behaviour. However, on calculating variance from RTD data (spread of the distribution - see table 4.2 and section 2.2.7 for its value and information about its calculation respectively) it shows a marginal decrease in variance value with increase in temperature profile (Table - 4.2A variance changes from 1.02 to 1.03). This is similar to the theoretically derived results of Janssen et al. (1979) which showed that for a model counter-rotating twin screw extruder, the viscosity changes do affect leakage flows. The increase in temperature (reduced viscosity) gives a increased variance - a better

mixing. However this is in complete contrast with the results of Kemblowski and Sek (1981) on a single screw extruder who showed that the viscosity of the melt is inversely related to variance. Thus decreased temperature profile increases the viscosity which increases the spread about RTD curve as shown by increase in value of variance.

However, as the temperature profile is reduced at zone 3 and 4, coinciding with the position of the melting disc. At this place the polymer temperature is lower than that in Run A4, and thus melting disc offers higher resistance to the polymer melt during passage through it which is then reflected in the higher current consumed. It also shows a high load on the motor as indicated by the screw torque values (increased from 2.78 to 3.34 KNM). This increase again shows that the polymer has a higher viscosity.

c. Filled volume: The change in temperature profile can affect the filled volume either by changing the melting position and thus changing the melt zone length or by simply increasing the filling in a given melt zone. As already discussed earlier, the start of the melting zone in the present extruder is fixed by the position of the melting disc. However, it was observed that the filled volume increases with increase in temperature profile (see calculated filled volume in Table-4.2 A). A similar increase was observed by Walk (1982) in non-intermeshing twin screw extruder. However, as the increase in filled volume is not substantial the consequential effect on mean and minimum residence time remains non significant. This is similar to that reported by Walk (1982) as shown in Fig 4.29. Janssen et al. (1979) reported a marginal increase in mean residence time.

4.3.3 Effect of screw speed: This is one of the easily attainable

variable available on the processor. Although in a real industrial sense the operational screw speed is always the maximum available, because maximum throughput is desired.

The screw speed is the most comprehensively studied variable. Various investigators have studied its effect on RTD. In the present work effect of screw speed on RTD was studied with two pulley systems.

a. Small pulley system: In this case most of the variables were studied at three screw speeds. Although individual effects are reported under separate headings the general trend of screw speed in all of these variables is studied.

b. Large pulley system: The small pulley originally fitted by GKN Windsor in the drive assembly was replaced by a large pulley manufactured at Brunel University with the view of increasing the screw speed and thus throughput. However, for ease of understanding both the cases are studied and discussed together. It is worth noting that in all the cases the throughput at each screw speed was kept at maximum. In the small pulley system this maximum was restricted by the emergence of melt out of the vent port, while in the case of large pulley system, the throughput was restricted due to limited available torque, and thus complete filling of the screw sections could not be achieved. The results for various conditions discussed are given in Figures 4.33 to 4.39.

In general, it can be said that by increasing screw speed, laminar mixing increases due to the frequent reorientation of the melt. The shear rate imposed on the polymer also increases.

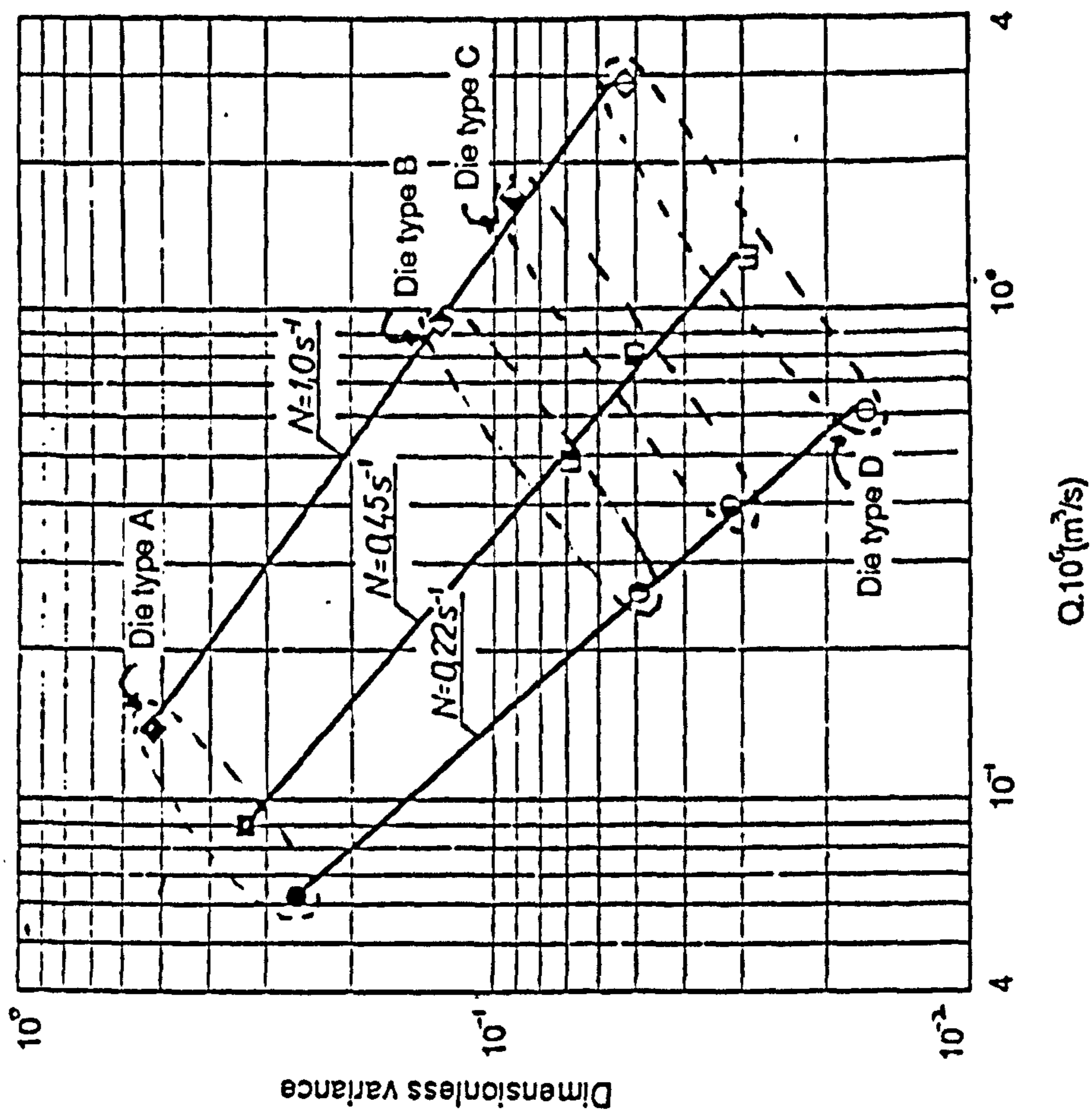


Fig. 4.32 Dimensionless variance Vs volumetric throughput for potato syrup extrusion (Kembloski & Sek 1981)

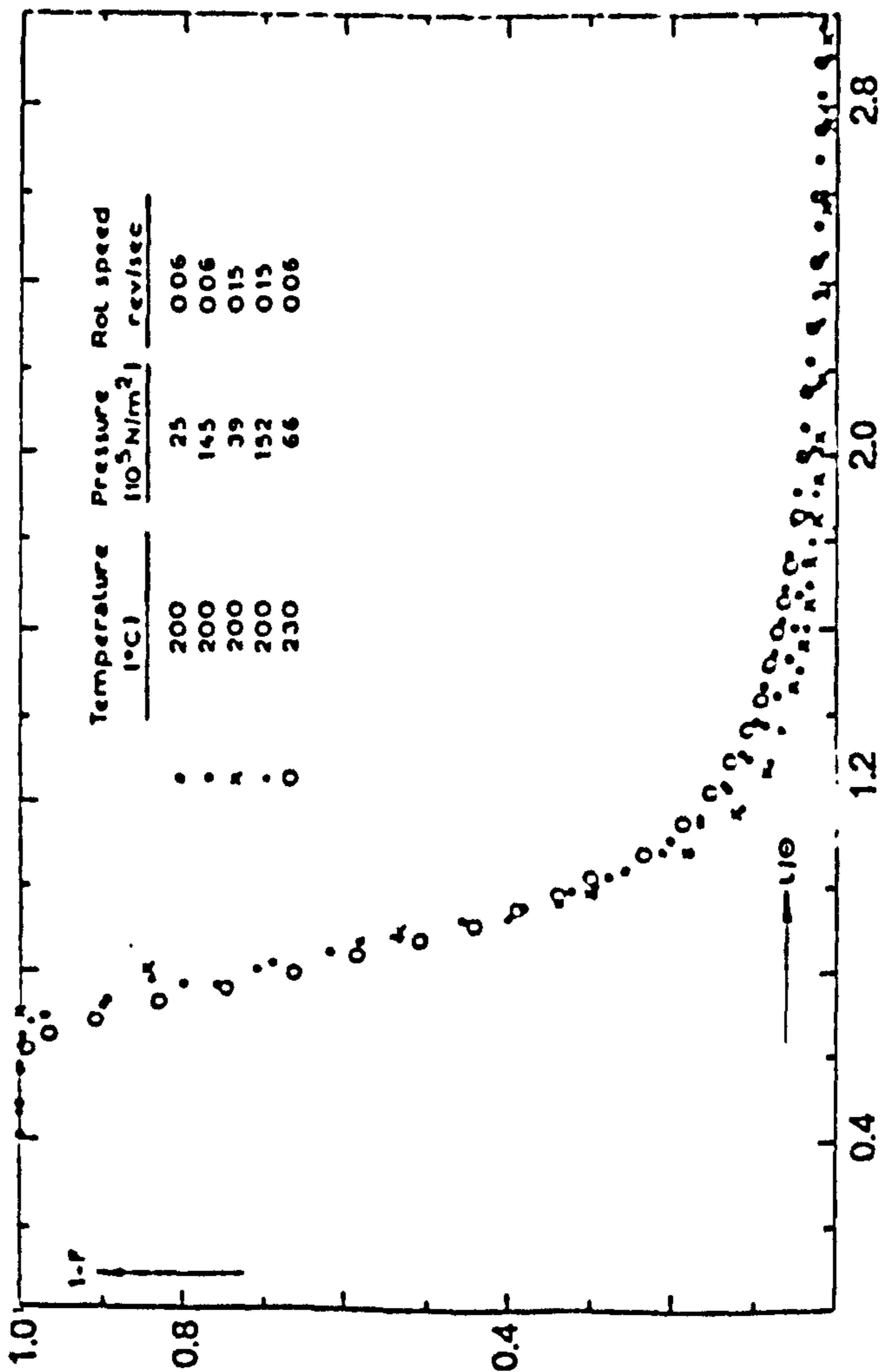


Fig. 4.31 RTD for various operating conditions (Janssen & Churchill 1978).

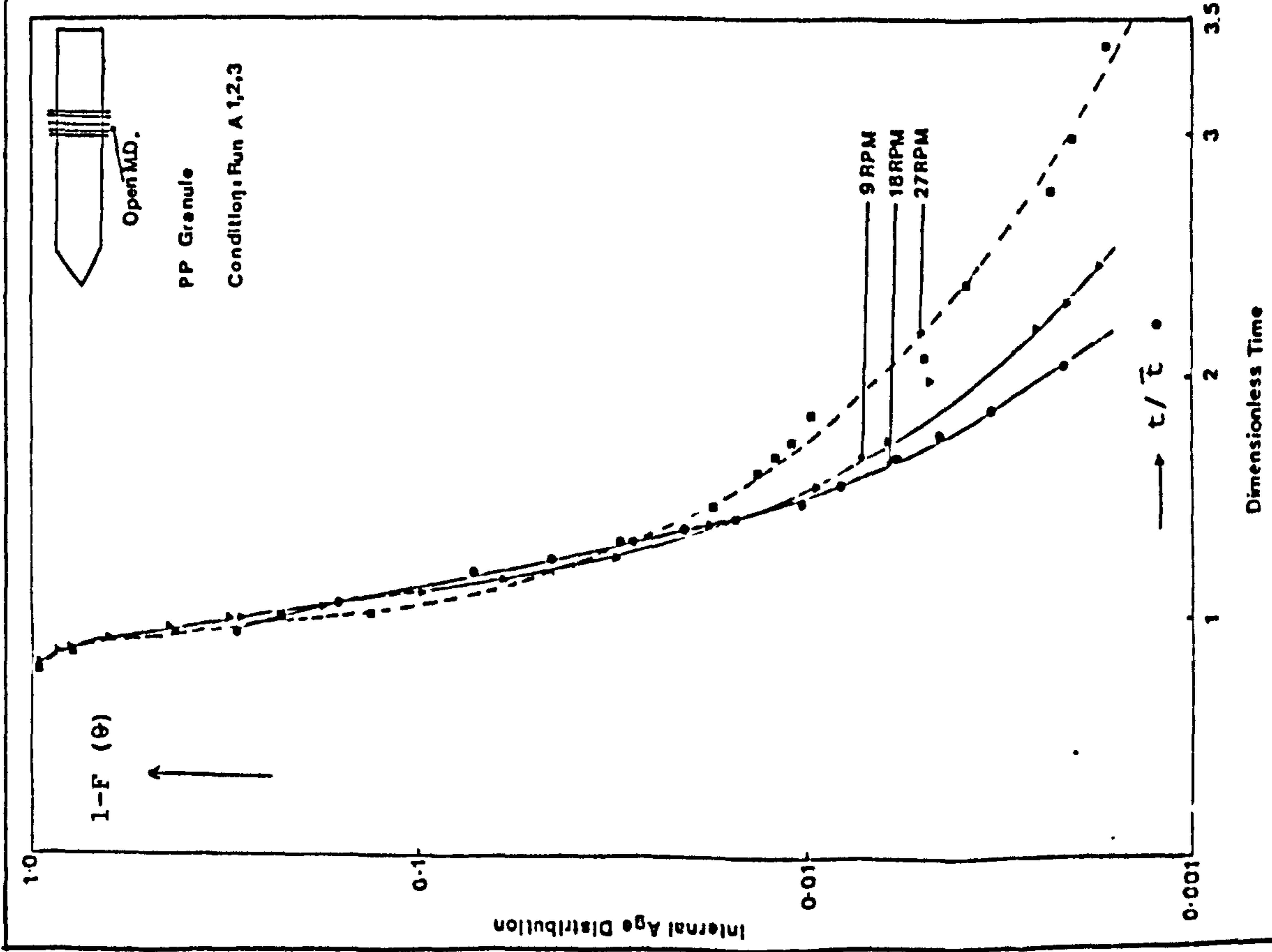


Fig. 4.33 RTD for upstream-open mixing disc screw configuration.

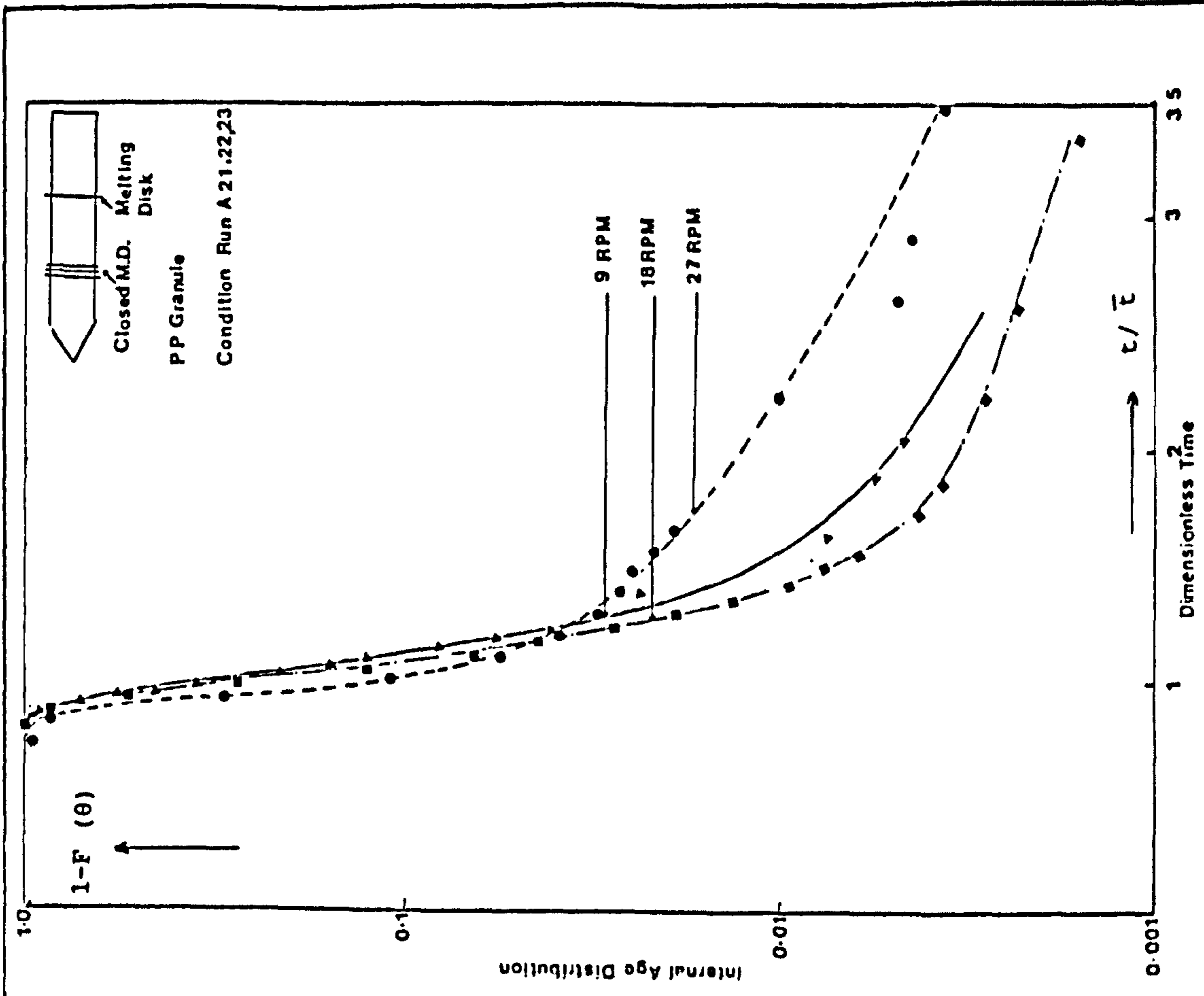


Fig. 4.34 RTD for downstream-closed mixing disc screw configuration.

Effect of screw speed on RTD.



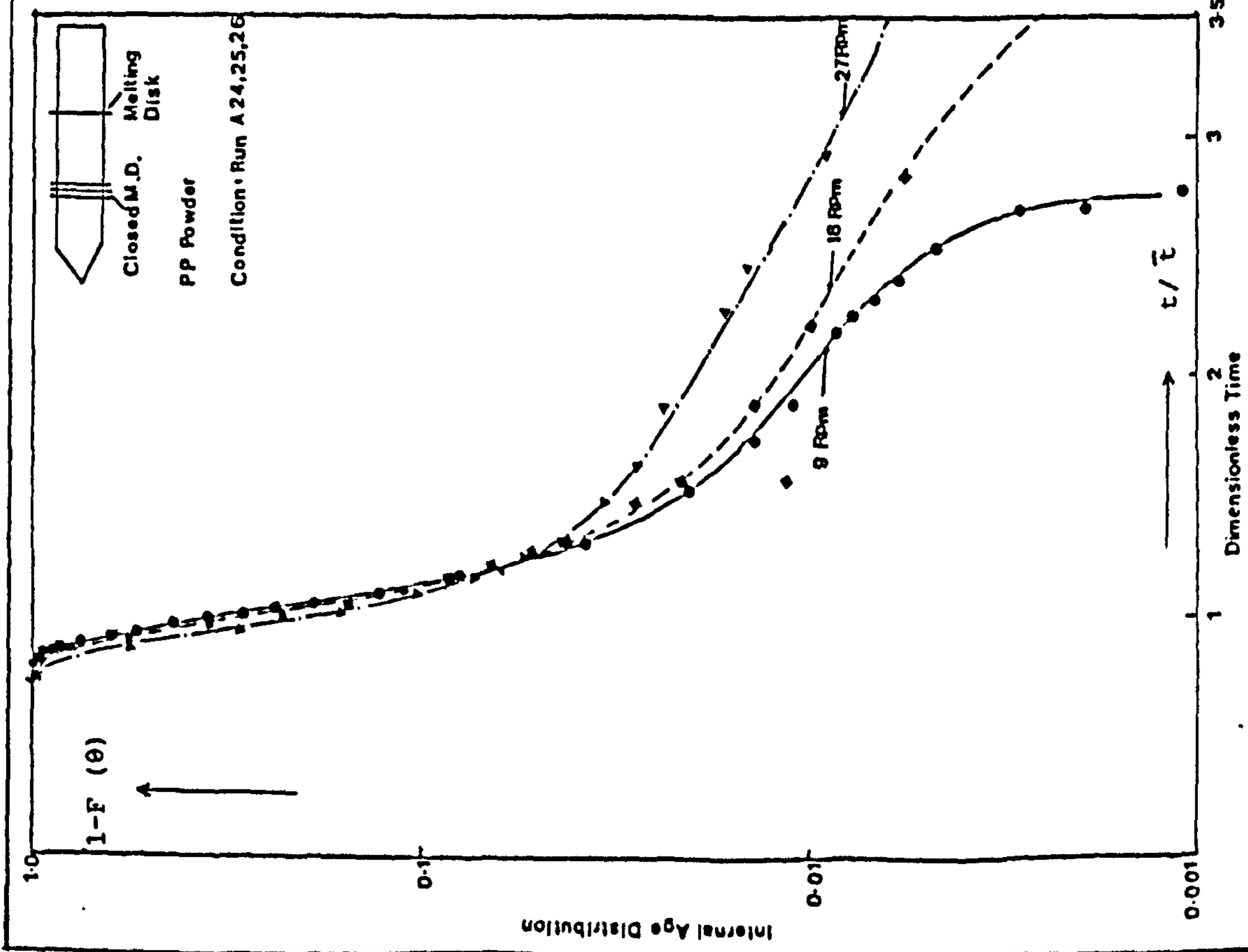


Fig. 4.35 RTD for downstream-closed mixing disc screw configuration (Powder Polypropylene).

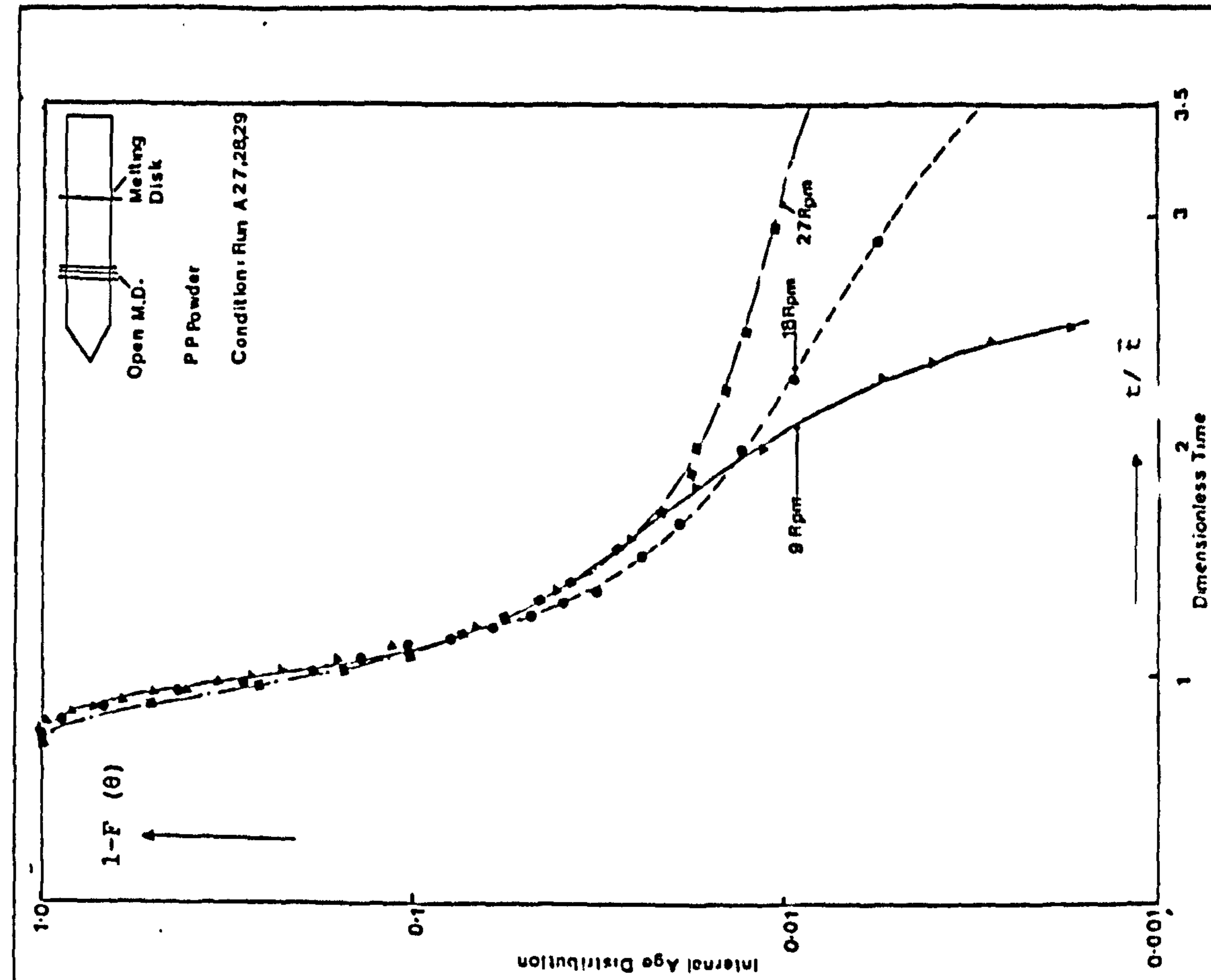


Fig. 4.36 RTD for downstream-open mixing disc screw configuration (Powder Polypropylene).

Effect of screw speed on RTD.

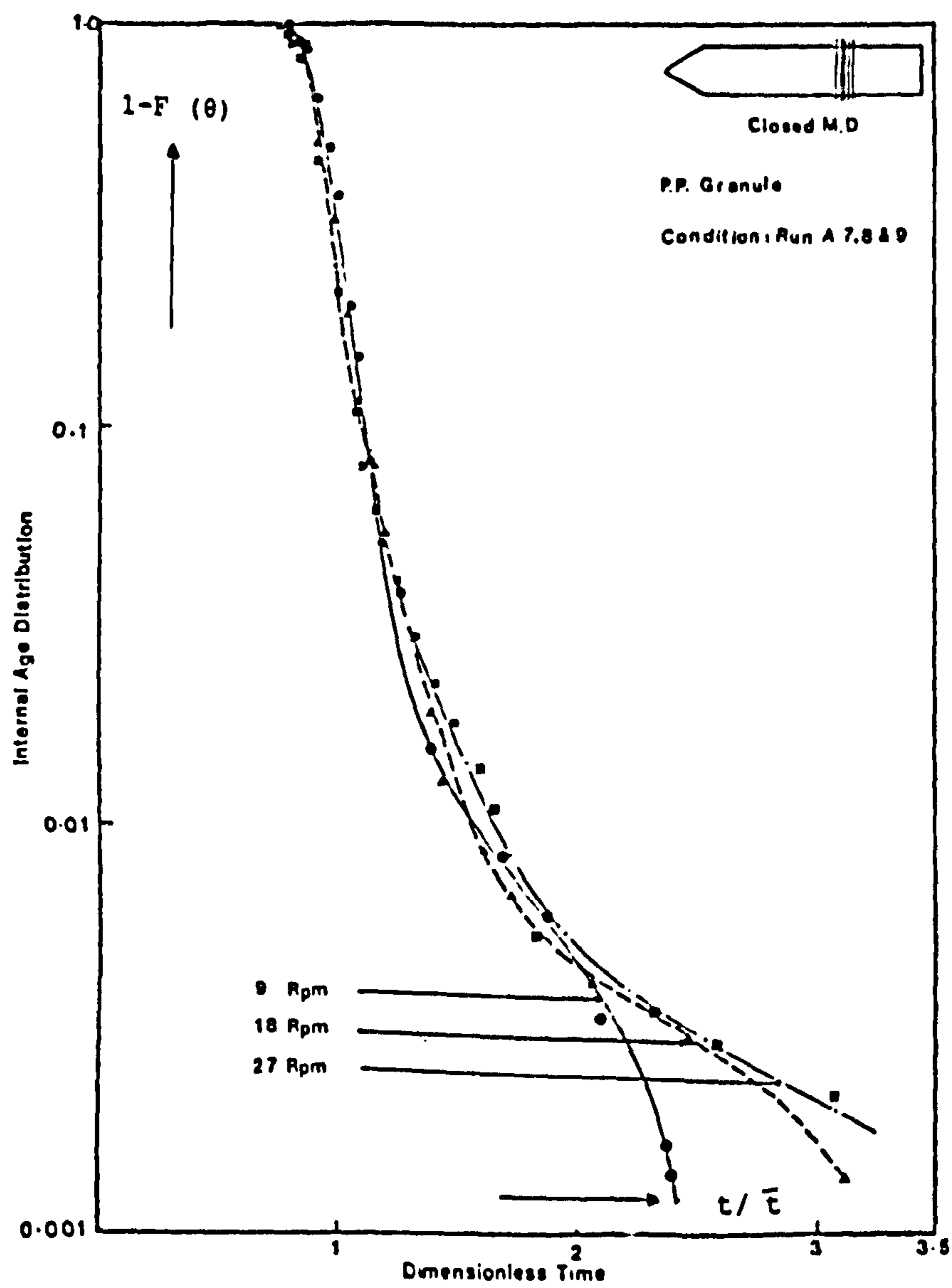
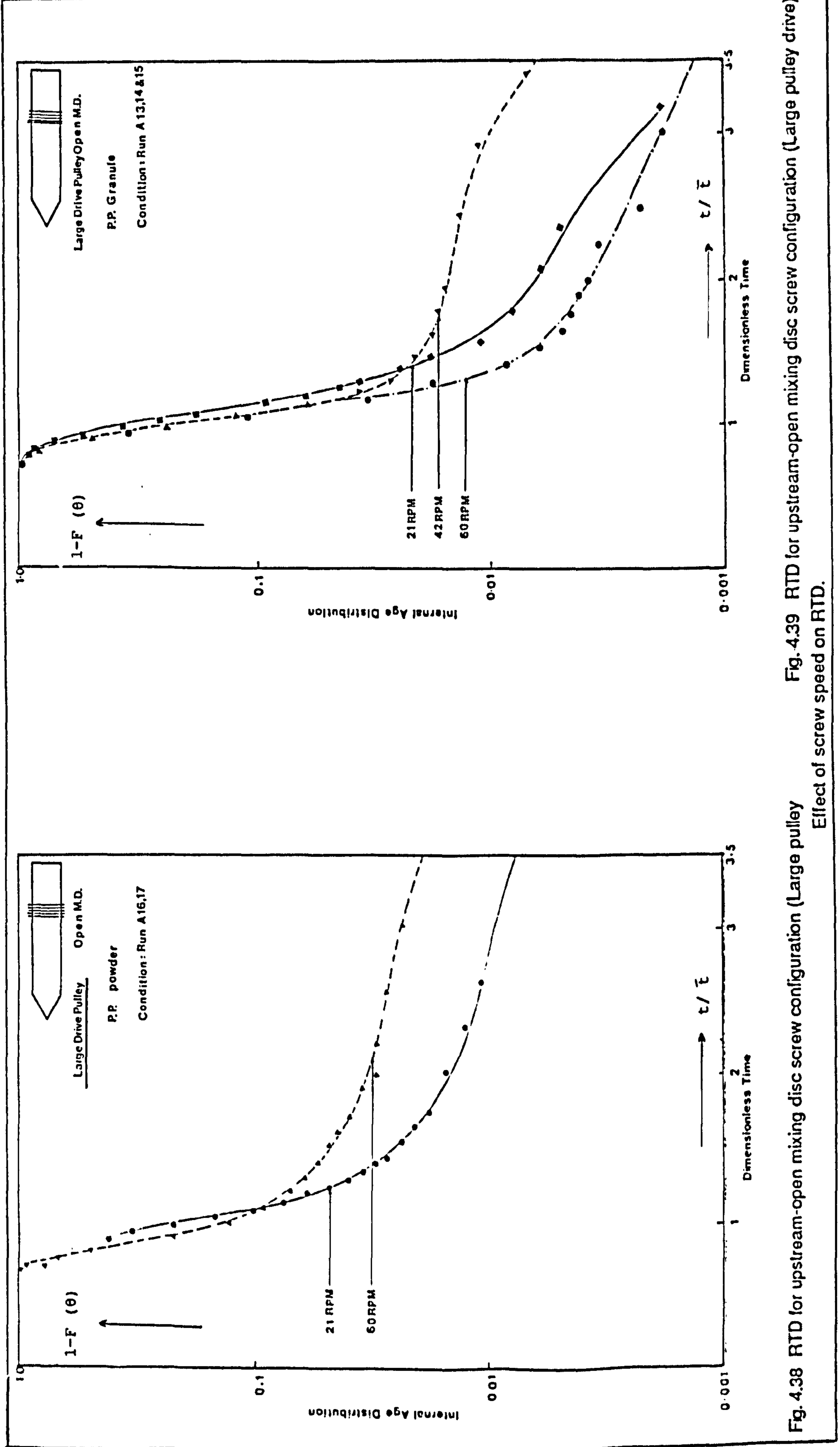


Fig. 4.37 RTD for upstream-closed mixing disc screw configuration.

Effect of screw speed on RTD.



$$\text{(shear rate = } \frac{\text{equivalent diameter} \times \text{screw speed}}{\text{channel depth}} \text{ )}$$

However, associated with these is the decrease in residence time which tends to limit the effects of shear rate and laminar mixing. This is due to the relatively low time exposure to these factors.

Before looking into the general trends of effect of screw speed, it would be better to look into the basic differences in mixing and associated factors in the two pulley systems, because this will later help to explain the overall trends of screw speed effects.

The set of experiments with the large pulley system shows a low mean residence time, low filled volume and a higher value for specific energy consumption. The shorter mean residence time results because of higher screw speed and consequently faster movement along the path. The low filled volume is due to the limited available torque in the design of the machine. The calculated values of filled volume are given in Table 4.2A. This is also confirmed by the barrel withdrawal experiments which show partially filled screw for large pulley system runs which are similar to the low throughput cases (Fig 4.11). The higher values for specific energy consumption can be attributed to local frictional heat generation which is related to the shear rate applied.

The effect of screw speed on RTD shows some interesting trends, which can be broadly classified into three categories.

1. Group A: In this case the flow shows a move towards more axial mixing with the increase in screw speed. This type of behaviour can

be said to be more the general type. The increase in screw speed leads to increase in melt conveyance per unit time. Exit area remaining the same, there is an associated increase in melt accumulation under pressure and thus more tangential pressure build up. The pressure has more effect on the leakage flow through tetrahedron gap i.e. at the intermeshing site more material tends to be pushed into the main tetrahedron flow ( $F_{TM}$ ), and thus less material is likely to go through ( $F_{TS}$ ) small tetrahedron gap which completely misses one whole rotation (see section 4.4.1.A). Similarly net drag flow would also be reduced due to excessive pressure build up tangentially. Furthermore the increase in the screw speed will also tend to increase the melt temperature rise due to mechanical dissipation. The other leakage flows, however insignificant thus might be, would obviously increase in backward direction. Herrmann, Burkhardt and Jackopin (1977) have theoretically shown, for a self wiping twin screw extruder, that the velocity distribution can be influenced by changing the screw speed or throughput, and thus velocity distribution can be altered considerably by preselecting these parameters.

However, it should be clear that pressure alone does not cause the effective widening of RTD curve because with a free outlet (Kemblowski and Sek 1980) the screw speed alone does have a profound effect in a single screw extruder.

So as discussed above, the increase in screw speed leads to flow with more axial mixing. This type of behaviour is found in all of the small pulley system runs with powder as feed material (Fig 4.35 and 4.36) and in run with "closed" mixing disc in upstream position with granules as feed material (Fig 4.37).

The reason for this type of behaviour in runs with powder feed is quite clear. Faster heat transfer and melting due to increased surface area occurs in powder. Once molten it shows normal behaviour as described above. However, in a run with closed mixing discs in upstream position (Fig 4.37) there is enough pressure build up in upstream position due to restricted flow passage through mixing discs. This leads to the relatively higher heat input in polymer and subsequently it behaves in manner as described above.

Similar results, as discussed above in this group A, were obtained by Schott and Saleh (1976) in plasticating single screw extruder, by Kemblowski and Sek (1981) and Rauwendaal (1981) in twin screw extruder. Kemblowski and Sek (1981) have shown that for a given die type, increase in screw speed and its consequential increase in throughput rate shows increase in variance (Fig 4.32). The RTD curve shows a trend similar to group A for various die geometries. But as these results are plotted on linear-linear scale, the effect does not show up effectively.

2. Group B: In this case the flow shows less axial mixing with initial increase in screw speed, and then it moves towards more axial mixing with further increase in screw speed. This type of behaviour is found in runs with open mixing disc configuration in upstream position (Fig 4.33) and closed mixing disc configuration in downstream position (Fig 4.34) - both of these runs being with small pulley system and polypropylene granule feed. As explained in group A section, the melt state determines the trend in total conveying behaviour as a result of varying speed. However, in this case the granules conduct heat slowly due to smaller surface area (vs powder). As

there is less resistance in both of the above cases (Fig 4.33 and 4.34 in the first due to open configuration and in the second because just one mixing disc is present. Thus because of easy passage there is less pressure build up and thus less melting. On increasing speed (from 9 to 18 rpm) probably there is slight build up of pressure before melting disc, but due to increased speed the overall net result is relatively less melting and therefore move towards more plug flow. However, on further increase in screw speed (18 to 27 rpm) probably there is now sufficient pressure build up at melting disc position, and therefore the flow behaviour produces more axial mixing.

3. Group C: In this group the behaviour is quite the opposite to that of group B. In this the flow shows initial increase in axial mixing with increase in screw speed. However, with further increase in the screw speed the flow becomes more of the plug flow type. This type of behaviour is found in runs with "open" mixing disc in upstream position with large pulley system with polypropylene and polystyrene granules as feed material (Fig 4.39 and 4.48). The reason for this type of behaviour can largely be attributed to the melting mechanism. On studying the fundamental principles of melting in extruder it is quite obvious that polymer gets energy from heater bands and from dissipation of mechanical energy. The low heat conductivity of polypropylene (0.12 of solid and 0.16 of melt W/mK) causes the mass in the middle of the screw channel to remain relatively cool. At low screw speeds the dissipation of mechanical energy is insignificant, and the melt is heated with a temperature somewhat below the barrel temperature. Accordingly the heat flux is routed from the wall of the extruder to 'cold' polymer, and the temperature profile has a minimum in the centre of the channel.

At high screw speed, especially in large pulley system, the expenditure of mechanical energy increases and the amount of heat passing to the polymer from the heater decreases on account of the shortening of the time for which the polymer remains in the extruder. So as a result, with the increase in screw speed, the temperature of the melt decreases (due to increase in heat generated by shearing and at the same time reduced heat transfer from heater bands). This is confirmed from shock cooling experiments which clearly show the presence of unmolten centre due to inadequate heating.

As for a particular shear rate, the melt with lower temperature is more viscous, which would result in more energy consumption and also show a more plug flow behaviour. So the centre with cold polymer will have more plug like flow at higher screw speed (large pulley system) which could be the reason for group 'C' type behaviour. The polypropylene powder behaves in a manner as described in group A type behaviour. This is due to better heat transfer and thus better melting. Sek (1979) has shown that radial temperature distribution has significant effect on RTD.

Similar results to that of group 'C' are reported by Lidor and Tadmor (1976), Walk (1982). Lidor and Tadmor (1976) theoretically derived RTD results of simulation with a constant flow rate and varying screw speed for 2.5 and 6 inches diameter single screw extruder (Fig 4.40 and 4.41). Furthermore the effect of screw speed while maintaining the flow rate at maximum value shows a similar trend. Similarly Walk (1982) has shown that in non-intermeshing twin screw extruder using PMMA as feed material at constant feed rate that the variance decreases with increase in screw speed and thus shows less axial mixing.



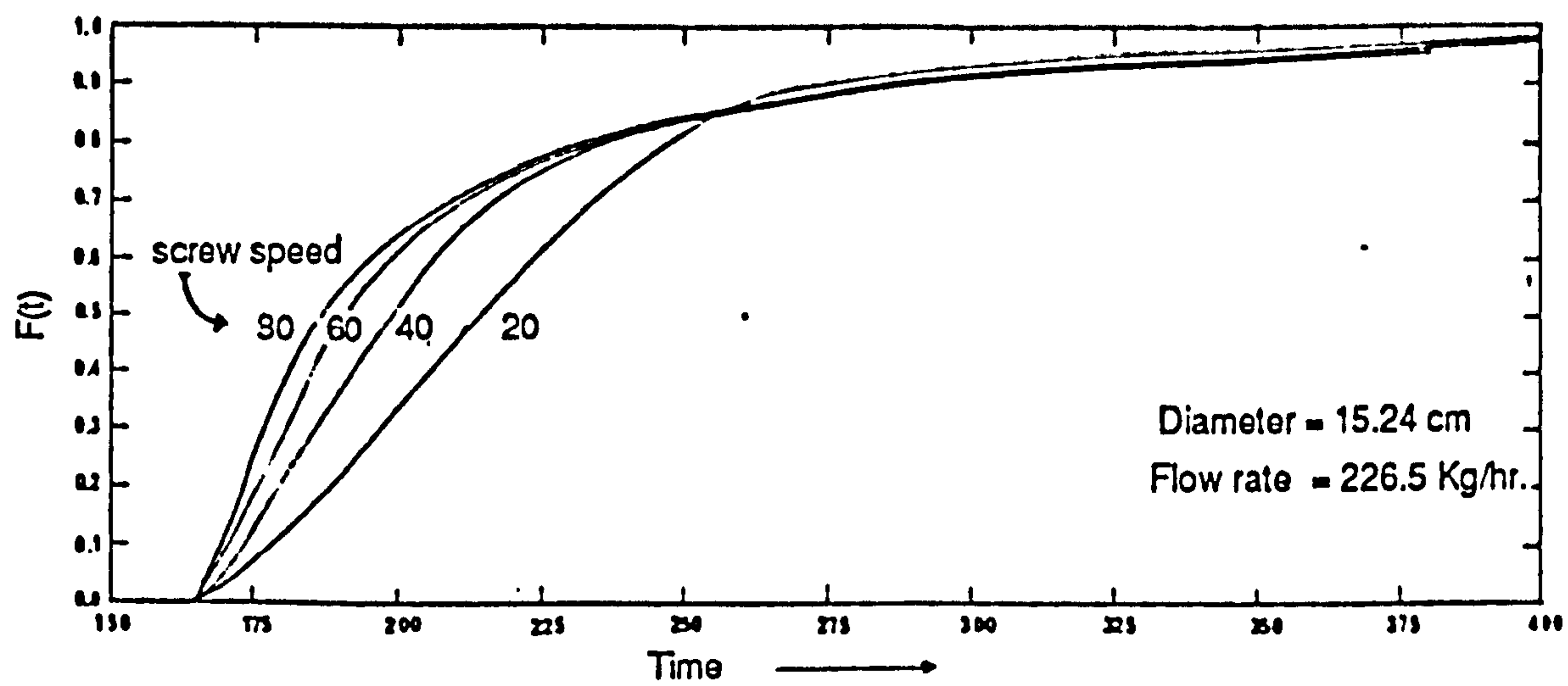


Fig. 4.40  $F(t)$  for various screw speeds (After Lidor & Tadmor 1976).

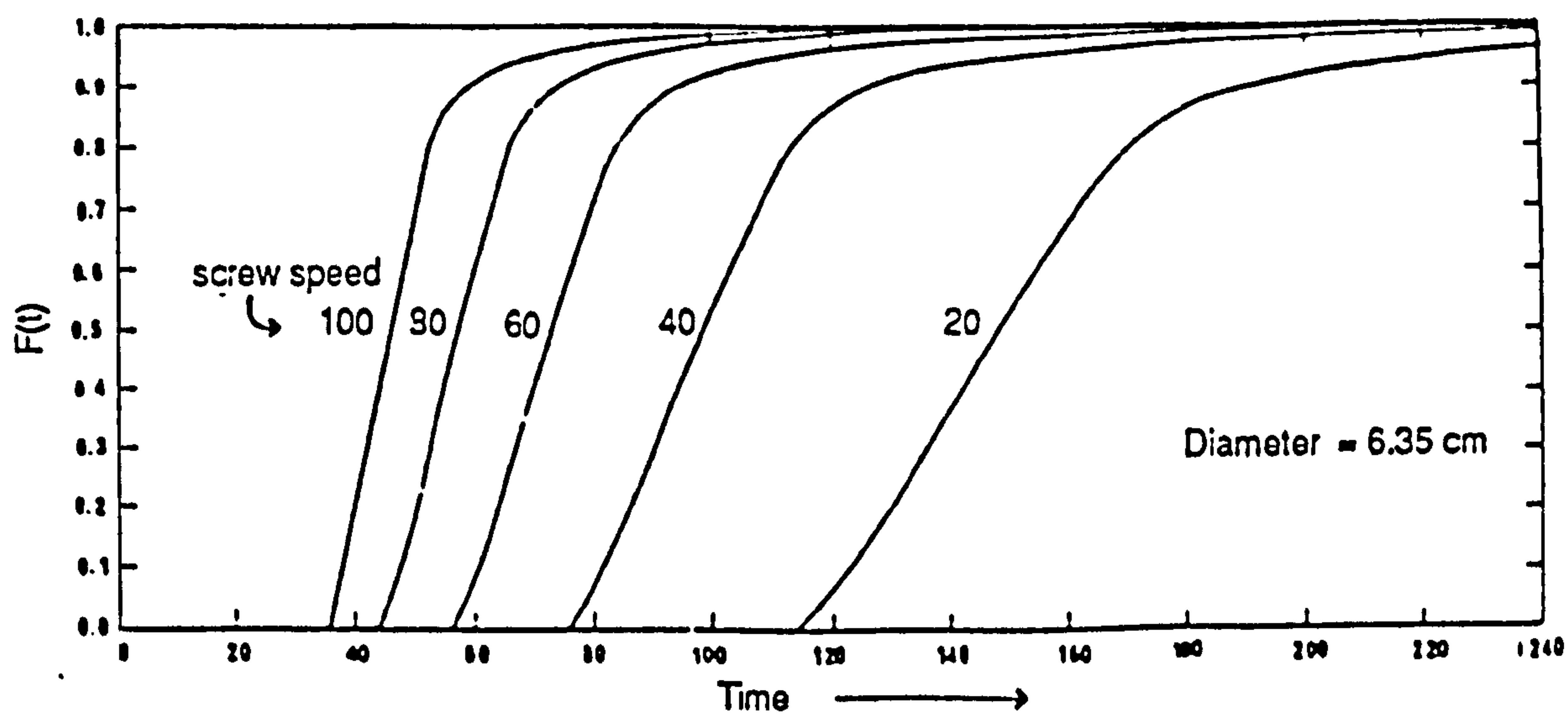


Fig. 4.41  $F(t)$  for various screw speeds with flow rate adjusted to get a constant length of melting (After Lidor & Tadmor 1976).

4.3.4 Pulley size: This variable has already been discussed in section 4.3.3 - screw speed.

4.3.5 Mixing disc: The mixing discs are the special feature of GKN Windsor extruder and offer variations in the screw design. It has been shown by Todd (1975) that screw design is one of the variables which has a significant effect on axial mixing characteristics (Fig.4.42).

The mixing discs consist of five pair of slotted discs. Depending on their position along the screw length, they can act as melting discs (in upstream position) or mixing disc (in downstream position) where they impart considerable distributive mixing.

The effect of mixing disc configuration and position along the screw on RTD is studied. The details of the conditions used are given in section 3.4.2 B. The position of mixing disc together with other arrangement are given in Fig 3.2 and 3.3 . The effect of mixing discs is analysed systematically as follows.

A. Effect of mixing disc configuration in upstream position: In this case all five pairs of mixing discs are situated in the upstream position. In this position two configurations are used - open and closed. The conditions for these runs are given in Table 4.1 and plotted in Fig 4.33 and 4.37 (Run A 1, 2, 3 and A 7, 8, 9).

In the upstream position, the mixing discs work mainly as melting discs. The energy required for melting depends on the raw material, which is shown in Fig 4.43. This melting could be induced quickly by

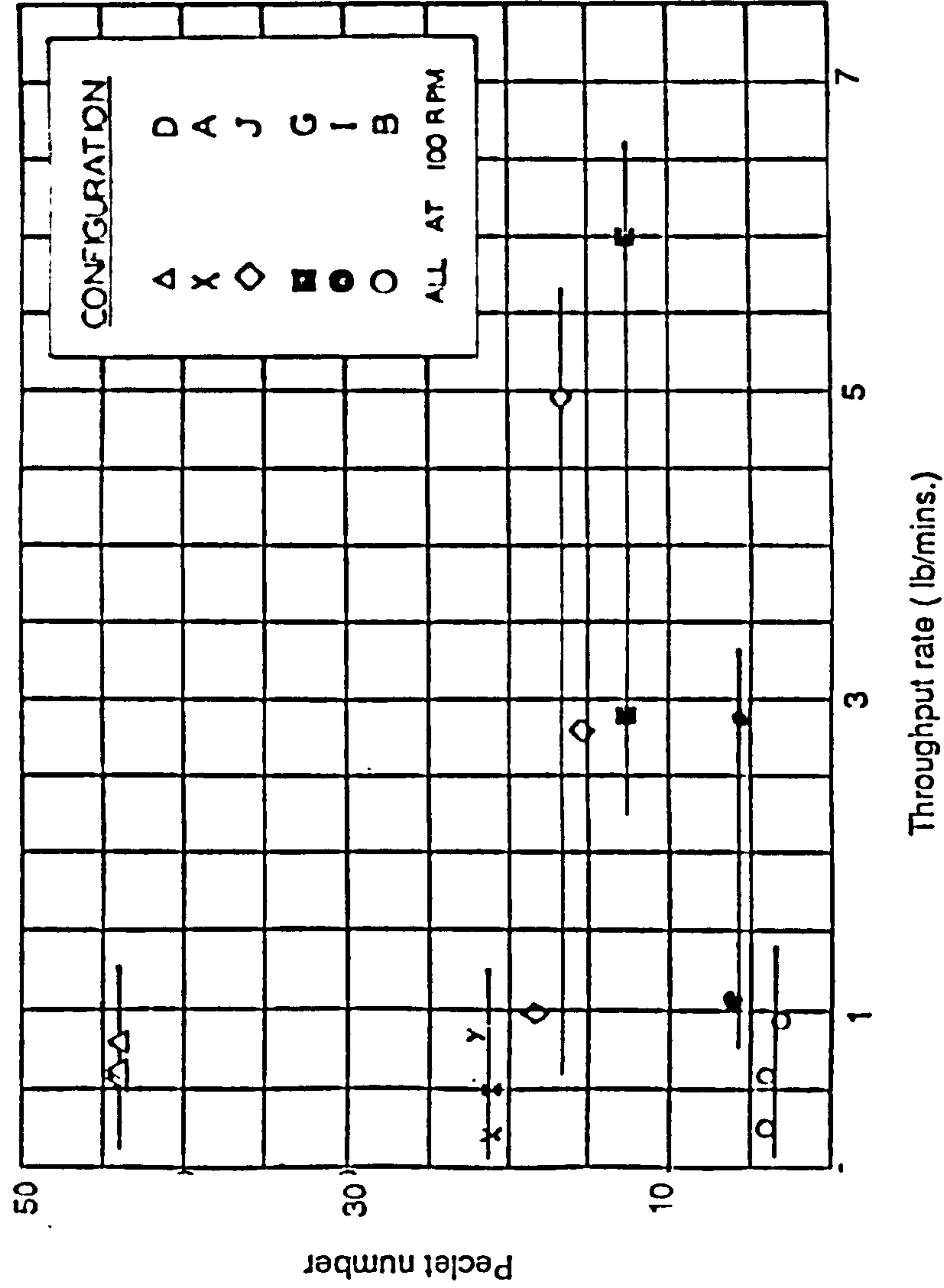


Fig. 4.42 Effect of feed rate on Peclet number for various screw configurations (After Todd & Irving 1969).

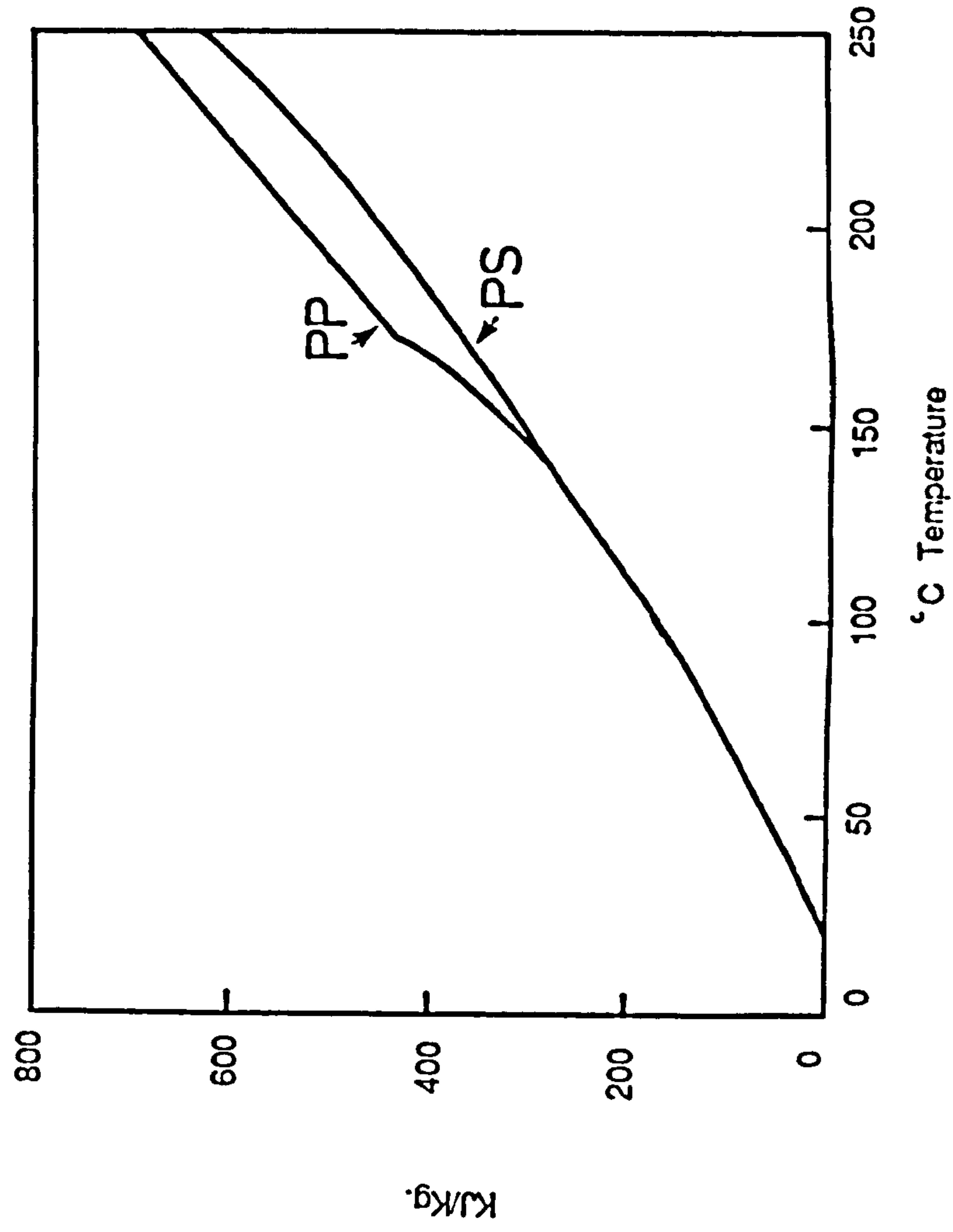


Fig. 4.43 Enthalpy of polymers used.

creating a high pressure bed of  $200-500 \text{ MN/m}^2$  (only applicable in high pressure extruders). However, single compression does not give satisfactory melting. The melting achieved by mixing disc is considered to be more satisfactory. In this the polymer melting is achieved as follows.

The heat for polymer melting is derived from internal friction or shearing of the polymer and from conduction of heat from heater bands. The mixing disc mixes the molten polymer with unmolten material and thus causing shearing of material. This in turn gives rise to heat generation which helps melting.

Thus mixing discs at this stage act as a barrier which completes the melting process within a short screw length. The material fills the screw threads in front of the mixing discs to overcome the resistance or the pressure barrier imposed by the mixing discs. A backup of specific length is formed ahead of the mixing discs. The angular displacement of the mixing discs (in closed mixing disc situation), which are axially arranged one behind the other, enables the material to flow through the slot of previous mixing disc into the two adjacent slots of the next mixing disc and thus providing a limited intermixing of the material.

In closed disc configuration, the flow path for polymer melt is more complicated than that formed by open disc configuration. Thus closed disc would offer more tedious path, and consequently more pressure is required to overcome this. Therefore more energy would be required for this purpose which is then transferred from the screw to the product through frictional forces and would generate heat. This results in higher energy input for closed disc configuration as

substantiated by output/current figures. These figures indicate that higher output/current is achieved for open disc showing more power consumption with closed disc configuration.

The filled volume (Table 4.2 A) studies show that closed disc configuration does give higher filled volume compared with open, presumably due to better melting which is obviously due to high energy input (as discussed above). This causes the melt to become less viscous which could cause more axial mixing as reflected in the RTD curves (discussed later).

The mean residence time (M.R.T.) for closed mixing disc configuration is higher than that for open, showing better axial mixing for closed disc configuration. The same trend is found in variance (Table 4.2A) which is higher for closed configuration. Although at higher screw speed (27 rpm) the value for variance is the same for both and so are the RTD curves. This is presumably due to enough pressure build up at this high speed (27 rpm) at start of mixing disc zone open configuration that is enough to cause melting.

On comparing the RTD curves (Fig 4.33 and 4.37) it becomes quite clear that both of these curves at various speeds do not change substantially as found in downstream settings (see below). However, on comparison between these two settings the open mixing disc configuration is more screw speed dependent than closed one. So it can be said that the upstream mixing discs give an ideal setting for dispersion. This is because the temperature of the polymer melt is rather low and thus it is quite viscous at this stage. This helps in the dispersion for which other requirements are high torque, large residence time and higher shear stresses. In this setting the melt

which is highly viscous at low temperature (due to low overall residence time up to this point) passes through narrow, wedge-shaped gap between the segmented mixing discs and the barrel wall.

B. Effect of mixing disc configuration in downstream position. In this case one pair of mixing discs is left in the upstream position whilst the remaining three pairs\* are moved downwards along the processing section to be situated at 13 D position (Fig.3.2 and Table 3.1 ). Two mixing disc configurations viz. open and closed are used. For each setting three screw speeds are used. The conditions for these runs are given in Table 4.1 and are plotted in Fig 4.35 and 4.36 (run A24 to A29).

The mixing discs in upstream position cause polymer to melt, and it is then carried forward by other screw sections where the temperature of the melt rises due to conduction and shearing. At the second stage of mixing discs (i.e. in downstream position), the melt is less viscous. At this point, these discs breaks up the polymer flow pattern. Thus it breaks up and disperses the unmolten solid bed in polymer melt and thus enhances melting by increasing the contact area and thus heat transfer. Besides this function, these melting discs at this position also thermally homogenise the polymer melt. Obviously at this point the pressure is once more consumed while passing through the melting discs, though pressure drop is not of the same magnitude as it is in upstream position (due to reduced viscosity). This energy consumption

---

\*Moving mixing disc into two positions leads to the necessity for blanks to be used, and therefore total of 4 rather than 5 mixing discs can only be used.

(throughput per unit current) is shown in the figures (Table 4.2B). In the closed disc configuration, throughput per unit current is the lowest followed by open. (Results from 9 rpm open disc configuration seem to be an anomaly.) The reason for this is similar to that explained above in "upstream" mixing discs settings. The closed disc configuration offers the maximum restriction to the flow and thus consumes maximum energy.

The mixing discs, being slotted in radial direction, do not offer a helical flow path to the polymer melt. Instead they break up the polymer melt into several segments - due to the presence of the radial slots. Passage through these discs breaks up the velocity flow pattern present in the polymer melt regime. This act gives some longitudinal and a good deal of transverse mixing. The flow mechanism through mixing discs in a single screw extruder is described by Fingerale (1973), which is shown in Fig 4.44. However in a twin screw extruder this flow behaviour will get further modified by the interrupting influence of the intermeshing of the other screw. This will then generate a somewhat modified overall flow to that shown by Fingerale Fig 4.44 . In the case of open disc configuration, presumably most of this circulating flow goes into the next set of spaces while for closed discs this individual circulating flow is divided into two parts and thus offers more splitting. However, this statement is based on the limited work in this region and also from speculation based on its simple geometry.

As discussed before, the heat for melting is derived from shearing of the polymer melt and from conduction from heater bands. So in the downstream setting of mixing discs some shearing is done by the one mixing disc in upstream position while the rest shearing is derived

Fig. 4.44 Flow pattern through slotted discs (after Fingerale).

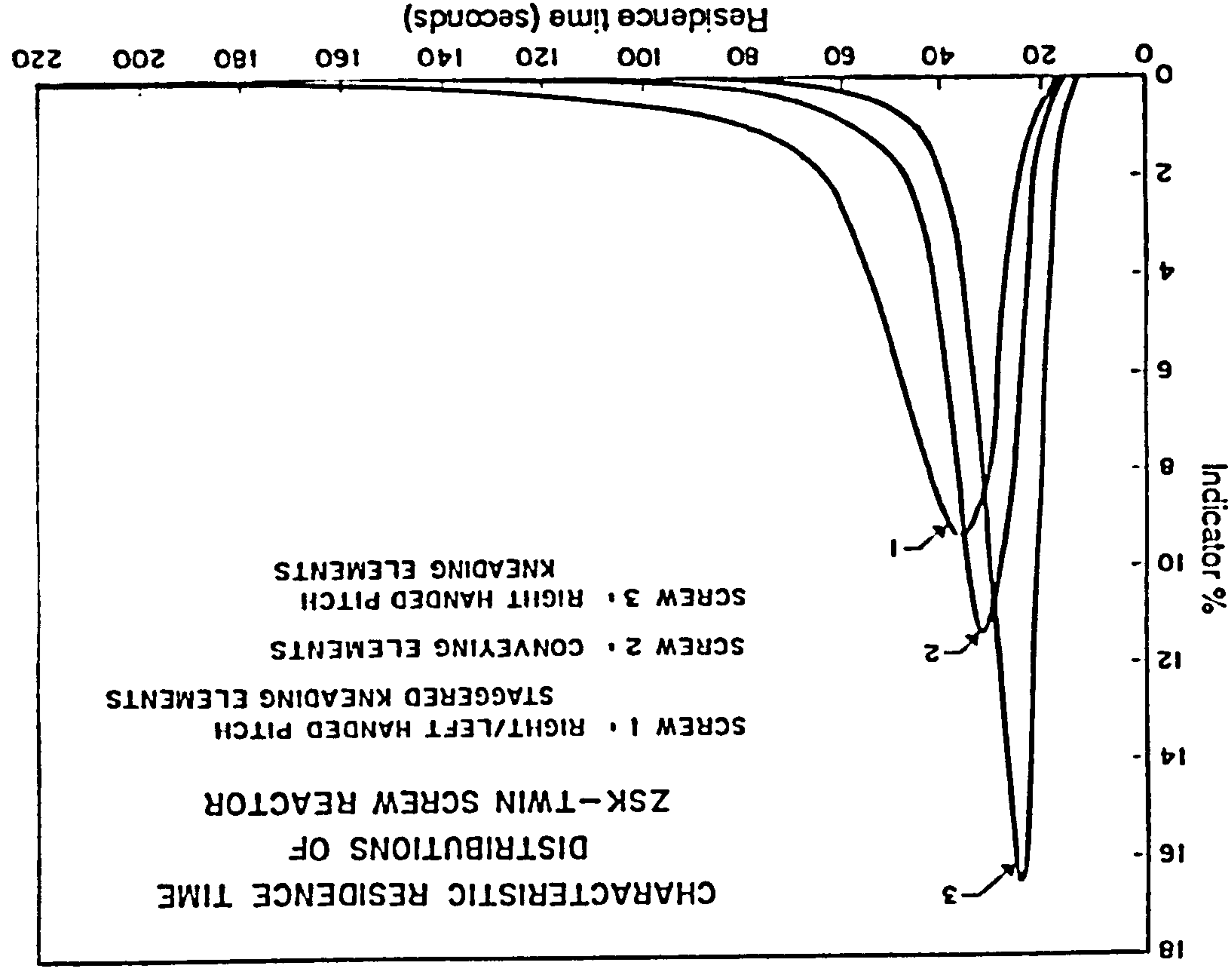
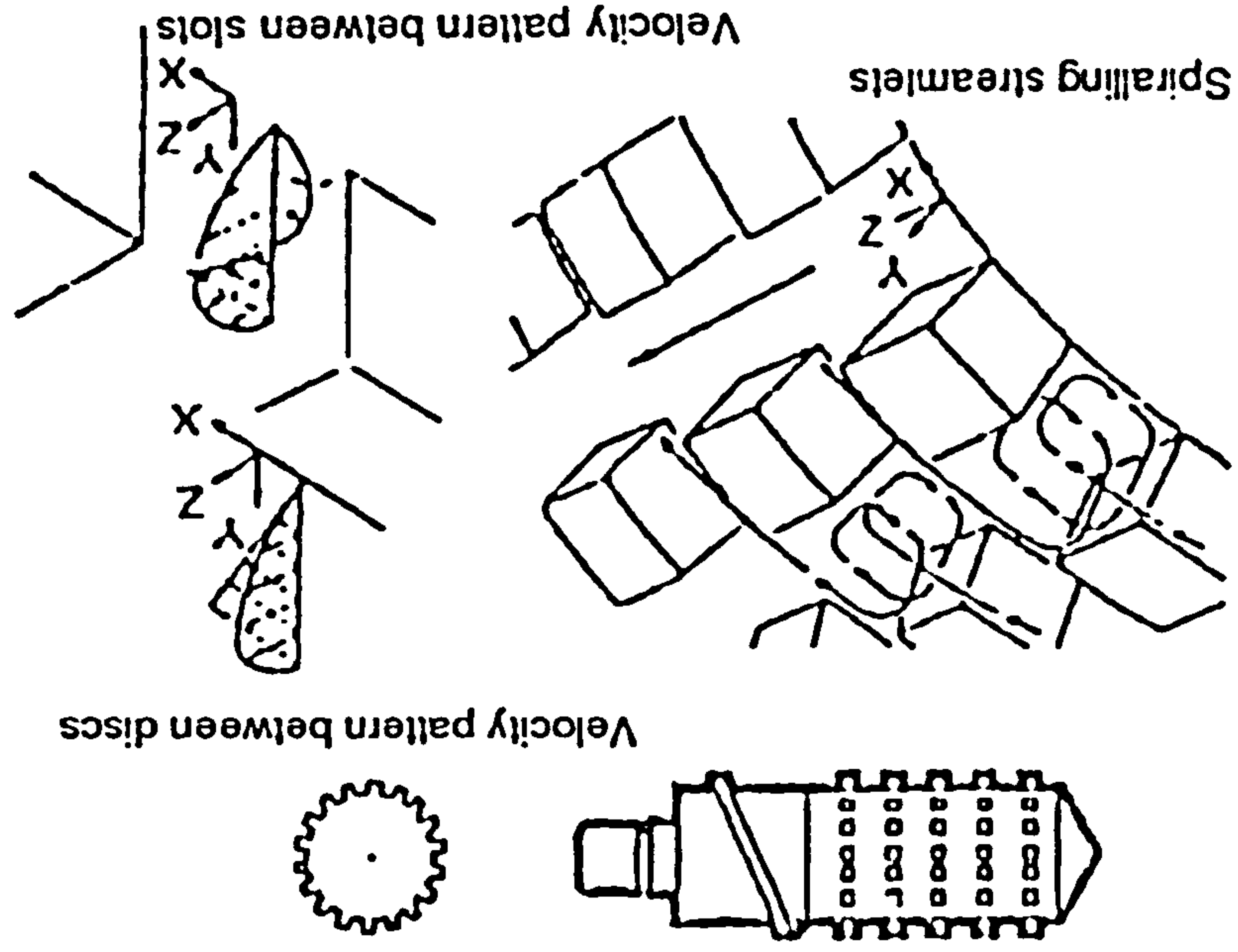


Fig. 4.45 RTD for various screw configurations (After Herrmann & Eise 1981).



from the other mixing discs in downstream position. As discussed before, closed mixing discs offer maximum resistance and thus give lowest throughput per unit current. This leads to more energy input which causes maximum melting, leading to high compaction and consequently higher filled volume. So as discussed in section 4.2.3 the maximum filled volume is achieved at 9 rpm. The increase in screw speed does not cause any improvement for this closed disc configuration. However, for open mixing discs at low screw speed, the filled volume is low due to the poor melting by first melting disc in upstream position and smaller contribution by open discs in downstream position. But increase in screw speed causes pressure build up at first melting disc and consequently an increase in filled volume occurs. These results are similar to the work by Herrmann and Eise (1981). They showed that alternating left and right handed pitched kneading discs (similar to closed discs of present study) result in maximum degree of fill and higher mean residence time than open mixing disc configuration.

The flow through mixing discs is quite different from the normal conveying through the screw pitch. The molten polymer passes through the slots of the mixing disc, and it undergoes orientation and shearing. In general it can be said that the mixing produced by shearing alone is linearly proportional to the shear applied (Ng and Erwin 1979). The mixing achieved by this mechanism is considered quite inefficient. However, due to orientation caused by the segments of the mixing disc and also by the interaction of the mixing discs of the other screw, much superior mixing is achieved. Thus in these mixing discs the mixing becomes more efficient on the available area by countering the tendency of the area to be oriented parallel to the shearing plane. The combination of separating the melt flow and

wiping the melt is nearly an ideal situation from mixing point of view.

The theoretical work by Ng and Erwin (1979) has shown that increase in number of reorientations exponentially increases the interfacial area. Similarly Dekker (1978) and Fingerale (1973) have shown in single screw extruders, the beneficial effect of mixing section in achieving homogeneity in the extrudate temperature.

The RTD curve (Fig. 4.35 and 4.36) does show an interesting trend. Both of the settings (open and closed) show that increase in screw speed moves RTD curve towards more axial mixing and thus moves towards laminar flow. On comparing the two configurations in downstream position at various screw speeds it becomes clear that whilst at 9 rpm closed discs show more plug flow type behaviour than open discs, at 18 rpm the differential in two settings is not high, and at 27 rpm both the settings give nearly same curves. The value of variance does support the above findings and trend.

Similar results are reported by Herrmann and Eise (1981) who showed that alternating right and left handed pitch kneading discs resulted in greater longitudinal mixing than conveying elements with constant pitch and right handed mixing discs gave the least (Fig 4.45).

4.3.6 Effect of melt pressure: Extruders are fitted with a die which then forms an integral part of the system. In the extrusion process, a melt pressure build up is required in front of the die so as to overcome the flow resistance of the die. The pressure at the screw tips depends on the following.

- (i) Throughput rate.
- (ii) Geometry of the flow channel in the head and die.
- (iii) Rheological properties of the material being extruded.

For a given system, all other variables being constant, increase in throughput increases the pressure build up at the screw tips. The geometry of flow channel and die have a profound effect. The die could be designed to give a required pressure at the screw tips by creating resistance to flow. The pressure build up at the screw tip helps in melting the "remaining" unmolten polymer. This is true in high pressure systems where a pressure of 200-500 MN/m<sup>2</sup> is developed as compared to GKN Windsor extruder where only a modest pressure (1.5-5 MN/m<sup>2</sup>) is built up. Therefore in the case of a run with high screw speed (Run A15) the polymer throughput shows that the centre of polymer melt remains unmolten or rather partially molten.

In the present study the pressure of the system was varied by adjusting the slot height in the die and thus changing the restriction to polymer flow. This in turn creates a back pressure. Overall, three slot heights in the die were used, these being 2.15, 4.8 and 6.25 mm (Run A7, 10, and A12 - for details see Table 4.1). These gave a melt pressures of 4.12, 3.79 and 2.65 MN/m<sup>2</sup> respectively in the melt pool in the vicinity of the screw tips. The rest of the variables, including throughput were kept constant. The RTD curves from these three conditions do not show as large and pronounced differences compared to effect of other variables on RTD (Fig 4.46). The increases in pressure at screw tips (from 2.65 to 3.79 and finally to 4.12 MN/m<sup>2</sup>) lead to an increase in axial mixing and thus broader RTD curves. This trend can be explained by looking at the effect of pressure on the flow mechanism in a co-rotating extruder. The pressure changes at the

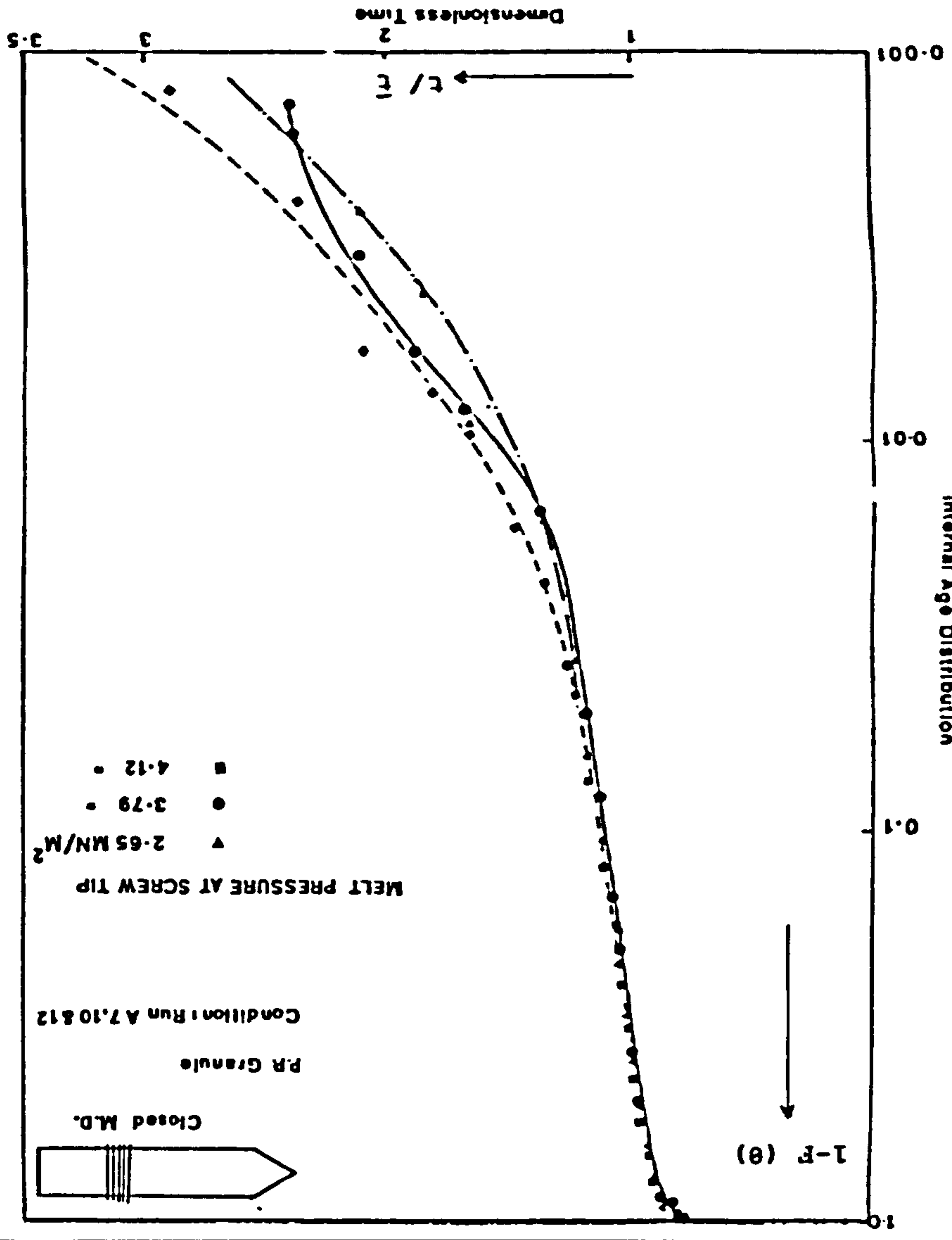


Fig. 4.46 Effect of melt pressure at screw tips on RTD.

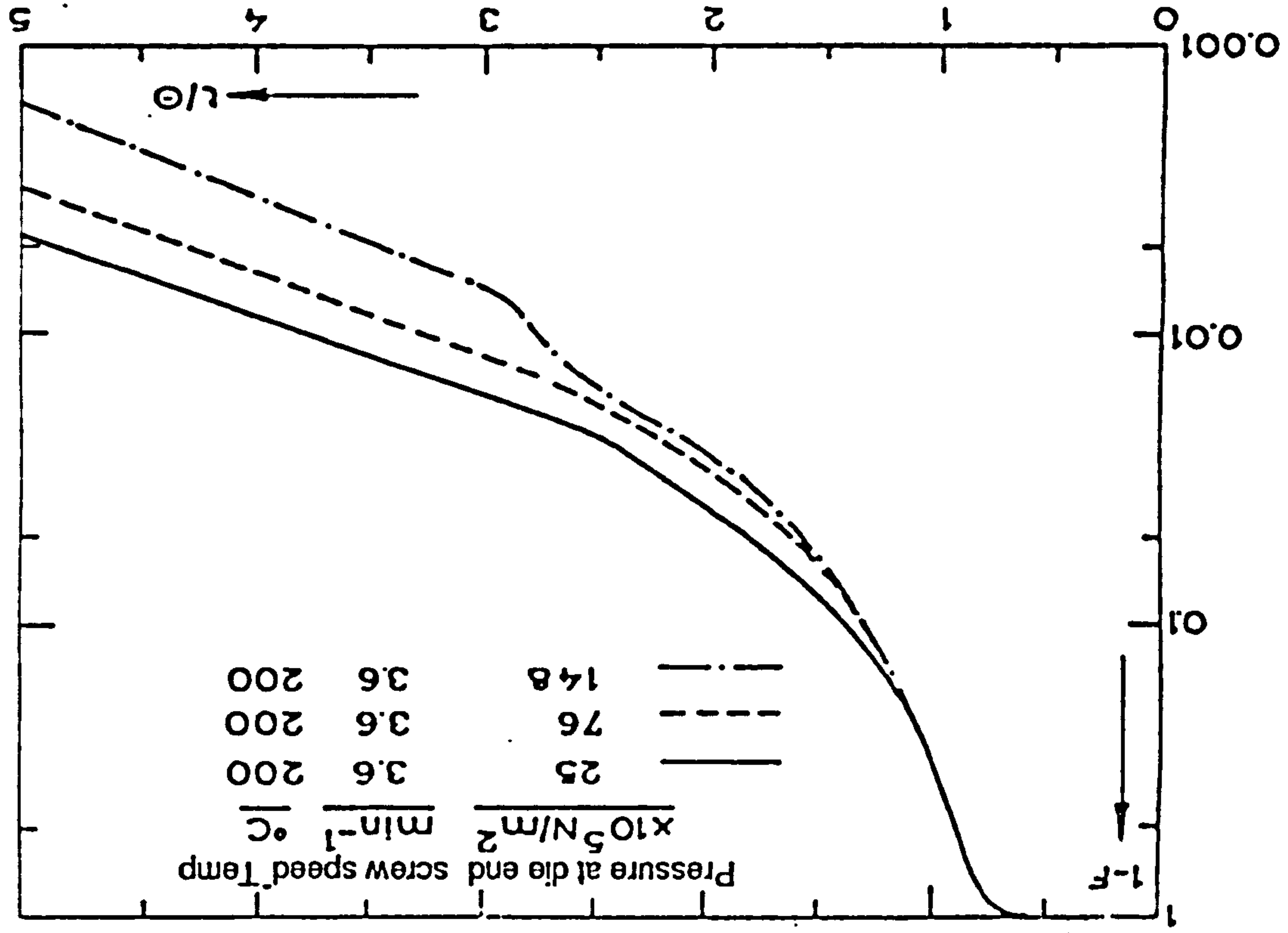


Fig. 4.47 The effect of die pressure on the tail of RTD at low screw speed (After Janssen & Churchill 1978).

screw tips lead to change in polymer conveying and leakage flows etc. In a co-rotating twin screw extruder, the conveying of the melt takes place as a result of combination of the frictional and viscous forces and also from the physical wiping action of the other intermeshing screw. The intermeshing screw physically prevents the material from rotating with the screw. A barrier is formed for backflow due to intermeshing regions thus giving a limited positive displacement action. However, as discussed above, the frictional force's contribution comes into play with the effect of the pressure on it. Generally speaking, the frictional forces are tied in with the pressure generated at the location and they increase with increase in pressure. (Therefore it is more effective at higher pressures). Thus increase in pressure (which partially travels back from screw tip) leads to increase in conveying and thus tends towards more positive flow. But the viscous force's (discussed above) contribution is in the opposite direction. The increase in pressure leads to better contact with hot metal and imparts resistance to the polymer flow. Both these factors tend to increase the overall rise in temperature. Blyumental and Safulin (1978) have shown that higher die pressure in a single screw extruder is associated with higher average temperature of the melt.

As the results show above, the conveying mechanism, in the range of pressures studied, shows a more axially mixed flow with increase in pressure. The initial rise in pressure from 2.65 to 3.79 MN/m<sup>2</sup> changes the curve marginally, but further increase in pressure (from 3.79 to 4.12 MN/m<sup>2</sup>) leads to a big shift in overall curve especially in the tail region. The conveying in this co-rotating twin screw extruder is more dependent on the viscous forces than the frictional ones. Furthermore the increase in pressure at die end results in increase in

polymer melt temperature thus leading to lower viscosity of the polymer. Thus lower viscosity would obviously have a substantial effect on the conveying and would work towards a broader RTD curve.

The above explanation could be used to explain, quite systematically, the other published work. Bigg (1973) for a single screw extruder has done quite fundamental research in the subject and found that for a Newtonian fluid the RTD curve remains the same for different values of  $G_2$  (ratio of pressure flow and drag flow). However, in non-Newtonian fluids, Bigg (1973) showed that the deviation from Newtonian behaviour increases as the power law index decreases. For a particular power law index (as power law index of 0.2 in Fig 4.22), RTD curve broadens with increase in  $G_2$  value (increase in pressure or decrease in throughput rate). At this point, as explained in above paragraph, the viscous forces play a major part in conveying and lead to a lower viscosity and thus more leakage flow and broader RTD curve. This can be seen in Fig 4.22 where flow becomes more axially mixed when  $G_2$  value is increased from 0.5 to 1.5. Similar results are reported by Mohr et al. (1957), Todd and Irving (1969) and by Janssen (1978) at high screw speed when the pressure is increased from 4 to 6.3 MN/m<sup>2</sup>.

Furthermore, Bigg (1973) showed that on further increase in  $G_2$  value, the flow becomes less axially mixed, and at one stage it develops an inflection beyond which it tends to become more of plug flow type (Fig 4.22). This can be explained by the flow behaviour, as discussed above. By increased throughput rate, the volume of polymer melt inside the channel increases, associated with the increase in pressure development. As a result the frictional forces start to act. Similar results are reported by Janssen (1978) at low screw speed (Fig 4.47) and also at high speed when the pressure is increased from 6.3 to 11.1

$\text{MN/m}^2$ . In that case the curve for  $14.8 \text{ MN/m}^2$  pressure condition also shows an inflection, as discussed above.

The dimensionless residence time is relatively independent of die pressure. Janssen et al. (1979) found similar results, and they concluded that this is associated with the relatively small change in the number of fully filled chambers. From the data in Table 4.2A it is clear that increase in die pressure is associated with decrease in stagnation time for 1 % of the material. It progressively decreases from 1.67 to 1.57 and finally to 1.49.

4.3.7 Effect of physical form of polymer: Polypropylene polymer (of similar molecular composition) in two physical forms, in granular and powder form, was compared. Two types of pulley were used covering both screw speed ranges, low screw speed range (Run A21 to A26 as in Fig 4.34 and 4.35) and high screw speed range (Run A13 to A17 as in Fig 4.39 and 4.38).

On comparing powder with granules in general, it becomes quite clear and obvious that RTD curve for powder shows a much pronounced axially mixed system. The difference in the behaviour of powder and granules arises from different internal friction between particles, increased surface area of the powder and the lower bulk density of the powder. The increased surface area, as shown later, leads to faster melting of the powder.

The polypropylene powder has a bulk density of  $500 \text{ kg/m}^3$  as compared to  $578 \text{ kg/m}^3$  of granules. This leads to less input of powder (as compared to granules) at feed point. As at low screw speeds (with small pulley system) the throughput rate is limited by the conveying

capacity of the screws, the powder should show less throughput and this is found in experiments (Run A21 to A25). However, at high screw speeds (with large pulley system) the throughput rate is restricted by the torque capability of the extruder. Therefore the type of polymer showing low energy consumption should show a higher throughput. This is shown by the powder system and therefore powder shows higher throughput rates. The reason for low energy consumption for powder can be explained on the basis of powder's faster and easier melting ability. Assuming that the powder and pellets are spheres, then the calculated times for complete melting by conduction alone are 0.13 and 0.83 seconds respectively.

The polypropylene powder starts melting faster and earlier (due to increased surface area) and therefore would give a higher filled volume for both low and high screw speeds (Table 4.2A). As discussed above powder also shows a low energy consumption and thus higher amount of polymer processed per unit current (throughput per unit current) for both speeds.

The powder shows a higher variance or spread about mean residence time. The polypropylene granules in large pulley system do show different behaviour (Fig 4.39). It has been discussed in detail in Group C of section 4.3.3. The melt pressure at the die end is directly related to the throughput rate. The polypropylene powder runs have low throughput at low speed range as compared to granules and thus show a low pressure at die end. At the high screw speed the opposite is true.

4.3.8 Effect of polymer type: Polymers are non-Newtonian fluids and their rheological properties vary considerably from one to



another. In the present study polypropylene and polystyrene granules were compared. The same processing conditions were used for both the polymers except for processing temperatures. The details of the temperature settings on the extruder are given in the notes for Table 4.1, except to say that these represent the normally used set temperature in industry for the respective polymers.

On comparing the flow behaviour of polystyrene and polypropylene, the RTD for polystyrene shows less dependency on the screw speed (i.e. it does not change significantly) compared to that for polypropylene (Fig 4.39 and 4.48). Furthermore the RTD curves for polystyrene show overall more axial mixing than polypropylene. This behaviour can be explained by comparing the rheological characteristics of these polymers (Fig 4.1 ). These results were obtained using capillary rheometer using only one capillary die, as only the comparative values of the viscosities were of interest. Thus the entrance effect was not taken into account and Rabinowitch corrections not applied. So the reported viscosities are higher than the true viscosities. Anyway, on comparing these rheological results (Fig 4.1 ), polystyrene shows a higher apparent viscosity for a given shear rate and this difference increases with increase in shear rate. It shows a power law relationship for large range of shear rates. This may be one of the reasons for less dependency of flow characteristics of polystyrene on screw speed.

Polystyrene melt is quite viscous and this leads to the relatively higher power consumption to process this melt. As, at this high screw speed range, the throughput is restricted by torque available in extruder assembly, this leads to a rather low volumetric throughput for polystyrene. This is the case as shown in Table 4.1. The

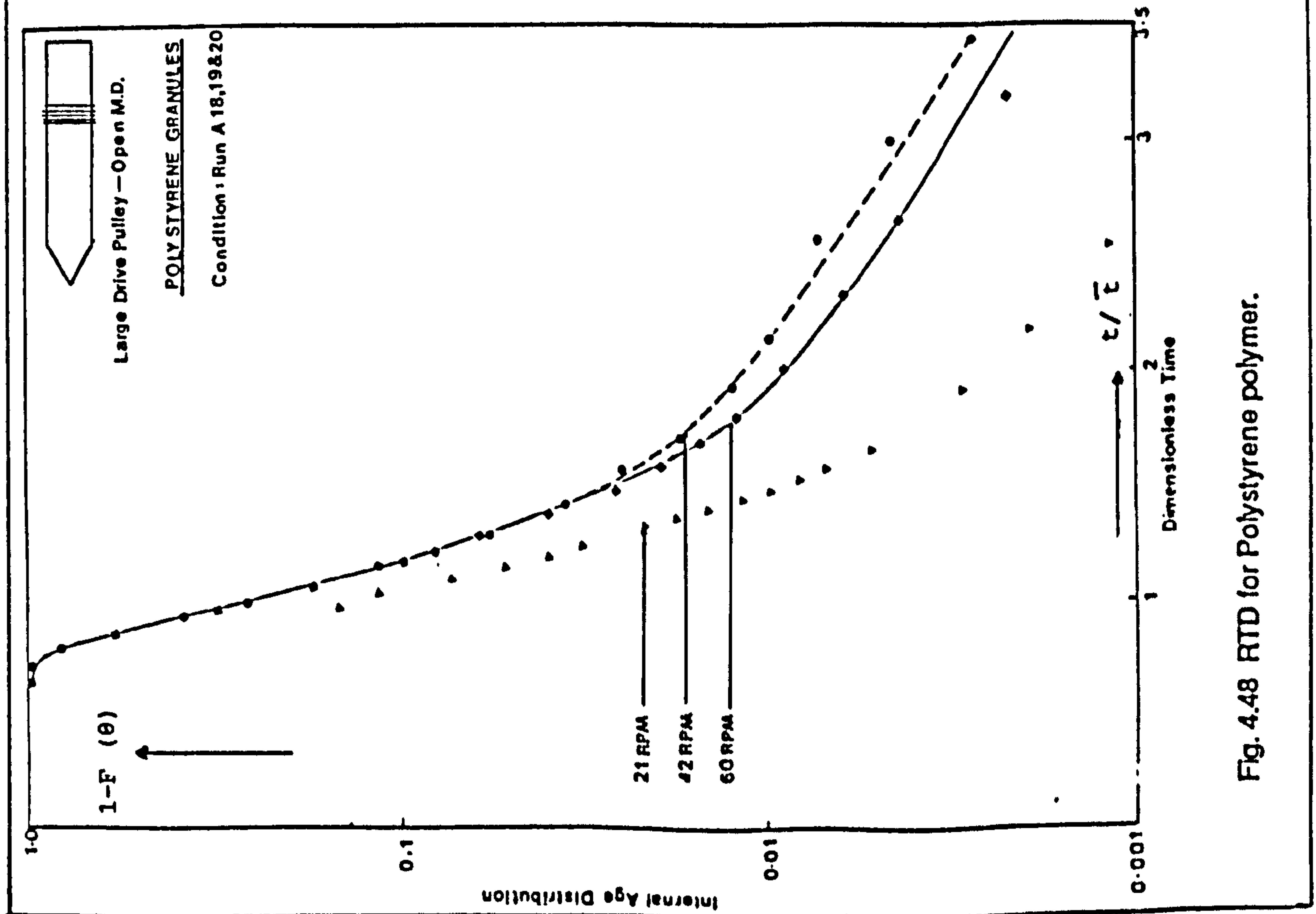


Fig. 4.48 RTD for Polystyrene polymer.

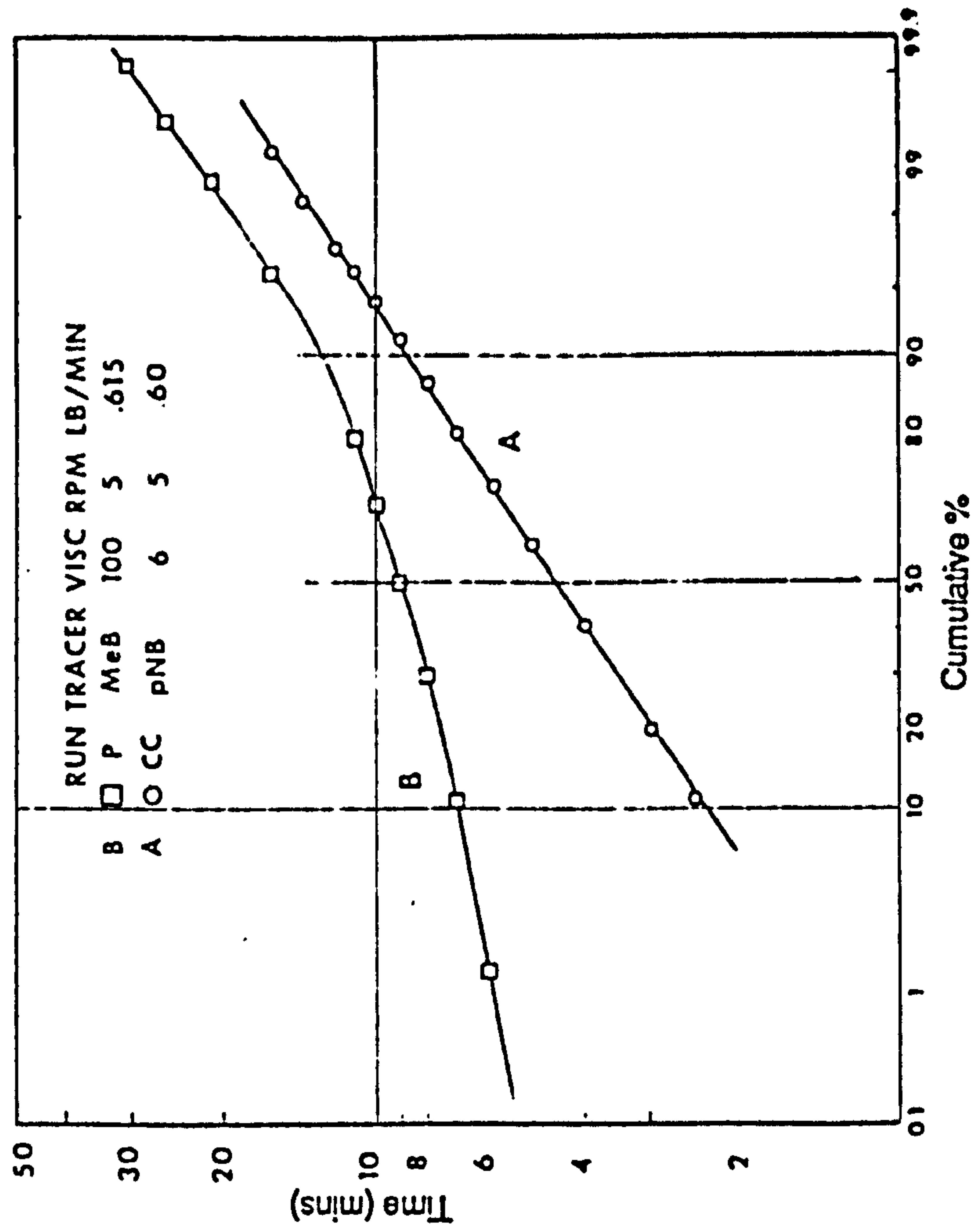


Fig. 4.49 Effect of viscosity on RTD (After Todd 1975).

polystyrene's volumetric throughput is quite low as compared to polypropylene. Thus polystyrene runs show low filled volume (Table 4.2A- Say polystyrene's  $5988 \text{ cm}^3$  as compared to  $8480 \text{ cm}^3$  of polypropylene). This low filled volume leads to more space available in the screw sections in which polymer melt can move around over itself and this leads to a higher mean residence time (Table 4.2A-7.8 minutes for polystyrene as compared to 7.2 minutes for polypropylene). This fluffing and mixing leads to a higher axial mixing and a high variance ( $\sigma_g^2$ ) for all the three speeds in polystyrene.

As we know, the polymer type affects the melting behaviour / heat requirement. For a similar heat input different polymers would give different ratios of molten to unmolten polymer and this in turn would determine the degree of fill. This would then determine the flow profile and RTD in the main stream. Furthermore, the flow characteristics are different for different polymers and so is the melt zone length which would affect the RTD. Polypropylene granules show a higher volumetric throughput as compared to polystyrene ( $5.85$  vs  $3.96 \text{ m}^3$  per hour) which in turn would lead to less axial mixing for the polypropylene material.

In comparison with polystyrene polypropylene has lower density ( $905$  vs  $1150 \text{ kg/m}^3$  of polystyrene ), higher melting temperature and lower thermal conductivity ( $0.16$  vs  $0.18 \text{ W/mK}$  of polystyrene).

On the basis of the calculations carried out elsewhere (Janssen 1978) the amounts of heat required to reach the usual processing temperatures are  $690 \text{ kJ/kg}$  and  $505 \text{ kJ/kg}$  for polypropylene and polystyrene respectively (Table 4.6). From these calculations it becomes clear that in polypropylene the mass in the middle of the

screw channel remains relatively cool and melting takes a longer time. This was confirmed by shock cooling experiments, described in section 3.5 . In this study an unmolten polymer core was observed at high screw speed. So at 60 rpm, the high screw speed, the heat transfer is quite low and melting is really restricted, thus showing more plug flow (Fig 4.39 and 4.48). However, when polypropylene powder is used, this plug flow behaviour is not observed simply because in powder the heat transfer is substantially better.

TABLE 4.6 PHYSICAL PROPERTIES OF POLYMERS USED

No.	Physical properties	Units	Polypropylene Granules GWM 22		Polystyrene Granules Lustrex HF66 Ext	
			at Room Temp.	Melt <sub>0</sub> 230 °C	at Room Temp.	Melt <sub>0</sub> 165 °C
1.	Density	kg/m <sup>3</sup>	905	750	1150	990
2.	Bulk density	kg/m <sup>3</sup>	0.58 <sup>1</sup>		0.62	
3.	Melting point	°C	160-66		95-104	
4.	Melt flow index		4.0 <sup>2</sup>			
5.	Thermal conduct. <sup>A</sup>	w/m <sup>0</sup> K	0.12	<u>0.16</u>	0.14	0.18
6.	Friction coeff. <sup>A</sup> agaist mild steel	at 20 <sup>0</sup> C	0.32		0.22	
		at 80 <sup>0</sup> C	0.16		0.25	
7.	Amount of heat re- quired to reach usual proc. temp. <sup>A</sup>	kJ/kg	690 (250 <sup>0</sup> C)		505 (220 <sup>0</sup> C)	

<sup>1</sup>) Bulk Density of powder is 0.5 g/cm<sup>3</sup>.

<sup>2</sup>) For polypropylene granules it was measured at 230<sup>0</sup> C under load of 1.16 kg.

For polypropylene powder mfi value is 22 measured at 190<sup>0</sup> C under load 10 kg.

<sup>A</sup>) Dekker (1976).

## *CROSS CHANNEL FLOW AND TRANSVERSE MIXING*

In this section, the results obtained by the shock cooling experiments are analysed. By systematic study of sections cut along the screw channel, the flow path of the polymer melt inside extruder together with the influence of the various leakage flows was analysed. The study was supplemented with study of transverse mixing along the extruder. Later on in the chapter it was tried to relate the progression in transverse mixing with the overall flow mechanism.

4.4 Flow mechanism in extruder: As described above, the flow mechanism inside the twin screw extruder was established by using colour tracer technique. The flow mechanism in twin screw extruder is rather difficult to understand because of its three dimensional nature. Therefore it has been tried to explain this with the help of diagrams together with sections taken from frozen polymer skeleton.

### Schematic explanation for various diagrams showing Flow Mechanism

For ease of understanding the flow behaviour of various zones is shown by painting the screw skeleton. The three photographs of this screw skeleton showing different flow regimes are given in Fig 4.50, 4.51 and 4.52. These diagrams give a three dimensional understanding of this complex flow which is rather difficult to grasp. This is supplemented by a summary of various leakage flows showing their mode of grouping together with their mode of rotation. This is then supplemented by diagrammatical representation (Tentative model) of flow mechanism in pictorial form (Fig 4.54). This is then supplemented by "where to where" schematic diagram (Fig 4.55). In part A (Fig. 4.55 A) of this diagram, the flow into the start of number 2R

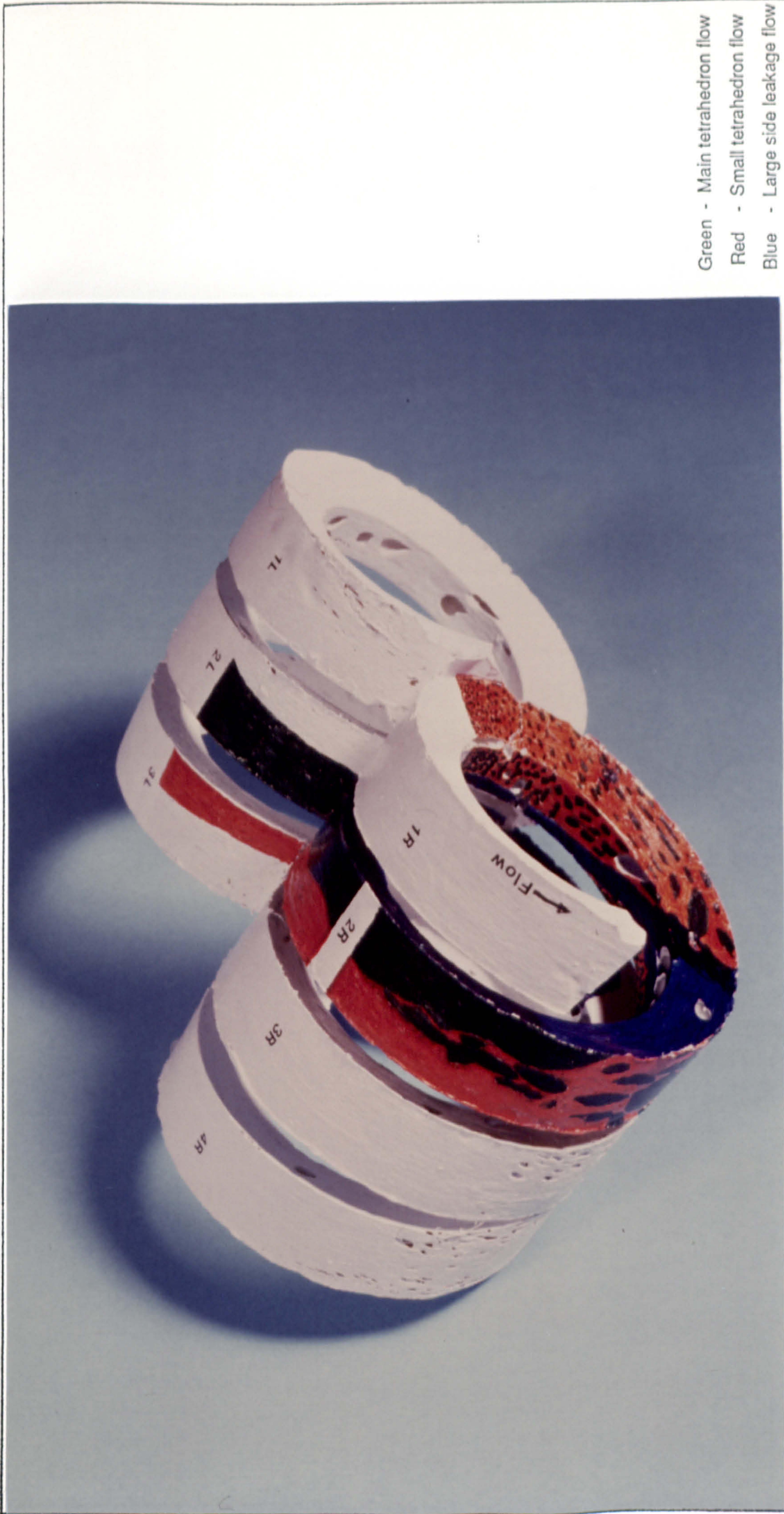


Fig. 4.50 Tentative flow model (photographed from top) showing origin and initial mixing of two tetrahedron flows. The spatial position changing of large leakage flow is also shown.

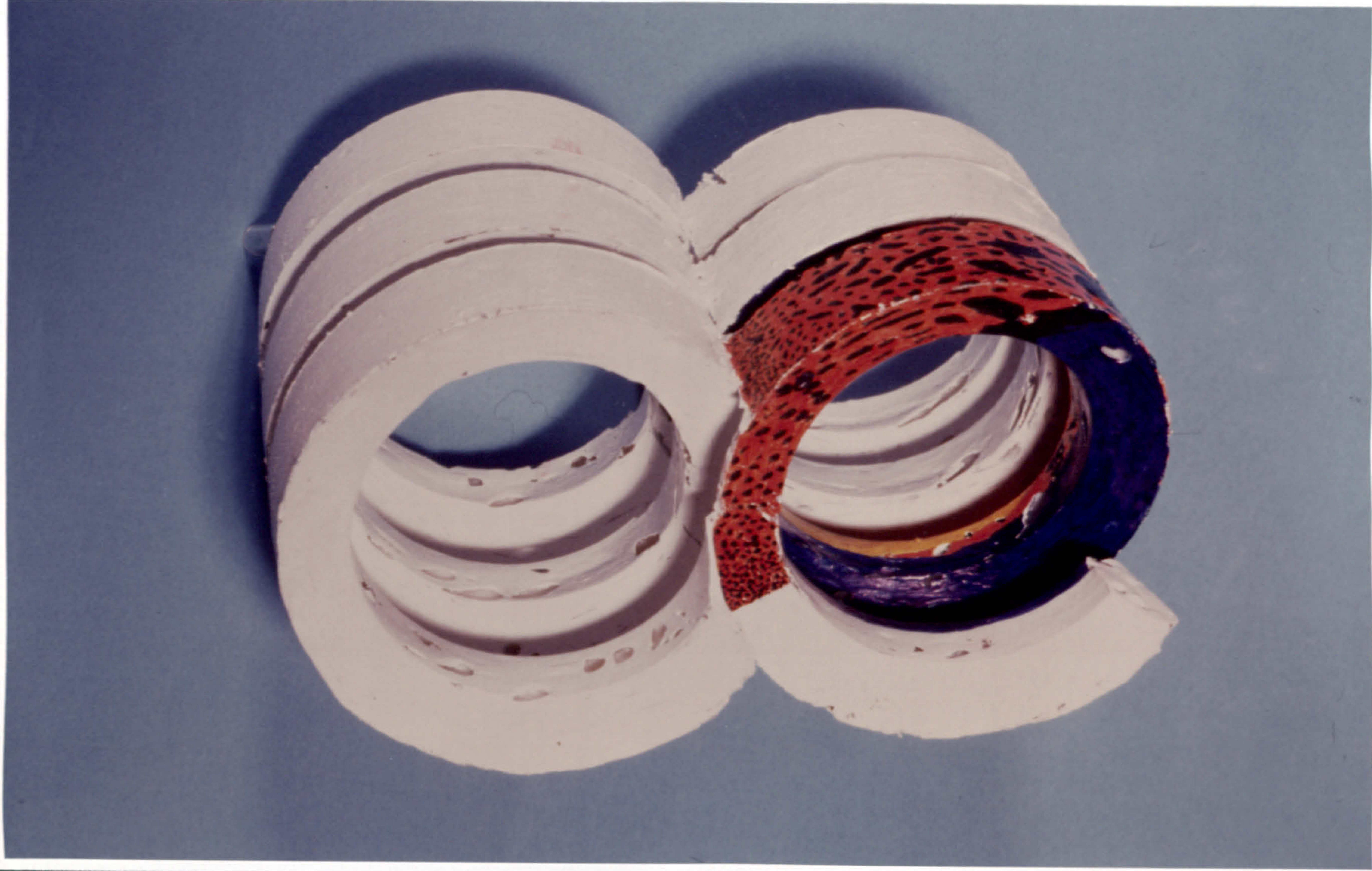


- Green - Main tetrahedron flow
- Red - Small tetrahedron flow
- Blue - Large side leakage flow
- Yellow - Central flow

Fig. 4.51 Tentative flow model (photographed from underneath c.f. Fig.4.50 position) showing origin of central flow and large side leakage flow. Also seen is intermixing of tetrahedron flows.



Fig. 4.52 Tentative flow model showing (from underneath) the spatial shifting of various flows.



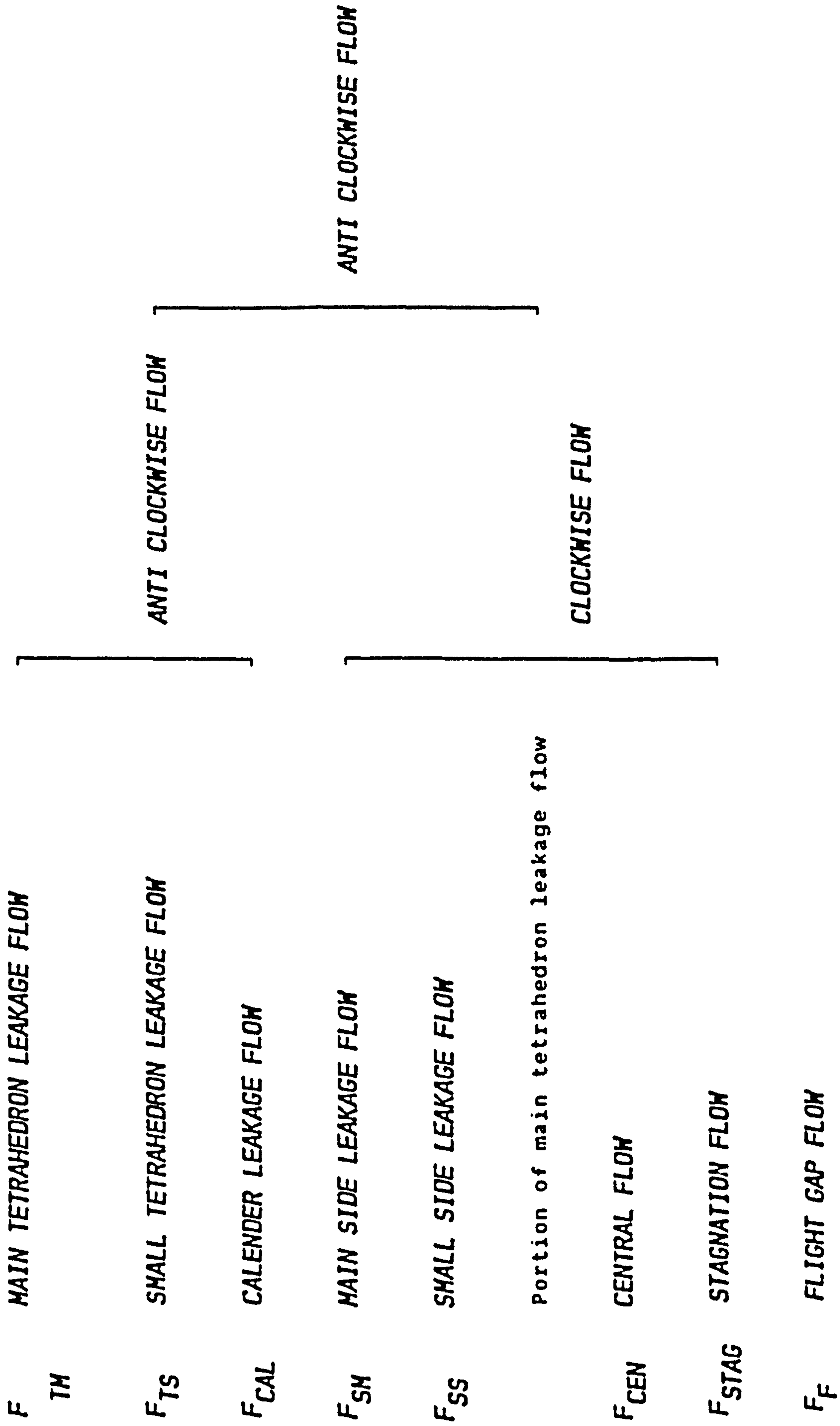
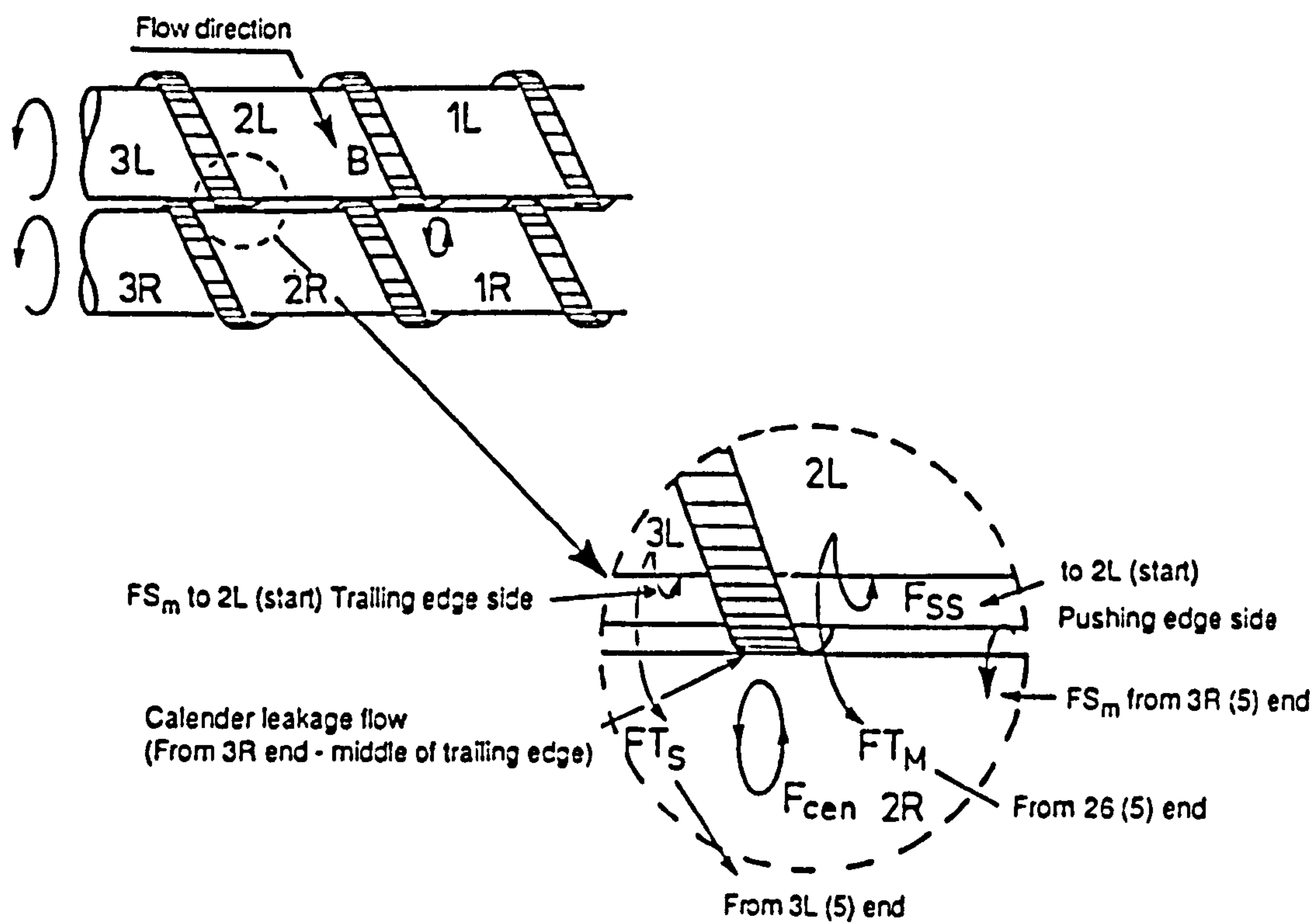


FIG. 4.53 VARIOUS LEAKAGE FLOWS IN CO-ROTATING TWIN SCREW EXTRUDER.



- $F_s$  - side leakage flow
- $T_s$  - Tetrahedron leakage
- $F_{cen}$  - Central flow
- $F_{cal}$  - Calender leakage flow

Fig. 4.54 Tentative model for flow mechanism in co-rotating twin screw extruder.

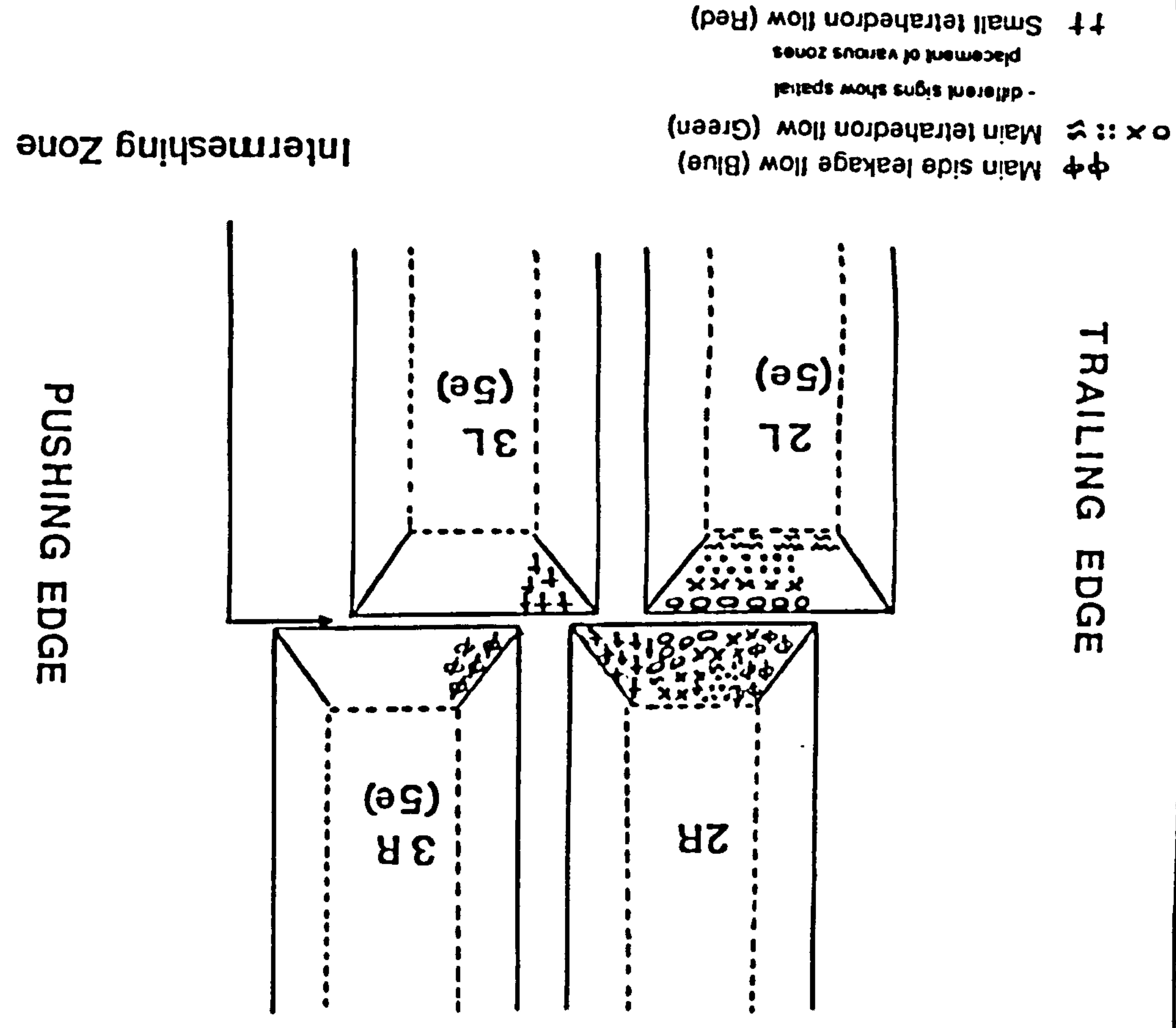


Fig. 4.55 A Schematic representation of polymer flow "Where to Where".

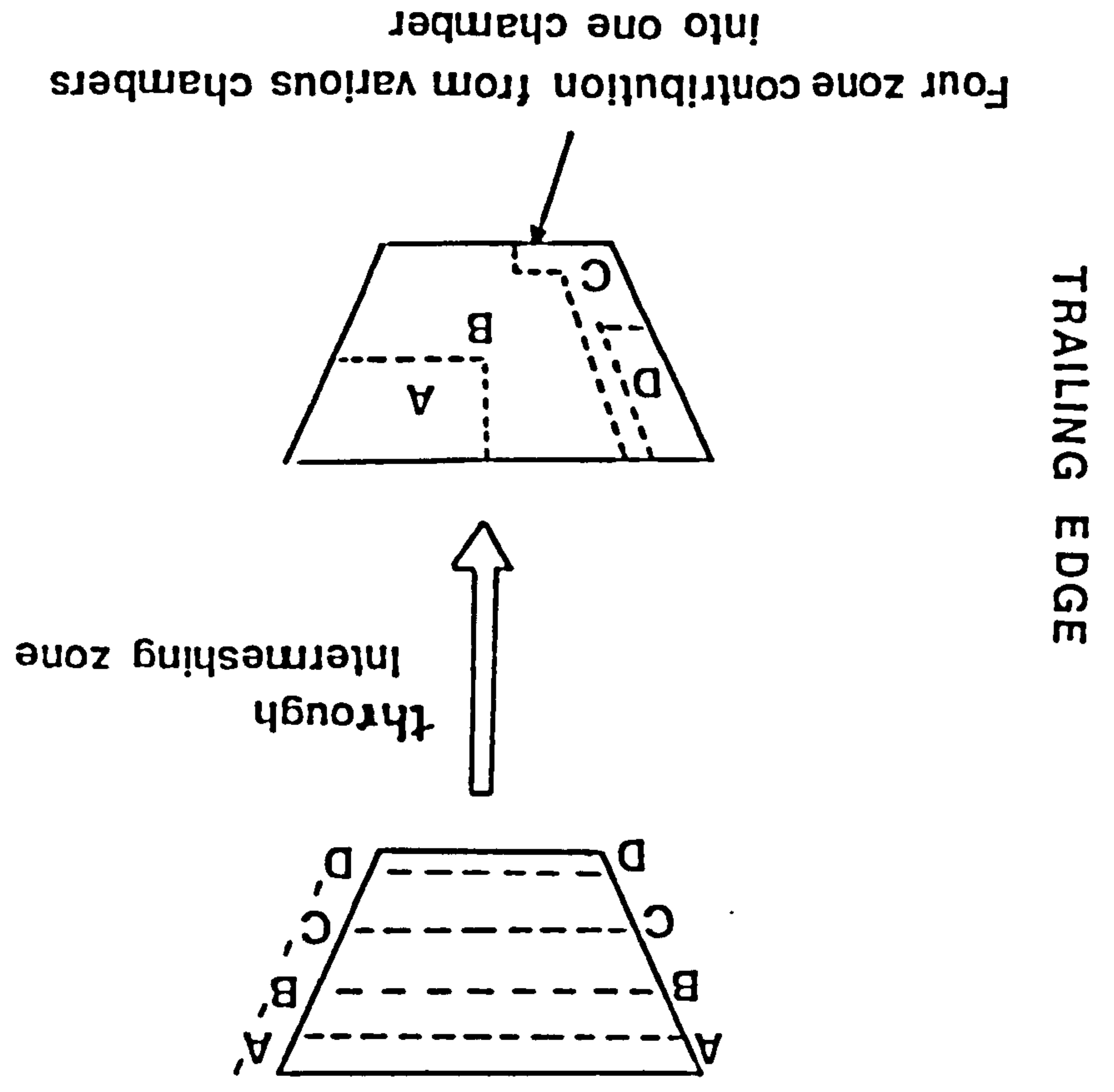
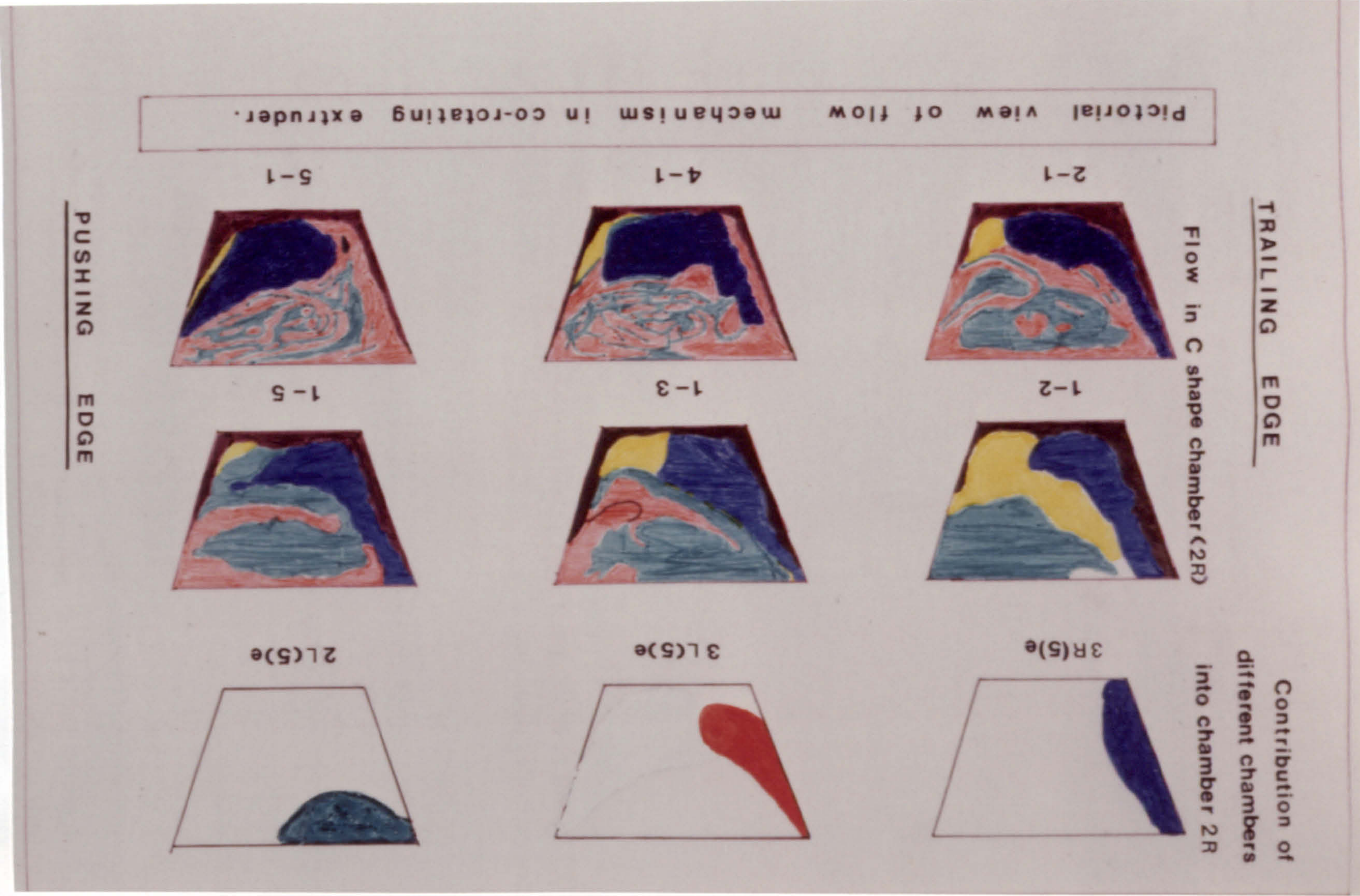


Fig. 4.55 B Diagrammatic explanation of flow through intermeshing zone.

"C" shape chamber is shown (see Fig.4.50 for explanation of 2R etc.). It shows that polymer melt comes from end of the 2L, 3L and 3R "C" shape chambers. In part B of this figure (Fig.4.55 B), the effect of intermeshing zone on the shifting of spatial position transversely in "C" shape chamber is shown. Once this basic concept is clear, the pictorial view of flow mechanism is given in Fig 4.56, the colour scheme remaining basically the same, as that used in Fig 4.50 to show polymer melt flow. The flow and mixing within 2R "C" shape chamber is shown in last two rows with first row showing the polymer flow contribution into 2R from different chambers of screw. In Fig 4.57 the original sections from screw skeleton are shown, from which the exact pictorial view of Fig 4.56 is made. The section A shown in Fig 4.57 is the one showing stagnation places in flow (white material vs. black main region). Fig 4.58 shows the sections from screw skeleton in various planes showing transition from one plane (2L) to other plane (2R) through a  $90^{\circ}$  rotation on flow axes. In between the two sections are shown the horizontal section through 2R in various planes 1 to 4 as shown in diagram. These sections substantiate the flow model and show the evidence of main tetrahedron leakage flows as shown in Fig 4.56. In Fig 4.59 the flow through intermeshing zone is shown by actual sections from screw skeleton. So by cutting sections through intermeshing zone, one screw section is cut transversely while the corresponding other one being cut longitudinally. The later sections show the various planes, e.g area AA' etc. as shown in Fig 4.55 B's top section picture.

#### Tentative model of flow mechanism in co-rotating Twin Screw Extruder

GKN Windsor 250x is a co-rotating, closely intermeshing and conjugated twin screw extruder. The flights and screw channels are trapezoidal



Main side leakage flow (blue)  
 Main tetrahedron flow (green)  
 Small tetrahedron flow (red)

Fig. 4.56 Pictorial view of tentative flow mechanism in co-rotating extruder.

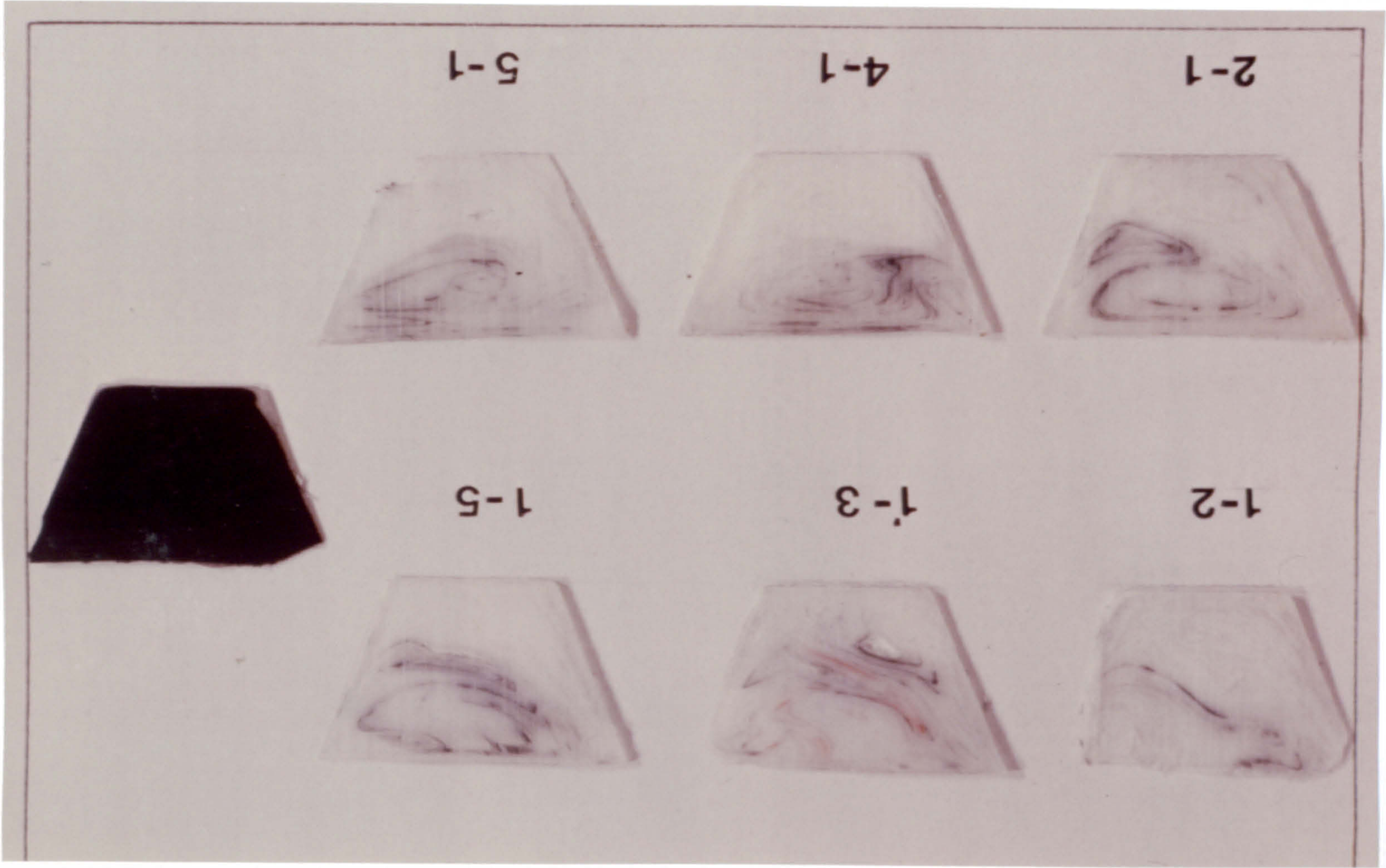
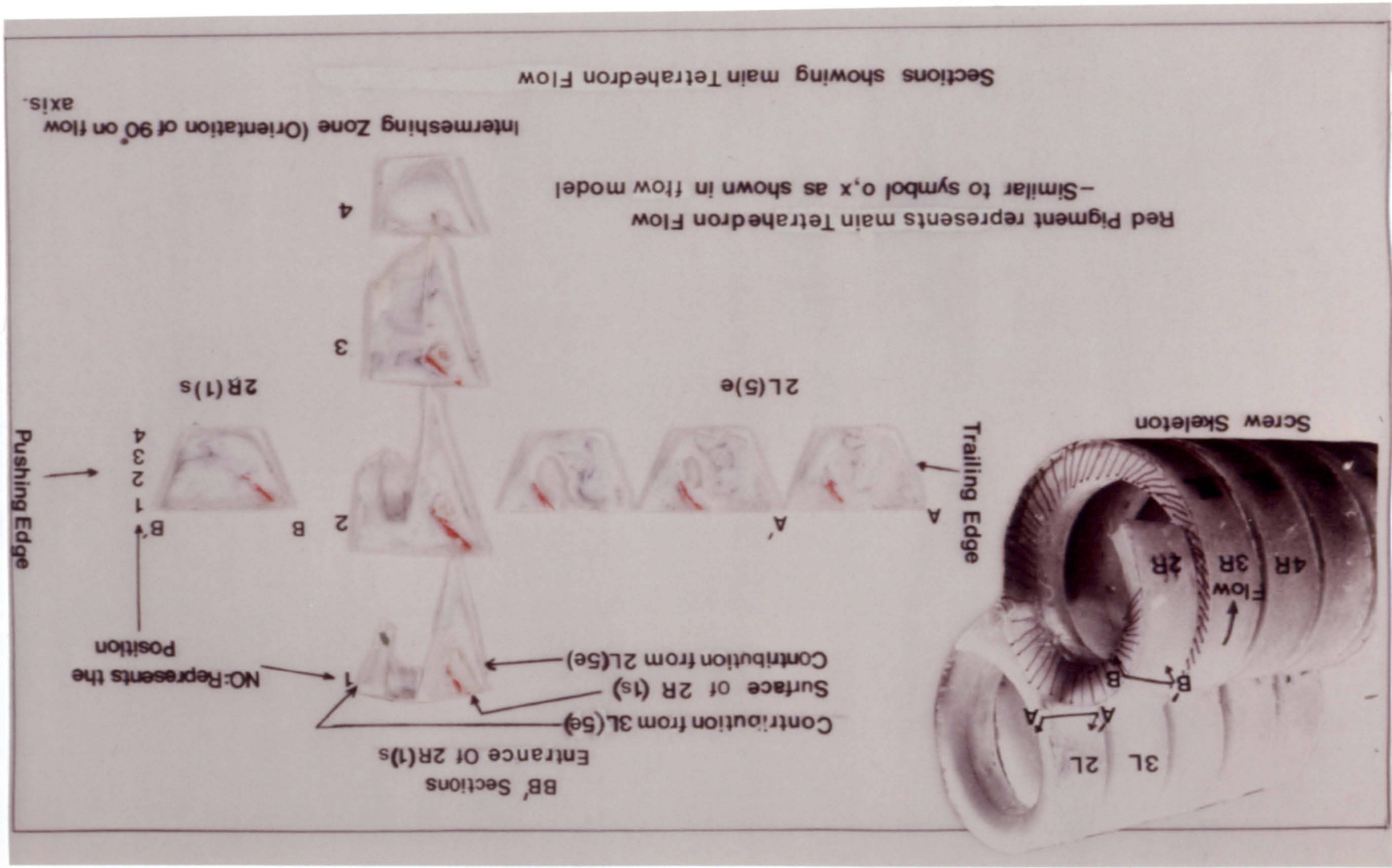


Fig.4.57 Flow mechanism in "C" shaped chamber.

Fig. 4.58 Sections showing main tetrahedron flow.





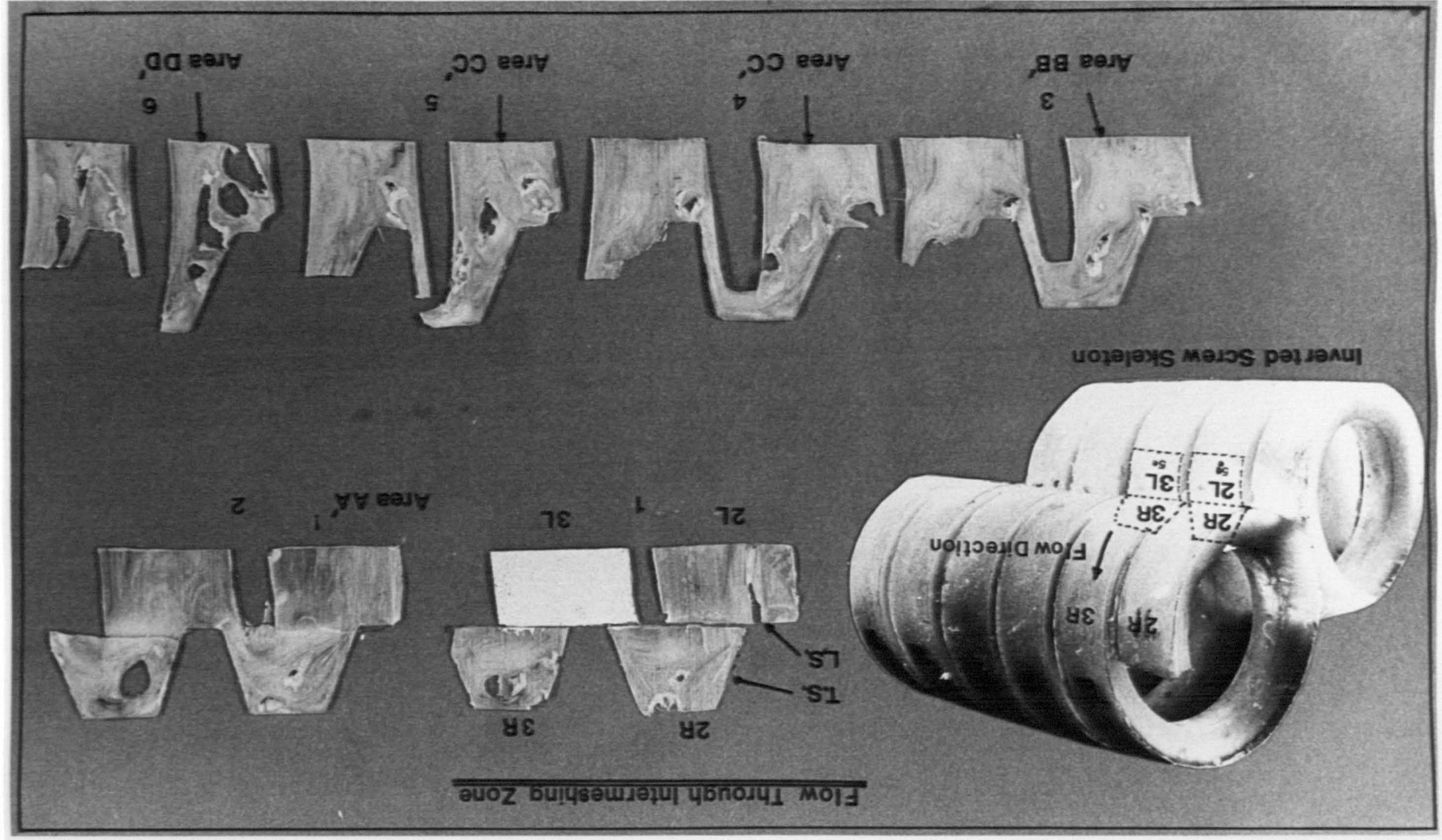


Fig.4.59 Sections showing flow through intermeshing zone.

shaped which result in a high degree of interchannel penetration. The polymer melt flows as a result of the frictional and viscous forces. During this flow, the polymer melt rapidly adjusts to an equilibrium configuration and behaves as a viscous material. On approaching the intermeshing zone, the polymer is prevented from remaining on the present screw and pushed into the chamber of the other screw. Thus it follows a shape of "figure 8" pattern (without the centre portion of 8) along the length of extruder. The intermeshing zone splits the incoming polymer melt into several streams which move to various places according to their position in the channel. These then flow into variety of new positions in various channels thus leading to transverse as well as axial mixing.

This flow can tentatively be described systematically by first analysing the types of various flows, their origins, the position they occupy soon after passage from intermeshing zone, their subsequent mixing with other flows and finally their behaviour in passage along the whole of the chamber in next intermeshing zone.

The flow mechanism is discussed with reference to

4.4.1 Various flows, their origins & positions

4.4.2 Flow behaviour in passage along the 'c' shape chamber

4.4.1 Various flows, their origins & positions: For ease of understanding, in the following discussion, an example has been taken to show the polymer melt flow from various channels to 2R channel (Fig 4.54). The following flows constitute the main flow within the twin screw extruder.

A. Tetrahedron Flow : As the polymer reaches the intermeshing

zone, the flank of one flight acts as wedge and forces the material out of the channel of the other screw. This happens because the screw velocities in the intermeshing region are in opposite directions. Therefore a limited amount of melt passes through intermeshing region (from top of the screws to bottom) while almost the entire volume is transferred via the open edge area to the opposite screw. This flow thus forms a flow path of figure of 8 pattern (without the centre portion of 8) while at the sametime moving in axial direction. During this process, due to conjugated screw profile (intermeshing without much gap) and staggered arrangement of the screw, it gets divided into two unequal parts. This is more clearly shown in Fig 4.50 and 4.56 where  $F_{TM}$  is represented by green colour and  $F_{TS}$  is by red colour.

Both of these flows constitute the bulk of the flow and are assisted by the motion of the screw flight surfaces. However, the flow is much greater through the wide gaps than the narrow one. As it can be seen, the tetrahedron gap is connected with the side gap, but it relates to flow between opposite chambers in the two screws.

Similar flow was shown by Howland and Erwin (1983) in a counter-rotating, non-intermeshing, twin screw extruder. They showed that the material flows backwards in the region created by the flight sweep. This flow then moves in the intermeshing zone, just behind the flight. This flow then penetrates and forms a reoriented region across the depth of the channel. This is about the same as tetrahedron flow in the present work. They showed further that everytime the material passed through the apex, a substantial reorientation took place. They concluded that this occurs because of the angle (approximately  $140^{\circ}$ ) at which the converging flow from each screw intercepts each other. So this collision together with the transfer of material from one shear orientation to another results in this enhanced reorientation.

On contrary, Bigio and Erwin (1985) found that the standard conveying elements used in a self wiping co-rotating twin screw extruder do not reorient the interfaces relative to the streamlines. The flow in the intermeshing region shows that the interfaces behave smoothly with the turning of the flow. In the present work similar results, as above for co-rotating, were obtained. Although at the intermeshing zone a complete change of direction takes place, but nevertheless the stream remains oriented. So Fig 4.58 shows the presence of red streak even after the passage from one channel to the next one of other screw.

(i) Main Tetrahedron Flow ( $F_{TM}$ ): It originates from the pushing edge side (of 2L) of the opposite screw (Fig 4.50 & 4.54). It passes through intermeshing zone, slightly pushed back by the flank of the flight of this new chamber (2R in Fig 4.54). This is because the screws are displaced in respect to each other in axial direction, and this pushing back of melt is called wedge restraint. This phenomenon (wedge restraint) reduces the tendency of the material to rotate in channel, thus increasing its conveying in axial direction. Fig 4.60 shows wedge restraint in GKN Windsor which is caused by the wide crest of the screw. This rather wide wedge restraint produces considerable restriction in cross section and deflection in direction of the material. As compared to this, the narrow crest causes small wedge deflection in direction (Fig 4.61).

This leakage flow carries material along the sequence of chambers numbered 3L → 3R → 3L → 2R towards the die end (Fig 4.50 and 4.54). As clearly shown in Fig 4.56, the flow path available to polymer melt dictates that the main tetrahedron leakage flow enters the trapezoidal channel from the top of the trailing edge's side. This is shown as green colour in Fig 4.56 and by signs (ox'~) in Fig 4.55A. But the

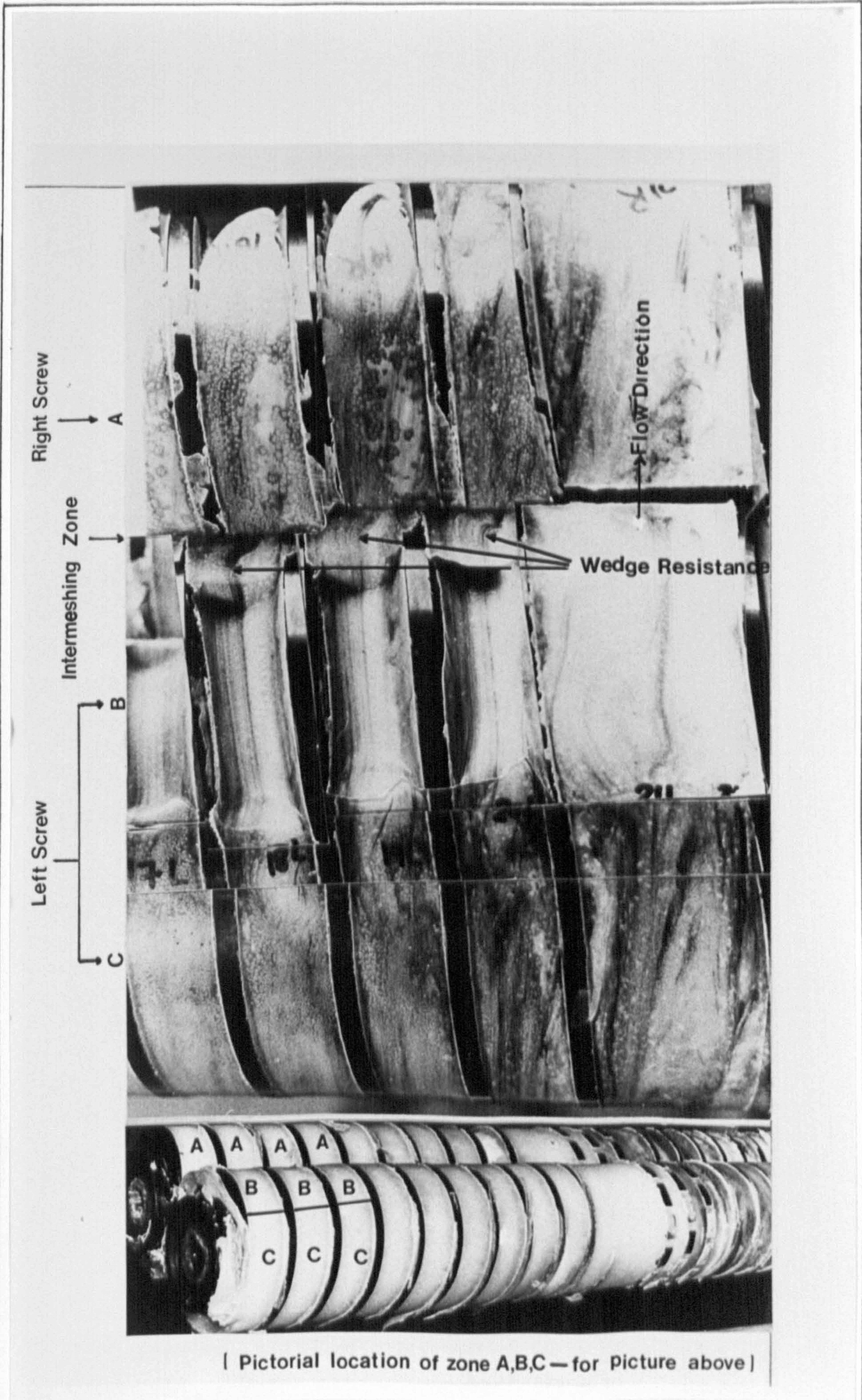


Fig. 4-60 Picture showing wedge resistance in GKN Windsor.

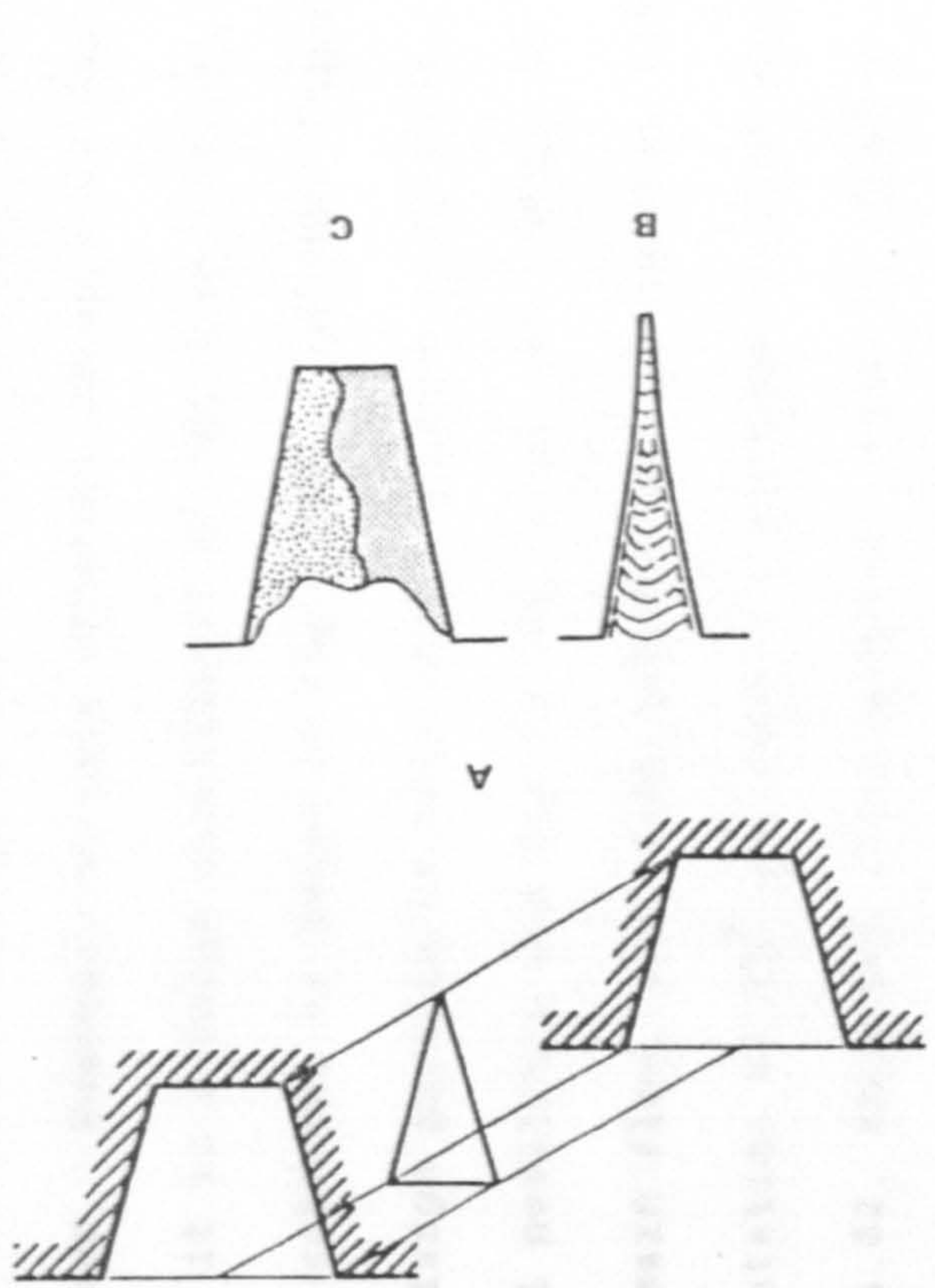
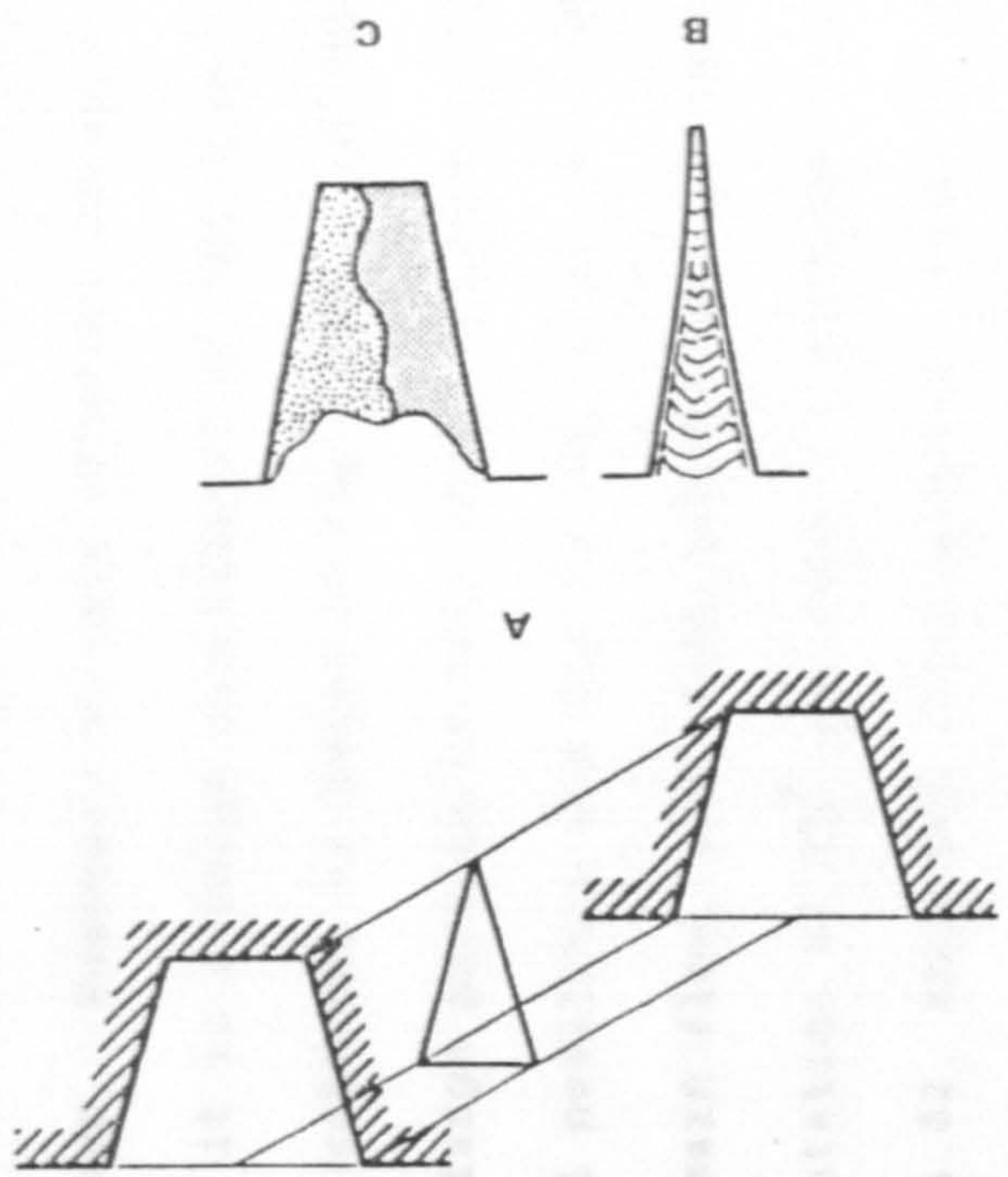


Fig. 4.61 Diagram showing change of flow direction of the wedge volume (A, B) and change of direction of material flow as a function of screw crest(C) - Alter Hermann and Jackopin.

Fig. 4.62 Triangular flow path and intermixing of various flows (after Martelli 1983).



melt from this flow occupies mostly the middle top portion of trapezoidal channel (Fig 4.56 and 4.55A). Furthermore, in Fig 4.58 the flow path from 2L to 2R is shown by sections cut from frozen polymer. However, as this consists of most of the polymer melt flow, i.e. it is a large constituent of the flow, it can be divided into four subzones as shown in Fig 4.55B. In this figure it is shown that the large portion of this flow occupies positions A and B. These final positions are due to the result of change of shape of channel for main flow, i.e. from trapezoidal to another trapezoidal at orientation of  $90^0$  and thus the passage becomes triangular, shown in Fig 4.62, thus the final position taken by elements C and D (or .. and -- in Fig 4.55A). This is once again substantiated by sections in Fig 4.59 where area AA', BB' etc. corresponds to that in Fig 4.55 B.

In the meantime when this lower zone C and D flows are passing through intermeshing zone, travelling downward in intermeshing zone, both of these come in contact with upgoing flow regime mainly consisting of main side flow ( $F_{SM}$ ). It is quite probable that main side leakage flow intermixes with downward position of  $F_{TM}$  (main tetrahedron flow), and thus together they occupy positions C and D (Fig 4.55A and B). These flows (C and D) move towards the trailing edge and lower down as well.

This main tetrahedron leakage flow intermixes with the small tetrahedron leakage flow of the previous chamber, e.g. flow from chamber 3 L, as shown in Fig 4.54 and quite clearly in Fig 4.50 where red and green colour mixes. Together these two flow form upper circulatory flow regime (Fig 4.56) which appears to rotate anticlockwise within itself, as described later.

As this flow follows the proper and wider path, it does not undergo excessive shearing action as compared to other flows. However as compared to the ordinary flow through the non intermeshing parts, this portion of flow experiences a higher level of shear (Hornsby 1987). Furthermore as this type of flow regime is followed by the majority of the polymer, this type of flow gives an average residence time. The heat conducted and shearing action undergone is normal.

(ii) Small tetrahedron leakage flow ( $F_{TS}$ ): As discussed above, this flow results from the smaller portion of the divided melt (as a result of division of melt by other screw flight). It originates from the trailing edge side (of 3L) of the opposite screw (Fig 4.54). It passes through the intermeshing zone, slightly pushed forward by the flank of the flight of this new chamber (2R in Fig 4.54 and 4.50). Thus this flow avoids completely one rotation around both screws, e.g. flow from 3L moves into 2R thus avoiding 3R and 2L chamber completely. Therefore the residence time for this portion is reduced drastically for such a journey.

The flow portion originating from the trailing edge location and enters through intermeshing zone into the top corner of the pushing edge's side. Thus it changes its position from one extreme to another extreme location. In Fig 4.56 and Fig 4.55 it is shown as red colour and by signs ++ respectively. Looking at the sections in Fig 4.59 it becomes quite clear that the space available for this flow (3L to 2R) through intermeshing zone is initially large (in section 1 and 2). But then it becomes rather narrow (in sections 3, 4 and 5), and then it discontinues (section 6). So quite a large amount of material must flow in rather short distance. This supposition is quite correct, as it becomes quite evident in Fig 4.57, the pictorial view of flow where



the flow seems to spread in very short time (Fig 4.56 in picture 1-3 and 1-5 and 2-1).

As explained above, it mixes very well with the main flow and together forms the upper flow regime. As the polymer melt passes through a narrow passage, it undergoes a high shearing as compared to other flows.

As explained above, the confluence of these two flows i.e. main and small tetrahedron leakage flows divide again into two unequal streams at the next intermeshing point. Thus each successive division into two stream doubles the cumulative mixing effect. Therefore the flow path itself imparts a considerable amount of mixing. This produces a more homogeneous melt, not just because of intermixing of different polymer stream but it also ensures a regular frequent redistribution of plasticized material between the area in contact with the screw flights and that in the centre of the flow path. Based on the above type of mixing Rheotec S.A. has designed staggered flights on the metering section of single screw extruder. These redistribute melt flow to give alternate contact as described above (Rheotec 1982) Fig.4.63 . This redistribution not only helps mixing but also averages out the shearing of polymer.

B. Side leakage flow: This occurs through the gap between the pushing (or trailing) face of the flight on one screw and the corresponding trailing (or pushing) face of the flight on the other screw. This gap is generally narrow on one side (connected to small tetrahedron flow gap) and broad on the other side (connected to the main tetrahedron flow gap). Therefore each channel end has one large ( $F_{SL}$ ) and one small side leakage gap ( $F_{SS}$ ). The large side leakage

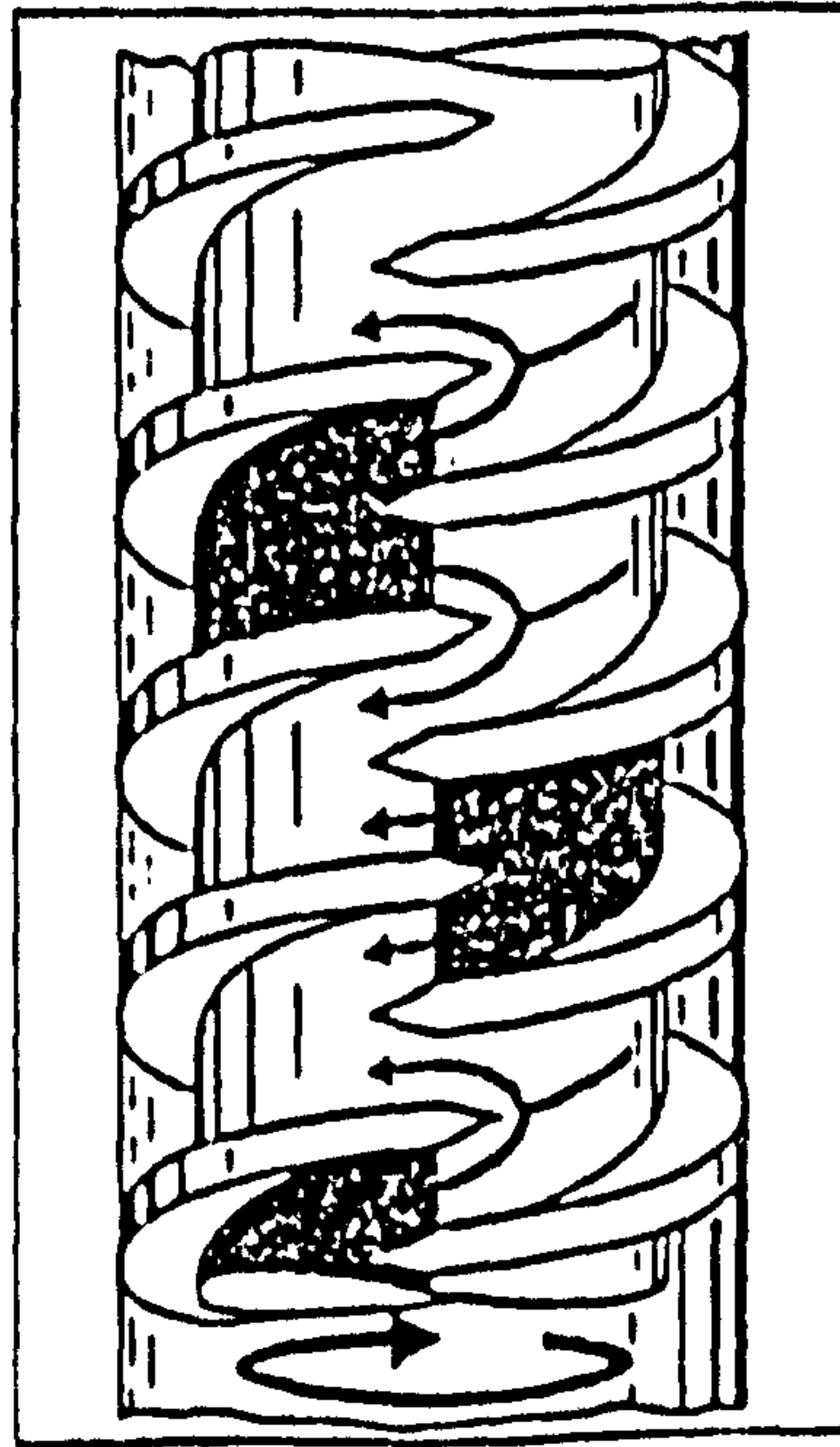
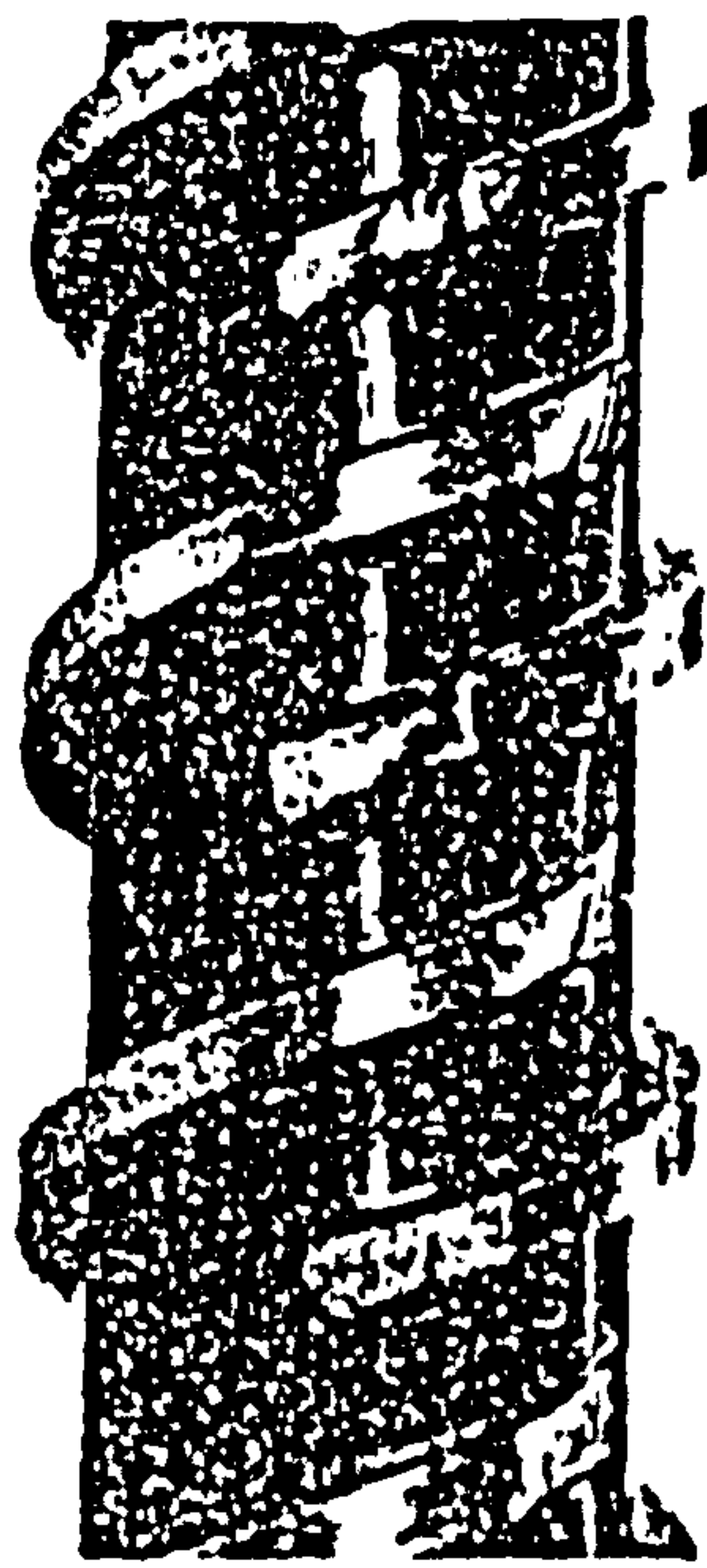


Fig. 4.63 Enhanced distributive mixing (ODM screw - Rheotec)

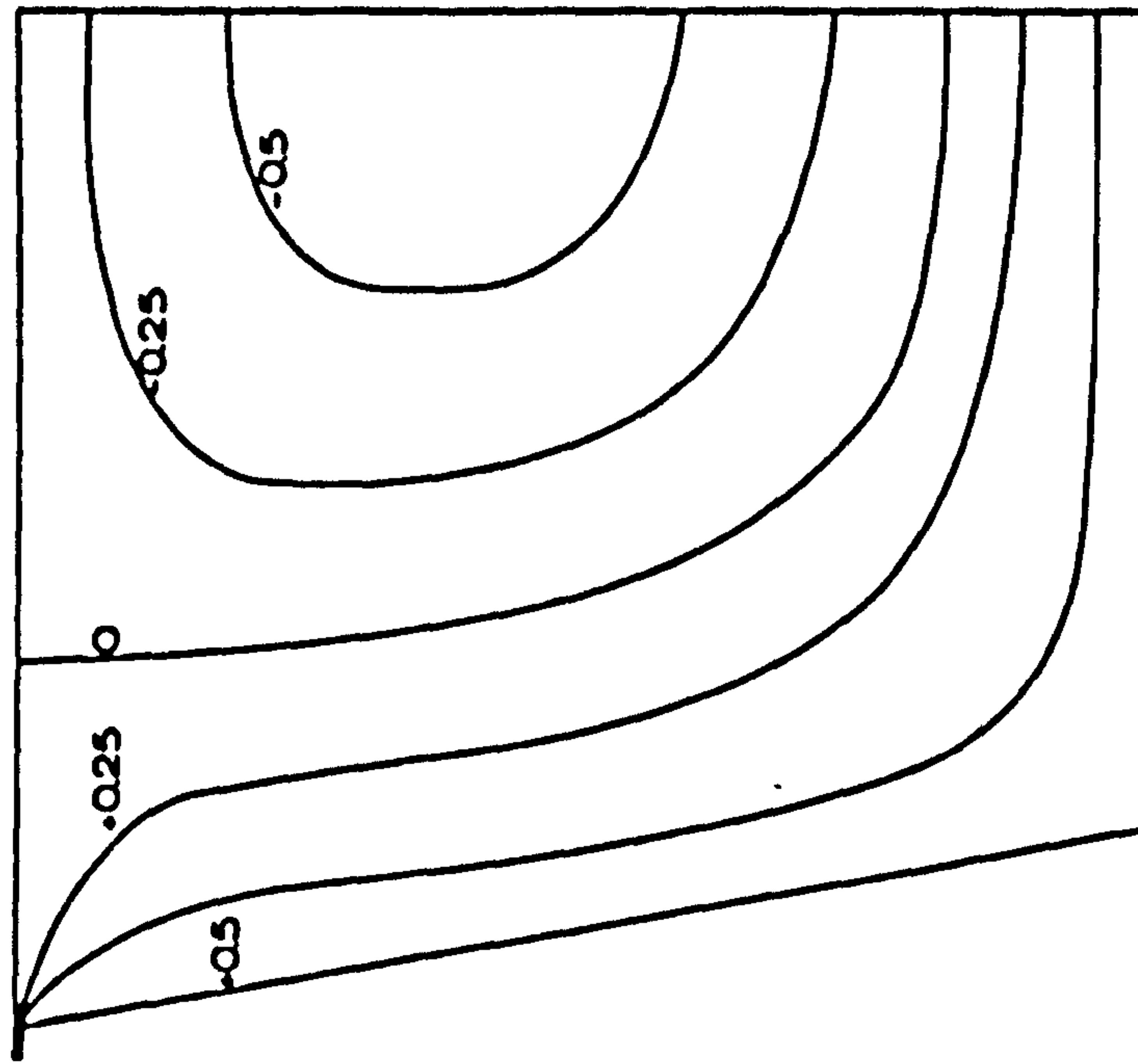


Fig. 4.64 Flow in the tangential direction with isotech numbers  
(after Janssen 1978)

flow ( $F_{SL}$ ) is shown as blue colour in Fig 4.56 and by sign of  $\theta\theta$  in Fig 4.55A. This originates on the trailing edge of the same screw (Fig 4.54).

This is the flow which takes place as a continuation of one chamber to the next chamber of the same screw, and it adds to that through the calender. So it can be said that this flow carries on as normal on its passage to next chamber on same screw thus escaping completely the other screw. As the screw velocities in intermeshing zone are in opposite direction, some of the polymer flow especially near edges undergoes reversal of flow and back in shape of  $\theta$  pattern flow. This flow thus undergoes intense shearing.

The pressure build up occurs primarily because of reduction in cross sectional area when material enters the intermeshing zone. However, this pressure build up is not the same for both sides of side gaps. The side gap towards main tetrahedron leakage flow would have a relatively small pressure build up, but this increases as this leads to gap which is quite narrow (The side gap of small tetrahedron gap). However, the small tetrahedron leakage flow has a relatively higher initial pressure which relaxes after entrance as it leads to flow into the main tetrahedron leakage flow area of the next chamber. As regards its initial destination soon after the intermeshing zone, the two portions of side leakage flow occupy the lower portion of the trapezoidal channel. The large side leakage flow ( $F_{SL}$ ) occupies the entire side portion of trailing edge side while the small side leakage flow ( $F_{SS}$ ) occupies the lower middle position towards pushing edge side (not shown in Fig 4.56, but can be considered to occupy portion next to central flow). These two sub flows do not mix with the other flow but keep their identity. Later on these two flows mix partially

with central flow (discussed later) and partially mix with part of main tetrahedron leakage flow (as described above). Unlike other flows, this is not reoriented at  $90^0$ , but remains in the same direction. Therefore it does not contribute to distributive mixing substantially.

It occupies the lower portion of the trapezoidal section, the main portion being situated towards trailing edge side (Fig 4.56). As discussed later, this flow intermixes with other flows and moves in overall frame of anticlockwise rotation (Fig 4.53). On its entrance to the next intermeshing zone, it occupies the position "C" and "D" of the main tetrahedron flow (Fig 4.55B).

This type of flow completely avoids the passage through other screw and thus reduces the residence time to half for that particular revolution.

C. Central flow: The polymer melt in front of the flight tip of the other screw (screw flight on trailing side of 2L channel) gets pushed from flight tip along in 2R channel flow direction. Thus the melt is pushed positively towards the end of 2R channel. This material undergoes a circulatory flow as shown in Fig 4.54. This material fraction will contribute to the positive conveying characteristics of the extruder. However, as the flight tip is not substantially wide, the contribution due to this is rather low.

As this flow is pushed positively, it gets exposed to little shearing and also has rather limited residence time. It continues to the next chamber as the central flow. This becomes quite evident in Fig 4.67 where centre region remains unpigmented till section 11R, although

slow reduction in area containing white polymer. This indicates that there is some intermixing with some other flow. Thus this central flow results in a fast moving centre which in some cases has shown the signs of being unmolten as well. This flow is represented by yellow colour in Fig 4.56. This occupies the centre of trapezoidal chamber and it mixes partially with the main side leakage flow. The way this polymer portion moves in screw is shown in Fig 4.51 and 4.52 by yellow colour.

D. Calender leakage flow: This flow occurs through the gap between root of one screw and flight land of the other. This is rather a misnomer as the relative movement of the screws (to each other) is such that no calendaring takes place. This also allows flow between adjacent chambers on the same screw. However, it is rather of insignificant amount and is therefore not shown in Fig 4.56. As screws are rotating against each other, a high amount of shearing action takes place. In contrast to counter-rotating extruder, no squeezing of the material between the flight tip of one and land of other screw's flight occurs. As a consequence the shearing undergone by this portion is less in co-rotating extruders as compared to that in counter rotating (Herrmann et al 1977).

E. Flight gap flow: This flow takes place through the gap between barrel and flight land which is similar to that in single screw extruders. It is responsible for melt leaking backward from one chamber to another chamber on the same screw.

F. Stagnation or hold back: This occurs due to the screw profile which does not completely wipe the other screw and has a small tip angle. This combination leaves layers of polymer melt which then tend

to stagnate for long time. In Fig 4.56 this is shown as black colour. The evidence of these stagnating layers is shown in section A of Fig 4.57. This section shows the presence of stagnating uncoloured polypropylene after eight minutes of black coloured polypropylene extrusion. However in contrast, Sakai et al (1987) on their work on model twin screw extruders (both co and counter-rotating extruders) have shown that the stagnant layer is absent in a twin screw extruder.

#### 4.4.2 Flow behaviour in passage along the 'c' shape chamber

In this case the subsequent flow within the channel till it approaches the intermeshing zone at end, e.g. the flow in 2R channel till the intermeshing zone at the end of 2R channel, is described. Once all the above mentioned flows pass through the intermeshing zone and enter into the new chamber, they tend to group and form two flow regimes (Fig 4.56). Hornsby (1987) has also reported the presence of two flow regimes, although no explanation for the presence of these regimes was given. This is in sharp contrast to a single screw extruder, where there is only one flow regime (Maddock 1959). As described above the top regime consists of main and small tetrahedron leakage flows, and calender leakage flow, while bottom flow regime consists of main and small side leakage flows, small portion of main tetrahedron leakage flow, and central flow. The stagnation flow and flight gap flow seem to contribute to both the regimes. (Fig 4.53).

The top flow regime has clockwise rotation, the bottom flow has anticlockwise rotation (analysed from the tracer studies). Looking at Fig 4.56 it becomes quite clear that both of these flows move in an overall flow regime of anticlockwise direction. This is opposite to the rotation hand of the screw element, a condition similar to single

screw extruders. This radial flow provides for radial mixing of the polymer, somewhat similar to that reported by Janssen(1978). He reported that the bottom volume mixes very slowly with the rest of the chamber volume. But whatever mixing is produced, it is the direct result of the rotation of fluid in X-Y plane. Similar results (presence of two flow regimes) to the current work are reported by Maheshri (1979) who has shown theoretically that because of down channel and cross channel flow, two separate flow patterns exist. He showed that on increasing the helix angle, the cross channel velocity component becomes as effective as the down channel velocity component and therefore the upper region becomes more prominent. This leads to more fluid separation (Fig 4.65).

In contrast to the above described flow, conveying in counter-rotating twin screw extruders and single screw extruders differs significantly. The conveying in a single screw extruder takes place in a helical circulating path (Tadmor 1966; Tadmor and Klein 1970). As compared to two flow regimes in twin screw, there is only one flow regime present. This is formed when the molten polymer on the barrel is collected by the leading edge of the screw and mixed with the previously molten material. This circulating flow is confined to the rear portion of the channel in each turn, whilst the forward portion is filled with the unmolten polymer. The molten portion gradually increases at the expense of the unmolten portion. Ideally this should produce completely a molten and homogeneous product before discharge from the screw. Similarly the flow in counter-rotating twin screw extruders differs from that in co-rotating twin screw extruders. In counter rotating there are basically two flow regimes (Janssen1978). But as compared to co-rotating, these do not exist as a separate entities. Instead, they exist one within the other one and are separated from

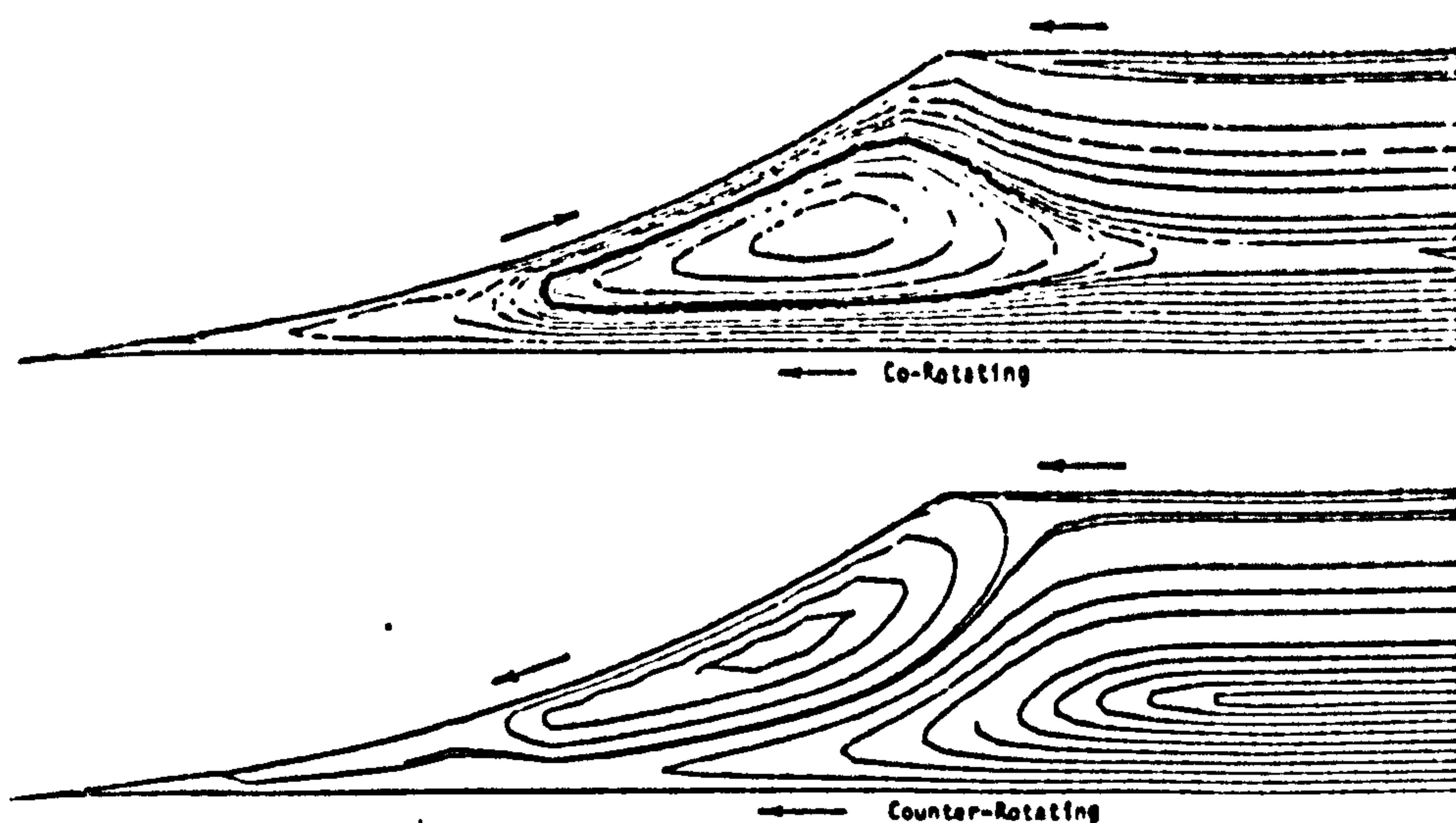


Fig. 4.65 A Streamlines in an end region of a twin screw channel of 15 degree helix angle (After Maheshri 1977).

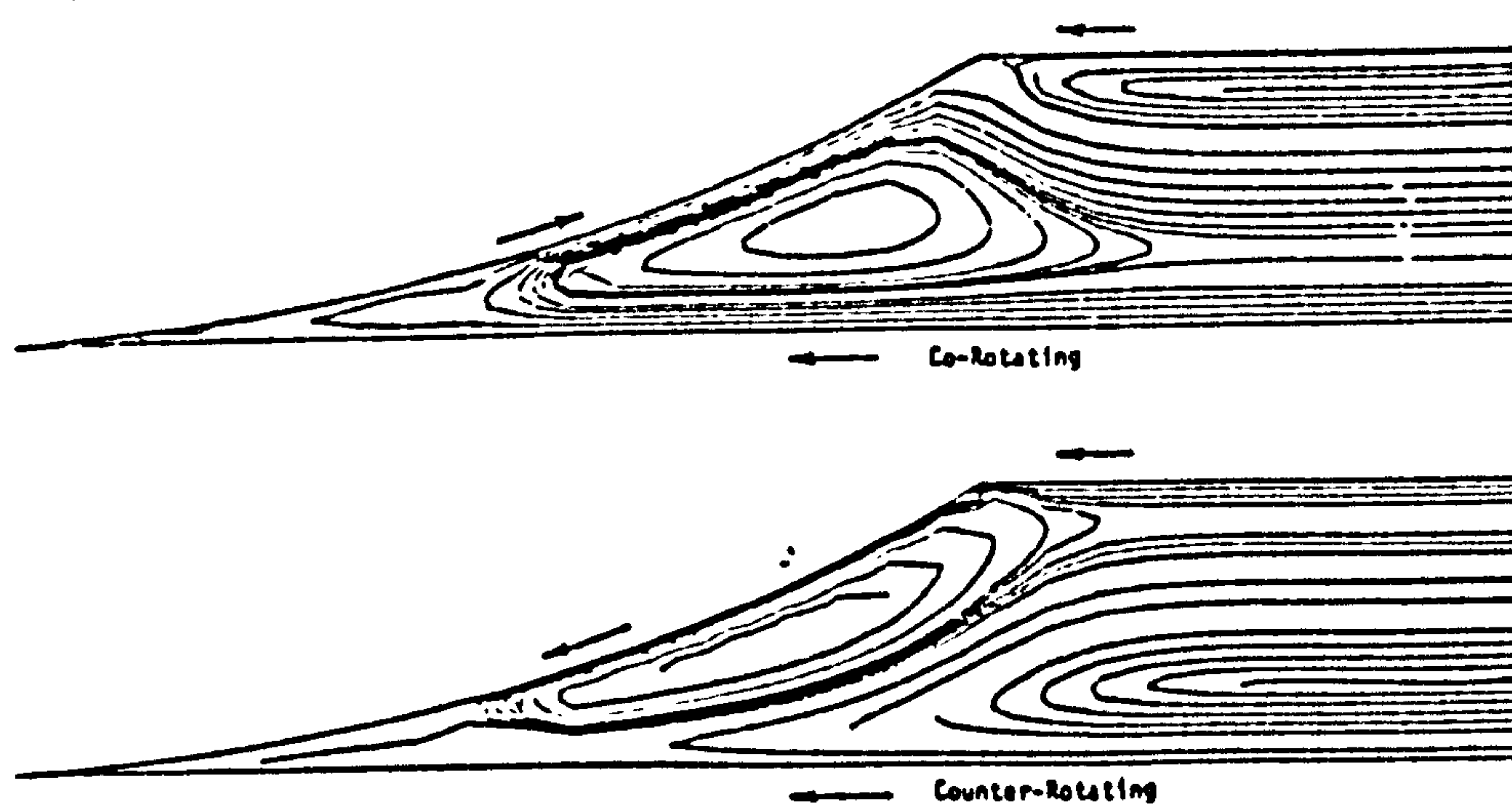


Fig. 4.65 B Streamlines in an end region of a 30 degree helix angle twin screw channel. (After Maheshri 1977)

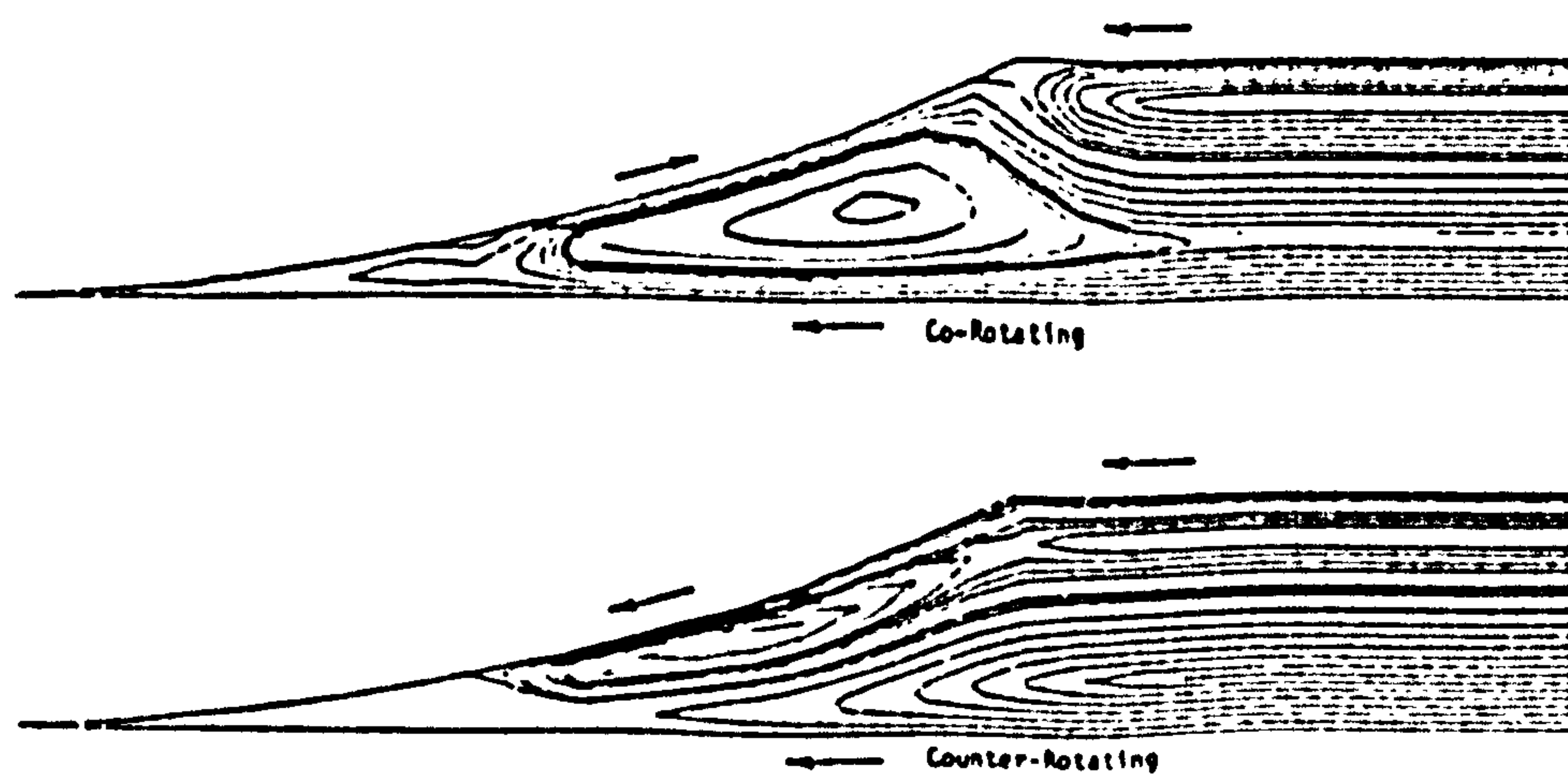


Fig. 4.65 C Streamlines in an end region of a 45 degree helix angle twin screw channel. (After Maheshri 1977)



each other by a layer of zero velocity (Fig.4.64).

Furthermore, the basic rearrangement of the polymer, on passing from one chamber to another chamber through the intermeshing zone, as discussed before, is quite complex process. The detailed diagrammatical representation is given in Fig 4.55 A and 4.55 B. This is in complete contrast to the flow in the counter-rotating twin screw extruder. In counter-rotating twin screw extruder Janssen (1978) has described the flow in similar fashion with the help of a diagram (Fig 2.4). This shows that unlike co-rotating extruder, the polymer in the regions near the flight wall, transfers to the opposite chamber while the corresponding polymer from the opposite chamber will move in a region near the middle of the channel. A horizontal plane of polymer, that goes to the converging side of the screw (made up of polymer in area near the zero velocity layer and from area next to it - towards flight wall) returns as a vertical plane. Furthermore, in the polymer area situated near the bottom of the channel, a remarkably closed and stable flow exists that mixes very poorly with the rest of the chamber unless the calender gap is sufficiently large. So the flow in counter rotating extruder is completely different from co-rotating twin screw extruder.

It is quite probable that the factors which would affect the down channel and cross channel flows would also affect the transverse mixing. These factors are helix angle, channel width/depth ratio, intermeshing gap, screw land/flight gap, channel curvature and end region influence.

4.5 Transverse mixing along the extruder: As mentioned above, this was studied for both the macro and micro-mixing along the extruder. In

this section, not only the progression of mixing along the extruder is discussed, but also it has been tried to correlate the transverse mixing with the flow model as proposed earlier.

4.5.1 Macromixing: The sections cut along the extruder do show a trend of macromixing and its progression along the length. This is shown by taking sections along the whole melt length of the extruder (Fig.4.67). The sample positions are clearly shown by photographs in Fig.4.66 . The sections clearly show the distributive mixing and presence of various different flows. In the first section (20 R) there is evidence of the presence of two different flow regimes: top and bottom. This once again confirms the presence of two flow regimes as proposed in the flow model earlier. The pigmented polymer layers are present on the edges which in later sections tend to slowly spread towards the centre. This gradual spreading of pigmented polymer in unpigmented polymer confirms the contribution of various zones in the mixing mechanism. The presence of unpigmented white centre in the centre of the channel indicates that this portion of the flow does not mix with the other region. The main side leakage flow (represented by blue colour in model Fig 4.55) does show fast mixing. This can be clearly seen by taking the reference position of these flows from Fig 4.55 and then seeing the progression of the mixing in Fig.4.65. This shows that whilst reasonably good distribution of pigments occurs by 13th channel for main side leakage flow, for the main tetrahedron flow it takes a further of two channels, and similar mixing is produced by the 11th channel (away from die). So the main tetrahedron flow (represented by green colour in Fig 4.55) together with other flows in the upper circulatory flow has slow but excellent distributive mixing. In this case the main side leakage flow does not mix with other flows but remains separate.

LOCATION OF SAMPLE POSITIONS

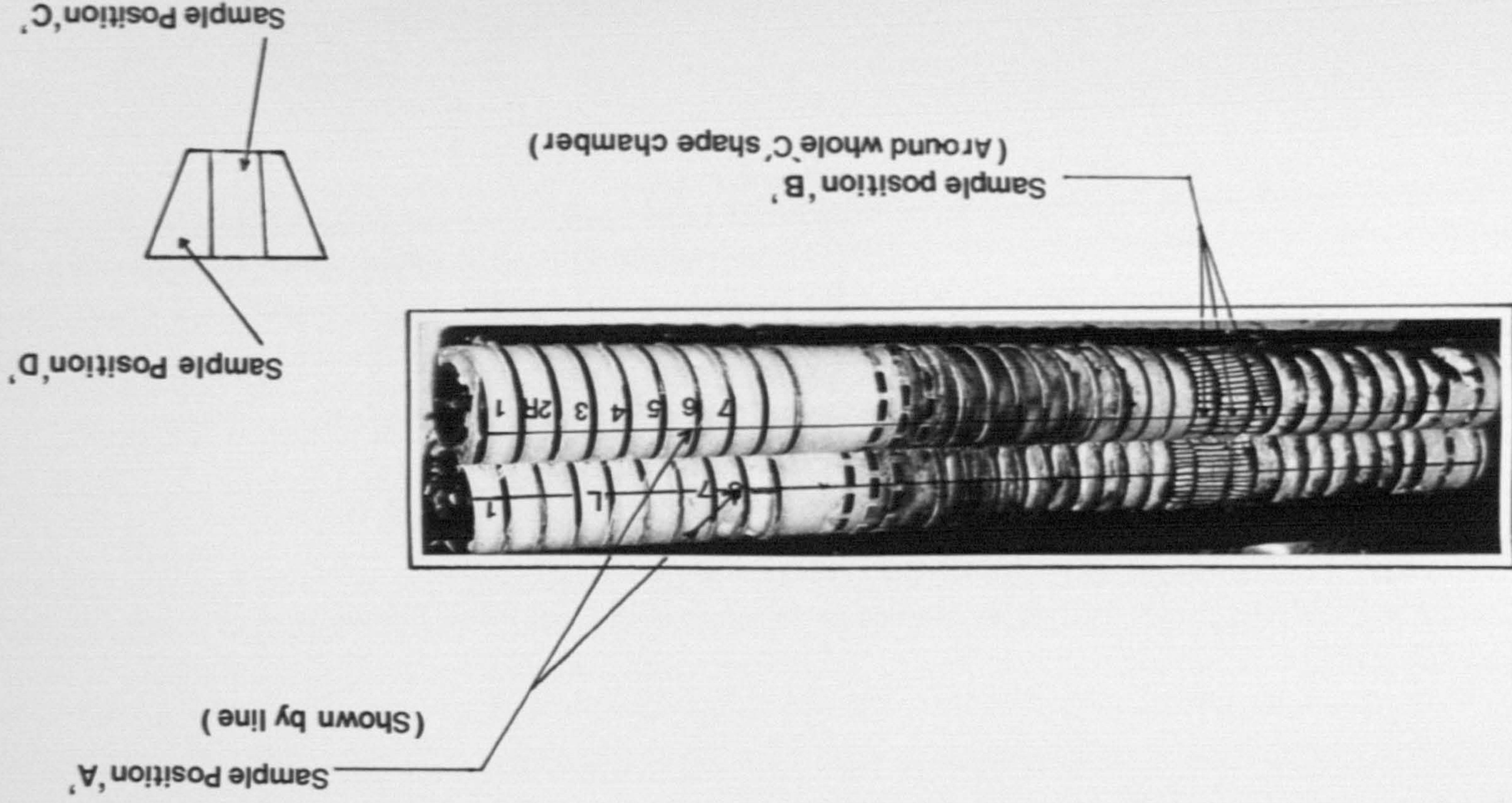


Fig. 4-66 Schematic diagram showing location of various sample positions.

The central flow (represented by yellow colour in the model) is quite obvious from section 16 L onwards to section 11 R where it is present as unpigmented polymer. This unpigmented centre shows that it poorly mixes with other flows and keeps its identity. As discussed above, the centre slowly decreases in area from all the sides, thus indicating that it intermixes with other flows (Fig 4.67). The central flow is once more clearly visible in the portion before the zone of mixing disc as white colour streaks. This central flow is a fast moving part, being pushed forward by the crest of the flight of other screw (Fig 4.54). This results in reduced residence time which is associated with poor heat transfer. The poor heat transfer which results in some unmolten centre, is surrounded by dark colour zone. This is clearly shown in sections of screw channel 6 L to 1 R. However, when the polymer passes through the open space and mixing disc, it tends to mix and evens out the different colours.

4.5.2 Micromixing: In this case the whole channel section was cut into three vertical pieces, as described in experimental section. However only one portion from side and the centre portion was analysed. Close examination of the sections shows that the polymer on the edge portion (Fig 4.68) shows better distribution of pigmented polymer in unpigmented polymer than the sections from the centre portion (Fig 4.69 ). This once again reinforces the observation made in macromixing which showed that the flows such as main side leakage flow and main tetrahedron flow are instrumental in getting a better distribution of the pigmented polymer. The sections cut from left screw skeleton edge (Fig 4.66 ) show the presence of streaks and rotational flows. It shows that different regions in the edge section have different degrees of distributive mixing. As the polymer progresses along the length, these streaks seem to become narrow and

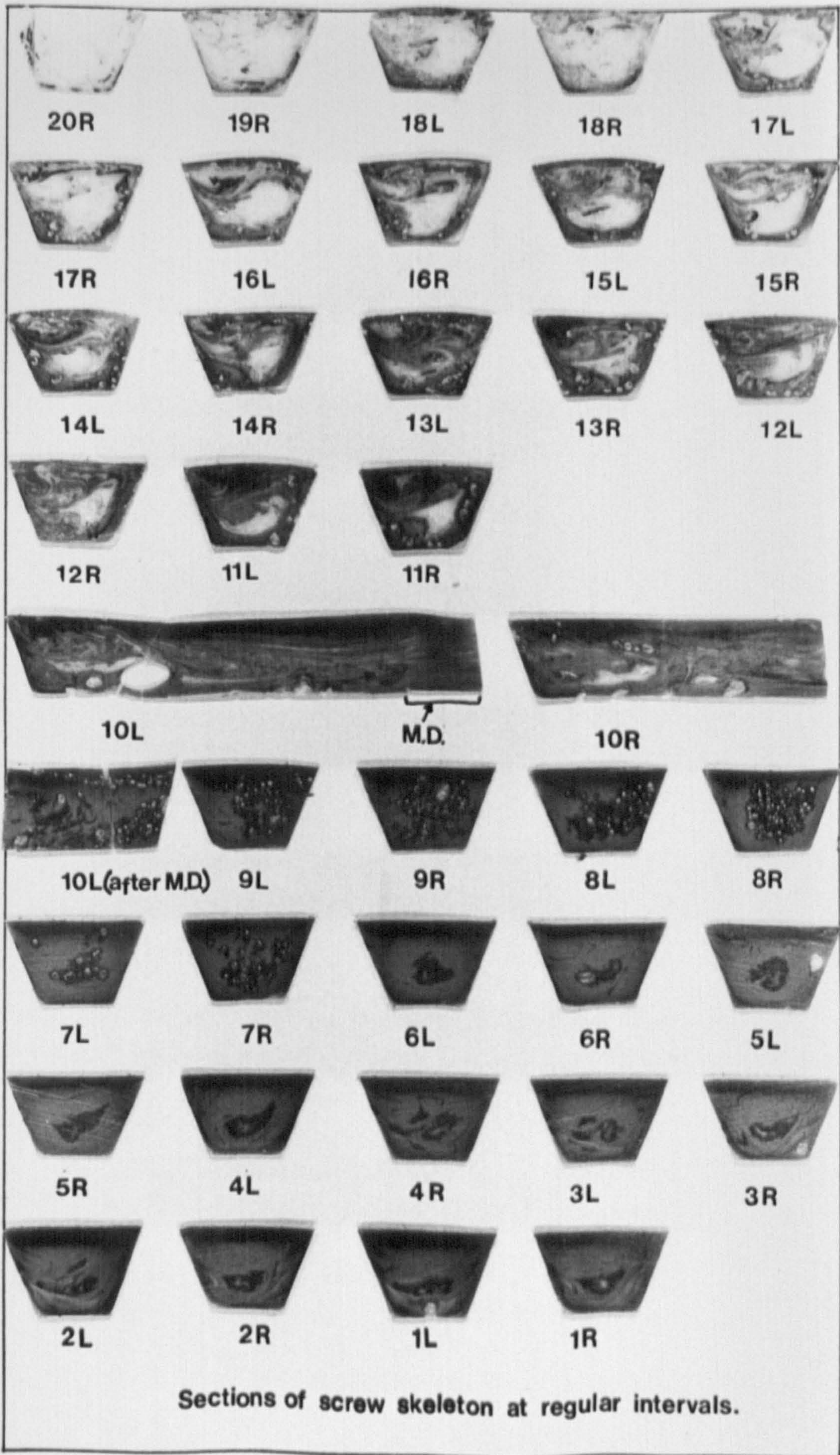


Fig. 4.67 Sections of screw skeleton at regular intervals.

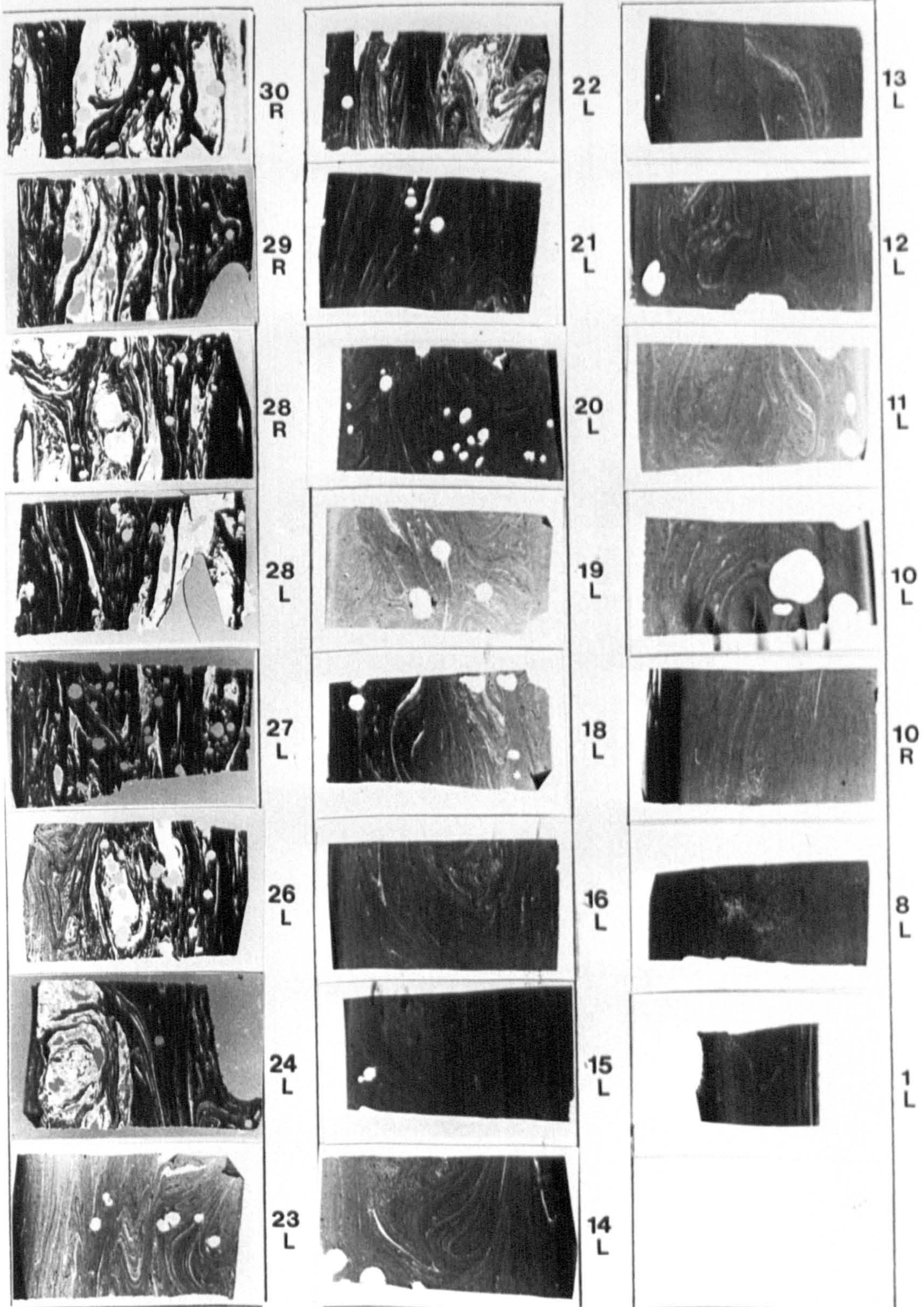


Fig. 4.68 Sections from the edge of chamber showing micromixing.

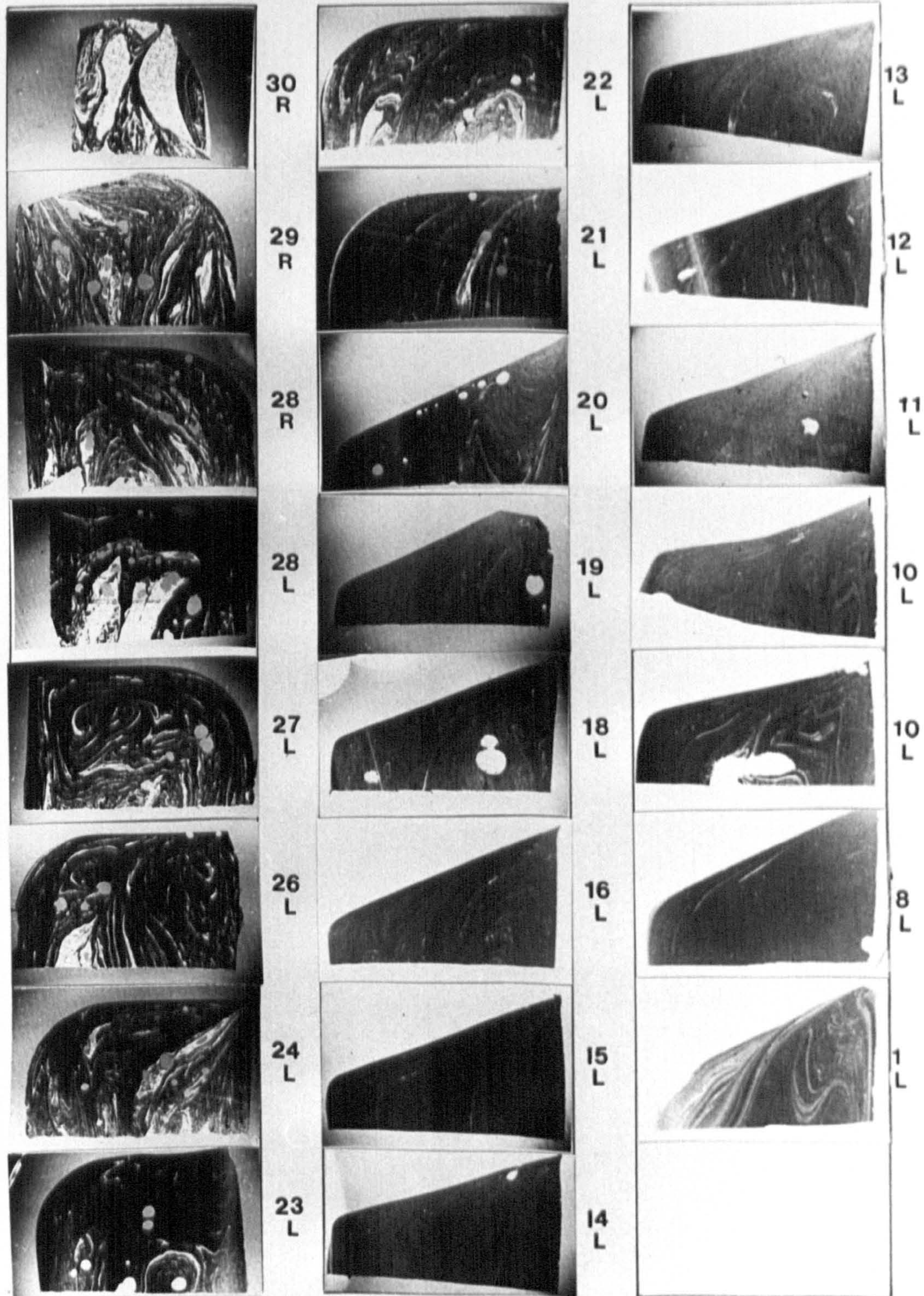


Fig. 4.69 Sections from the centre of chamber showing micromixing.

also less in number. However, in the centre sections these unpigmented areas are rather large and concentrated at some places only.

However an interesting observation was made from these sections. It was seen that a significant improvement in pigment distribution occurs in between 22 L and 20 L. This incidentally also represents a change in channel shape (from rectangular with curved edges to trapezoidal shape). This improvement in distribution could be attributed to the presence of interrupted flights or to the change in the shape of channel or optimum length for distributive mixing. From 21 L onward, however, there seems to be a slow improvement thus achieving good mixing by channel 8 L. In the later sections (from 20 L onwards) the sections show flow patterns but not of the same magnitude as before. The dark small particles are in fact masterbatch portions and not carbon black particles (e.g. in 15 L, 14 L etc.). These portions of the masterbatches also raise a question about the GKN Windsor's capability as compounding extruder.

The above observations made from micro and macromixing suggest that these techniques are quite useful, and they have a potential for testing screw design and also to study the other processing variables on transverse mixing.

#### **4.6 RELATIONSHIP OF RTD AND TRANSVERSE MIXING STUDIES**

Now after proposing a flow model for twin screw extruder and studying the influence of some variables on RTD and on other associated characteristics, it is reasonable to combine the observations made from both of these studies and get an overall picture regarding the twin screw extruder's behaviour.



The polymer melt, in GKN Windsor twin screw extruder, is conveyed semi positively in the "C" shape chambers (as compared to counter-rotating where there is a positive conveyance due to the closed "C" shape chambers). So friction does play a small part in conveying. This is because co-rotating extruders basically have interconnected "C" shape chambers so there is no direct cut off in flow direction (vs. counter rotating extruders). But at the same time the screws wipe each other and so there can be no prolonged stagnation and this action also leads to semi positive conveyance.

As the Reynold's number for molten polymer flow in a pipe is of the order of 0.01 (due to the polymer's very large viscosity value), so the mass diffusivities are so slow and residence times so short in an extruder that there is essentially no micromixing due to diffusion. As a result the mixing in a twin screw extruder is caused by shear and velocity gradient. The relative motion between the extruder barrel and the screws and also in between screws themselves creates a velocity gradient. The molten polymer is sheared in both the down channel and the cross channel directions. So the distributive mixing is caused by semi positive conveying (leading to shearing and velocity gradient) and also the varied available passages to the polymer melt which results in residence time distribution.

So any factor which influences either of the above two, tends to affect RTD. As discussed before, some of the variables effects on RTD can be traced to the flow mechanism. However before discussing the effect of variable, it is tried to establish the interrelationship between the two - namely - RTD and flow mechanism.

The basic mode of melt conveyance within this extruder, as described above, is semi positive. The flow mechanism within the extruder leads to different residence times within the extruder. So the changes in the flow mechanism, maybe due to changed flow path or maybe the relative increase or decrease of specific leakage flow, result in change of RTD. So the procedure and the way by which the flow mechanism and RTD are affected can be discussed under the following two headings.

A. Polymer flow path

B. Polymer melt's flow characteristics

A. Polymer flow path : The flow path contributes considerably in spreading RTD. The flow path in a co-rotating extruder is basically the shape of figure of 8. The passage formed by the intermeshing of the two trapezoidal channels is triangular in shape and its area is defined by the angle of the flank of the flights (Fig 4.61). Due to this change of shape, from trapezoidal to triangular at intermeshing zone, a considerable amount of reorientation of the material takes place (although not as much as in counter-rotating extruder). As the whole of the flow direction changes, through  $90^{\circ}$ , this reorientation causes an optimum mixing. During this  $90^{\circ}$  reorientation some flow paths are changed and thus it causes distributive mixing. Furthermore due to differential positions occupied by the polymer within the screw channels, the differential linear velocities cause the different flow of melt. So high linear velocity for the layers near the tip of flight and lower for those near the core of the screw. This differential flow also contributes to mixing, due to the differential velocity and different total path length available.

Besides the above, the position taken by the melt within the screw channel also determines the flow path taken by the polymer melt. The polymer melt situated on the trailing edge of the channel (main side leakage flow - represented by blue colour) tends to remain on one screw, thus missing the other screw completely. Supposing this flow follows the same pattern all along the length, this would virtually result in halving the mean residence time (see later). While some polymer, that located on the trailing edge (small tetrahedron flow - represented by the red colour), tends to move into next chamber of the other screw, thus missing one whole of the 8 shape travel along the two screws. This flow would reduce its residence time within the extruder substantially. Probably it is this flow which gives the minimum residence time within the extruder. This leakage flow is represented by in Fig 4.55 A ff. The polymer in centre (central flow - represented by yellow colour) is pushed forward by the crest of the other screw. So this portion travels relatively faster than the rest of the polymer within the channel. This fast travelling polymer melt, although following the defined path (shape of 8), due to forced conveying, would have reduced residence time. However the flow followed by the polymer located on the pushing side of the screw seems to be rather normal i.e. it follows the normal 8 shape flow path and takes an average residence time (based on semi positive conveying and travelling in defined 8 shape path). While doing this, it will obviously result in average residence time, because this flow makes up the majority of the polymer flow. This is confirmed by the shock cooling and sectioning of the polymer screw skeleton (see Fig 4.54A) where it is shown to constitute the major part in the section. As described before, these flows tend to regroup into two flow regimes, which tend to rotate either clockwise or anticlockwise. Besides the polymer melt in "C" shape chamber also shows an overall spiral motion.

All of the above mentioned phenomenon tend to contribute towards the spread of longitudinal flow and RTD.

So it can be seen from the above description and discussion on the various flows that it is the relative effect of the various flows which would determine the net RTD. So, e.g., if the variable factor affects the flows such that there is a substantial increase in the small tetrahedron flow, then the comparative value of mean residence time would decrease with a shift of the curve towards left (Fig 4.17), i.e. the portion of the flow would show more short channelling.

B. Polymer melt's flow characteristics : The polymer melt's flow characteristics contribute considerably in spreading of RTD. The polymer in the pre-mixing discs zone is in non molten state. So distributive mixing, due to the flow profile in polymer does not take place, consequently it becomes plug flow. But due to different flow paths formed, along the screw, some spread in RTD occurs in this region (as discussed above). On its passage across the mixing discs, the polymer starts to melt. This brings about the change in flow characteristics as material tends to stick to the heated metal and shows a laminar viscous flow. Further along heat is generated by shear in polymer melt. The melt flow is affected by various parameters viz: viscosity, shear rate, shear stress and temperature. Thus in extrusion, factors which could affect one or more of these parameters, do affect melt state and thus RTD.

As the polymer is a bad conductor of heat, temperature non uniformity exists. Therefore the viscous flow in polymer becomes quite non uniform due to different temperatures and shear rates applied, according to the position in "C" shape chamber. The portion of

material which sticks to the screw surface is transferred from one screw to the other in the intermeshing zone and thus forced conveyance exists. Material can stick to a warm screw thus reducing effective chamber volume and thus the throughput.

4.6.1 Typical effects of a variable : As discussed above, a simple approach is taken to discuss the interrelationship between the RTD and flow model while discussing the effect of mixing discs configuration. From the shock cooling experiments and flow visualisation studies, it is clear that the filled volume decreases on changing the configuration from closed to open in upstream position (Run A1,2,3, and 4 and A7,8 and 9) . The lower filled volume is due to the volumetric restriction imposed by the vent port (the closed disc configuration melts more efficiently, due to better pressure buildup, as compared to open and thus better compaction). The lower filled volume leads to low pressure build up at die inlet (from 4.41 to 3.72 MPa at 27 rpm - Table 4.1 A) which in turn affects the flow profile in the main stream. As a result the RTD curve shifts towards a less positive (i.e. more axially mixed) and becomes more dependent on the screw speed. The greater dependence of RTD curve (and therefore of mixing) on screw speed at open disc configuration as compared to closed can be explained on the basis of melting mechanism together with the increase in central flow with increased screw speed. In closed discs, the pressure is enough to cause melting whilst in open disc configuration the melting pressure is not sufficiently developed. Furthermore the reduced residence time together with limited heat input also causes reduced melting. (see section 4.2.3) .

The mean and minimum residence times increases and also the variance about the RTD curve increases. The cause for this can be explained on

the flow visualisation studies. It becomes quite clear from these studies that the less filled volume in the chambers will promote the leakage flows such as small tetrahedron flow and side leakage flow at the expense of the main tetrahedron flow which remains more or less constant. The small leakage flow is caused by the polymer located on the trailing edge of the flight (small tetrahedron flow - represented by the red colour in Fig 4.55). Whilst large side leakage flow is caused by the polymer situated on the trailing edge of the previous flight of the same screw (represented by blue colour). The small tetrahedron flow tends to move into next chamber of the other screw, thus missing one whole of the 8 shape travel along the two screws. Thus this flow reduces its residence time within the extruder substantially. Similarly the large side leakage flow tends to miss out the other screw completely virtually reducing the residence time to half. So this increased contribution of these flows results in the increase of minimum residence time within the extruder.

The reduced pressure at die inlet, which travels back along the extruder also enhances these flows (rather imposes less restriction to it). The reduced pressure also affects mixing in the "C" shape chamber and also leakage from flight tips. Besides, limited melting could also affect the unmolten centre position which then affects the flow behaviour. The melting behaviour affects the flow and RTD in numerous ways.

Similar to the above explanation, other factors (screw speed, mixing discs position etc.) which affect the melting behaviour within the extruder, also act in the similar manner.

## CHAPTER 5 CONCLUSIONS

1. A flow model is proposed which describes material transport within a co-rotating twin screw extruder. The overall material flow takes place in an anticlockwise manner along the screw channel, but comprises two separate flow regimes. Both of these regimes maintain their identity throughout the course of flow in the "C" shaped chamber. Based on the model, "where to where" diagrams are constructed which illustrate material transport. The model is substantiated by flow patterns obtained from screw sections taken from an industrial extruder using polypropylene. The model differs substantially from models used to describe flow in both a single screw extruder and a counter-rotating twin screw extruder.

2. The two flow regimes in the channel rotate in opposite directions and are present predominantly in the upper and lower regions of the channel. The upper flow regime rotates anti-clockwise, and is made up of main and small tetrahedron flow, and "calender leakage flow". The lower flow regime rotates clockwise and is made up of main and small side leakage flow, a portion of main tetrahedron leakage flow, and central flow.

3. The flow studies show conclusively that the position of the melt after it crosses the intermeshing zone is dictated by the actual flow path available at the intermeshing zone, together with the amount of polymer that must pass along a particular path. The melt from a particular site ahead of the intermeshing zone therefore occupies a predestined site after passing through the intermeshing zone.

4. Based on the explanation given above, it is concluded that the

main tetrahedron flow in a particular channel originates from the pushing edge of the screw in the opposite channel. However, on crossing the intermeshing zone it enters the top of the trapezoidal channel next to the trailing edge due to staggering of the channels. The actual flow path available, which is gradually constricted from the top to the bottom of the trapezoid, forces most of this material to occupy predominantly the middle top portion of the trapezoidal channel. In contrast, the bottom portion, which has the narrowest available flow path in the intermeshing zone, occupies a site on the trailing edge together with the main side leakage flow. In summary, as a result of the change in shape of the channel at the intermeshing zone, the various portions of the tetrahedron flow occupy different locations after passing through the intermeshing zone. The spatial shifting of this flow is substantiated by the flow patterns.

5. The small tetrahedron flow in a channel originates from the trailing edge of the previous channel from the opposite screw. The staggering of the channels gives rise to a connection and thus it misses one rotation around both screws. On passing through the intermeshing zone, it occupies the top corner of the pushing edge of the trapezoidal channel. Due to the short flow path available, together with the necessity for a large amount of material to flow in this short distance, the polymer is forced to move much faster in this region. This results in spreading of this flow in the mid-upper portion of the chamber and thus it intermixes with the main tetrahedron flow. This spreading and intermixing is substantiated by the flow pattern. Although in both the tetrahedron flows a perpendicular change of direction takes place at the intermeshing zone, the orientations within sections remain approximately unchanged, thus producing little distributive mixing.



6. The side leakage flow originates on both the pushing and trailing walls (towards the lower regions) in the previous channel of the same screw, and it continues in the same position after passing through the intermeshing zone. However the flow on the trailing edge (main) is substantially larger than that on the pushing edge (small).

Micromixing studies show that faster mixing is achieved in the region where this flow dominates, compared with the regions where main tetrahedron flow dominates. Unlike other flows, this flow does not change direction after passing through the intermeshing zone. It contributes mainly to a rotating flow regime which is confined to the lower portion of the trapezoid.

7. Material originating in the centre of a channel meets a screw tip in the intermeshing zone due to staggering, and is forced into the centre of the corresponding channel of the other screw. Due to its position it is referred to as the central flow. It undergoes circulatory flow and adds to the positive conveying. It mixes rather poorly with the other flows which results in a fast moving centre. It undergoes little shearing and has limited residence time. It has been confirmed by the presence of an unpigmented central zone in the trapezoidal channel.

8. In addition, "calender" leakage, flight leakage and some stagnation are also present. The presence of stagnation is conclusively shown by the presence of stationary zones next to the edges of the trapezoidal channel.

9. Both micro- and macro-mixing studies along the screw length have been correlated with the proposed flow model. The presence of an

unpigmented and sometimes unmolten centre, and the relatively slow progression of mixing in the centre (the region of main tetrahedron flow), compared with edges (the region of main side leakage flow), tend to confirm the flow model.

10. The reasons for a link between the reduced minimum residence time and increased axial mixing are shown to be related to the various leakage flows. Similarly, the increased dependence of axial mixing on the screw speed with an open disc configuration, compared with a closed, can be explained on the basis of the melting mechanism together with the increase in central flow with increased screw speed.

11. Axial mixing in a co-rotating twin screw extruder was established by studying residence time distribution (RTD) by using various tracer techniques. As the tail of the distribution is of paramount importance, two tracer techniques, ashing and radioactive, were studied for their reproducibility.

The ashing tracer technique, as compared with the radioactive technique, cannot detect at low levels (below 1%), and therefore requires a high tracer concentration. The method involving slow degradation of polymer followed by pyrolysis of carbonaceous products gives reproducibility for up to 98% of the total flow. Being easily accessible and easy to use, it can be used for preliminary studies.

Within the radioactive tracer technique, three methods for the determination of the tracer concentration were investigated. The gamma ray technique gives reproducibility for up to 90% of the flow. Although the detection limit for this technique is lower (below 0.1%), the reproducibility achieved by this is inferior to the ashing

technique. The beta-gamma ray method shows a reproducibility of up to 99% . Gamma ray spectroscopy is found to be the most accurate, sensitive and reproducible technique (for up to 99.5% of the total flow).

12. Factors which may affect the reproducibility of RTD results over the range tested, are named in descending order of their influence on the RTD results. These are: location of sample position; first sample time; agglomeration of tracer compound; amount of tracer used and sampling duration. The number of samples within a given time does not affect the results. However two extrusion runs with similar running conditions make accuracy above 99% of the total flow difficult due to extruder's fluctuations

13. Melting is brought about by the imposition of constrictions in the flow path by the mixing discs. Thus the initial melting is achieved over a remarkably short distance leaving a portion of polymer unmolten. After this initial start, the progress of melting corresponds with a steady decrease in the size of the solid core located in the middle of the chamber, which is surrounded by the molten polymer. Thus it resembles the melting mechanism in large single screw extruders. However this solid core can be broken by the interruptions in the flow path.

14. The role of the mixing discs is proved conclusively. In the upstream position, they melt the polymer by imposing constrictions in its flow path. This is enhanced by the closed configuration as compared with an open one (more restricted flow path) which is shown by the increase in filled volume and increased axial mixing. As the difference is more pronounced at low screw speed it further confirms

the view that a critical pressure must be attained ahead of the mixing discs in order to achieve an optimum filled volume.

In the downstream position the mixing discs act as distributive discs thus improving the mixing by interrupting the flow patterns, illustrated by improved axial mixing results. The RTD in this position is more sensitive to the screw speed, than that in the upstream position. This pronounced effect further confirms the distributive function of these discs in the downstream position.

16. The relationship between screw speed and filled volume (at maximum attainable throughput rate), is determined by the overriding factors of available torque, pressure build-up from the mixing discs in the upstream position and their associated effect on the melting mechanism. In most cases the filled volume was found to increase with an increase in screw speed.

17. The filled volume gives a qualitative representation of the effects of variables on RTD. The filled volume is found to be directly related to the throughput rate. An increase in throughput rate results in an increase in filled volume, which restricts the free movement of polymer melt. Thus there is an associated decrease in mean residence time, and more positive flow.

Similarly, polypropylene granules, as compared with powder, show a higher throughput rate and therefore more restricted movement of polymer. This is associated with decreases in both minimum and mean residence times and more positive flow, as above. This is in sharp contrast to powder, which shows more stagnation due to a low throughput rate (because of the lower bulk density) and enhanced

melting, which creates a longer molten path in which the RTD can become more broader.

18. Polystyrene shows a continuous flow with increased axial flow, which is more dependent on screw speed. This is in contrast to polypropylene which shows the presence of two segregated flows. This behaviour could be due to the presence of a central unmolten zone which results from the lower thermal conductivity and higher total energy requirement for melting polypropylene.

19. The effect of screw speed on axial mixing shows three distinct trends. In most cases, an increase in screw speed using a small pulley gave rise to an increase in longitudinal mixing. However in some runs there was a decrease in axial mixing at an intermediate screw speed, compared with the lowest speed. This can be explained by poor melting and compaction. It is possible to relate these two types of behaviour with the net percentage pressure change.

However, in a system using a large pulley, a third trend in flow behaviour was observed due to the restricted heating and torque available. In this case the initial increase in screw speed produces an increase in the longitudinal mixing, but a further increase in screw speed results in a decrease in axial mixing. It also results in a lower mean residence time and a lower filled volume.

20. A trend in the effect of pressure on RTD was also observed. An initial increase gives rise to a broadening of the RTD curve but a further increase leads to reduced axial mixing and the tail becomes shorter, improving cleaning efficiency.

**REFERENCES**

- Adams R.L., Soc.Plust.Eng., Technical papers, 20, pp469- (1974).
- Baedecker P.A., Analytical Chemistry, 43, No:3, pp 405-410 (1971).
- Bigg D., Ph.D.Thesis, Mixing in a single screw extruder (1973).
- Bigg D. and Middleman S., Ind.Eng.Chem.Fundam., 13, No:1, pp66- (1974).
- Bigio D. and Erwin L., Ann.Tech.Conf.of Soc.of Plast. Engr., pp 45-48 (1985).
- Bird R.B, Stewart W.E., Lightfoot E.N., Transport phenomena, Wiley, New York, (1960).
- Blymental M.G. and Safulin D.M., Plasticheskie Massy, No:9, pp44- (1978)  
(Translated by Mosley R.J., Int.Poly.Sci.& Tech, 6, No:1, pp T/73 (1979)
- Booy M.L., Poly.Eng.Sci., 20, NO:18, pp 1220- (1980)
- Cox A.P.D., Williams J.G. and Isherwood D.P., Poly.Eng.Sci., 21, pp89- (1981)
- DeBoo and Schneider R.G., Ann.Tech.Conf.of Soc.of Plast. Engr., pp 625- (1978).
- Dekker J., Kunststoffe, 66, pp130- (1976).
- Dekker J, Plastic and Rubber: Processing, pp14- (1978).
- Denson C.D., Hwang Jr.B.K., Ann.Tech.Conf.of Soc.of Plast. Engr., pp 107-110 (1980).
- Dobroth T., Druhak G. and Erwin L., Ann.Tech.Conf.of Soc.of Plast. Engr., pp124-(1984).
- Gailus D.W. and Erwin L., Ann.Tech.Conf.of Soc.of Plast. Engr., pp639- (1981).
- Golba Jr.J.C., Ann.Tech.Conf.of Soc.of Plast. Engr., pp 83-88 (1980).
- Hansmann J., Gummi.Asbest.Kunststoffe, No:9, pp632- (1978).  
(Translation: Inter. Poly.Sci and Tech. 6, No:2, ppT/107- (1979).

- Herrmann H., Burkhardt U. and Jakopin S., Ann.Tech.Conf.of Soc.of Plast.Engnr., pp481-87 (1977).
- Herrmann H. and Eise K., Ann.Tech.Conf.of Soc.of Plast. Engnr., pp614-617 (1981).
- Hirshberger M. "Two dimensional non Newtonian flow in rectangular channel" M.S.Thesis, Dept of Chem.Eng., Technion,Haifa,Israel (1972).
- Hornsby P.R., Plastics and rubber processing and application, 7, (4), pp 237 - 240 (1987).
- Hornsby P.R.,Singh D.P. and Sothern G.R., polymer Testing, 5, pp 77-97 (1985)
- Howland C. and Erwin L., Ann.Tech.Conf.of Soc.of Plast. Engnr., pp113- (1983).
- Janssen L.P.B.M. and Churchill J.W. ed., "Twin Screw Extrusion" Chem.Eng.Monograph,Elsevier Scientific Publication Co. (1978).
- Janssen and Smith J.M., Proc.Cong.,on Poly Rheology and Plastic Processing PRI/BSR Loughborough, pp160-69 (1975).
- Janssen L.P.B.M.,Smith J.M., Plastics and Rubber : Processing and application, pp 90- June (1976).
- Jewmenow S.D. and Kim W.S., Plaste and Kautschuk, 20, pp356- (1973).
- Kao S.V. and Allison G.R., Polym.Eng.Sci., 24 (9), pp645-651- (1984).
- Kemblowski Z. and Sek J., Polym.Eng.Sci, 21(18), pp1194- (1981).
- Kim V.S.,Skatschkow W.W. and Jewmenow S.D., PlasteKautschuk, 20, pp696- (1973).
- Kim V.S.,Skatschkow W.W. and Jewmenow S.D., Plaste und Kautschuk, 22, pp730-734 (1975).
- Kim V.S.,Skatschow and Stungur J.W., Plaste und Kautschuk, 23, pp665- (1976).
- Kim V.S.,Skathkove V.V. and Stungur Yu.V., Plaste u Kautschuk, 25, pp352- (1978).

- Kruger P., "Principles of Activation Analysis", Wiley Interscience (1971).
- Kruder G.A. and Nunn R.E., Ann.Tech.Conf.of Soc.of Plast. Engnr., pp648- (1981).
- Levenspiel O., "Chemical Reaction Engineering", ISBN 0-471-53016-6, Wiley, NewYork (1972).
- Lin S., Ph.D. Thesis 1982, Brunel University, Uxbridge, England.
- Lindt J.T., Proceedings congress on Polymer Rheology and Plastic Processing PRI/BSR Loughborough, pp132- Sep(1975).
- Lindt J.L., Polym.Eng.Sci., 21, No:17, pp1162- (1981).
- Lidor and Tadmor, Poly.Eng.Sci., 16, pp450-62- June(1976).
- Lovegrove J.G. and Williams J.G., J. Mech. Eng. Sci., 15, pp 114-122 (1973); also, *ibid.*, 195-199.
- Maddock B.H., S.P.E. Journal, 15, pp383-(1959).
- Maheshri J.C. and Wyman C.E., Ind.Eng.Chem.Fundam., 18, No:3, pp226- (1979).
- Maheshri J.C. and Wyman C.E., Polymer Eng and Sci., 20, No:9, pp601- (1980).
- Martelli F., S.P.E. Journal, 27, pp25- Jan (1971).
- Martelli F. G., Twin Screw Extruders : A basic understanding, ISBN0-686-481739, T-C Publications CA. (1983)
- Mohr W.D., Saxton R.L., Jepson C.H., Industrial and Engineering Chemistry, 49(11), pp1857- Nov(1957).
- Mokhtarian F. and Erwin L., Ann.Tech.Conf.of Soc.of Plast.Engnr., pp - (1982).
- Ng K.Y. and Erwin L., Ann.Tech.Conf.of Soc.of Plast.Engnr., pp241-245 (1979)
- Nichols R.J., Golba J.C. and Shete P.K., Tech papers, AIChE 75th Anniversary meeting, Washington D.C., 1983.



- Nichols R.J. and Kheradi F., Ann.Tech.Conf.of Soc.of Plast.Engnr., pp134- (1983).
- Pinto G. and Tadmor Z., Polym. Eng.Sci, 10, Nu:5, pp279- Sep (1970).
- Rahim W., Ann.Tech.Conf.of Soc.of Plast.Engnr., pp77- (1980).
- Rauwendaal C.J., Puly.Eng.Sci., 21 (16), pp1092- Nov(1981).
- Rauwendaal C.J., Polymer Extrusion; ISBN 3-446-14196-0  
Hanser Publishers,Munich 1986.
- Rheotec -ODM Screw : Modern plastics international, pp36- Feb(1982).
- Roemer M.R. and Durbin L.D., Ind.Eng.Chem.Fundam. 5, pp120- (1967).
- Sakai T., Hsshimoto N. and Kobayashi N., Ann.Tech.Conf.of Soc.of Plast.Engnr., pp 146-151 (1987).
- Schott N.R.,Saleh D.V. Ann.Tech.Conf.of Soc.of Plast.Engnr., pp 536- (1978)
- Sebastian D.H. and Biesenberger J.A., Ann.Tech.Conf.of Soc.of Plast.Engnr. pp121-123 (1984).
- Shah S., Wang S.F., Schott N. and Grossman S., Ann.Tech.Conf.of Soc.of Plast.Engnr., pp 122-127 (1987).
- Sherider L.A., 78th National meeting,American Institute of Chemical Engineers, SaltLake City, Utah, (1974).
- Sterlinski S., Analytical Chemistry 40, Nu:13, pp1995-98, Nov(1968).
- Suchanek H.J. and Feng L.X., Kunststoffe, 74, No:8, pp459- ,(1984).
- Suchanek H.J. and Potente H., Ann.Tech.Conf.of Soc.of Plast.Engnr., pp 117- ,(1983).
- Tadmor Z., Polymer Eng. Sci., 6 ,pp 185 - (1966).
- Tadmor Z and Klein I.,:Engineering Principles of Plasticating extrusion, Van Nostrand, Reinhold, New York (1970).
- Todd D.B.,Polymer Eng and Sci 15, Nu:6, pp437-43, June(1975).
- Todd D.B.,Irving H.F., Chem.Eng.Prog., 65 Nu:3, pp85-, Sep(1969).
- Tucker C.S., Nichols R.J., Ann.Tech.Conf.of Soc.of Plast.Engnr, pp117- 121,(1987).

Uhland and Dienst, Ann.Tech.Conf.of Soc.of Plast.Engnr, pp36-40,(1980)

Ulmer and Werner:DBP 2029337 (1970).

Vermeulen J.R.,Scargo P.G.,Beek W.J.,:Chem.Eng.Sci.,26,pp1457- (1971).

Walk C.J., Ann.Tech.Conf.of Soc.of Plast.Engnr., pp423- May(1982).

Werner H. and Eise K., Ann.Tech.Conf.of Soc.of Plast.Engn.,pp181-  
(1979).

Wolf and White, Ann.Tech.Conf.of Soc.of Plast.Engn., pp439-42, (1975).

Wolf and White DH, A.I.Ch.E.J. 22 (1), pp122-31, (1976).

White and Wolf, Ann.Tech.Conf.of Soc.of Plast.Engn , pp532- (1978).

Wyman C.E.,Polym.Eng.Sci., 15 (8), pp 606-611, Aug(1975).

Zuillichem DjV,Swart J.G.,Buisman G,: Lebensm-Wiss.u.Technol.,6(5)  
(1973).